SAFETY IN MINES RESEARCH ADVISORY COMMITTEE

SIMRAC

Final Project Report

Title: PRECONDITIONING TO REDUCE THE INCIDENCE OF FACE BURSTS OF HIGHLY STRESSED FACES

Author/s: N Lightfoot, D H Kullman, A Z Toper, R D Stewart, M Grodner, A L Janse van Rensburg and P J Longmore

Research Agency: CSIR: MININGTEK

Project No: GAP 030 Part 1

Date: JANUARY 1996

ACKNOWLEDGEMENT

The CSIR: Mining Technology Preconditioning Team (i.e. the authors of this report) would like to gratefully acknowledge that the work reported here results entirely from funding provided by SIMRAC as project GAP030.

The work has enjoyed the cooperation and support of the South African Gold Mining Industry, and in particular that of Blyvooruitzicht Gold Mine and Western Deep Levels South Mine where the main research sites are situated. The team would like to thank the management of both mines for their cooperation in allowing the field site to operate on their mines. In addition we would like to express our gratitude to all the personnel on these mines that have given us much needed assistance during the course of our field experiments. Without the help of the people on the mines none of this work would have been possible.

Finally, gratitude goes to the members of SIMRAC, SIMGAP and GAPREAG for their enthusiastic support of the preconditioning research programme over the last three years.

TABLE OF CONTENTS

1. INTRODUCTION

Preconditioning, or destressing as it was initially called, was first introduced as a means of ameliorating rockburst conditions in deep mines by the management of the East Rand Proprietary Mines (ERPM) in the early 1950's with the cooperation and guidance of the CSIR (Roux, et al, 1957). The principle on which destressing was based at that time was that "The occurrence of rockbursts might be reduced or their violence decreased by increasing the depth of the fracture zone at the face of the working stope". The argument for this was based on the concept that if the holes drilled at right angles into the face were blasted they would advance the depth of fracturing and in so doing transfer the high stress zone further away from the face into the solid. Furthermore, should sudden failure occur in the high stress zone only limited damage would result because of the cushion effect of the 'destressed' zone ahead of the face

Field trials were carried out by ERPM in the 1950's to assess the feasibility of destressing, or preconditioning, as a safety measure to reduce the incidence of rockbursts. The results of these trials were encouraging. For example, the incidence of rockbursts per area mined was reduced by 36%; the number of severe rockbursts was reduced by 73%, and the frequency of on-shift rockbursts dropped to almost zero. However, despite these apparent benefits preconditioning was not generally accepted by mines as a viable and safe mining method. To address this problem the Chamber of Mines Research Organisation initiated a programme to re-investigate preconditioning as a viable, safe mining method in the late 1980's.

Field trials at West Driefontein mine were carried out to assess the viability of drilling 30 metre long preconditioning blast holes. Following this, work was transferred to Blyvooruitzicht Gold Mine, where a pillar adjacent to a fault was extracted using preconditioning. Following this successful experiment, a further three sites have been used for experimentation.

Work on the current site at Blyvooruitzicht Gold Mine began in April 1990 using preconditioning holes that were fanned out sub-perpendicular to the stope face. The intention is to extract a long strike pillar using preconditioning to reduce the risk of rockbursts at the face. Initially the mining was in an updip direction. However, in an attempt to improve the effectiveness of preconditioning, the panels were changed to breast in September 1992. This new layout allowed for the drilling of face parallel preconditioning holes. On the whole this has proven to be a more successful preconditioning and mining geometry.

In late 1994 it was decided that although face parallel preconditioning appeared to be well suited to the mining of long and narrow strike pillars, it would be difficult to implement in a normal deep-level longwall production environment without imposing considerable delays in the mining cycle. For this reason a new experimental site was opened on a deep-level longwall on Western Deep Levels South Mine. Experiments have been undertaken at this site with drilling short face perpendicular preconditioning holes as a standard addition to every production blast. Experiments to date indicate that it is possible to implement this method in deep-level longwall mining environment without significant disruption to the mining cycle. In addition, there appears to have been a significant decrease in the impact of rockbursts at this site.

2. ALTERNATIVE METHODS OF PRECONDITIONING

A number of different drilling methods and mining configurations have been used during the years of experimental preconditioning experimentation. The drilling methods have been

- face perpendicular long holes
- face parallel long holes
- face perpendicular short holes

The mining faces have been in remnant pillars, stabilising pillars and production longwalls. The faces in pillars have been oriented both up-dip and on strike. The production longwall faces have all essentially been up-dip faces. Currently, only two methods of drilling are being used by Miningtek and each of these is specific to a particular mining geometry. The current preconditioning systems involve

- face parallel long holes ahead of breast panels in remnant strike pillars
- face perpendicular short holes in up-dip panels on a production longwall

Both methods are operating successfully and guidelines have been published describing the specifics of implementation for each. The guidelines are briefly summarised below.

2.1 GUIDELINES FOR FACE PARALLEL PRECONDITIONING

Layouts to maximise the integration of preconditioning into a pillar mining operation are described by Kullmann, et al, 1995 and Lightfoot, et al (1995). All the results obtained thus far are based on the results obtained from a limited number of research sites on one reef type (the Carbon Leader Reef). An overhand mining layout is required to drill up-dip preconditioning holes from the leading panel below. The holes must be drilled beyond the length of the panel to ensure a full preconditioning effect along the entire face length. The hole must be stemmed to prevent excessive energy loss through the collar of the hole, potentially resulting in damage to support units in the stope. Panel lengths should ideally be 15m and not exceed 20m to ensure that the preconditioning holes can be drilled and blasted in a single shift, depending on the capabilities of the drilling equipment and ground conditions. If not, loss of the drill bit and rods as well as the hole becomes more likely.

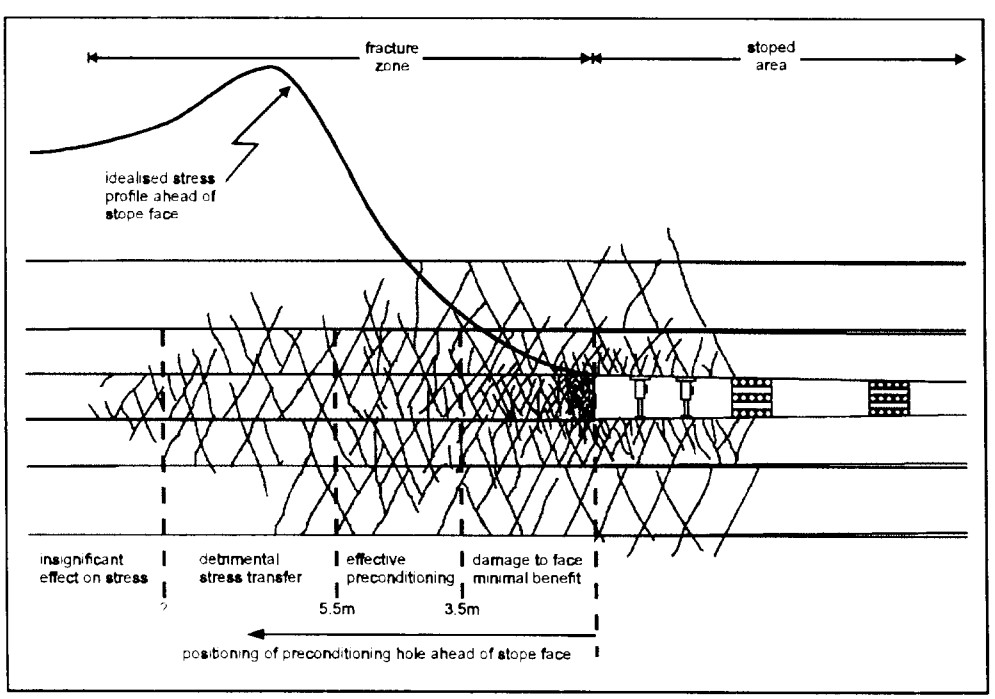

Figure 2.1: Effects of positioning an 89mm diameter preconditioning hole at varying distances ahead of the stope face.

An 89mm diameter percussion drilled hole should be positioned from 3.5m to 5.5m ahead of the panel face and blasted with an ANFO or emulsion type explosive. Smaller holes should be positioned somewhat closer to the face to account for the smaller charge. For the most effective results, the hole should be drilled as close to the reef plane as possible but remain at least 50cm from the proposed hangingwall contact to prevent direct blast damage to the hangingwall. The optimal distance ahead of the face of the preconditioning hole can only be determined by experimentation (Figure 2.1 and 2.2). Holes positioned too close to the face will result in damage to the stope face area. Holes too far ahead of the face can even be detrimental to face stability as the stress redistribution resulting from a blast can reload the stope face (Lightfoot, et al., 1994, Kullmann, et al, 1994).

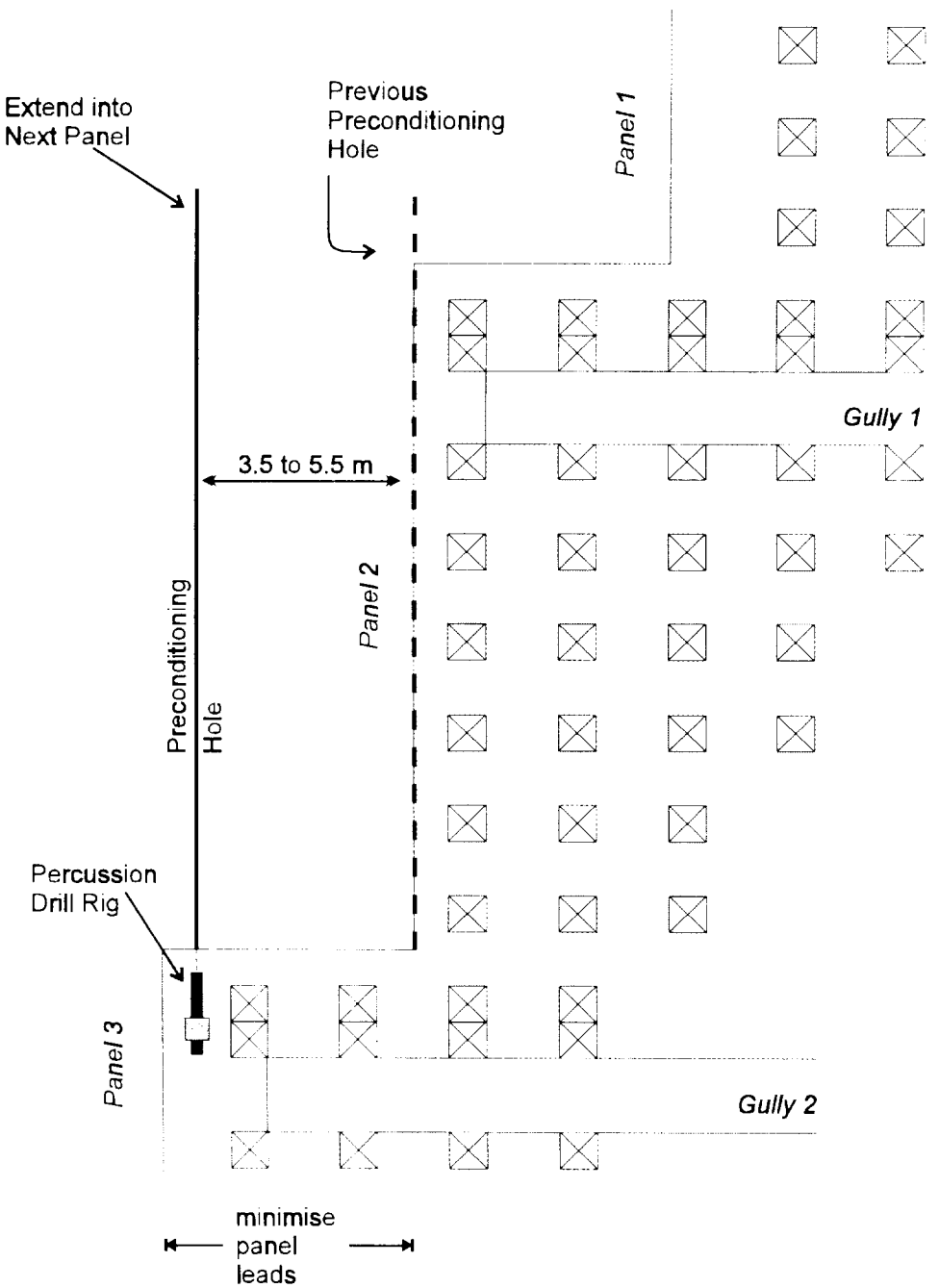

Figure 2.2: Face parallel preconditioning layout in an overhand mining sequence. In the example case Panel 2 has been mined to the temporary limit (the previous preconditioning hole position) and the next hole is drilled up to 5.5m ahead of the current face position.

Blast optimisation is a compromise between the blast size and the time required to achieve this blast. A larger diameter hole can be positioned farther ahead of the face, effectively preconditioning a larger volume of rock. This results in a more efficient cycle as there would be less stoppages for preconditioning. However, a larger hole drilled in more highly stressed ground is more difficult to drill. The benefits of preconditioning are also time dependent, and too much time between blasts could result in an excessive strain energy accumulation which could result in a rockburst. Hole diameter also affects the efficiency of stemming and explosives (especially ANFO).

2.2 GUIDELINES FOR FACE PERPENDICULAR PRECONDITIONING

The diameter and the length of the preconditioning holes should be about 40 mm and 3 m respectively (Toper, et al, 1995). This allows usage of the drilling machines and drill steel presently available on most mines.

In order to achieve maximum effect, the preconditioning holes should be drilled in the plane of the rock to be preconditioned (i.e. on-plane with reef). Since the effective area of a preconditioning hole was determined as 1.5m in radius, the spacing between preconditioning holes along the face should be maximum 3 metres (Figure 2.3). This technique uses a three day cycle. Once the face has been cleaned and prepared for the next round of preconditioning, the drilling of new preconditioning holes commences. For this round the preconditioning holes are offset from the previous ones by almost 50 cm along the strike direction. On the third day the preconditioning holes are drilled 50 cm offset from the sockets of the previous day's preconditioning. Since the panel face is advanced almost 3 metres in a three day cycle, the preconditioning holes on the fourth day should be drilled at the same positions as those of the first day.

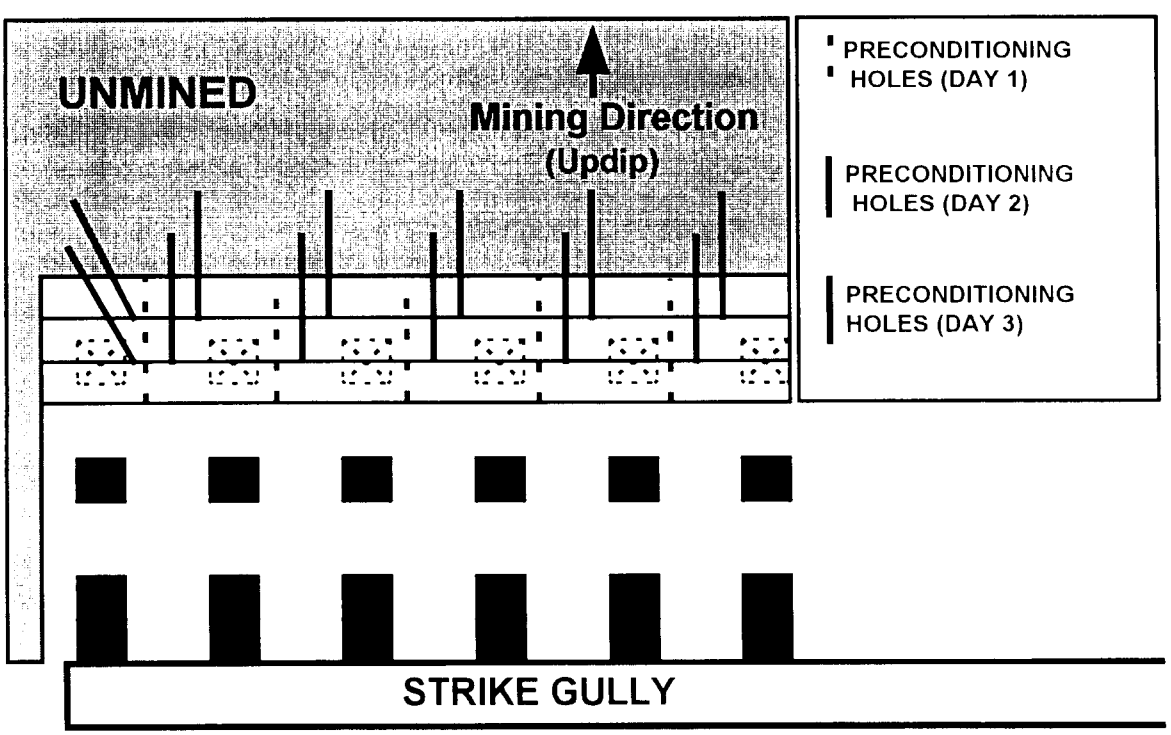

Figure 2.3. Diagram showing the face perpendicular preconditioning layout for a three days cycle. The maximum distance between preconditioning holes is 3m.

The updip preconditioning holes should be drilled at right angles to the face at mid-stope height in order to reduce the chance that a hole drilled as part of the normal production round will intersect a preconditioning hole. The closest point between the production and the preconditioning holes is at the collar and when properly drilled, the production holes are drilled away from the preconditioning holes. Either knock-off or button bits could be used for

drilling of the preconditioning holes. Knock-off bits are recommended as they eliminate taking the drill steels out at the end of the shift for re-sharpening.

It is believed that the rock (first 3 metres from the face) to be preconditioned is in fractured condition, even if some of the fractures are tightly closed by clamping forces. Thus a low shock energy and high gas energy explosives would have a better effect in opening and extending pre-existing fractures and discontinuities. ANFO (ammonium nitrate fuel oil mixes) explosives are recommended for preconditioning but were not available at the project site. Powergel cartridges were used instead to charge the preconditioning holes, 15 cartridges being required for each hole, only 2/3rds of the total length being charged (i.e. 2 m). To date preconditioning with emulsion explosives has been quite successful.

The charging of preconditioning holes should be by top priming the explosive charge to facilitate easier removal of primers from misfired preconditioning holes. One emulsion cartridge can be used as a primer and should be initiated with a Nonel or electric detonator. A reliable and accurate electronic initiation system should ideally be used. But, if none is available at that particular stope, an existing initiation system can be employed. The application of fuse/ igniter cord systems is not recommended due to the difficulty of obtaining the proper firing sequence of preconditioning holes in relation to the production holes. To ensure the proper firing sequence, all preconditioning and production holes are charged by 2.1 m long fuses and the fuses of the preconditioning holes are connected to the igniter cord approximately 1 m forward. This enables the preconditioning holes to be fired with almost a 1 m burden in the strike direction (i.e. before the neighbouring production holes are fired).

Since the preconditioning holes are charged for 2/3 of their total length, the remaining 1 meter should be tamped with a competent stemming material. Clay, bentonite, angular sand or a combination of these could be used for tamping the preconditioning holes.

3. PRECONDITIONING FOR REMNANT PILLAR EXTRACTION

3.1 HISTORICAL REVIEW

COMRO's involvement in preconditioning began in 1987 with experimentation at West Driefontein Gold Mine where the 32-12W stope was being mined into a large remnant along the Western Deep Levels boundary (Rorke, et al, 1988). The technique being implemented made use of long, face parallel holes drilled along the length of the 30m panels. The 76mm diameter holes were positioned between 2.5m and 3.5m ahead of the face and drilled within a shift. The panels mined beyond the line of the previous preconditioning holes and hence the spacing between preconditioning holes averaged about 8m.

Following a trial period of five months of test drilling, preconditioning was implemented in two panels. Once the technique was optimised, all five panels within the stope were being preconditioned. A total of 18 preconditioning blasts were taken in the eleven month period of the project. The project was terminated when the technique could not be integrated into the new layout which was required as the stope was approaching a seismically hazardous structure.

The effects of the preconditioning blasts are reported to be very similar to that being observed at the current Blyvooruitzicht site, 17-24W (see Section 3.2 below). Convergence associated with a preconditioning blast of 5mm to 40mm, face scaling of up to 300mm, and a lack of damage at the face following large seismic events were all reported. An observed reduction in low angle fracturing compared to non preconditioned panels resulted in improved hangingwall stability, which may partly account for the lack of seismic damage.

Preconditioning was then initiated on Blyvooruitzicht Gold Mine in the 18-13W stope; an up-dip panel along a protection pillar for seismically active structures (Rorke et al, 1990). A series of 30m long, 76mm diameter holes fanned out from the dip gullies were planned to be drilled into the entire pillar with the intention of "preconditioning" the pillar with one blast. Eventually, only the holes on the edge of the pillar could be drilled to nearly their full length. The other holes were drilled to only 10m. Difficulties experienced with drilling into the core of the pillar provided some insight regarding the condition of the pillar. The pillar was eventually mined out without incident by fanning the preconditioning holes drilled from the up-dip gullies at five different face positions.

Improved hangingwall stability was reported to be due to steeper extension fractures following the introduction of preconditioning. Although most of the preconditioning holes were 10m long, it was reported that experimentation elsewhere (no details given) indicated that the preconditioning effect did not extend more than 4m ahead of the face.

The 30-24W stope on Blyvooruitzicht is situated near the boundary pillar to Western Deep Levels. This dip pillar was 40m wide and 150m long with the top of the pillar terminating on a stabilizing pillar. Initially, the pillar was being conventionally mined but after problems with consistently poor ground and several large seismic events, the mine decided to implement their own preconditioning project in mid 1990. They requested that COMRO monitorthis project. The method of preconditioning was similar to that used at the 18-13W stope; 10m long holes fanned out from the dip gullies. Difficulties with drilling and frequent damage to support and the collar area of the holes all resulted in production delays.

Problems also arose due to the mining by Western Deep Levels of two large longwalls just to the south of the boundary pillar. The resulting stress changes in the preconditioning stope resulted in a significant increase in seismicity. A large rockburst in October 1991 resulted in several fatalities. This prompted a change in the preconditioning layout to face parallel drilling. However, before any progress could be made with this technique, the stope had to be abandoned due to increasing seismicity. No production blast has been take in the stope since February 1992.

3.2 THE BLYVOORUITZICHT GOLD MINE 17-24W FIELD SITE

3.2.1 Site description

The preconditioning project at BGM is continuing at the 17-24W stabilising pillar (Figure 3.1) which is situated on the Carbon Leader Reef at a depth of over 1,900m below surface. The pillar is about 40m wide and extends for 300m on strike in an east / west direction. The site is very isolated; the current mining faces are about 250m from the nearest pillar and 400m from the closest mining. Extensive mining around the pillar has led to shearing along the top and bottom edges of the pillar, resulting in complete closure of back areas extending to the pillar itself. Support in these back areas consisted of timber packs and pipe-sticks.

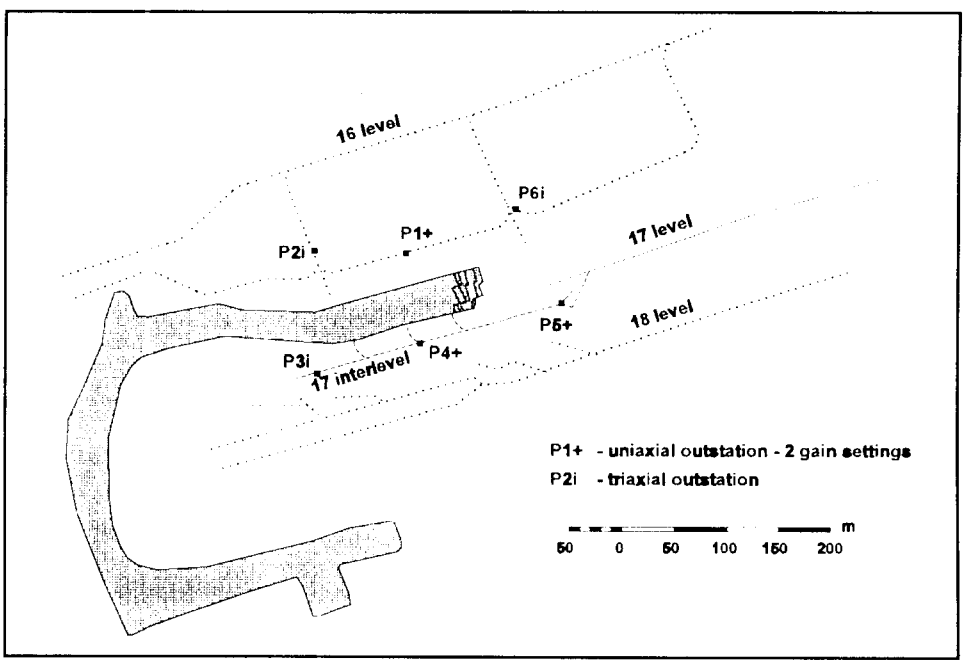

Figure 3.1: Plan of 17-24W stope and layout of the microseismic network around the current faces.

3.2.2 Preconditioning layout

The current research site at 17-24W was initially to be mined in the strike direction. During the establishment of the faces, a rockburst resulted in the loss of access to those faces. The layout was then changed to up-dip mining with 18m long faces and 13m long preconditioning holes being fanned out from the dip gullies. Mining of the pillar began in April 1990, but drilling difficulties and damage to the collar area of the holes delayed production. In an effort to reduce these delays, a face parallel preconditioning layout was implemented with the second phase of up-dip mining in mid 1991. However, dense support and poor ground conditions resulted in poor positioning of the drill rig and in some cases, holes were drilled 10m ahead of the face. The blasting in such confined conditions resulted in damage to the collar of the hole and support units, again resulting in production delays. This then prompted a change in the stope layout and in September 1992, mining on strike began in conjunction with face parallel preconditioning. This consists of an advance heading at the bottom of the stope leading two full panels (Figure 3.2). Panel 2 is preconditioned from the gully in the advance heading and panel 1 (top) is drilled from the gully that is footwall lifted at the top of panel 2. In terms of the efficiency of both preconditioning and production at the site, the change in mining layout has had positive results, some of which are described below.

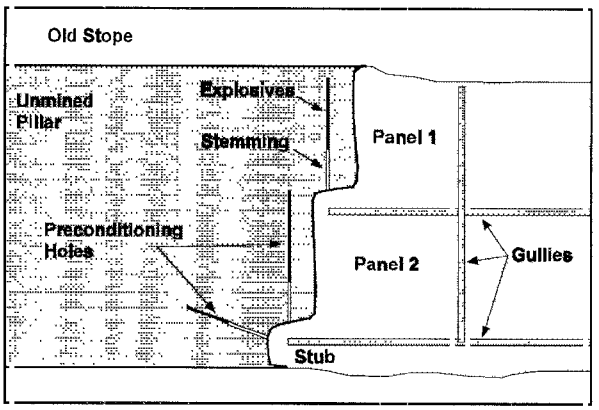

Figure 3.2 Current layout of preconditioning holes for breast mining configuration at 17-24W stope.

Panel leads of 8.5m are required for the current face parallel preconditioning holes in order to meet mine support standards but this has had no detrimental effects on hangingwall stability. The major delays to production have been the result of poor ground conditions in the panel 2 gully and dip gullies which are bounded by major fracture sets. Minor delays have resulted from mechanical failure of the water jetting equipment and more recently, labour shortages.

In an effort to overcome the hangingwall stability problems, a new stope layout was proposed and accepted by mine management (Figure 3.3). The intention is to move the bottom gully out of the major fracture zone along the bottom edge of the pillar. At the same time, dip gullies will be oriented on an apparent dip direction to create a more oblique angle with the face parallel fracture sets.

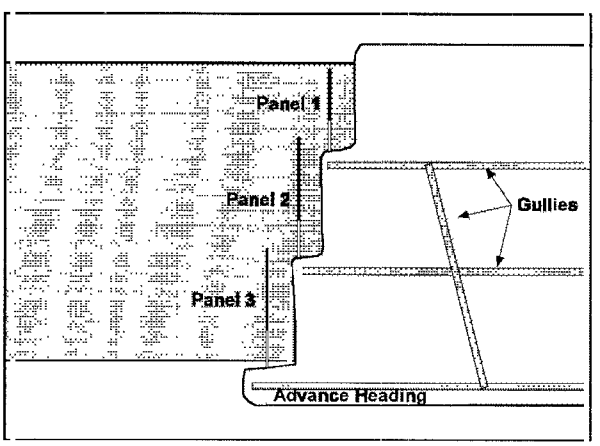

Figure 3.3: New stoping layout of 17-24W.

The current layout with the stub at the bottom of the pillar makes it impossible to drill a face parallel preconditioning hole ahead of the stub. In an attempt to provide preconditioning to the stub area, a preconditioning holes are drilled out from the stub sub-parallel to the edge of the pillar (Figure 3.2). Although this is far from ideal, some reasonable results have been achieved from these blasts. The combination of 5m of stemming from the panel 2 preconditioning hole and the nearly 8m of face length in the stub results in the bottom 13m of the pillar not being adequately preconditioned. With the new layout, the lower portions of the pillar can now be much more efficiently preconditioned.

3.2.3 Seismic coverage

As adequate monitoring of the preconditioning site is essential to any assessment of the effectiveness of preconditioning, sufficient microseismic coverage of the site has been ensured throughout the preconditioning experiment at 17-24W. If the general seismicity

patterns of the site can be evaluated, an understanding of the effects of preconditioning on those patterns can be gained. The effectiveness of preconditioning can also be determined from an analysis of the seismicity directly associated with recorded preconditioning blasts.

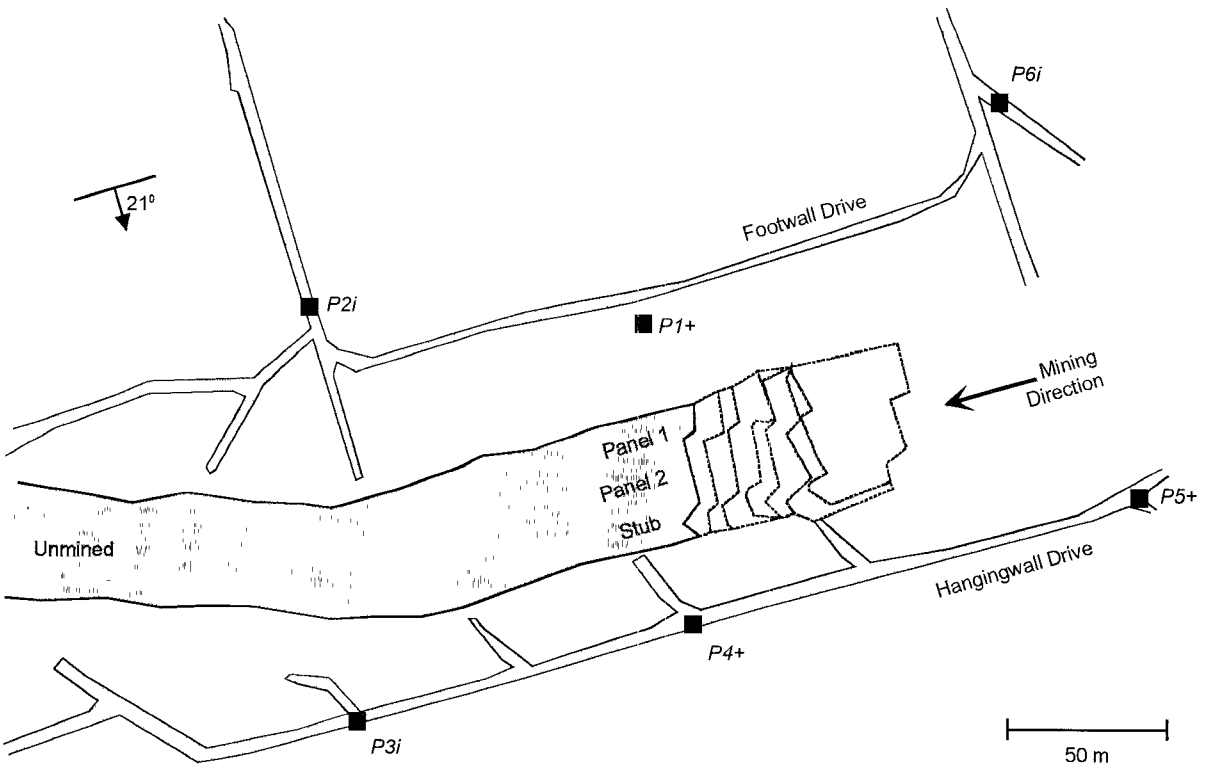

Figure 3.4. Plan of the Blyvooruitzicht Gold Mine 17-24W preconditioning site, showing the geophone positions for the PSS network which is monitoring the seismic activity from the site. Uniaxial geophone sites which have a high- and a low-gain channel are labelled e.g. *'P1+'*, while triaxial geophone sites are labelled e.g. *'P2i'*. The current face position is that of mid 1995, previous positions of the stope faces are indicated by the dashed lines.

A Portable Seismic System (PSS), developed at the Chamber of Mines Research Organisation (now the CSIR Division of Mining Technology), has been used for the microseismic monitoring of the preconditioning experiment at the 17-24W site. The PSS has been described by Pattrick et al (1990). Briefly, the system consists of a network of appropriately sited transducers which are grouted at the ends of boreholes drilled into the rock mass from underground excavations, and which are connected to nearby transducer outstations which amplify the transducer signals. From the outstations, the signals are passed along electrical cables to the Data Acquisition Unit (DAU), which digitises the signals. The function of the DAU is to detect and capture seismic events, and to pass the information on to a data computer (PC), which is usually situated on surface. The DAU communicates with the PC via modems and standard telephone cables. The standard PSS can accommodate a maximum of 16 transducer channels. The 17-24W PSS uses geophones to measure ground velocity at the recording sites.

The current layout of the PSS network with respect to the 17-24W preconditioning site is shown in Figure 3.4. The preconditioning site is relatively isolated from other mining areas, and it was thought that the seismicity recorded from the site would reflect mostly the response of the pillar to the stresses induced by the mining activities at the site, with limited external seismic influence. As can be seen in the figure, the PSS network covering the preconditioning site is well balanced with respect to the area of interest and provides close coverage of the seismic activity at the site, with good sensitivity and location accuracy. The horizontal extent of the network is 200 metres in the strike direction and 150 metres in the dip direction, but the vertical extent is just over 30 metres (centred about the plane of the reef),

so that the accuracy of location of out-of-plane seismic events in the vertical direction is not as good as in the horizontal directions. Most of the recorded seismicity originates close to the reef horizon (within about 15 metres of the reef plane), so that this is not a serious limitation.

The 17-24W PSS network consists of six recording sites, these being three triaxial sites (e.g. 'P2i' in Figure 3.4) and three uniaxial sites (e.g. 'P1+' in Figure 3.4). The uniaxial sites measure only the vertical component of the ground velocity. The network has good sensitivity, recording seismic events of magnitude down to M = -2.0 from the preconditioning site with adequate signal-to-noise ratios on most channels. Unfortunately, the PSS has a relatively limited dynamic range, which results in saturation of the waveforms recorded at the closest sensors for events of magnitude greater than about M = 1.0. While accurate locations of such events are still possible, the magnitudes are underestimated.

In an attempt to overcome this limitation, at least in part, adjustments were made to the uniaxial outstations, so that the signals from each of those geophones were recorded on two channels, one at the normal gain, the other at a reduced gain. The signals from larger seismic events, which saturate the higher-gain channels, can be processed on the lower-gain channels, so that useful source information can also be obtained for these events. The lower-gain channels have proved their worth repeatedly in the recording of larger events which originated from the preconditioning site.

Blyvooruitzicht Gold Mine also uses a PSS for the recording of mine-wide seismicity. Although the location accuracy of this network is inferior to that of the PSS in the vicinity of the 17-24W preconditioning site, the network does have sufficient sensitivity to record the larger seismic events which originate from the site and to provide reliable magnitudes for these events. However, some of the events are large enough to saturate too many of the channels of the 17-24W PSS to allow the network to provide an accurate event magnitude. When this happens the magnitude is obtained from the mine-wide system, while the location is obtained from the 17-24W PSS.

The 17-24W PSS network has good location accuracy for seismic events which originate from the preconditioning site. This was verified by the locations determined by the PSS for preconditioning blasts recorded during the breast mining phase at the preconditioning site. These were compared with the physical locations of the blast centres and the average difference in location was found to be 5.4 $\pm$ 3.0 metres. This location accuracy lends a high degree of confidence to studies of migratory patterns which have been observed in microseismic event locations in the rock mass ahead of the mining faces. These migratory patterns are related to the stress redistribution which takes place in the rock mass during mining and preconditioning activity at the preconditioning site, and form an important part of the analysis of the effectiveness of preconditioning.

In general, the PSS has proved itself to be a reliable system. Occasional communications problems have, however, been experienced between the DAU underground and the data PC on surface. Also, the aging DAUs have become decreasingly reliable. This has resulted in some loss of data, such that occasional gaps are to be found in the seismic database. The DAUs are shortly to be replaced with newly constructed counterparts.

3.2.4 Other Instrumentation

Convergence data is currently being acquired with the use of convergence-ride stations. This involves the use of bolts installed in the hangingwall and footwall. Through triangulation daily measurements are resolved into the principal convergence and ride components of ground movement (Piper and Gürtunca, 1987). The convergence/ride stations are quick to install, easy to use and inexpensive.

The maintenance of convergence-ride stations can be a problem at the Blyvooruitzicht site because of deteriorating ground conditions in the back areas and the rapid convergence rate. Stations often become inaccessible 8m from the face. Loss of stations also occurs as a result of shake-out from preconditioning blasts, large seismic events, and at times even support installation over the stations. At present, three stations are installed in each panel, not only to

record variations in movement in different areas of the stope, but also for some redundancy in the event of the loss of a station. A virtually complete database of convergence measurements is available since the start of the breast mining phase of the preconditioning project.

The Ground Motion Monitor (Black Box) is being investigated as a tool for use in the practical implementation of face parallel preconditioning. Design modifications to the standard Monitor itself have allowed for the installation of individual sensors on either the hangingwall, face or footwall, or all three at once with a single box. Currently, ground accelerations are being recorded for each preconditioning blast and compared with the data obtained from the PSS, convergence / ride stations and observations of the change in ground conditions after the blast. Essentially, the black box is intended to take the subjectivity out of the observation of face condition and replace it with measured values of the ground response to the preconditioning blast. This will provide, at least partially, for the evaluation of the effects of the stemming area of the hole and beyond the end of the hole in situations where the hole has been drilled short of the full face length. The monitors may also be used to evaluate the effects of varying explosive types, hole sizes and hole positions. It is likely that the results obtained from the current research site will be used to optimise blast layouts on new sites on the same reef type or even different reefs.

3.3 PRECONDITIONING BLASTS

3.3.1 Summary of the preconditioning blasting

In the 39 months since the change to breast mining in September 1992, 3724 centares have been extracted from the 17-24W preconditioning site. This corresponds to 93 metres face advance, an average of 2.39 metres per month (28.6 metres per year). The production rate has been maintained fairly steadily throughout this period, although it was somewhat higher in 1994, in spite of a three-month production stoppage in order to improve the conditions of the access ways and of the stope support. This temporary suspension of production was based on the recommendation of researchers at CSIR Mining Technology, after some disturbing trends had been identified in the seismic data recorded from the preconditioning site.

Figure 3.5 compares the cumulative production from the site with the cumulative seismicity. While the production rate remained fairly constant, a slight increase can be seen in the seismicity rate from late 1993 until the time of the production stoppage in mid 1994. After the stoppage, the seismicity rate returned to the values of early 1993. The trend which was the primary cause of concern is shown in Figure 3.6, and indicates an alarming increase in the release of seismic energy at the preconditioning site from November 1993, without any corresponding changes being identifiable in the production rate or in such factors as the mining geometry. This increase in the seismic energy release rate occurred without a marked increase in the overall seismicity rate, but rather resulted from an increase in the rate of occurrence of larger ($M \geq 1.0$) seismic events at the site.

The change in the pattern of seismic energy release prompted the CSIR Mining Technology researchers to recommend temporary suspension of production in order to improve the conditions of the access ways and of the stope support. After the three-month production stoppage, the recorded seismic energy release returned to a fairly steady rate, at a slightly higher level than that which prevailed in early 1993, as can be seen in Figure3.6. It appears that the production stoppage allowed the rock mass ahead of the stope face to stabilise and return to a state of greater equilibrium.

During this period 51 preconditioning blasts were detonated at the 17-24W preconditioning site. A total of 4328 kg of explosive was used in 722 m of preconditioning holes, an average of 85 kg per 14 m preconditioning hole. The average time between preconditioning blasts was 24 days, and this has been maintained fairly consistently throughout the three-year period. During 1995 15 preconditioning blasts have been carried out, six in each of panel 1 and panel 2, and three in the advance heading (stub). The details are summarised in Table 3.I.

Table 3.I. Summary of preconditioning activity at 17-24W preconditioning site. The 5 preconditioning blasts of 1992 are not included in this summary.

	Number of blasts	Average amount of explosive (kg)	Average length of hole (m)	Average days between blasts
Total	51	85	14	24
Panel 1	19	74	13	60
Panel 2	22	111	18	56
Stub	10	49	8	104
1995	15	67	12	24
1994	15	85	15	24
1993	16	88	14	24

On average the blasts undertaken in 1995 have been smaller than those in previous years as a result of a greater degree of difficulty in the drilling of the preconditioning holes than in previous years, so that a number of blasts were detonated in holes that were shorter than planned. The greater length of time between stub blasts is the result of the geometry of the hole: with the hole being oriented on strike, the ground is affected for a greater distance ahead of the face, so that the stub is preconditioned only every second cycle, on average.

3.3.2 Analysis of preconditioning blasts

A number of criteria are used in the assessment of the effectiveness of each preconditioning blast at the 17-24W preconditioning site. These criteria were developed in an attempt to minimise subjectivity in the assessments. The criteria are:

- The seismic magnitude of the recorded blast event
- The number of seismic events recorded from the site in the 24 hours following the blast
- The magnitude of the largest event in the subsequent seismicity
- The degree of spatial migration evident in the subsequent seismicity
- The convergence recorded on the following day

In the assessment, account is taken of:

- The amount of explosive used in the blast
- Whether or not there was a production blast in another panel on the same day
- Whether the convergence measurement was made in the panel of the preconditioning blast or in another panel

The rating system which has been developed is outlined in Appendix *A*. Appendix *B* contains a detailed summary of all preconditioning blasts which have been detonated at the preconditioning site since September 1992, and includes a rating for each blast. Note that the rating system is conservative, so that an acceptable preconditioning blast is one which scores 30 per cent or more. A very effective blast would score 50 per cent or more. The average rating for all preconditioning blasts to date is 38 per cent, with 70 per cent of preconditioning blasts having scored 30 per cent or more. The average ratings by panel and by year are given in Table 3.II.

It is clear from Table 3.II that preconditioning blasts set off in panels 1 and 2 have typically been more effective than those set off in the stub. This is related to the orientation of the preconditioning holes in the stub and to the fact that shorter preconditioning holes with less explosive have been used in the blasts there. The relative lack of effectiveness of the stub blasts is a source of concern, as this area of the pillar is the site of a substantial concentration of stress, which may be aggravated by the effective preconditioning of panels 1 and 2. The new mining layout which is shortly to be implemented should alleviate this problem considerably.

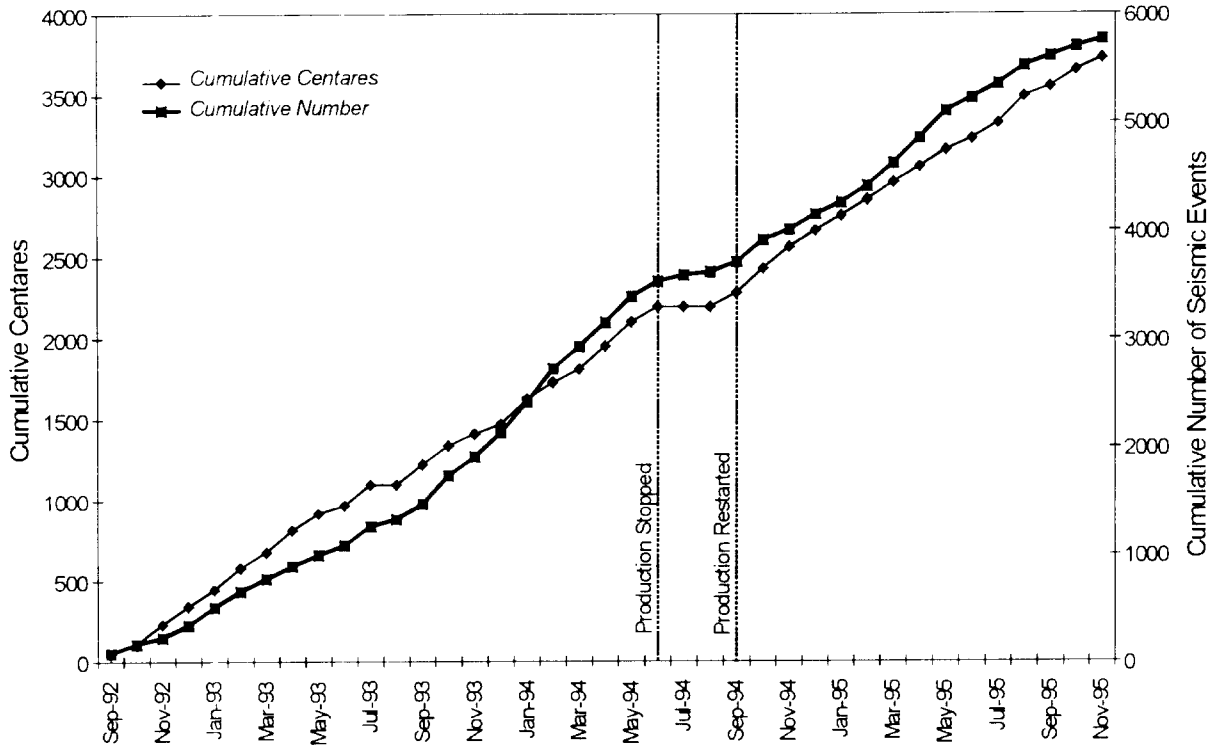

Figure 3.5. Plot of the variation in cumulative production and cumulative seismicity rate recorded from the BGM 17-24W preconditioning site during breast mining.

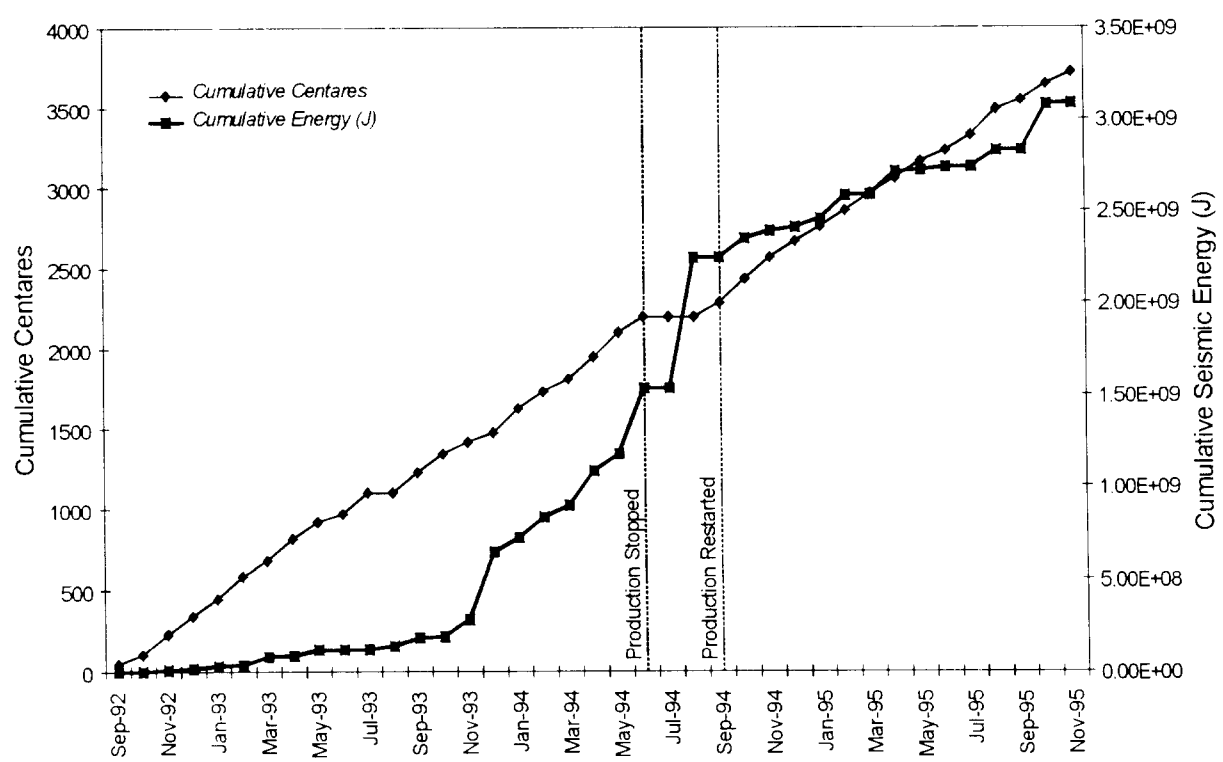

Figure 3.6. Plot of the variation in cumulative production and cumulative seismic energy release rate recorded from the BGM 17-24W preconditioning site during breast mining.

Table 3.II. Summary of 17-24W preconditioning blast ratings. The rating system is described in Appendix A: in summary >30% = acceptable; >50% = very effective.

	Average rating (%)	Blasts above 30% rating (%)
Total for the pillar	38	70
Panel 1	40	79
Panel 2	41	76
Stub	28	40
1995	33	73
1994	39	67
1993	40	69

From Table 3.II, it can also be seen that the average preconditioning blast which was set off in 1995 was less effective than that of previous years. This is attributed to the more frequent drilling difficulties which were encountered during the past year. The average blast rating for 1995 preconditioning was only 33 per cent. However, 73 per cent of all blasts in 1995 rated 30 per cent or above. Most of the preconditioning blasts during 1995 scored 30 or 40 per cent, the highest score being 60 per cent. This indicates that, while few blasts were "very effective", the majority of blasts produced an "acceptable" effect in the rock mass. The rating in previous years was more varied, with a greater proportion of "very effective" blasts (scoring 50 per cent or more), but also a larger number of ineffective blasts.

The preconditioning blasts with low ratings (20 per cent or less) have generally followed inadequacies in the preparation of the blast (incorrect hole positioning or orientation, drilling difficulties, insufficient stemming, etc.). Other ineffective blasts have been produced by short or small-diameter holes with less explosive, especially for the stub blasts. An exception to this is the panel 1 preconditioning blast of 18 May 1994 (rating: 20 per cent). This blast was well prepared and yet appeared to produce very little preconditioning effect. The reason for this was that a production blast in panel 2 on 12 May triggered a large (M = 2.2) seismic event very close to the face of panel 1, which effectively destressed the rock mass ahead of the panel 1 face just prior to the detonation of the panel 1 preconditioning blast. The preconditioning blast therefore had no work to do in the rock mass and so was "ineffective".

The average rating for the 33 preconditioning blasts which have been set off without any concurrent production activity is 41 per cent. The average rating for the 18 preconditioning blasts which have been followed by at least one production blast in another panel on the same day is 34 per cent. This result indicates that if a production blast occurs in a neighbouring panel on the same day as a preconditioning blast it has little effect on the results of the preconditioning process. On the other hand, it has been found on a number of occasions that a production blast on the day following a preconditioning blast can be effective in the release of stored strain energy from the rock mass by way of the triggering of larger seismic events. Examples of this phenomenon are the panel 2 production blast of 30 June 1993 (following a panel 1 preconditioning blast on 29 June) which triggered two $M \geq 0.0$ events in panel 2. and the panel 2 production blast of 11 January 1995 (following a panel 1 preconditioning blast on 10 January) which triggered two M = 1.7 events in panel 2 and the stub.

3.4 QUANTITATIVE ANALYSIS OF THE EFFECTS OF PRECONDITIONING

Although the preconditioning team at Miningtek are confident that preconditioning is having a beneficial effect in improving safety while mining the stability pillar at the Blyvooruitzicht Gold Mine 27-24 West site it is necessary to quantify this effect. If preconditioning is of benefit then it must be affecting the local rock mass in some way that is measurable. Seven objective methods of quantifying the effects have proven to be of value to date at this site, these are:-

- Integrated data analysis
- Seismic analysis
- Convergence monitoring
- Ground motion monitoring
- Assessment of face dilation
- Analysis of mining induced fracturing
- Seismic tomography

The first six of these methods are described in more detail below. The seventh method (i.e. seismic tomography) is described in detail in a later chapter. The different methods have been used for a varying degree of time and, as such, are at various stages of maturity, with some techniques currently yielding more significant results than others. In general the analysis simply requires more time and data in order to describe quantitatively the effects of preconditioning on the rock mass.

3.4.1 Integrated Data Analysis

A considerable amount of data has been gathered from the 17-24W preconditioning stope at Blyvooruitzicht Gold Mine since the change to the breast mining layout. The diagnostic areas for which the data is virtually complete include recorded seismicity, convergence measurements near the stope face, and production and preconditioning blasts. To deal with this large amount of data, a systematic approach of data analysis is required. This requires the ability to retrieve and relate data rapidly. Microsoft Access® is a relational database management system which has the capability to store, correlate and retrieve information quickly according to user defined relationships. Basic evaluations can also be conducted easily but more detailed analyses are better carried out within a spreadsheet (such as Microsoft Excel®).

This database currently contains five tables of the most basic information and consists of seismic event details, convergence - ride data, and blasting records (Figure 3.7, Table 3.III). The seismic events table is constructed directly from the Events file from the PSS system. Source parameters will be included in the near future. The new Windows™ based PSS software is structured around an Access database which would allow for the importation of the entire seismic database very conveniently into this database. Access is also being investigated for storing and calculating convergence - ride data which is currently being stored in a spreadsheet. All blasting data are being compiled directly within the database. The Blasting table contains all blasts (production, precondition, and development) since all are being recorded by the seismic system. All blast events are flagged appropriately within the seismic events table by the location method category.

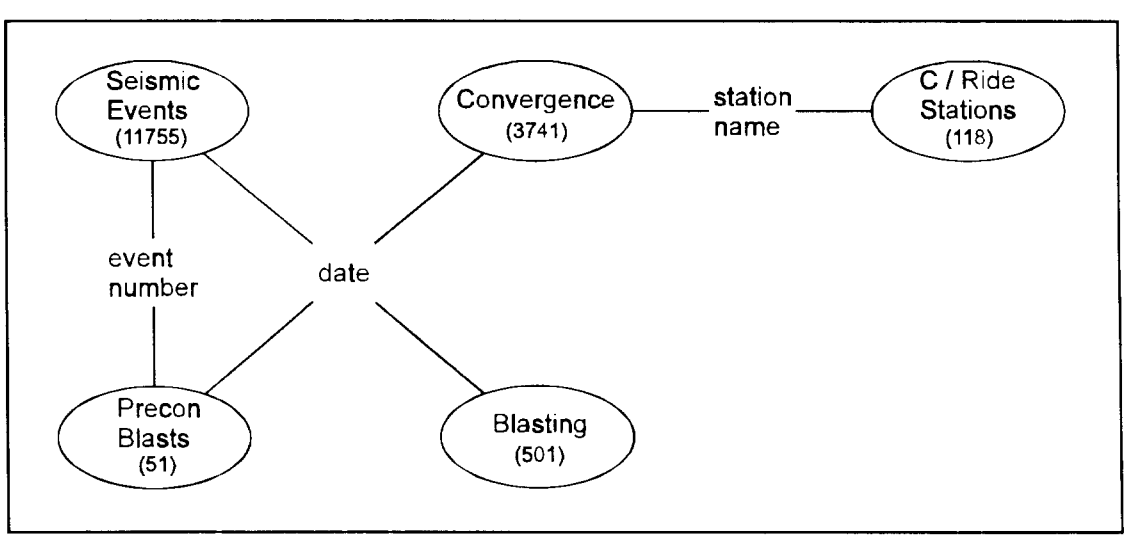

Figure: 3.7 Schematic of the relationships between tables within the database. Shown are the number of entries within each table as of mid December 1995.

Table 3.III: Data tables of relevant information from the 17-24W preconditioning site.

Seismic Events	Convergence Data	Convergence - Ride Stations	Preconditioning Blasts	Blasting (all)
Event number	Station name	Station name	Date	Date
Date	Date	Installation date	Panel	Panel
Time	Dip ride	Termination date	Blast rating	Face length blasted
X co-ordinate	Strike ride	Install dist to face	Mass of explosive	Area blasted
Y co-ordinate	Convergence	Term dist to face	Explosive type	
Z co-ordinate	Distance to face	X co-ordinate	Length of hole	
Location error	Comments	Y co-ordinate	Stemming length	
Magnitude		Comments	Hole diameter	
Location method			Event number	
			Magnitude of blast	
			Subsequent events (yes/no)	
			Largest subsequent event	
			Seismic migration (yes/no)	
			Comments	

At this stage in the analysis, this is the only data that warrants inclusion in the database. Many of the other evaluation techniques have been 'one-off' investigations which may or may not be followed-up at this site (for example: seismic tomography, ground penetrating radar and digital photogrammetry). Fracture mapping has been used to identify fracture sets that influence the behaviour of the pillar and ground motions within the stope. It will also be used to investigate variations in fracture development ahead of the panel faces due to variations in the size and positioning of preconditioning holes and the use of various explosives. Such information can be included with the preconditioning blasts if sufficient information is available.

3.4.2 Seismic activity associated with preconditioning

Since the change to breast mining in September 1992, 51 face-parallel preconditioning blasts have been set off at the 17-24W site. The full seismic history of all but three of these blasts was recorded by the monitoring PSS. This history includes the blasts themselves as well as the seismicity occurring at the site in at least the 24 hours following each blast and has allowed the development of a considerable understanding of the processes occurring in the rock mass in response to precondition blasting.

Some 80 per cent of the recorded preconditioning blasts were detected as seismic events with magnitudes in the range

$$(\textit{mass of explosive} / 100) \pm 0.5.$$

where *mass of explosive* used for the blast is given in kilograms (Appendix C). This would be expected for a seismic efficiency of about one per cent. Two of the recorded preconditioning blasts had magnitudes above this range, indicating an additional release of stored strain energy from the rock mass above that which would arise from the normal interaction of the explosive with the rock. The rock mass in the vicinity of these two blasts (one in panel 2 and one in the stub) had clearly been carrying excess load which was relieved by the preconditioning. Eight of the recorded preconditioning blasts had magnitudes below the range given above. These were mostly blasts from short holes with small quantities of explosive or blasts from incorrectly laid out holes or holes which had proved difficult to drill and which had not been drilled to the planned length.

The seismic data has shown that effective preconditioning blasts induce stress transfer away from the preconditioned area, release stored strain energy from the rock mass and can beneficially affect the stress concentrations in areas of the rock mass adjacent to the preconditioned area. The seismic expression of preconditioning in a rock mass includes the blast event itself, an increase in the rate of induced microseismicity following the blast, and the triggering of any separate larger seismic events by the blast.

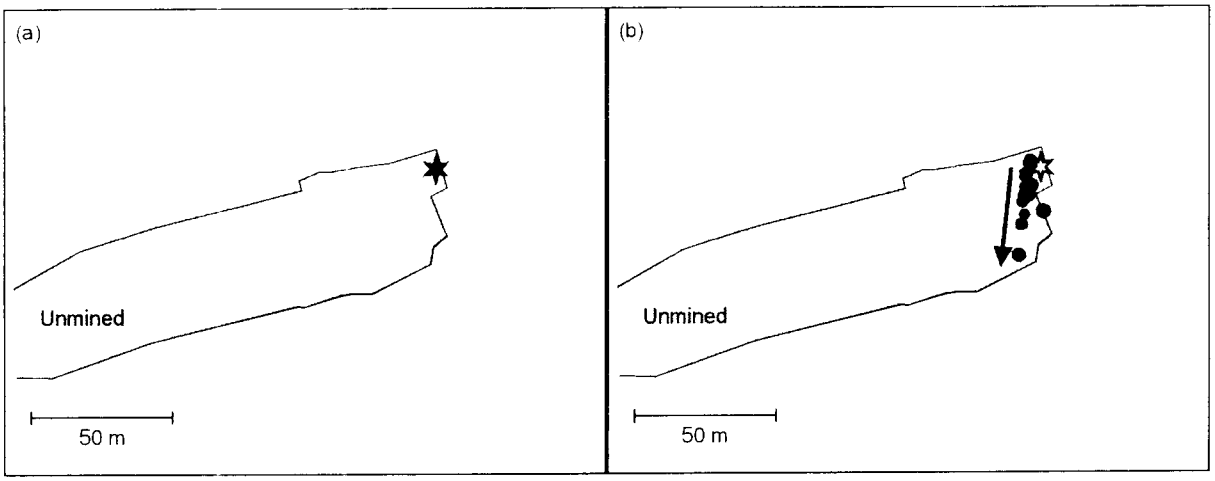

Figure 3.8: Panel 1 preconditioning blast of 26 November 1992. (a) Location of recorded M = 0.7 blast event (star). (b) The trend of the spatial migration of microseismicity (circles) recorded in the following 24 hours is indicated by the arrow.

The recorded microseismicity following effective preconditioning blasts exhibits spatial migration away from the vicinity of the preconditioning blasts, indicating the transfer of stress further ahead of the face of the preconditioned panel and towards unpreconditioned ground. Figure 3.8 shows an example of the effects of a preconditioning blast in panel 1 on 26 November 1992. Figure 3.8*a* shows the location of the blast event (M = 0.7) as recorded by the PSS. Figure 3.8*b* shows the spatial distribution of the microseismicity which was recorded by the PSS in the following 24 hours. This seismicity showed a clear migratory trend away from panel 1 towards panel 2 and the stub (advance heading), indicating the transfer of stress away from panel 1 after the preconditioning blast. Figure 3.9 shows an example of the similar effects of a preconditioning blast in panel 2 on 22 December 1993. Figure 3.9*a* shows the location of the blast event (M = 1.0) as recorded by the PSS. Figure 3.9*b* shows the spatial distribution of the microseismicity which was recorded by the PSS in the following 24 hours. This seismicity concentrated further ahead of the face of panel 2 (i.e. away from the working areas), as well as in the stub and panel 1, indicating the transfer of stress away from the vicinity of the preconditioning blast. This example illustrates the need for a correct sequencing of the preconditioning of adjacent panels. The preconditioning blast in panel 2 transferred some of the stress from panel 2 back onto panel 1. It was thus important that panel 1 had been destressed prior to the panel 2 blast, or the stress transfer might have loaded the rock mass ahead of panel 1 to failure.

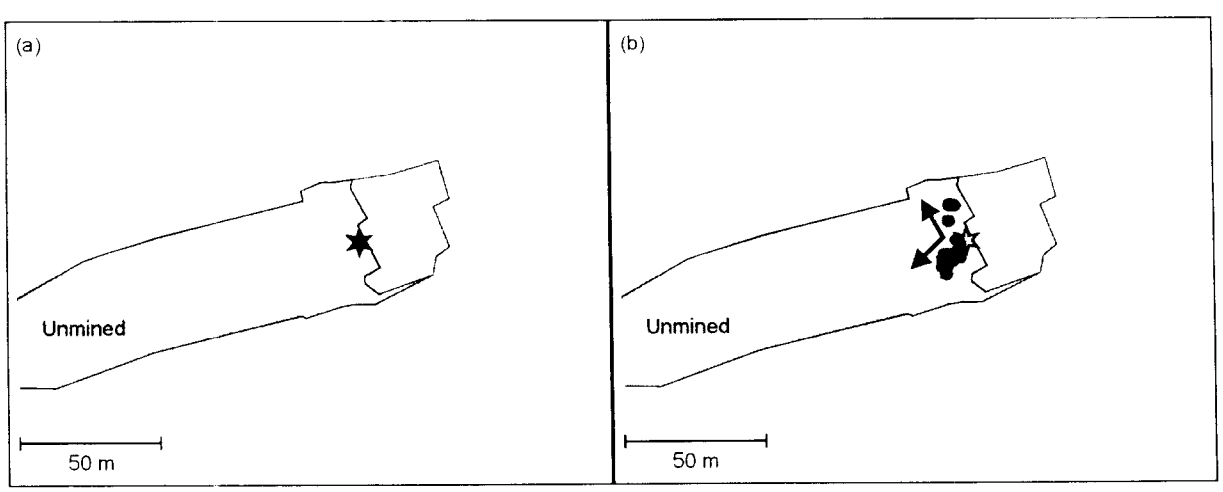

Figure 3.9: Panel 2 preconditioning blast of 22 December 1993. (a) Location of recorded M = 1.0 blast event (star). (b) The trends of the spatial migration of microseismicity (circles) recorded in the following 24 hours are indicated by the arrows.

Effective preconditioning blasts have been found to release stored strain energy from the rock mass through the triggering of separate larger seismic events. While these have resulted in some damage to the working areas on occasion, it is significant that the events were triggered at a time when there were no workers in the stope, so that the strain energy which had built up in the rock mass ahead of the stope faces in response to the mining activity was released without injury to workers. The PSS location of the panel 1 preconditioning blast event on 31 March 1993 (M = 0.8) is shown in Figure 3.10*a*. This preconditioning blast facilitated the release of stored strain energy by triggering an additional M = 0.4 event in panel 1 (Figure 3.10*b*). Note that the subsequent microseismicity migrated away from panel 1, indicating that the vicinity of the blast had been effectively destressed.

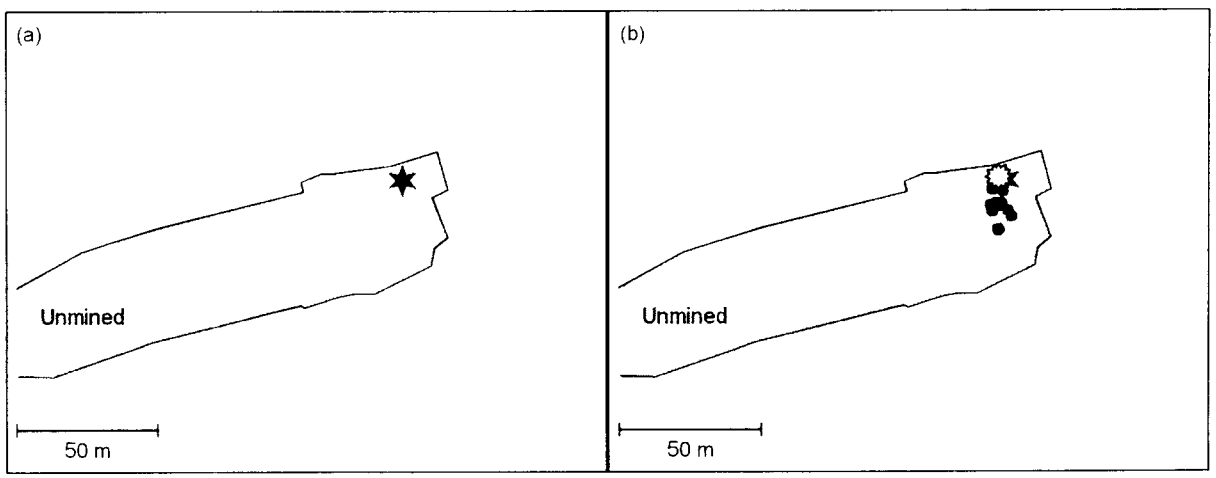

Figure 3.10. Panel 1 preconditioning blast of 31 March 1993. (a) Location of recorded M = 0.8 blast event (star). (b) Microseismicity (circles) induced in following 24 hours, including triggered M = 0.4 event (white star). The face positions shown are not current with the faces at the time but reflect the most recent 3 monthly survey update.

Through the mechanism of stress transfer in the rock mass, effective preconditioning blasts beneficially alter the stress concentrations in adjacent areas. The panel 1 preconditioning blast on 28 October 1994 was recorded as an M = 0.9 seismic event by the PSS (Figure 3.11*a*). The subsequent microseismicity migrated down-dip (Figure 3.11*b*), indicating the transfer of stress away from panel 1 into panel 2. The addition of load to the rock mass ahead of panel 2 then triggered a large (M = 2.1) seismic event in that area (Figure 3.11c), releasing the strain energy that had accumulated there. The destressing of both panel 1 and panel 2 in sequence suggests that additional load was then being carried by the rock mass ahead of the stub face, a supposition borne out by the subsequent triggering of a large (M = 1.5) seismic event in that area by the production blast in the stub face (Figure 3.11*d*). All of the mining faces were thus effectively destressed by the one preconditioning blast in panel 1, on that occasion.

It is interesting to note the circumstances that preceded the preconditioning blast described above. After the three-month production stoppage from July to September 1994, it was decided to precondition all three faces before restarting the production activity at the site. The first of those blasts, on 20 September in panel 1, went according to plan and was effective in preconditioning the rock mass ahead of the panel 1 face. The preparations of the following blasts, on 26 September in panel 2 and on 29 September in the stub, were marred by drilling difficulties, and neither of those blasts produced a discernible preconditioning effect. Thus, the panel 1 preconditioning blast on 28 October took place at a time when neither panel 2 nor the stub had been effectively destressed, which conditions undoubtedly contributed to the particularly impressive results of that blast.

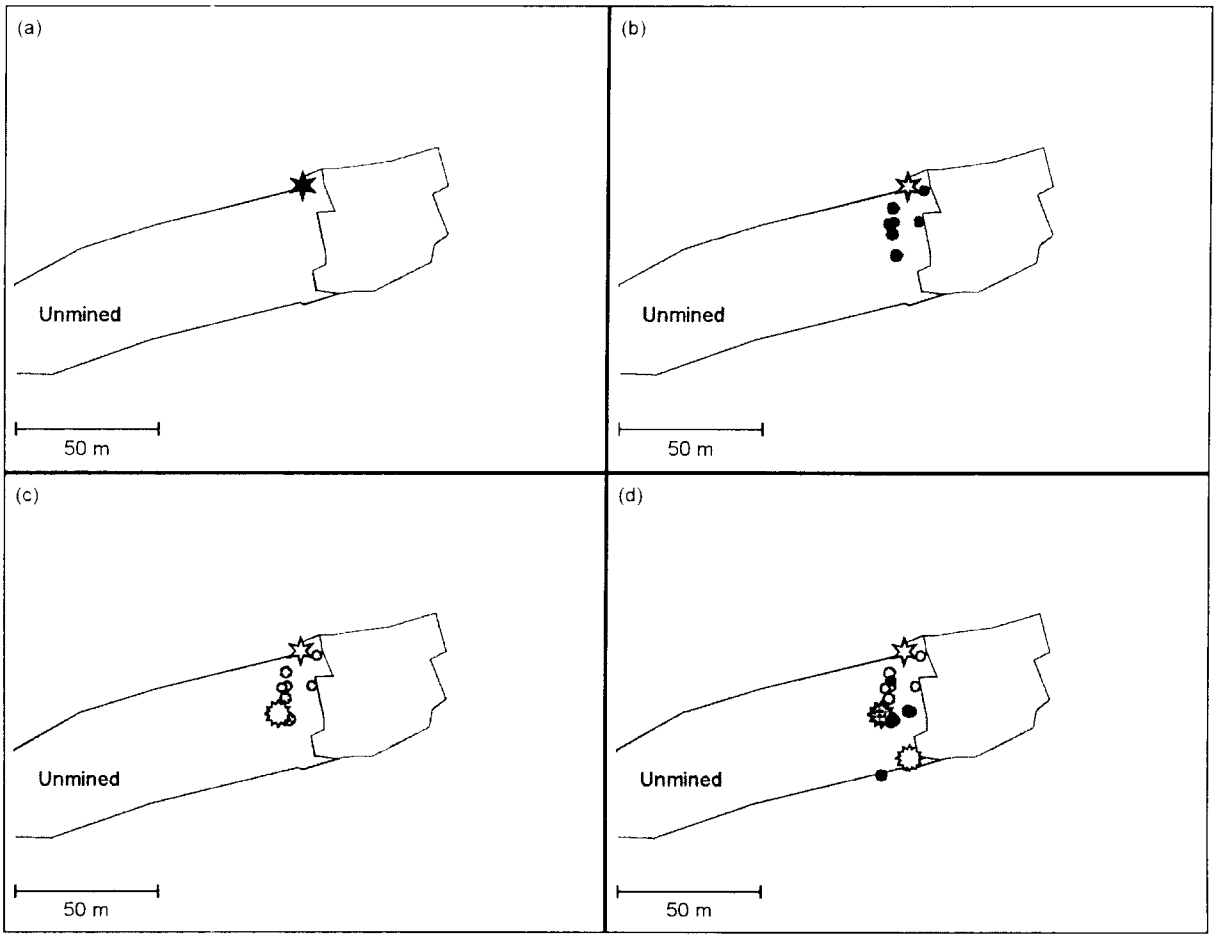

Figure 3.11. Panel 1 preconditioning blast of 28 October 1994. (a) Location of M = 0.9 blast event (star) recorded at 13:47. (b) Spatial migration of subsequent microseismicity (circles). (c) Location of M = 2.1 event (white star) triggered at 16:21. (d) Location of recorded face blast events (darker circles) and M = 1.5 event (white star) triggered at 18:36.

A similar example of the effects of preconditioning is shown in Figure 3.12. A panel 1 preconditioning blast on 10 January 1995 (Figure 3.12*a*) caused stress transfer away from panel 1 towards panel 2 (Figure 3.12*b*). A production blast in the panel 2 face on the following day then triggered the instability which had developed in the rockmass ahead of panel 2, releasing the stored strain energy by way of two large (M = 1.7) seismic events (Figure 3.12*c*).

While well executed preconditioning blasts have been proved to have very beneficial effects on the stress state and condition of the rock mass ahead of a stope face, it is important to note that poorly executed preconditioning blasts are either ineffective or can, in fact, negatively affect the stress state of a rock mass. Defective preconditioning blasts caused by the drilling of the face-parallel preconditioning holes too far ahead of the face either have no effect on the stress condition at the face or, in the worst case, can actively add to the load carried by the face. Seismically, the results of a preconditioning blast set off too far ahead of the face are a small blast event (assessed with respect to the amount of explosive used), little induced microseismicity, and no triggering of larger seismic events by the blast. Examples of such defective preconditioning blasts are the panel 1 blast of 2 January 1993 and the panel 2 blast of 10 February 1994. In the latter case, the same hole was charged and blasted again on 28 February 1994, after the face had been advanced by production blasting, to much better effect.

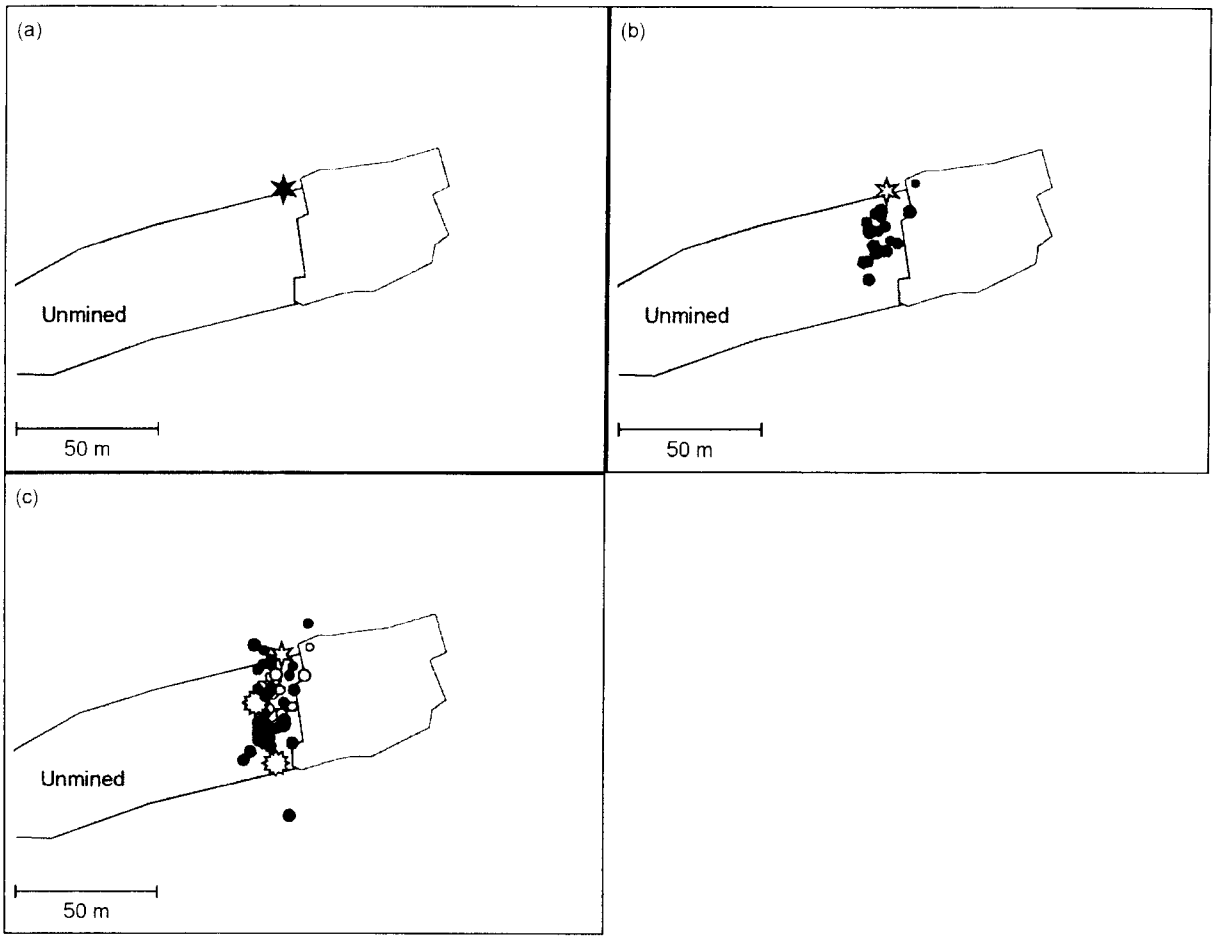

Figure 3.12. Panel 1 preconditioning blast of 10 January 1995. (a) Location of recorded M = 0.7 blast event (star). (b) Spatial migration of microseismicity (circles) recorded in following 24 hours. (c) Location of recorded face blast events (darker circles) and triggered M = 1.7 events (white stars) of 11 January 1995.

On occasion, drilling difficulties have necessitated the abandonment of a preconditioning hole before it was completed requiring the drilling of a second hole in close proximity to the first. In a number of such cases, even though the first hole was grouted closed, the results of the preconditioning blast have been unsatisfactory. There has been clear physical interaction between the holes during the blast, often with a significant amount of blow-out damage between the collars of the holes. While the blasts themselves have generally been adequate as shown by the magnitude of the recorded blast event, there has been little induced microseismicity and no triggering of larger seismic events by the blast, indicating a lack of interaction of the blast with the stress field in the rock mass ahead of the stope face. Such defective preconditioning blasts have occurred once in the stub (on 22 January 1993) and four times in panel 2 (on 16 April 1993, 26 September 1994, 29 March 1995 and 4 October 1995), but not in panel 1. This history is a clear reflection of the greater degree of difficulty which has been experienced with the drilling of preconditioning holes in panel 2 than in the stub or in panel 1. The average length of preconditioning hole for panel 2 has been 17.9 metres, compared with 12.8 metres for panel 1 and 8.4 metres for the stub. The drilling has typically been easier for panel 1 as well, because it is the portion of the stope face which carries the least amount of stress.

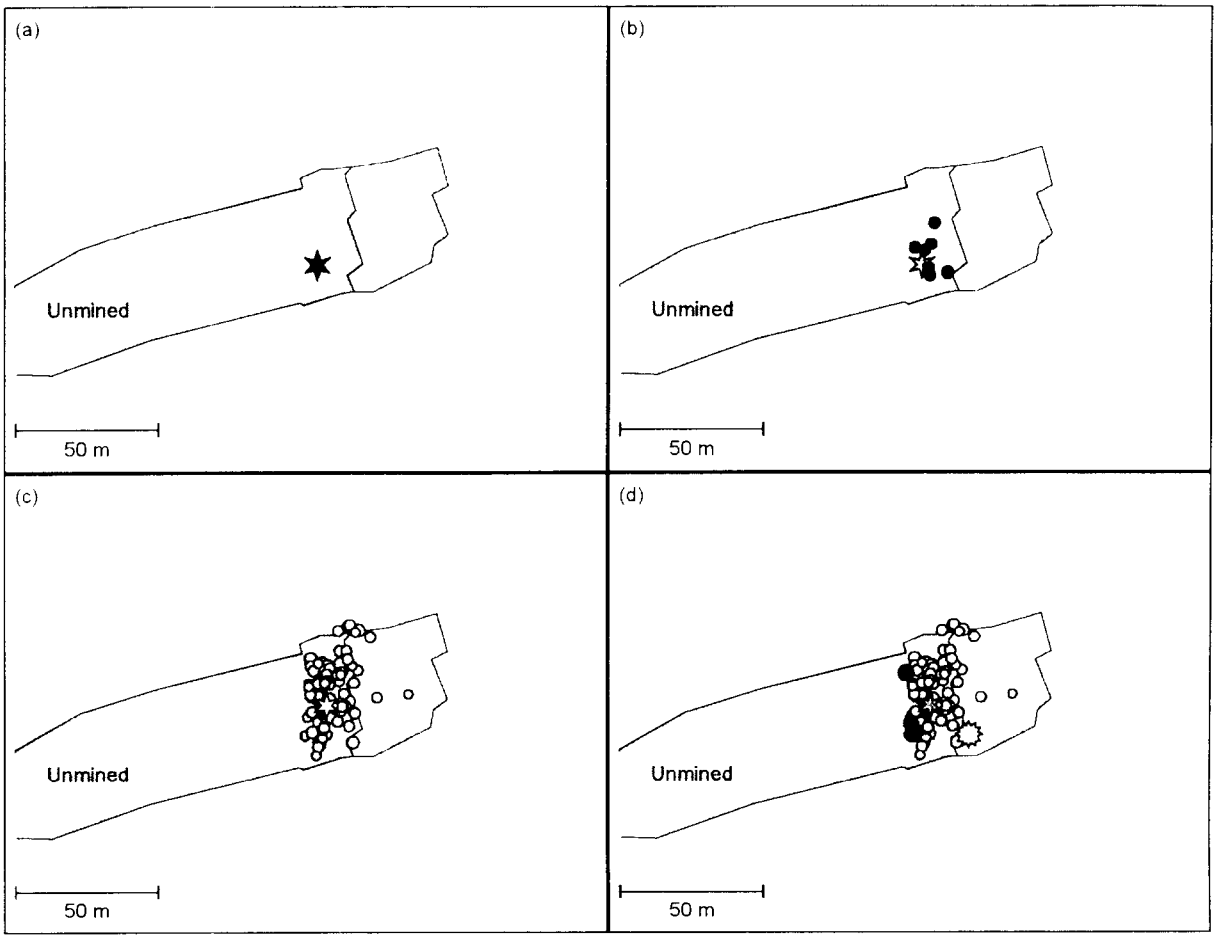

Figure 3.13. Preconditioning blasts of 11 April and 15 April 1994. (a) Location of recorded M = 0.4 stub preconditioning blast event (star), of 11 April. (b) Locations of microseismic events recorded soon after the preconditioning blast. (c) Location of recorded M = 1.4 panel 2 preconditioning blast event (white star), of 15 April. The microseismic events associated with three face blasts which preceded the preconditioning blast are shown as circles. (d) Location of damaging M = 2.3 event (white star) triggered by preconditioning blast. The microseismic events associated with the preconditioning blast are shown as darker circles.

The importance of the correct sequencing of the preconditioning of adjacent panels was mentioned earlier. An example that serves to illustrate the importance of correct sequencing is the pair of preconditioning blasts that were set off in April 1994. This was the only occasion to date on which the stub was preconditioned immediately before the preconditioning of panel 2. The preconditioning blast of 11 April 1994 was set off in the stub (Figure 3.13*a*) without panel 2 having been preconditioned beforehand. The stub preconditioning hole was oriented effectively perpendicular to the stope face, with the intention of remobilising the pillar-edge parallel fractures that are prominent ahead of the stub face. The result was that the preconditioning blast was effective further ahead of the face than it would have been had the hole been oriented parallel to the face. The net effect was to drive the stresses back towards the face, mostly in the area between the stub and panel 2 (Figure 3.13*b*). This area is generally not effectively preconditioned, due to the neutralising effect of the stemming near the collars of the stub and panel 2 preconditioning holes. The three production blasts which took place over the following days do not appear to have altered the stress state between panel 2 and the stub significantly. On 15 April 1994, a preconditioning blast was set off in panel 2 (Figure 3.13*c*). This seems to have had the effect of adding further to the stress which had concentrated in the area between panel 2 and the stub, and a large (M = 2.3), damaging, seismic event resulted, locating on the face between panel 2 and the stub (Figure 3.13*d*).

3.4.3 Convergence Data

Table 3.IV compares the daily convergence rates for production and preconditioning blasts. All measurements were made within less than 10 metres of the advancing face. For production blasts, only a full face length blast in the one panel was considered. Similarly, only preconditioning blasts with a rating of at least 30% and not accompanied by a production blast were considered. The average convergence for the production blasts is based on nearly 100 data entries, but the preconditioning database is more limited with less than 10 entries for each result quoted.

As the stub is only an advance heading, there is usually no room to accommodate a monitoring station, hence there exists little data for this region. Nevertheless, the main trends are apparent.

A production blast in panel 1 has a reasonably limited effect on the other panels; similarly, blasting in the adjacent panel has relatively little effect on panel 1. The strong influence of a panel 2 blast on the stub is probably the result of the limited face length of the stub and the fact that most of the stub is situated in the extensive fracture zone along the bottom edge of the pillar.

Table 3.IVa: Average induced daily convergence as a result of production blasting. This is shown graphically in Appendix C.

		Production Blasting in			No Blast
		Panel 1	Panel 2	Stub	
Convergence* (mm/d) Measured in	Panel 1	9.6 ± 4.2	5.3 ± 7.1	4.2 ± 6.1	2.4 ± 1.3
	Panel 2	6.0 ± 3.6	23.1 ± 19.5	8.8 ± 9.0	3.8 ± 2.4
	Stub	3.0 ± 2.3 [1]	14.4 ± 9.6 [1]	8.3 ± 3.8 [1]	2.8 ± 1.6

Table 3.IVb: Average induced daily convergence as a result of precondition blasting

		Precondition Blasting in		
		Panel 1	Panel 2	Stub
Convergence* (mm/d) Measured in	Panel 1	18.3 ± 13.7	12.1 ± 11.2	14.2 ± 13.8
	Panel 2	5.0 ± 3.9 [1]	28.0 ± 19.1	
	Stub	*Insufficient Data*		

* Reported as mean ± standard deviation

[1] Limited data set

Preconditioning blasts from holes positioned 5m ahead of the face have a greater effect on the convergence than do the production blasts. This is especially evident from the convergence recorded after the a preconditioning blast in the panels other than the one actually being preconditioned. This is due to the more global effect of the preconditioning blast which is indirectly achieved as a result of stress transfer into unpreconditioned ground. The high standard deviations reported for the preconditioning blasts is largely due to the variability in the conditions in which the blasts are carried out. Several blasts have been less successful than expected, resulting in a lower convergence and others have triggered large events resulting in a very large convergence in all panels.

3.4.4 Ground Motion

To date, six preconditioning blasts have been monitored with black boxes installed at the face of the panel being preconditioned (Table V). The first two were with the original unit with the sensors inside the box and the entire box had to be bolted onto the face; only one box was installed for each of the two blasts. The other four blasts were monitored with externally mounted sensors. The configuration of these boxes was either one triaxial cell or three uniaxial cells per box (Figure 3.14). As many as 9 sensors (all uniaxial) have been installed for the recent preconditioning blasts.

Table 3.V: Ground motions recorded from black box monitoring of preconditioning blasts. Results are given only for those sensors placed on the face. Accelerations are quoted in the direction perpendicular to the face.

Date	Panel	Magnitude of Blast	Ground Acceleration at Face (m/s²)		
			within charge length of hole	at top end of charge length	beyond end of charge length
10/01/95	P1	0.8	> 980*		
29/03/95	P2	0.3			4
23/09/95	P1	0.4	>1082*		
04/10/95	P2	1.0	>1049*	253	
16/11/95	P1	0.5	> 992*	418	205
05/12/95	P2	0.8	> 1073*		505

* saturated waveforms

Figure: 3.14: Instrumentation of a preconditioning blast with Ground Motion Monitors. Note the sensors on the face, hangingwall and footwall (shown by the arrows).

Although only a few preconditioning blasts have been monitored to date, specific responses are becoming apparent. The effects of the blast appear to diminish quite dramatically beyond the charge in the hole. Even at the end of the hole, the ground accelerations are considerably less than towards the centre of the charge. However, in two instances, sensors were placed at the bottom end of the charge length, and accelerations in excess of 1000m/s² were recorded with the waveforms being saturated. The difference in ground response between the area near the collar of the hole and at the top of the hole may be due to the geometry of the panel. Further investigations are required.

High vertical motions in the footwall are probably due to the positioning of the preconditioning hole in the footwall of the reef plane and can be overcome by repositioning the hole close to the reef plane. High horizontal motions in the hangingwall are not well understood at this stage.

The development of the black box itself is not yet complete and some problems still exist in the data acquisition. Full waveform analysis is currently not possible due to response

problems with large events (including saturation of the recorded signal), and hence, only peak accelerations are being reported.

3.4.5 Dilation of the Stope Face

A good preconditioning blast will result in a varying degree of scaling of rock off the face and shake-out of loose rock from the hangingwall. The extent of this will depend largely on the fractured nature of the rock and the extent of barring undertaken by the stope crew. On several occasions, however, a considerable amount of dilation has been noted on the face (Figure 3.15), providing more evidence to support the model of preconditioning (Lightfoot, 1993, Lightfoot, et al, 1994 and Kullmann, et al, 1994) and its interaction with the rock mass. The amount of dilation, however, is extremely difficult to quantify to any degree of accuracy with conventional measuring techniques.

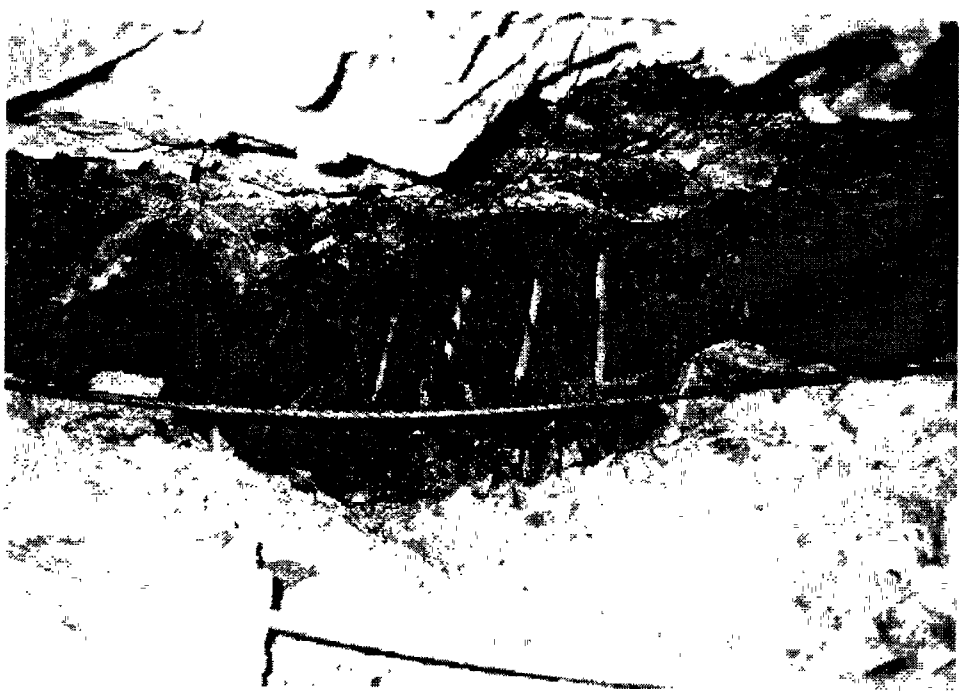

Figure 3.15: View of the stope face after a preconditioning blast. Dilation of the face is clearly indicated by the open fractures enhanced by paint lines initially put on for a ground penetrating radar scan before the blast. Scaling of rock from the face has resulted in the removal of paint lines on both sides of this area.

During 1995, Miningtek has collaborated with University of Cape Town, to develop a photographic technique to evaluate changing conditions underground. This technique, called digital photogrammetry, is intended for use in the investigation of the effects of preconditioning on the stope face, namely, to measuredilation of the face into the open stope and the opening up of pre-existing fractures. Images of the face are captured with the use of a high resolution digital camera. The exact position (with an accuracy of less than 1mm) of the face and features on the face are obtained before and after the preconditioning blast. Image processing can then provide information in the format of contour maps, 3D surface plots (Figure 3.16) and cross-sections. The volumetric change resulting from the dilation of the face can be easily determined (Smit and Rüther, 1995).

At this stage, the image processing is not entirely automated with the amount of user interaction varying depending on the program's ability to detect and match points of interest in adjacent images. The biggest constraint with the use of this technique for underground analysis is in providing a fixed control point to establish a co-ordinate reference system. This point needs to be reasonably close to the face to minimise the number of images needed to tie in the control point to the face. The problem that arises is that no point near the face

remains fixed relative to any other point, especially after a blast. Certain assumptions have to be made with regard to a reference point and these can only be evaluated with respect to their validity once the comparison of before and after blast images is made.

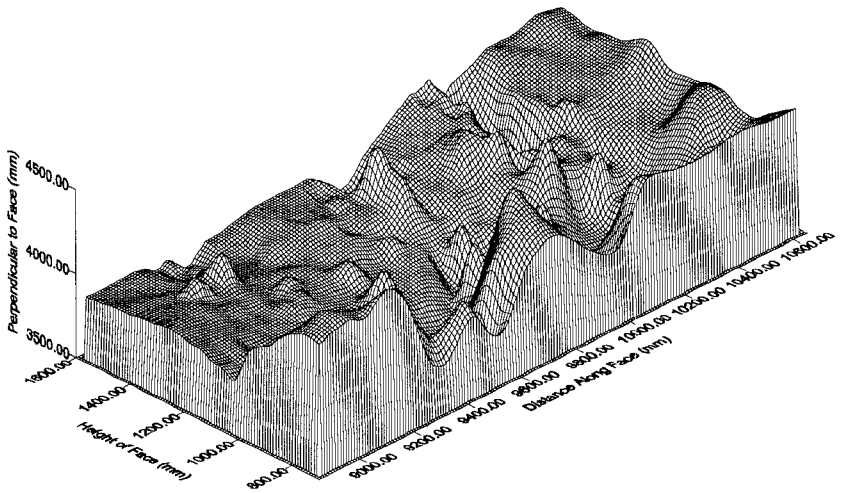

a) Before the preconditioning blast

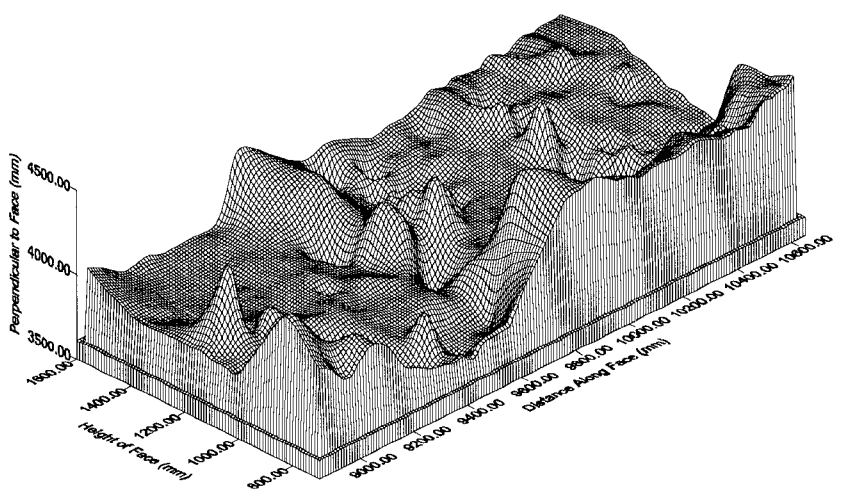

b) After the preconditioning blast

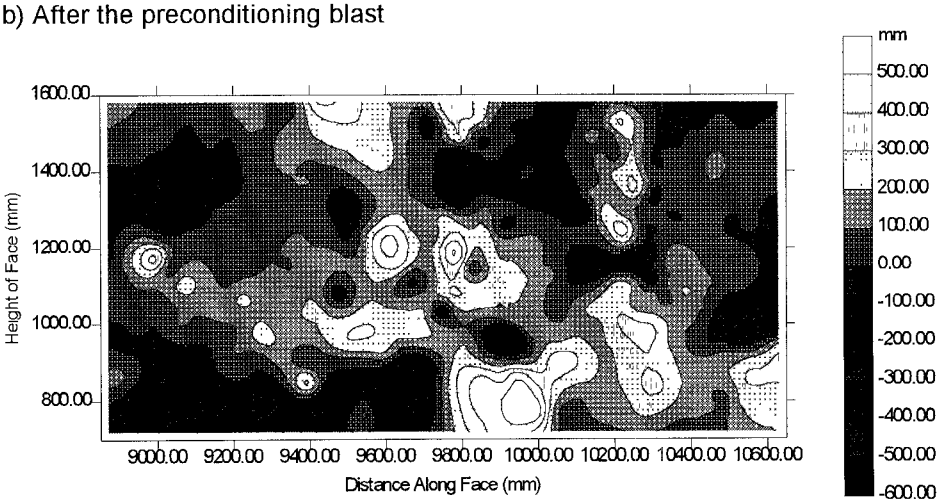

c) The difference between before and after the preconditioning blast

Figure 3.16: Three dimensional surface plots of the stope face for before (a) and after (b) a preconditioning blast and c) a contoured plat of the difference between the two. With this information, an estimate of the volumetric dilation can be made. It is claimed that the accuracy of the survey is possible to less than 1mm error in any direction.

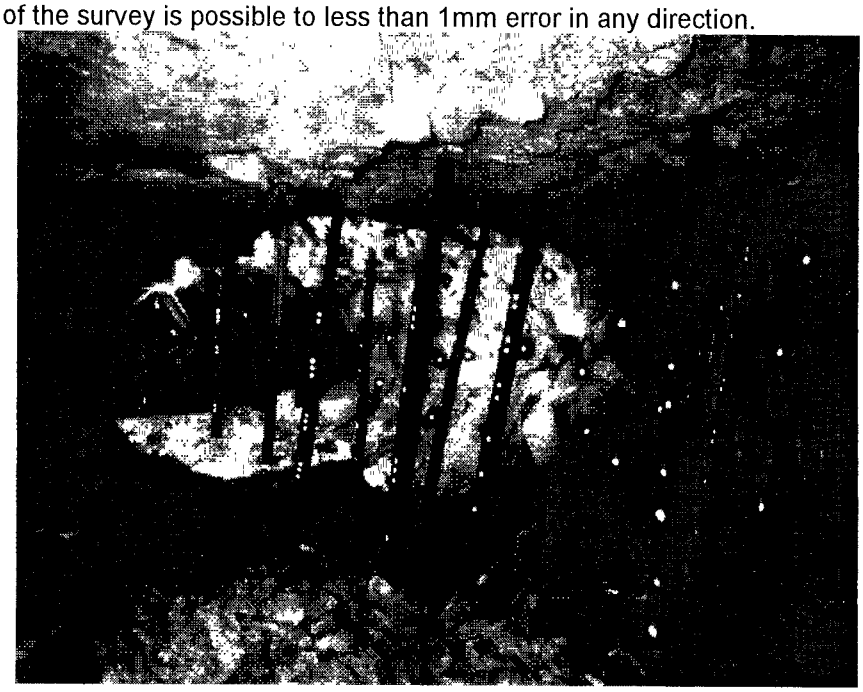

Figure 3.17: Target poles with control points placed along the face to match successive images. A Ground Motion Monitor (orange) installed on the face can be seen between the poles on the right.

Image capture is not a time consuming matter but the image processing can take some time depending on the amount of user interaction that is required. Problems could arise from poor image quality, insufficient overlap of successive images, insufficient control point locations, or difficulties in matching control points in successive images. Control points are placed on target poles down the face to enable matching of successive images (Figure 3.17). At this stage, digital photogrammetrey is seen only as a research tool.

3.4.6 Fracturing

Drummond and Grodner carried out detailed mapping of the preconditioning site and although their methods were slightly different, the high quality of the data collected allowed the two sets of data to be analysed together. Both workers collected data on the strike, dip, frequency and type of fracture. Descriptions and notes made by Drummond were used to determine details of persistence and movement of the fractures. Positions of major fractures were also mapped and later plotted on a 1:200 scale plan of the area.

The data was entered into worksheets shortly after being mapped underground. Graphs developed from these worksheets were then used to analyse the data for trends in orientation (both dip and strike) as well as factors such as type and rating. Fracture rating combines persistence and frequency of the various fractures in an attempt to determine the dominant fractures. It should be noted that this is not an absolute value, but rather is relative to the other fractures at the specific site.

The majority of fractures fall into one of four strike directions (see Figure 3.18). The most abundant set has a wide range from 10° to 40° to the face (in a clockwise direction) and make up about 26% of the total. The most prominent single group (approximately 25%), are those orientated at 90° to the face (the orientation of the various fractures was in all cases recorded relative to the panel face). Face parallel fractures (those with a strike of less than 10° or greater than 170° to the face) account for approximately 6% of all fractures. There is a

further clustering (±20%) of fractures at an angle of between 110 and 140° to the face, whilst the remaining 25% of fractures appear to be evenly spread and as such are not significant in analysis.

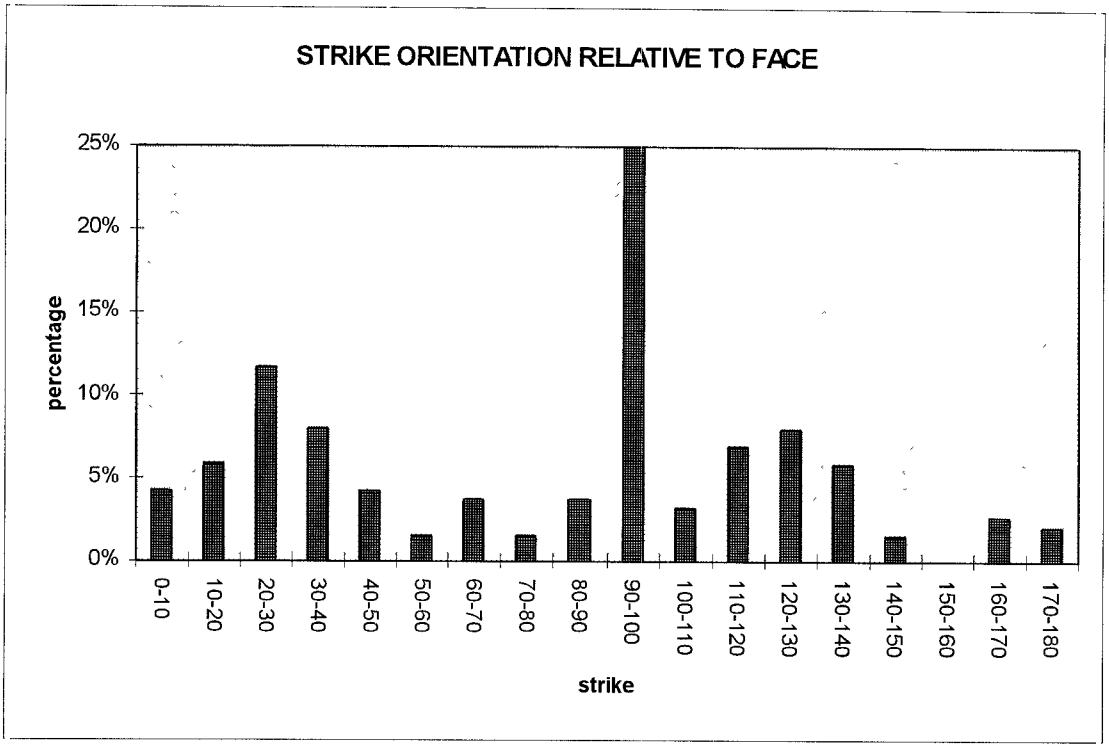

Figure 3.18 : Orientation of fractures relative to face. Strike is measured in a clockwise direction facing towards panel face.

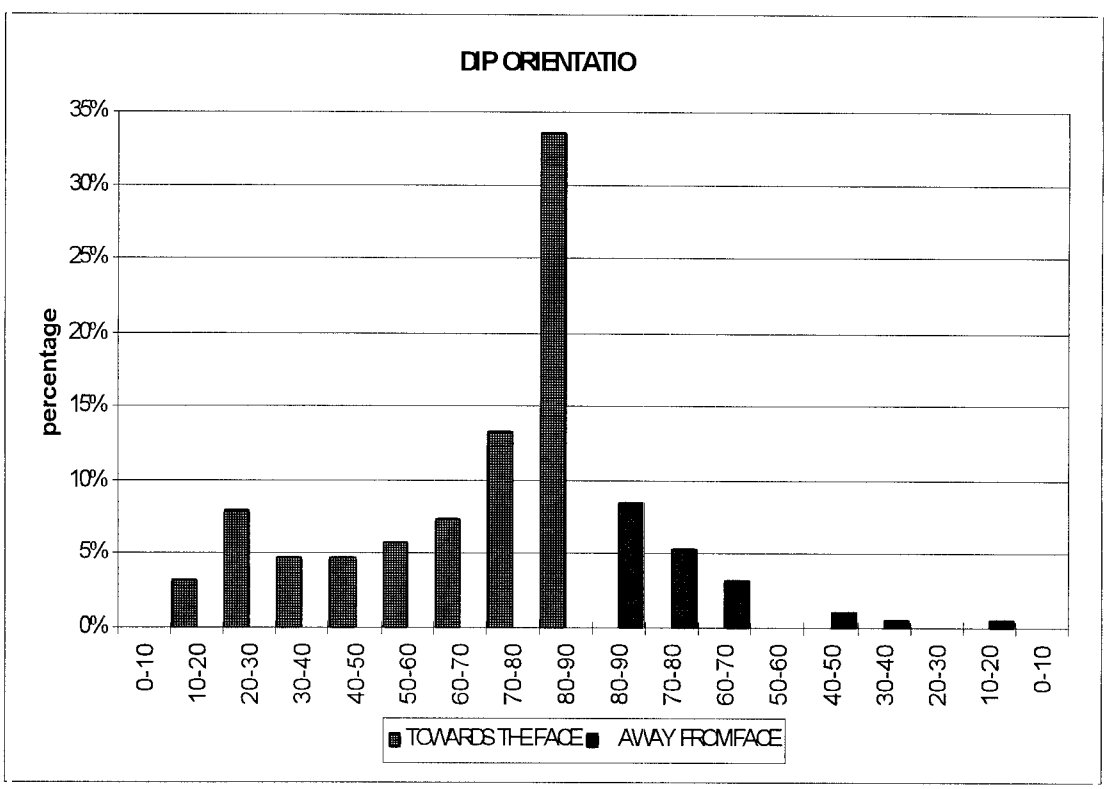

Figure 3.19 : Dip direction of all fractures relative to face.

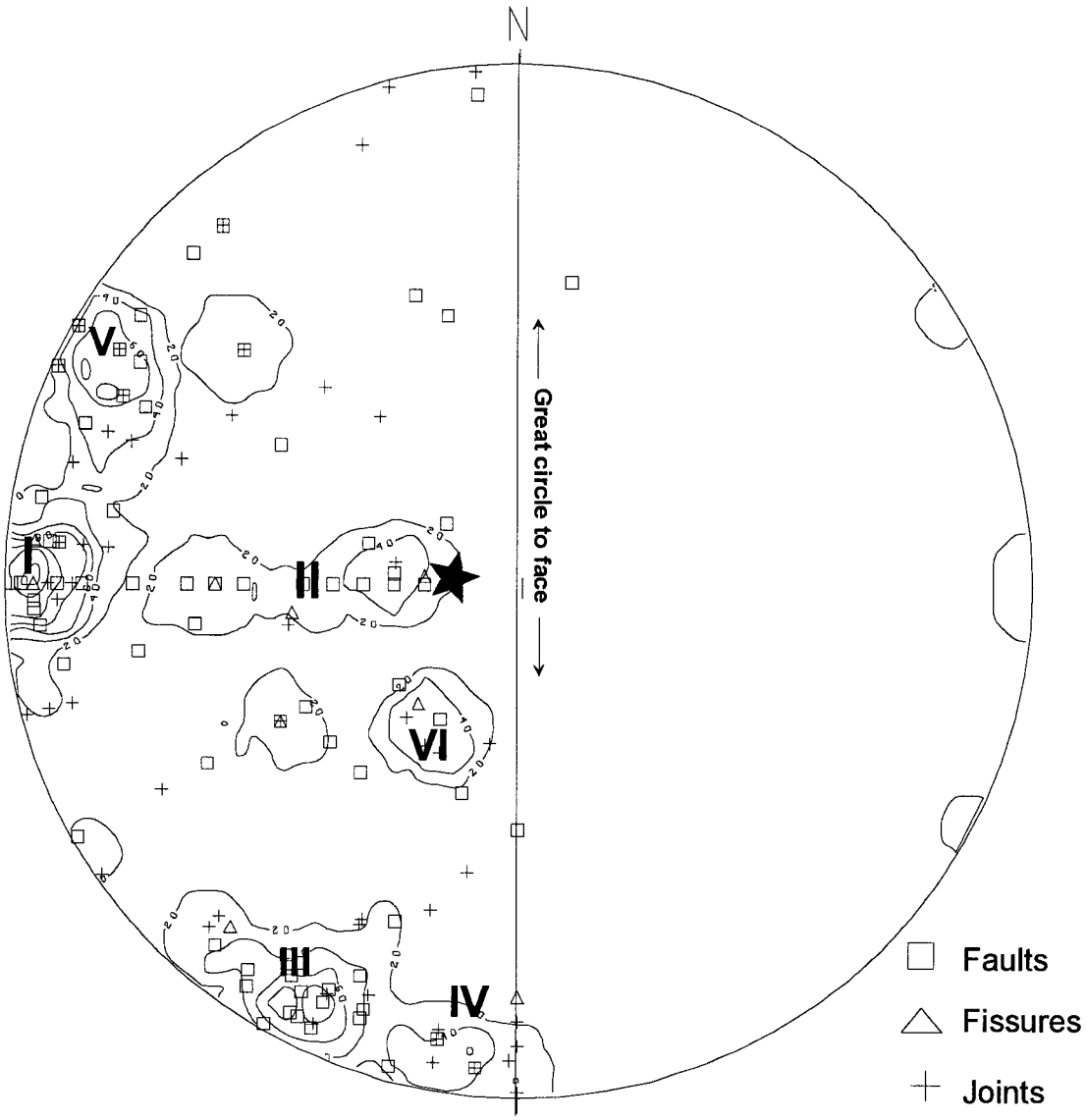

BLYVOORUITZICHT PRECONDITIONING SITE

Figure 3.20 : Schmidt-Equal Area Net, lower hemisphere projection of poles to all fractures. Fractures are classified into 6 major groupings based on dip and strike orientation (see text for details).The star indicates the position of the pole to the reef plane, values on contours are in percentage

The bulk of fractures (some 33%) are almost vertical in dip (see Figure 3.19) and in fact 60% of all fractures are steeply dipping, being orientated between +70° and -70°. A positive dip indicates a dip towards the face and a negative a dip away from the face. Almost 30% of the fractures have an intermediate dip of between 50 and 60° toward the face. The remaining 10% may be termed low inclination fractures as their dip lies between 10 and 30°.

By combining the dip and dip direction of the various fracture types, the different sets may be identified. Figure 3.20 is a stereo-net (lower hemisphere projection) of poles to all the fractures mapped and shows the six sets of fractures identified for this particular site.

Group I: Group I consists of steeply dipping face perpendicular fractures - their dip varies between -80° and +80° at a strike angle of between 85° and 95° to the face. Underground

these are observed as low persistence joints occasionally with calcite infill of up to 2 mm thickness.

Group II: The second major cluster, Group II also lie more or less perpendicular to the face, but have a shallower dip of between 50° and 60° towards the face. These are sinuous (often vein quartz filled) joints and faults that appear to interconnect the fractures of Group III. It was initially thought that they had been displaced by faulting within the plane of the reef. However subsequent investigation showed that the fractures actually curve slightly as they pass through the reef horizon. As the joints traverse the reef plane, their dip decreases, and then increases as the joints penetrate the footwall.

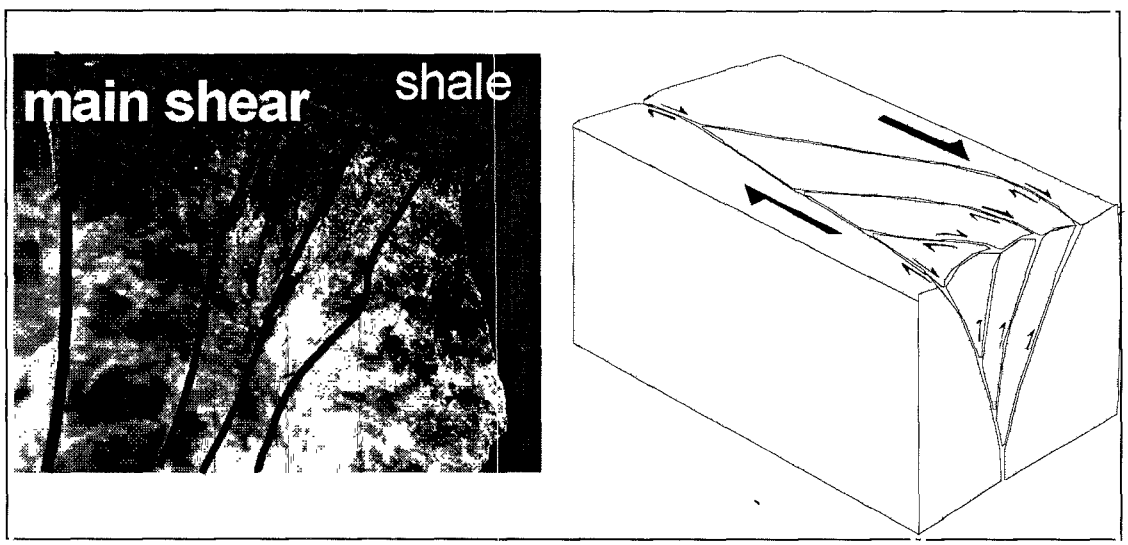

Figure 3.21 :Photograph of flower structures developed underground below the shale horizon, and block diagram explaining origin of these features. Note that shearing is perpendicular to the plane of the photograph.

Group III: This group of fractures which contains all fracture sets with a high rating, lie at an angle of 35° to 45° to the panel face (in a clockwise direction). The fractures in this group are clustered into distinctive steep dipping highly sheared zones containing both calcite and vein quartz (with occasional oblique slickensides). These sinistral shear zones are between 50 cm and 80 cm wide and occur at intervals of about 3m. White crushed quartzitic gouge is also common in these fractures which show several phases of movement. Fractures of this group have an orientation that is consistent with the regional trend of the dykes and faults across the mine. This suggests that the initial alignment of these fractures was strongly influenced by regional scale tectonics. Vein quartz filled faults represent the earliest fractures formed in this orientation. Calcite precipitated along these quartz filled fractures in the void spaces created by sinistral shearing. At a very late stage (probably due to current stoping and preconditioning), these fractures were abraded to form a fine white quartzitic gouge. Above the shale horizon in the hangingwall the fractures do not contain this white gouge. In addition to this, where the Group III shears intersect the shale horizon, flower structures (as described by Wilcox, et al, 1973) are developed (Figure 3.21). This indicates strike-slip shear has occurred along these fractures.

Associated with these shear-zones are the lower angle Group VI fractures.

Group IV: The fractures of Group IV are steeply dipping and are orientated approximately parallel to the panel face. These joints have a fairly low persistence and usually don't contain any secondary minerals. Some of the Group IV contain a whitish gouge similar to that of the Group III fractures.

Group V: This group lies at roughly 130° to the strike of the face at a steep angle of dip. These fractures interconnect with Group VI to form a distinctive hackly hangingwall.

Group VI: Fractures in this group are relatively uncommon and are generally associated with the more prominent Group III shear zones. Underground they occur as short (often gouge-filled) faults which terminate against Group III and sometimes Group I fractures.

Table VI contains a summary of all the fracture groups that were identified.

Table VI : Summary of the various fracture groups.

Fracture Group	Description
I	steeply dipping face perpendicular joints
II	intermediate dipping face perpendicular faults and joints
III	steeply dipping shear-zones lying at 40° to panel face
IV	steeply dipping face parallel joints
V	steeply dipping joints lying at 130° to panel face
VI	shallow dipping faults lying at 40° to panel face

3.4.6.1 Origins of the fracture groups.

As mentioned previously, the rock mass in this pillar has undergone a complex stress history. The fracture patterns developed in the pillar can be explained in terms of this history, indicating that none of them are the products of preconditioning alone.

Group I: These joints lie parallel to the long axis of the remnant pillar and were probably the first mining induced fractures formed. At both the top and bottom edge of the pillar these form the dominant fracture set, and the additional jointing further weakens the rockmass, causing large falls of ground to occur in these areas. The joints are thought to have formed early in the history of the pillar prior to closure of the stopes around it. This is most likely due to compressive forces induced on the pillar by mining out of the surrounding ground.

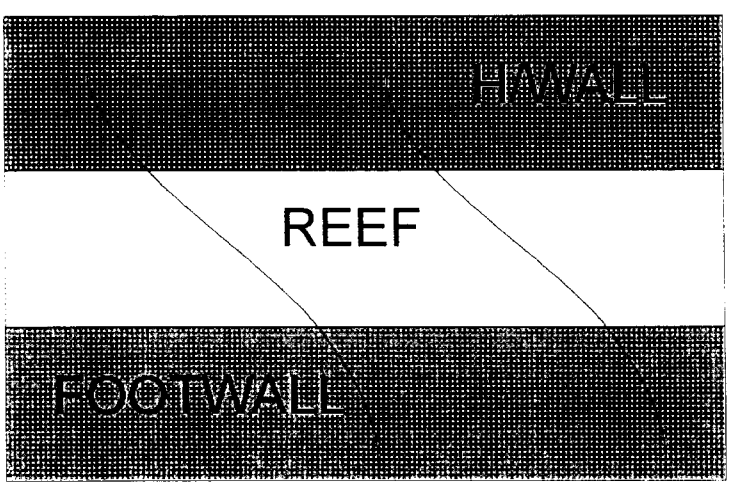

Figure 3.22: Sketch diagram showing how Group II fractures change in dip as they pass through the reef plane.

Group II: Although these fractures have a similar strike to Group I fractures (i.e. parallel to pillar axis), they lie at a much shallower dip. It is proposed that these fractures also formed due to the compressive forces applied on the pillar by the mining out of the ground around it. Time dependent dilation, particularly along the edge of the pillar would allow these fractures to widen forming water bearing fissures at the northern edge of the pillar. The water in these fissures appears to have originated from the mine stopes, as they contain large amounts of iron oxides, from rusted materials. Water from longer fissures generally contains more calcium rich minerals that have been dissolved from the overlying dolomites. Thus these dilational features are of limited length.

Of interest is the different response of the various materials to the pillar loading as evidenced by the orientation of the fractures. In both the hangingwall and footwall quartzite the fractures have a dip of about 65°, while within the narrow reef zone of grits and small pebble conglomerates the fractures may flatten out to as shallow as 40° (Figure 3.22).

Group III: The most prominent fractures observed in the preconditioning stope are the shear-zones of Group III (Figure 3.23). It is possible that these fractures originally formed during large-scale tectonic activity which affected the entire region, as Group III fractures have a similar azimuth to the major dykes and faults on Blyvooruitzicht Gold Mine. These slightly sinuous shears also lie more or less parallel to the overall face-shape of the pillar and are likely to be reactivated by mining activity and could result in the reactivation of these shears. An important observation is the regular periodicity of both their spacing and width, with zones of relatively unfractured rock in between. These zones are similar to the zones of fracturing described by Adams and Jager (1980), who identified them as zones of extensional fractures. Group III fractures are however observed as sinistral shear zones underground, often with an oblique movement component indicated by vein quartz slickensides.

Although Group III fractures initially appear to be shear zones, it becomes clear with more detailed examination that they initially formed in an extensional environment (indicated by the presence of void filling minerals such as vein quartz and calcite as well as small dilational features). The presence of white crushed quartz and offset joints indicates that there is a later component of shear to these extensional fractures. Only the Group III fractures that lie below the shale horizon have this powdery white quartzitic gouge associated with the vein quartz. In addition to this, the fact that flower structures (Figure 3.21) are limited to the hanging wall below the shale horizon indicates that the shearing is probably due to mining induced stress redistribution and/or preconditioning. The quartzitic gouge filled Group IV fractures also appear to be affected by this later phase of shearing and it is in fact the orientation and left lateral offset of these fractures which confirms the synistral sense of shear of the Group III shears.

Figure 3.23 : Hangingwall photograph showing some of the features within the Group III shear zone, large arrows represent sense of shear and numbers refer to fracture groups. Note that the shearing is concentrated within a distinct zone lying at about 40° to the face direction. Scale bar in lower left corner is 10 cm.

Group IV: The weakly persistent Group IV joints lie parallel to the panel face and appear to have formed as a result of stress release immediately ahead of the face. The lack of fault generated cataclastic minerals such as crushed quartzite gouge indicates that they were formed under extensional conditions and as such are correlated with the Zone 3 fractures of Brummer (1987). Brummer ascribes their formation to the presence of the free surface of the face nearby. The void created by mining reduces the strain on the minor principal stress axis

and thereby allows fractures to develop parallel to the major principal strain axis. If preconditioning causes the development of new fractures one would expect to see an increase in abundance of this group of fractures around the areas of the preconditioning blast.

However, the only place that fractures of this orientation increase in abundance is in Group III shear zones. Within these shear zones the Group IV fractures change character and appear as white quartzitic gouge filled faults and are, in fact, first order Reidel shears (Ramsey 1980). These shears, termed second order shears by Moody & Hill (1956) form *en echelon* at an angle of 30° (±15°) to the main shear.

Group V: Fractures of this group are the most difficult to explain in terms of applied stress, as they do not line up with any major stress directions that could have been, or currently are, acting on the pillar. It is likely that these fractures formed at the same time as Group IV fractures and now form interconnections between the steeply dipping Group IV joints, as a result of indirect tension in the fracture zone immediately ahead of the face. The tensile forces in this broken rock mass would, in turn, allow the initiation of thin fractures which could later collapse under the influence of gravity.

Group VI: These low persistence fractures are thought to have formed at the same time as the Group III fractures. As these fractures are confined to within and immediately adjacent to the Group III shears, many of them are also affected by the later stage of shearing. Fractures of this group represent second order Reidel shears which develop at approximately 90° to the original Reidel shears (Group IV in this case)

3.4.6.2 Chronology of fracture development

Fracturing of the rockmass in the pillar is thought to have occurred in the following sequence:

1) Formation of Group III fractures (probably as quartz filled veins) as a result of regional scale tectonism producing lineaments with a NNE-SSW orientation.
2) Groups I and II , pillar edge parallel fractures formed due to stress build-up in the pillar after the area around it had been mined out and prior to the closure of the stoped out areas.
3) Reactivation of Group III fractures by shearing. Group IV and VI faults were also developed as a result of this sinistral shear movement as second and third order shears between Group III faults.
4) Mining induced stress changes resulted in the formation of Group IV, face parallel, joints.
5) Finally the extensional Group V fractures formed due to indirect tension as a result of compressive forces in the fractured rockmass immediately ahead of the face

4. PRECONDITIONING OF DEEP LEVEL LONGWALLS

The first documented experiments with preconditioning, or de-stressing, as it was termed at the time, on deep South African gold mines was in the early 1950's on deep level production longwalls at ERPM (Roux et al, 1957). There is no documented evidence of further work in this field until COMRO's involvement in pillar preconditioning at West Driefontein in 1987.

The longwall destressing experiment at ERPM in the 1950's was undertaken in collaboration with the CSIR. Hill and Plewman (1957) make reference to previous de-stressing trials at ERPM and Rose Deep Ltd. but no information is available other than a comment that the first trial at ERPM did not appear successful but was considered inconclusive.

A detailed de-stressing experiment at ERPM began in 1953 with more than 45 stopes being evaluated using the technique which consisted of 3m, small diameter holes drilled into the production face at a spacing of 1.5m. These holes were then blasted independent of the production round about once every week. Eventually, the results from only 17 stopes (scattered across the entire mine) were used for comparative purposes for equal time periods of before and during de-stressing. The effects of the de-stress blasts include improved hangingwall conditions (possibly the result of observed steeper fracture planes), a more fractured stope face after production blasts and triggered large events.

The most significant results from this project was the dramatic reduction in severe rockbursts in the de-stressed stopes and the complete elimination of such events during the day shift. During the period of comparison, only 1 person was injured due to a rockburst during the de-stressing phase compared to 6 fatalities and 38 injuries before de-stressing. From an implementation perspective, a total of 780 days were required to carry out the de-stress work but the average production rate did not change, indicating that the drilling did not interfere with production.

4.1 THE WESTERN DEEP LEVELS SOUTH MINE FIELD SITE

In 1993 a proposal was made to Anglo American Corporation to initiate a preconditioning project on Elandsrand Gold Mine. However following further discussions it was agreed that this project be carried out at Western Deep Levels South Mine in the 87-49 Stope which had experienced face bursting in addition to mining difficulties due to rolls.

Seismic coverage of the site was provided by a PSS microseismic network, which monitored seismicity associated with the 81-49 stabilising pillar to the north of the proposed preconditioning site, as well as by the regional ISS network. These systems were not able to provide adequate coverage for the new site at the 87-49 stope. Consequently the decision was made to install another PSS. Commissioning of this PSS was delayed as a result of problems encountered during installation, including malicious damage to the cable, sensor installation problems and difficulties in establishing a data acquisition room.

Despite these problems progress has been made, particularly with respect to gaining an understanding of the rock mass response to mining from seismic data acquisition, fracture mapping and convergence and ride monitoring.

4.1.1 Site description

Miningtek began its preconditioning trial at Western Deep Levels South in May 1995, since when no serious difficulties have been encountered with the drilling of long face perpendicular holes. At present work is concentrating on the integration of up-dip preconditioning into the mining cycle. This has included training and supervision of the drilling crew and related personnel.

Currently three panels are being mined with preconditioning and methods for quantifying the benefits of up-dip preconditioning are being developed. Information being obtained includes microseismic data, fracture mapping and, convergence and ride monitoring.

The preconditioning trial was begun in May 1995. Since this time almost 200 preconditioning blasts have been carried out on six panels and $\pm 3000 m^2$ of face area has been mined. With regard to safety, during the seven month period since the start of the trials no face bursts have been reported, although three workers were injured in separate rock falls due to seismic events.

Although it is too early to draw the conclusion, there are some indications that preconditioning improves the mining conditions in addition to improvements in safety. One of these indications is the increase in face advance rate from 0.7m to 1.0m per blast, an increase of about 40%.

Also since the face parallel fractures extend further into the rock mass, better face break is achieved and the number of sockets on the face is minimised. Moreover the time required for drilling of the holes has reduced from an average of 15.4 minutes to 13.6 minutes/hole indicating that the five to six preconditioning holes can be drilled by the normal production crew given an additional 1.5 hours per shift,.

Currently research is being carried out to determine the change in the in-situ stresses as a result of preconditioning. This will only be completed in 1996.

4.1.2 Preconditioning Layout

A review of the face perpendicular preconditioning has also been carried out. This included an assessment of the early work by Roux and Hill (1957) at ERPM and Giltner's (1992) work on an alternative method to the preconditioning being implemented by COMRO at that time.

The ERPM experiment used short, small diameter blast holes and was applied in more than 30 stopes. Compared with conditions elsewhere on the mine, hangingwall and face conditions were markedly improved and it was also concluded that the incidence of rockbursting reduced.

Giltner's work also followed the ERPM Model but utilized small diameter holes (38 - 42mm) drilled 2.25m apart. The main difference of this work from the ERPM trials was that the preconditioning holes would be drilled and detonated as an integral component of the production blast.

Giltner had assumed that each individual preconditioning hole would have a diameter of influence of around 1.5 metres. The first stage in adapting Giltners proposal to a working technique was to test this assumption experimentally. Two 3m face perpendicular holes were drilled and blasted at Blyvooruitzicht Gold Mine preconditioning site on 14 December 1993. Ground Penetration Radar profiles were acquired before and after the preconditioning blasts. The effects of the experimental blasts were clearly visible as a strong change in the reflector pattern observed on the radar images (Figure 4.1). A clear intensification of pre-existing fractures was observed on post blast profiles. By comparing the before and after blast profiles it was concluded that the zone of effect around the face perpendicular preconditioning blast hole was around 1.5m in radius, double that assumed by Giltner.

The drilling procedure for the preconditioning holes allows for the use of drilling machines and jumpers presently available on most mines. This negates the need to purchase special equipment which may be difficult to position and operate in underground conditions. The drilling of preconditioning holes can be done by hand-held percussion drill machines with air-legs. It was anticipated that some drilling difficulties would be encountered during initial attempts at this preconditioning technique.

In order to achieve the maximum effect from the blast, it was proposed that the preconditioning holes be drilled on the reef plane. As the radial extent affected by the preconditioning hole has been determined to be 1.5 metres, the spacing between preconditioning holes along the face should not exceed 3 metres (Figure 4.2). Because of the limited space for drilling long holes in the face area of a normal stope, all preconditioning holes must be drilled in the spacing between neighbouring packs close to the face.

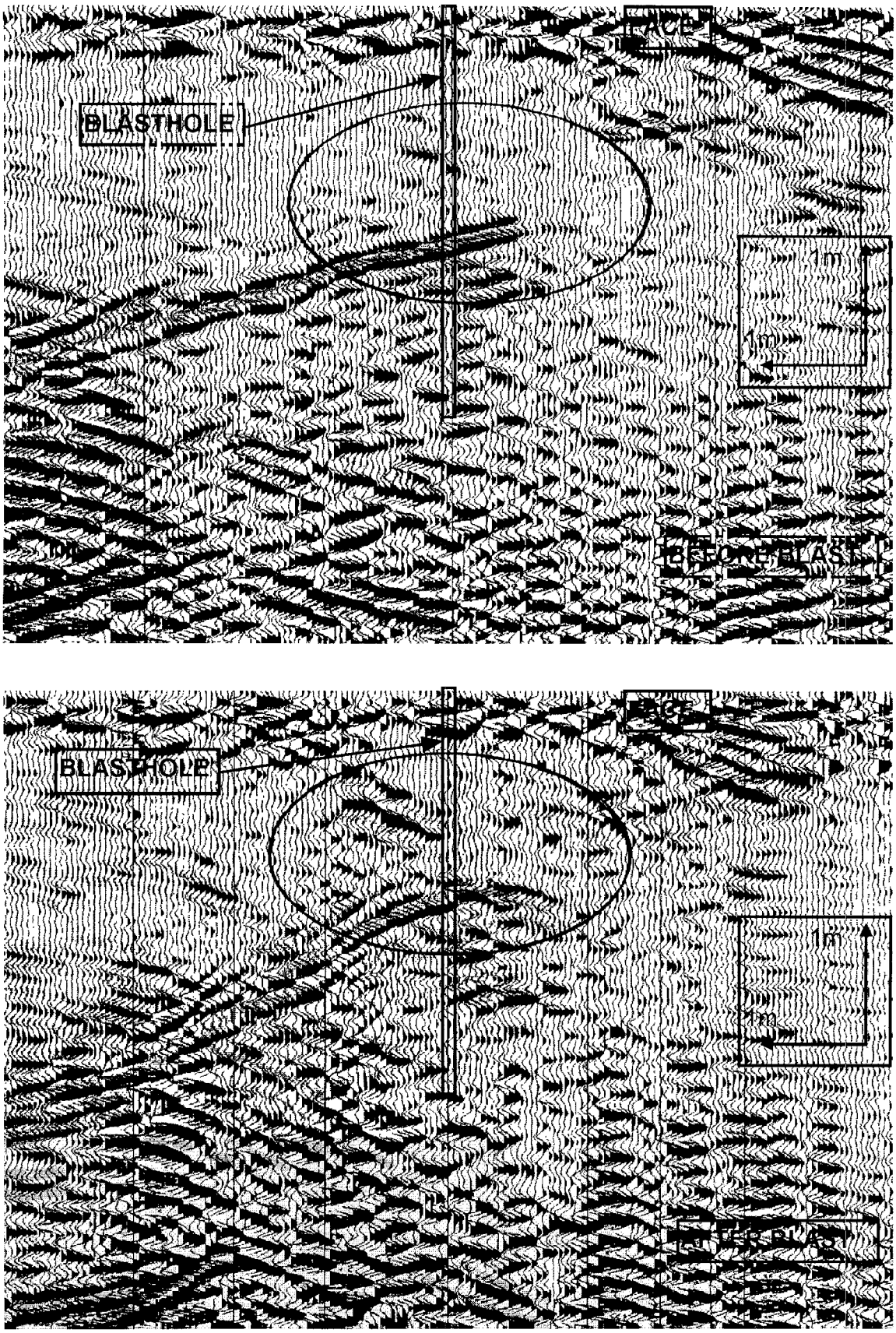

Figure 4.1: Ground Penetration Radar Scans.

The technique chosen for implementation experiments involves a three day cycle. Once the face has been cleaned and prepared for the next round of preconditioning, the drilling of new preconditioning holes commences. Each new round of preconditioning holes is offset from the previous ones by almost 50 cm along the strike direction in order to avoid drilling in the position of existing sockets. In this way the preconditioning holes drilled on the first day of a new three day cycle are drilled in the same position as those on the first day of the previous cycle. However, as three production rounds of roughly 1 metre face advance each have been taken between these two blasts there should no longer be any sockets remaining in these positions.

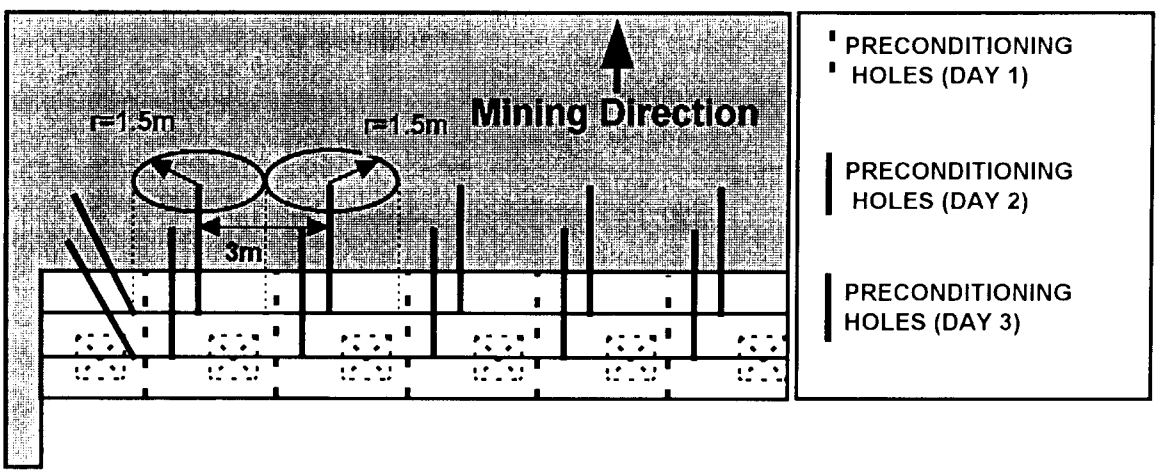

Figure 4.2: Layout of face perpendicular preconditioning holes, showing radius of influence of each hole (r=1.5m) and maximum recommended spacing between holes (i.e. 3m).

The up-dip preconditioning holes should be drilled at right angles to the face at mid-stope height in order to reduce the chance that a hole drilled as part of the normal production round will intersect a preconditioning hole. The closest point between the production and the preconditioning holes is at the collar and when properly drilled, the production holes are drilled away from the preconditioning holes. The intention is to use knock-off button bits to drill the preconditioning holes as this eliminates the need to take the long drill steels out at the end of the shift for re-sharpening.

In practice, a single 3 m long hole can be drilled in $\pm$15 minutes. Assuming that 2 machines are used to drill a given face, each drilling machine (or drilling crew) is required to operate for an additional 45 minutes. Alternatively one additional machine and drill crew can be allocated exclusively to the drilling of the preconditioning holes. The decision on which method is to be followed, increased drilling time or increased drilling labour, must be addressed based on the specific requirements of each preconditioning site.

4.1.3 Seismic Coverage

Although there was a seismic monitoring system in place in the vicinity of the 87-49W stope prior to the commencement of the preconditioning experiment, it was decided to install a dedicated PSS network for the seismic monitoring of the preconditioning site. Neither the mine-wide ISS network nor the PSS network monitoring the 84-49W stability pillar had adequate coverage of the 87-49W stope faces at the time. At the start of the project, just one panel was preconditioned. The analysis of the seismicity associated with the preconditioning required data of sufficient sensitivity and location accuracy to distinguish between the seismicity from the preconditioned panel and that from adjacent panels.

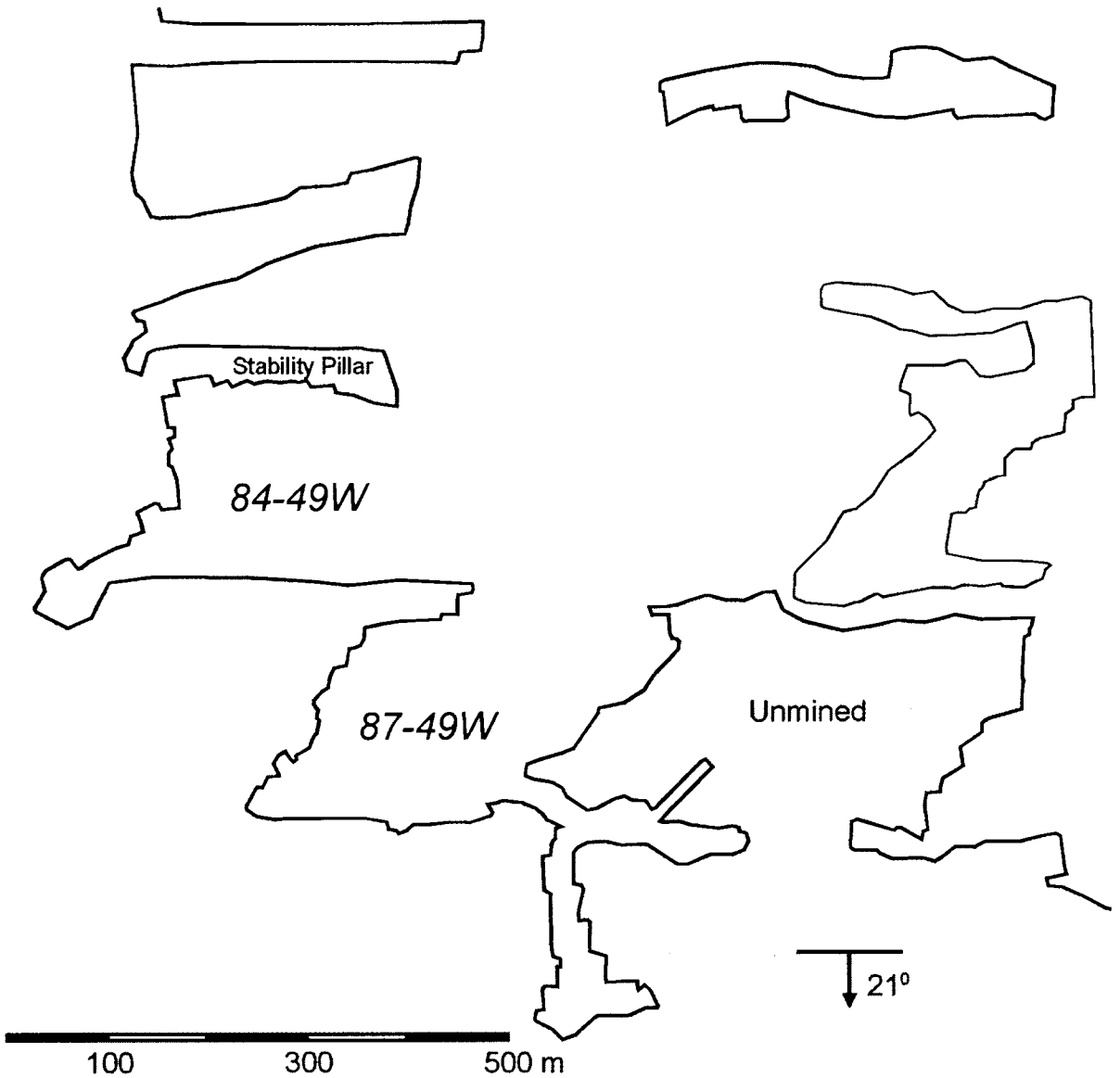

Figure 4.3: Plan of a portion of the WDLS 49 Line, showing the positions of the 84-49W stability pillar and of the 87-49W stope which is the site of the preconditioning experiment.

The positions of the 84-49W stability pillar and the 87-49W stope are shown in plan in Figure 4.3. The layout of the PSS network which was installed for the monitoring of the seismicity from the preconditioning site is shown in plan in Figure 4.4. The positioning of the five triaxial geophone sensors (labelled 'OS1i' to 'OS5i' in Figure 4.4) was a compromise between the desired coverage of the preconditioning site and the constraints imposed by the existing development around the 87-49W stope, the chief constraint being the lack of access to the south and west of the mining. The resulting network has dimensions of 350 metres in the strike direction, 200 metres in the dip direction and 85 metres in the vertical direction, roughly centred about the mining faces of interest. The PSS network was commissioned in September 1994 and has been recording seismic data since that time.

The sensors at 'OS1i' were installed at the end of a 10 metre down-hole drilled into the footwall quartzites from an 84 level footwall-access cross-cut. The sensors at 'OS2i' were installed at the end of a 15 metre horizontal hole drilled into the hangingwall lavas from an 84 level reef drive. The sensors at 'OS3i' were installed at the end of a 30 metre up-hole drilled into the lavas from an 87 level reef drive. The sensors at 'OS4i' were installed at the end of a 10 metre up-hole drilled into the quartzites from a follow-behind development on 87 level. The sensors at 'OS5i' were installed at the end of a 10 metre up-hole drilled into the lavas

from an 84 level cross-cut. The sites 'OS1i' and 'OS4i' have operated consistently since installation. One channel at each of 'OS2i' and 'OS5i' malfunctioned shortly after installation. Owing to difficulties with the grouting of the 30 metre up-hole, the sensors at 'OS3i' were not properly installed, so that the signals from these sensors are uncalibrated and useful for arrival-time picking only.

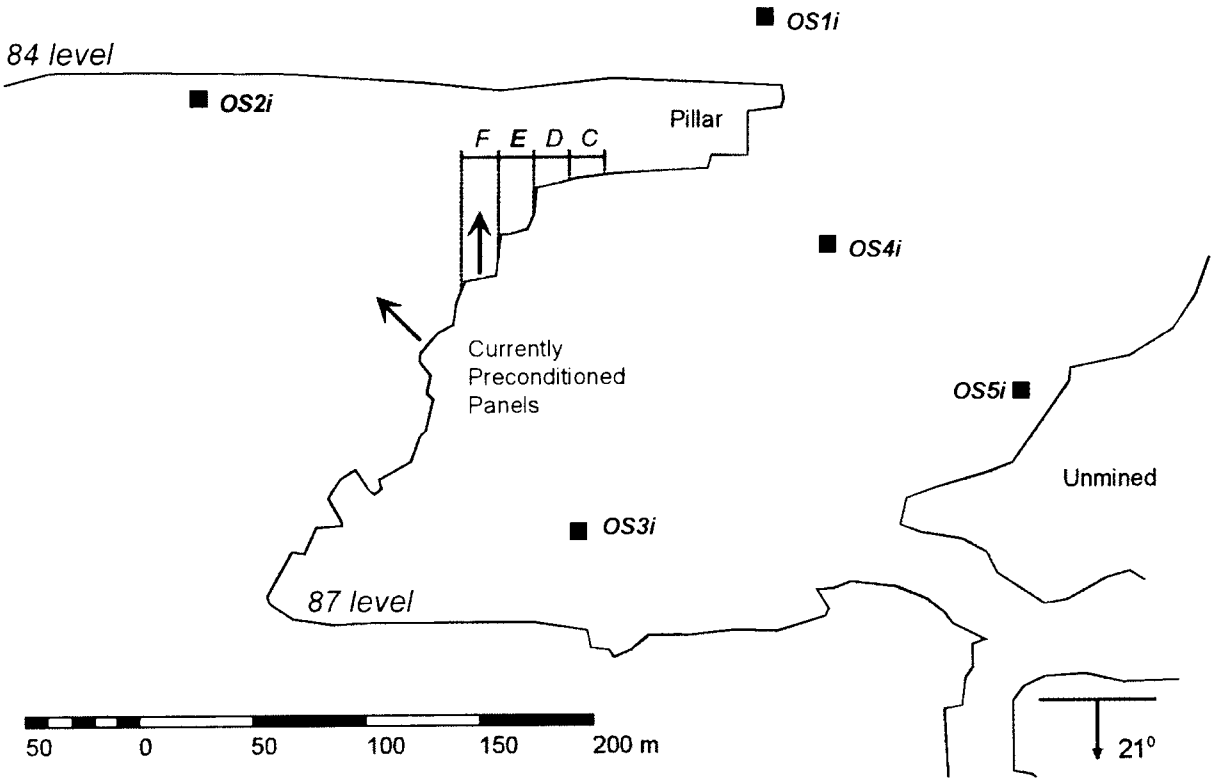

Figure 4.4: Plan of the WDLS 87-49W preconditioning site, showing the layout of the PSS network monitoring the experiment. The triaxial geophone positions are indicated by squares labelled *'OS1i'* to *'OS5i'*. Panels *'C'* to *'F'* are discussed in the text.

The data acquisition unit (DAU) is housed in an enclosure behind the waiting place near 'OS5i' on 84 level. The cables carrying the signals from the five triaxial geophone sensors are brought together at the DAU, where the data are digitised and passed through to a computer (PC) on surface. Numerous difficulties have been encountered with respect to the functioning of the seismic system since its commissioning. These have included the failure of several PC's in the initial period when these were operated in the harsh underground environment, the malfunctioning of the aged DAU's and damage to and/or loss of cabling between the DAU room and the outstations near the various sensor installations. Since the data PC has been moved to surface and the DAU's have been serviced (new DAU's have been purchased and will shortly be installed underground), data losses have been reduced significantly. While cable damage has been occurring less frequently of late, it does remain an occasional problem which compromises the quality of the recorded seismic data. Attempts are being made to supplement periods of lower quality or missing data from the data recorded by the mine-wide ISS system or the neighbouring PSS network.

4.1.4 Other Instrumentation

4.1.4.1 Convergence-Ride Measurements

A total of 43 Convergence-Ride Stations (Figure 4.5) have been installed and measured since the project in Western Deep Levels South mine was started. 23 of these have discontinued due to the difficulties in accessing the stations but measurements continued to be taken daily from the remaining 20 stations. The data are presented later in this report under "Quantitative Analysis of the Effects of Preconditioning" heading.

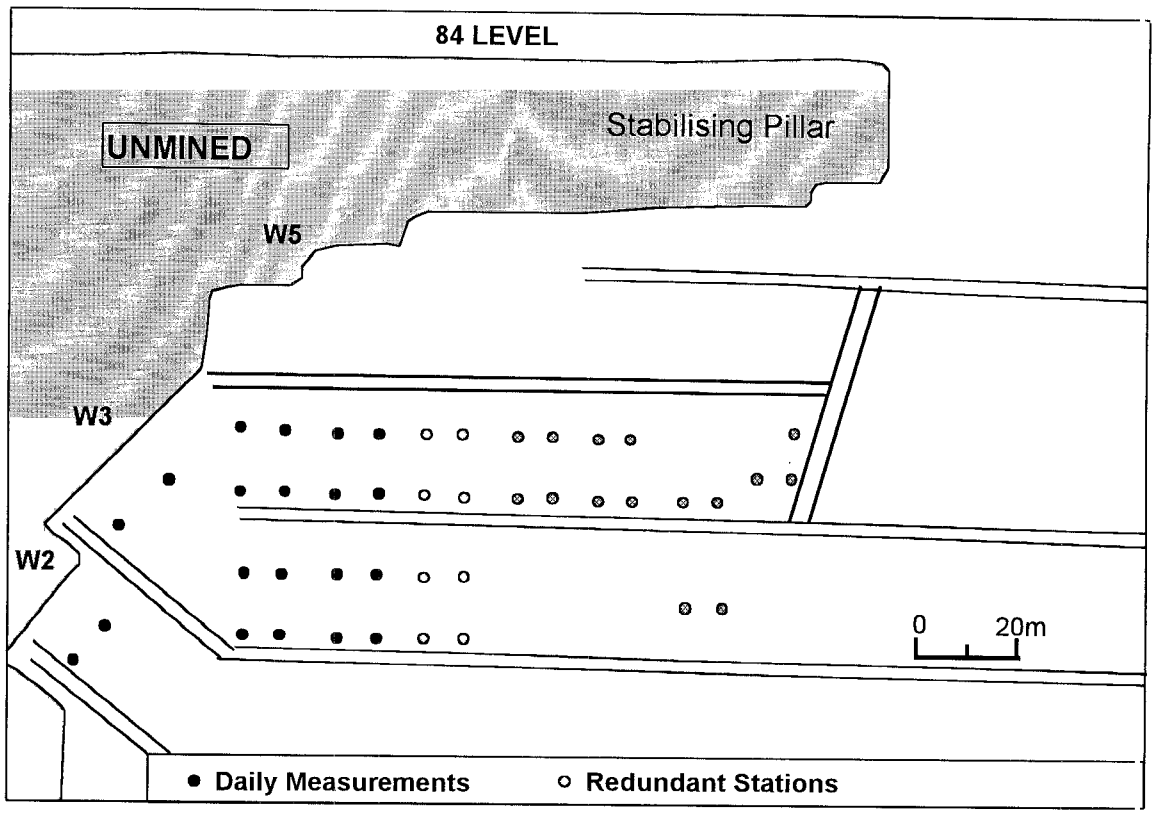

Figure 4.5: Positions of Convergence-Ride Measurement Stations.

4.1.4.2 Stress Determination

Strain Measurement (Stress Determination) studies have been initiated in September 1995. The idea was to determine the stress distribution profile ahead of a mining face in relation to the preconditioning and the face advance . The measurements would be taken before and after the preconditioning applied on that particular panel, and the comparison of these measurements would help quantify the effects of preconditioning. A total of 5 BX size instrumentation holes were to be drilled about 10-15m ahead of an updip panel. Unfortunately, at a depth of 6-7m, the holes started to collapse making the installation of the strain gauges impossible. However it has been decided to persist with the program because of its potential for quantifying the effects of preconditioning. This study will continue through 1996.

4.1.4.3 Ground Motion Monitoring

An array of 4 black boxes was installed in the preconditioning site in July 1995, and has operated continuously since then. The black boxes are generally placed close to a convergence-ride station and detailed fracture mapping was carried out around each of the boxes. Over 600 events have been recorded, with about 70% of these occurring during blasting time. The maximum peak particle velocity recorded to date is 780 mm/s. No rockburst damage has yet occurred in the immediate vicinity of a monitor.

4.2 QUANTATIVE ANALYSIS OF THE EFFECTS OF PRECONDITIONING

As with the Blyvooruitzicht field site it is important to quantify the effects of preconditioning on the rock mass in the vicinity of the preconditioned face. Four methods of objective quantitative analysis and a fifth more subjective technique are currently being used or developed at the WDLS site. These are:-

- Seismic analysis

- Convergence monitoring
- Rock fragmentation
- Analysis of stress induced fracturing
- Worker perceptions

These techniques are discussed in more detail below. The worker perceptions aspect is of considerable importance for the future acceptability of preconditioning as an implementable production tool. No studies of worker attitudes have as yet been undertaken and although this is not as scientific as the other analyses described here, it is nevertheless crucial that impartial studies begin in the near future.

4.2.1 Seismic Activity

A large (if somewhat incomplete) database of the seismicity from the 87-49W stope and surrounding areas has been recorded by the PSS monitoring the preconditioning site. The data appear to be well-behaved, with good correlation between data from the preconditioning network, data from the adjacent stability pillar PSS and data from the mine-wide ISS. Spatially, the seismicity recorded independently by both PSS networks exhibits similar trends, with a marked degree of clustering in the vicinity of the 84-49W, 87-49W and 89-49W stope faces (Figure 4.6). The linear spatial clustering of seismicity ahead of the 87-49W faces is more intense than that ahead of the 84-49W faces, where the stress conditions appear to be modified by the presence of both the stability pillar to the north and of the geological structures to the west. Both networks record a higher seismicity rate from 87-49W than from 84-49W and the seismic b-values are lower (i.e. there is a higher proportion of larger seismic events) for the seismicity from the former stope as well, indicating that 87-49W is the more seismically active area. The results from a comparison of data recorded by the two PSS networks between September 1994 and April 1995 are given in Table 4.I.

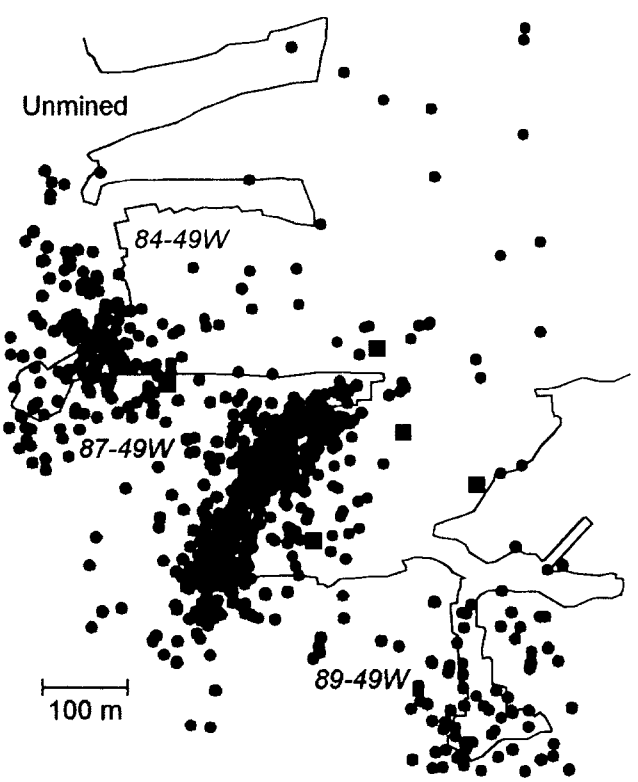

Figure 4.6. Plan of the seismicity recorded by the PSS monitoring the WDLS 87-49W preconditioning site during 1995. Seismic events of magnitude $M \geq 0$ are shown. The clustering in the vicinity of the 84-49W, 87-49W and 89-49W stopes.

Table 4.I. Comparison of seismic data recorded by two adjacent PSS networks on WDL South Mine. Kappa is an attenuation factor commonly used in seismic analysis.

		Preconditioning Site PSS	Stability Pillar PSS
Seismicity from 84-49W Stope	Number of events	303	280
	Smallest magnitude	-0.98	-1.39
	Average magnitude	-0.15	-0.15
	Largest magnitude	1.94	1.58
	Number of M>0 events	103	103
	b-Value	0.74	0.71
	Average estimated location error (m)	31	20
Seismicity from 87-49W Stope	Number of events	1275	379
	Smallest magnitude	-1.83	-1.18
	Average magnitude	-0.49	0.03
	Largest magnitude	2.08	2.40
	Number of M>0 events	257	177
	b-Value	0.71	0.65
	Average estimated location error (m)	17	20

The overall sensitivity of the preconditioning site PSS is greater than that of the stability pillar PSS, so that the former network records seismic events of smaller magnitudes. At the other end of the scale, the waveforms from the preconditioning PSS saturate for local larger events of smaller magnitudes, so that the magnitudes assigned to such larger events are less accurate. Clearly, the sensitivity and location accuracy of each network are better for the seismicity from the stope which is closer to that network. The estimated location errors given in Table 4.I are somewhat inflated by the fact that the simple velocity model used in the location error calculation of the recorded seismic events averages out the differing hangingwall (lava) and footwall (quartzite) P- and S-wave velocities for the rock mass in the area. The location accuracy of each network is better than the quoted figure for the seismicity local to that network, due to the encompassing of each stope in the monitored area by the respective network configuration and the fact that the least squares algorithm used to locate the events is independent of the velocity model. Above and below the reef horizon in vertical section and beyond the confines of each network in plan, increased scatter in the seismic event locations is evidence of the reduced location accuracies.

The seismic data recorded by the preconditioning PSS exhibit a well-developed clustering ahead of the 87-49W stope faces in plan and, to a lesser extent, about the plane of the reef in section. The shape of the clustering in plan approximates the mining geometry closely and there is evidence of the migration of the seismicity along with the advancing stope faces. The recorded seismicity rate has two clear peaks in time of day, corresponding to development blasting (at about 15:00) and to production blasting in the stope (at about 17:00).

From September 1994 until the commencement of preconditioning in May 1995, a background database of seismicity was recorded from 87-49W stope by the preconditioning site PSS. From 23 May 1995 to 14 August 1995, a single up-dip panel (labelled panel 'E' in Figure 4.4) was subjected to preconditioning. The location accuracy of the manually-located seismic data is sufficient to allow the comparison of the seismic characters of the preconditioned and adjacent panels before and after preconditioning, but not good enough for the expected stress-transfer processes induced by preconditioning ahead of the panel face to be identified. Changes in the spatial location of the seismicity with respect to the panel face are expected to be relatively small (compared with the distinct effect observed in the seismicity recorded after a face-parallel preconditioning blast). However, work is underway to refine an auto-location algorithm which is capable of very accurate locations (to within much

better than 5 metres) and which should facilitate the identification of spatial trends in the seismicity, should any such trends exist.

The up-dipping line followed during the mining of panel 'E' is indicated in Figure 4.2. A comparison of the seismicity recorded from panel 'E' and from adjacent panels ('D' and 'C', to the east of panel 'E', and 'F', to the west) before and during the preconditioning of panel 'E' is given in Table 4.II.

Table 4.II: Summary of seismic data recorded before and after the start of preconditioning of WDLS 87-49W panel 'E'. The values for b-value and kappa are given as average value ± standard deviation (Frequency - magnitude graphs for panel E are given in Appendix E).

Panel	Period *	b-Value	Total events	% M≥0 events	Average kappa (ms)
'C'	before	0.53 ±0.15	53	26.4	1.62 ±0.41
	after	0.47 ±0.17	30	30.0	1.53 ±0.47
	% change			*13.6*	*-5.56*
'D'	before	0.48 ±0.18	29	20.7	1.65 ±0.56
	after	0.58 ±0.18	39	17.9	1.58 ±0.40
	% change			*-13.5*	*-4.24*
'E'	**before**	**0.42 ±0.16**	**28**	**53.6**	**1.79 ±0.55**
	after	**0.60 ±0.16**	**58**	**24.1**	**1.59 ±0.42**
	% change			*-55.0*	*-11.17*
'F'	before	0.55 ±0.23	25	32.0	1.71 ±0.49
	after	0.51 ±0.10	109	33.0	1.61 ±0.47
	% change			*3.1*	*-5.85*

* Period
before: 01/01/95 to 22/05/95
after: 23/05/95 to 14/08/95

The change in the proportions of numbers of seismic events recorded from the various panels between the two time periods reflects the fact the mining activity shifted focus from the eastern portion of the stope (around panel 'C') to the western portion (around panel 'F'). While there were changes in the seismic characters of the adjacent panels after the start of preconditioning in panel 'E', the change within panel 'E' itself was clearly the most significant. This is to be expected, as the effects of preconditioning are thought to be confined mostly to the rock mass in the immediate vicinity of the preconditioning activity. The seismic data contain no indications of any preconditioning effect (positive or negative) on panels adjacent to panel 'E'.

The change in the seismic character of panel 'E' was most encouraging in terms of indicating the positive effectiveness of preconditioning. The seismic b-value increased markedly, indicating that the proportion of larger events in the seismicity recorded from the panel had decreased. This is confirmed by the 55 per cent decrease in the proportion of M≥0 events recorded from the panel. The manner of seismic energy release from the rock mass ahead of the panel face had been positively altered by the introduction of preconditioning.

The attenuation factor 'kappa' is an indicator of the quality of the rock in the vicinity of the source of a seismic event. A higher value for kappa indicates that the rock is relatively more fractured. After the change to preconditioning, the average value of kappa decreased by twice as much for the seismicity recorded from panel 'E' as it did for that from the adjacent panels. This would suggest that the seismicity ahead of the face of panel 'E' occurred further ahead of the face (i.e. in the less fractured ground) under the influence of preconditioning. The inference is that the preconditioning was transferring the stress concentration ahead of the advancing panel face away from the excavation, further ahead of the face and into the area of more solid rock.

4.2.2 Convergence data

The installation of convergence-ride measurement stations was initiated on 28 of September 1994. Since then a total of 43 Convergence-Ride Stations have been installed and measured at the project site in Western Deep Levels South Mine. Currently 20 of those stations are being measured daily. The remaining 23 stations are no longer monitored due to the difficulties in accessing the stations.

The total convergences are calculated from the actual measurements and plotted on the graphs (Figures 4.7 and 4.8 and Appendix C). The measurements show a very high convergences and rides due to the seismic events in the vicinity of the stope. In order to correlate the convergence-ride data with seismic data obtained from PSS, first the inelastic component of the total convergences had to be determined. Therefore a detailed Minsim-W modelling was conducted to determine the elastic component and the inelastic component was calculated by subtracting it from the total convergence. The next step is to correlate the inelastic component with the seismic data.

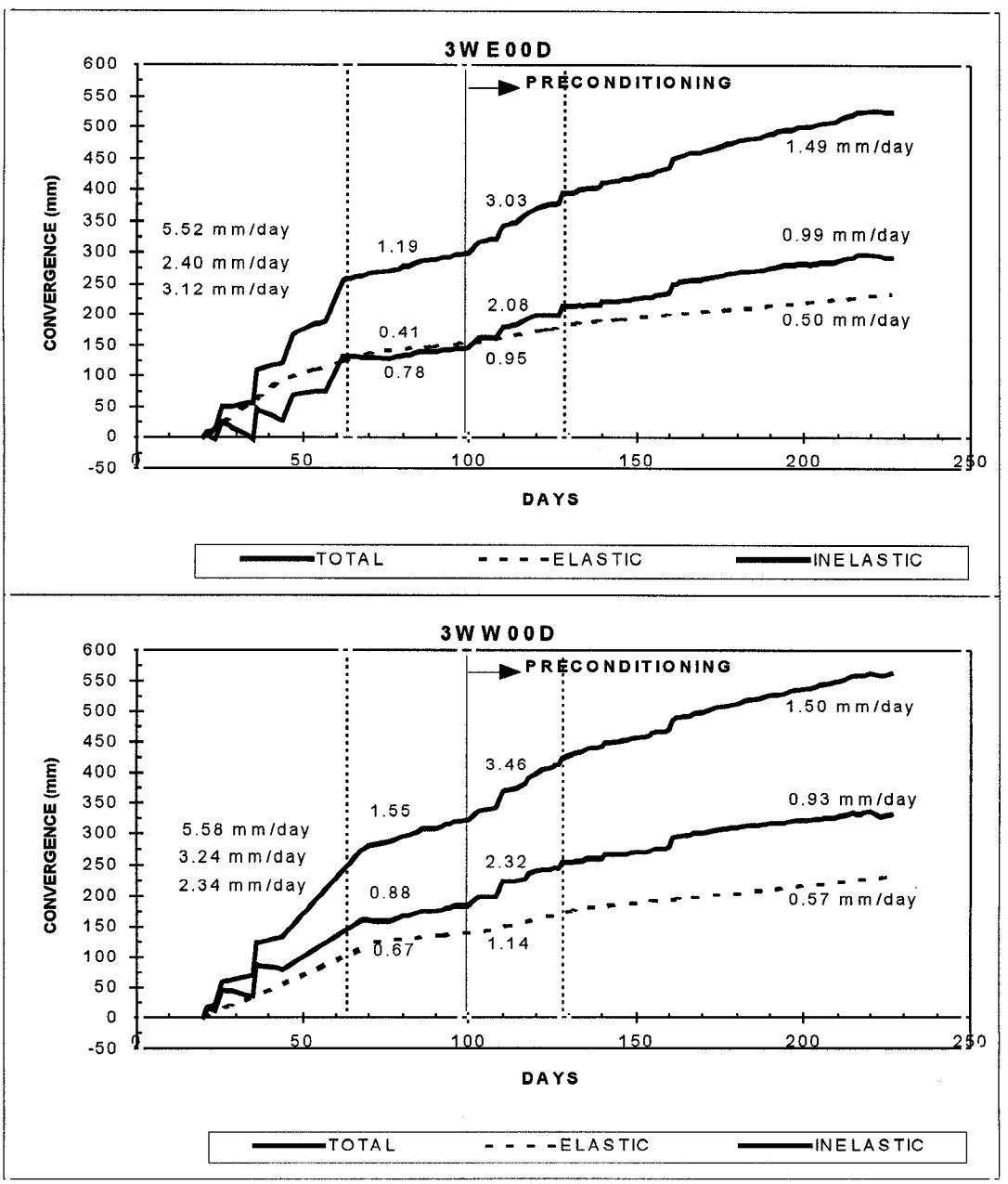

Figure 4.7. Convergence - Ride Measurements (Stations 3WE00D & 3WW00D). Convergence rates are linear regression gradients for the periods shown on the graphs.

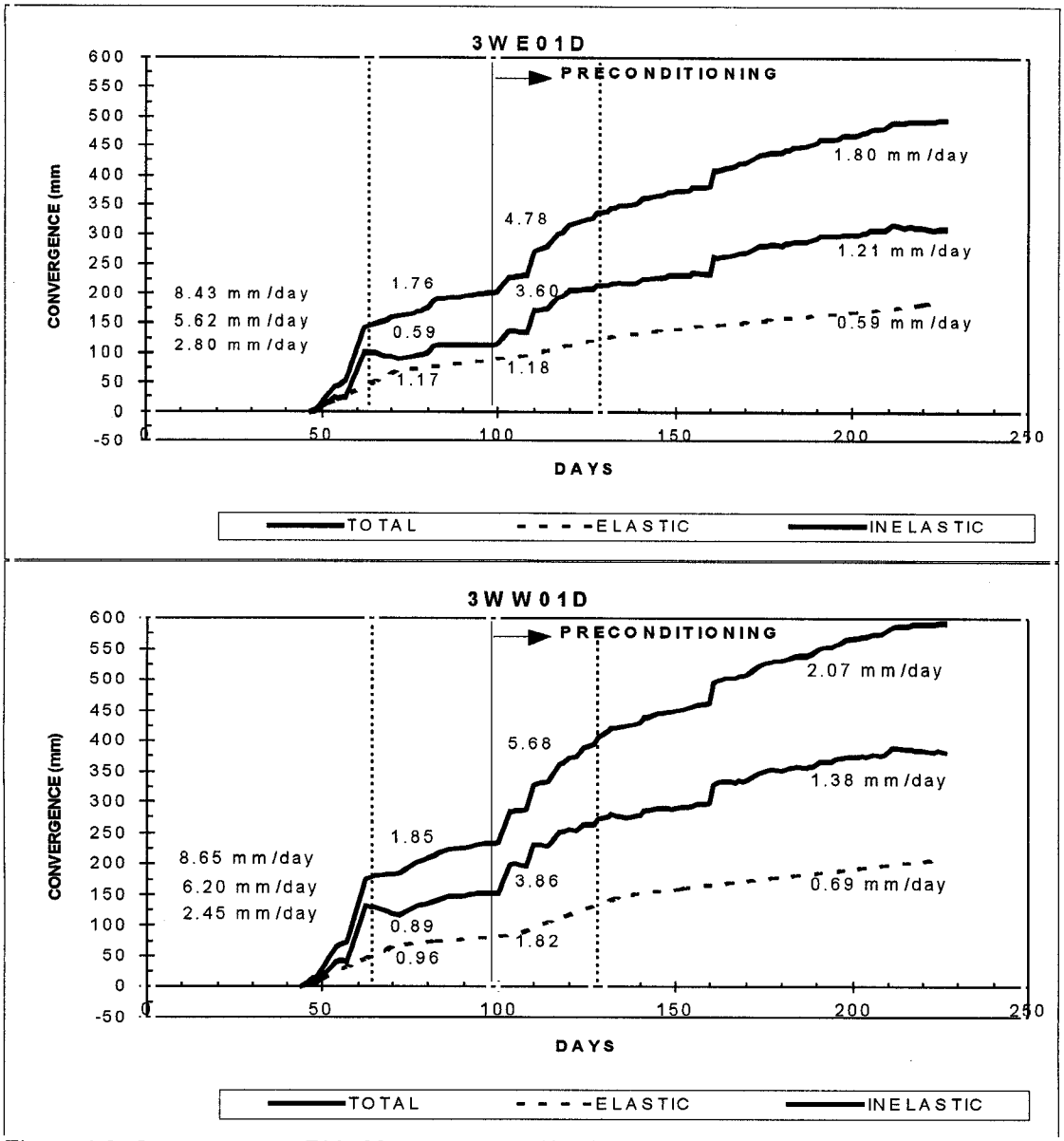

Figure 4.8. Convergence - Ride Measurements (Stations 3WE01D & 3WW01D). Convergence rates are linear regression gradients for the periods shown on the graphs.

The effect of the preconditioning on the convergence measurements is shown in Figures 4.7 and 4.8. The preconditioning was started on day 97 (23/5/1995). In these graphs measurements from 4 stations closest to the preconditioning panel are analised in four regions. The first region is from installation day to the day 62. In this region all 4 stations show very high convergences. Since the stations are very close to the mining face both elastic and inelastic components are very high (as they were expected). The second region is from day 62 to the initiation of preconditioning. The measurements are interestingly quite low. The decrease in elastic component would be expected since the distances from stations to face are increasing. The decrease in inelastic component can only be explained after the measurements are corrolated with seismic data. The third region is from initiation of preconditioning to the day 128 (this is a month after preconditioning). It is quite clear that the measurements from all 4 stations showed a significant increase in inelastic component. A slight increase in elastic component can be explained by the increase in face advance rate by the effect of preconditioning. The fourth region can be called as "settlement" region. In this region all measurements decrease back to a fairly consistent level of total convergence similar to the one in region 2.

The effect of preconditioning can not be seen in all other measurements from the stations (Appendix C) relatively far from the preconditioning panel. Since preconditioning has a local effect, this was also expected.

4.2.3 Fragmentation

The model of the mechanism of preconditioning describes the process as an injection of gas generated by the blast, opening up the existing fractures within the rock mass. Since the preconditioning blast is initiated just prior to the production blast, the production blast should be much more efficient in breaking the face. This is indicated by the improved advance rates being achieved in the preconditioned panels at WDLS and should also be seen in the improved fragmentation resulting from the production blast.

Automated techniques of image processing of fragmented rock are available and suitable methods of image analysis techniques could be the same as those described previously for the face dilation investigations at Blyvooruitzicht Gold Mine. A two-dimensional analysis of the blasted rock needs to be carried out using stereo images. To do this the analysis requires edge detection of the pieces of rock, which may require significant user input as the contrast in a pile of broken rock may not be sufficient for a fully automated process.

Improved fragmentation of a production blast will result in a more uniform particle size distribution, thus improving material handling and enabling faster face scraping, less secondary blasting, less chance of a hang-up in a boxhole and potentially less fines, thus improving gold recovery.

4.2.4 Fracturing around a deep level longwall

Approximately 600 individual fractures were mapped prior to the start of preconditioning on WDLS. A further 500 fractures have so far been mapped within the preconditioned areas. These fractures were classified into three types: faults, fissures and joints. Faults are fractures with visible movement indicators such as gouge or slickensides. Fissures are fractures with significant dilational features and the discontinuities with no or very minor displacement are termed joints. By far the most common fracture type are joints, (69% of the total). Faults made up about 31% of all fractures, and fissures were uncommon (less than 1%). The fractures were predominantly face parallel (Figure 4.9a) with a second cluster at approximately 90° to the face. The dip of the fractures is mainly at a high angle towards and away from the face (Figure 4.9b). A second set dips at an intermediate angle of approximately 40° and a third dips away from the face at an angle of up to 30°.

Five distinct fracture groups (Figure 4.9c) were identified based upon their spatial orientation (dip and strike). These groups have been labeled Groups I to V and are summarised in Table 4.III.

Table 4.III: Summary of characteristics of major fracture types.

GROUP	DESCRIPTION
I	Low angle, face parallel joints (and occasionally faults)
II	Steeply dipping ,face parallel faults and joints
III	Steeply dipping, face perpendicular faults and joints
IV	Moderately dipping (towards face) joints lying at an acute angle to the face
V	Moderately dipping (away from face) joints lying at an acute angle to the face

The majority of fractures are face parallel and steeply dipping (i.e. Group II). There is also a group of face parallel, low angle fractures that dip towards the face. These low angle fractures are restricted to the lava hangingwall and comprise Group I. Many of the shallow dipping fractures are actually extensional features that have developed later in the lava sub-parallel to the pre-existing joints and have a very low persistence, even though on a local scale they may appear abundant. Most of the steeply dipping face parallel (Group II) fractures occur predominantly at the face, and it is thought that these represent short, relatively intense, mining induced fractures. Both the low angle and the steeply dipping

fractures are predominantly face parallel and as such they split the hangingwall up into oblong blocks of rock. It is generally these blocks that fall out during a seismic event.

Group III fractures run perpendicular to the face and dip at approximately 80°. They are not as common as the face parallel fractures. They occur as joints or faults filled with a white gouge of crushed quartzite.

The fractures of Group IV and V lie at an acute angle to the face and have an intermediate dip towards and away from the face respectively. Fractures of these groups appear to interconnect Group I and II fractures and, as such, they have a low persistence.
The fractures mapped at the preconditioning site after the initiation of preconditioning fall into the same five groups identified in the stope before preconditioning was initiated (Figures 4.9d to 4.9f). However, the abundance of the fractures within these groups varies between preconditioned and unpreconditioned (normal) areas.

The Group I faults and joints, which appear to be restricted to the lava hangingwall are thought to have formed as a result of mining induced stress changes at or immediately in front of the face. These form parallel to the mining direction and can, in places, be linked to more steeply dipping intra-reef and footwall fractures. This would seem to indicate that Group I (shallow dipping) and Group II (steep dipping) fractures may in fact be the same fracture set. The different orientations would appear to be due to the different response of the various rock types to the same stress, rather than a series of different stresses producing different fracture patterns.

The existence of steeply dipping fractures in the hangingwall justifies the separation of specific steep dipping fractures into a different group. The low angle fractures of Group 1 can be correlated with the extensional fractures of Brummer (1987) and Roering's (1979) Type 3 fractures. Brummer (1987) suggests that these fractures form due to a reduction in the minor principal stress (that is by mining) allowing the rock to fracture in a uniaxial stress field.

Faults and joints of Group II are generally fairly persistent and are thought to have been formed due to the larger scale stresses applied to the unmined ground. Adams et al (1981) describes a series of steeply dipping face parallel shear fractures developed at periodic intervals ahead of the face,. The authors also noted that these shears develop furthest away from the face and conclude that these are probably the first to develop.

The Group II joints increase in intensity towards faults (also steeply dipping face parallel). These faults may be the shear fractures of Adams et al (1981) and Brummer (1987). Thus the more persistent faults and joints of Group II were probably the first formed fractures, and as mentioned earlier, formed due to larger scale stresses on bigger unmined blocks. The low persistence fractures in this group are thought to have formed at the same time as the shallow dipping (Group I) fractures.

The fractures of Group III are orthogonal to those of Groups I and II . A large number of these fractures developed in the immediate vicinity of a lag between adjacent panels. The fractures were concentrated within the first 3m of the open end of the panel and it is proposed that the same mechanism which caused the Group I fractures to develop, was also dominant here. All the other Group III fractures are thought to be the natural joint set described by Lightfoot *et al* (1994).Underground these fractures are observed as joints and faults (often with a white crushed quartzite infill) that are more persistent than the other fractures. This matches with the observations of Lightfoot et al (1994) who recommended that the mining layout should be altered so as to prevent mining in line with these features.

Fractures of Groups IV and V lie at an intermediate dip between Groups I and II and are uncommon in comparison to the other face parallel fractures (they were only identified after a large amount of data had been collected). These fractures form two distinct sets dipping at approximately 100° to each other and it would appear that they form after the fractures of all other groups as interconnections between the shallowly and steeply dipping face parallel fractures. The lack of fault material, either as gouge or as crushed quartzite suggests that both Group IV and Group V fractures are extensional features. It is proposed that these

fractures formed where Group I and II fractures were temporarily locked against each other, but due to the lowered minor principal stress of the area, extensional features could develop.

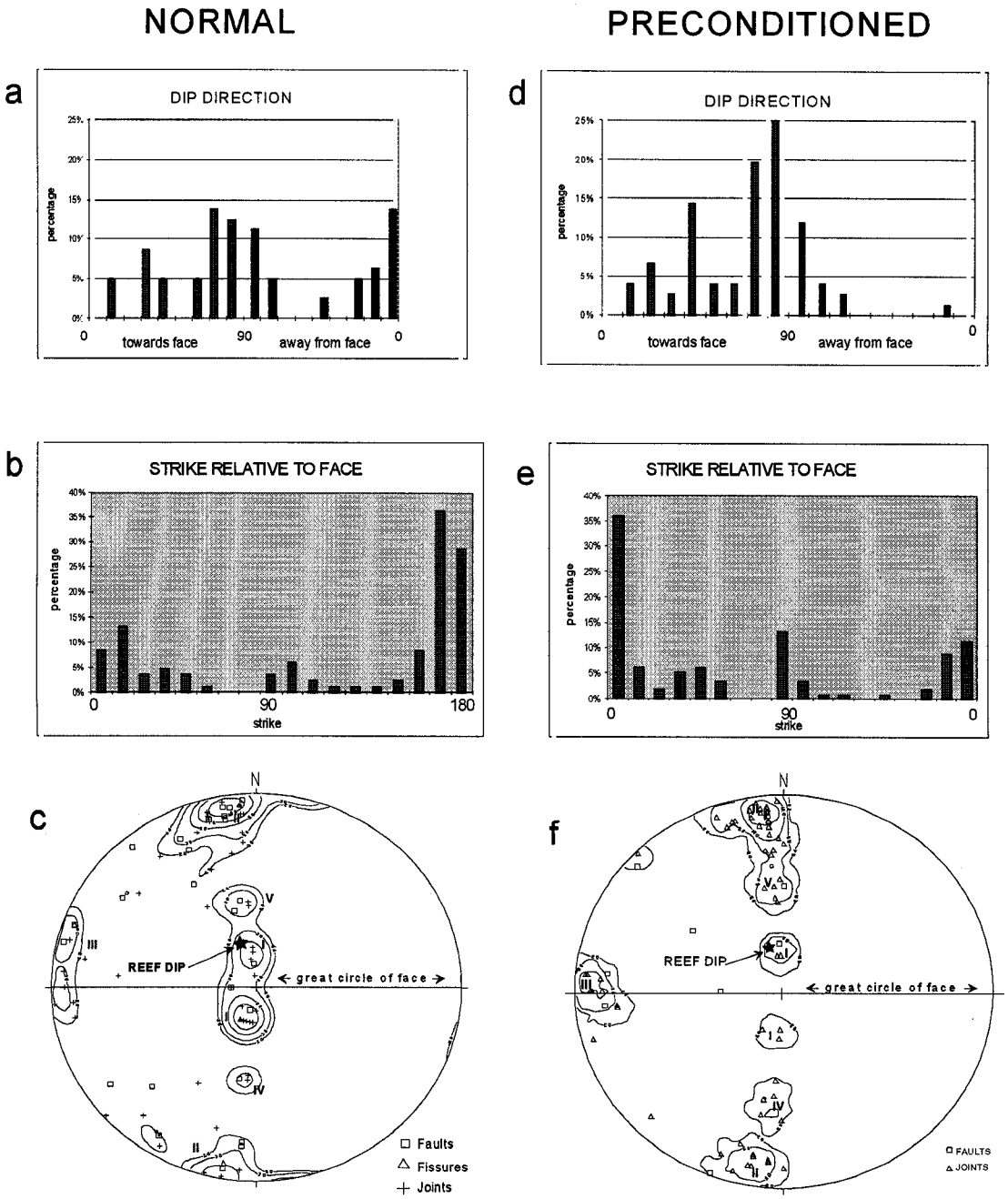

Figure 4.9: Summary of orientation data of fractures mapped prior to and after the initiation of preconditioning.
a)Dip orientation of fractures prior to preconditioning
b)Strike orientation of fractures prior to preconditioning
c)Schmidt Net (lower hemisphere projection) of poles to all fractures prior to preconditioning
d)Dip orientation of fractures after initiation of preconditioning
e)Strike orientation of fractures after preconditioning
f) Schmidt Net (lower hemisphere projection) of poles to all fractures after preconditioning (contours are in percent).Note the high degree of similarity in both the dip and strike orientations prior to and after the initiation of preconditioning.

It would seem that the fractures of Group III are the first formed fractures, followed by the majority of Group II fractures. Certain of the Group III joints (notably those that occur at the lag between panels) probably also form at the same time as most of the Group II fractures. After this the remainder of Group II and all of Group I fractures are thought to have developed. Finally Group IV and V joints can develop between the other pre-existing fractures.

Since the inception of preconditioning there has been a noticeable change in the appearance of the stope. This is because there has been a change in the fracturing of the rock mass around the stope. Despite this change, no new groups of fractures have formed. Rather the relative abundance of the existing groups have changed. There has been a significant increase (25%) in the number of steeply dipping fractures, whilst shallow dipping fractures have shown a 61% decrease in abundance in preconditioned areas (Figure 4.10a and 4.10b). Fractures of an intermediate dip do not show much variation in abundance between preconditioned and unpreconditioned (normal) areas. In normal areas fractures with an intermediate dip make up approximately 21% of the total, compared to 27% in preconditioned areas. It can therefore be assumed that, in terms of dip orientation of fractures, preconditioned stopes have steeper dipping fractures, than normal stopes.

The strike orientation of fractures in normal and preconditioned areas appears to have changed (see Figure 4.10c and 4.10d). There is a decrease in the number of fractures lying in between 0° to 30° and 150° to 180° (this is a band of more or less face parallel fracturing). Accompanying this decrease is an increase in fractures orientated in a direction of between 110° and 150°. However, many of the fractures mapped as part of the data-base of post preconditioning initiation fractures were recorded in panels orientated approximately 40° anticlockwise from the conventional updip panels. If the orientation of the fractures in these diagonal panels is considered relative to the face, the majority of the fractures classified in the 110° to 150° range, would actually be lying parallel to the face. This change in mining orientation has also resulted in a decrease of fractures orientated within the class 30° to 70°. Fractures orientated between 70 and 110° show an increase in abundance in preconditioned areas, but this can again be explained in terms of mining orientations. A large lag developed between adjacent panels and as the preconditioned panel mined up past this lag, it went through a zone of fracturing developed parallel to the lag. This led to an increase in the abundance of fractures orientated between 70 and 110°.

The same five fracture groups have been identified in both preconditioned and normal areas. The orientation (mean strike and dip vector) of the various groups is very similar (Table 4.IV). The strike vector azimuth of Groups II, IV and V appears to be very different in preconditioned and normal areas. But the azimuths are more or less 180° from each other, and so in fact the fractures lie almost parallel to each other. The spherical variance of the different groups is low, especially if compared to the spherical variance obtained if all the fractures are grouped together. In preconditioned areas this variance is 47.4 and 61.4 in normal areas. Thus the spherical variance of the groups is two orders of magnitude lower than that of the entire data-base. This indicates that the groupings identified are realistic. Thus, not only are the groups well defined within preconditioned and normal areas, but the orientations are very much the same in both mining conditions.

As a result of preconditioning Group I fractures decrease in abundance. In unpreconditioned panels these joints and faults account for approximately 25% of the fractures, whereas in preconditioned areas they make up less than 15% of the total. There are two potential reasons for this reduced abundance. It is possible that because preconditioning reduces the stress at the face that these stress fractures are not able to develop deep into the lava. Secondly the preconditioning blast may weaken the contact between the reef and the lava hangingwall by shearing and or dilation. There is evidence of shearing along both the top and bottom reef contacts, with the development of centimetre thick shear zones on the contacts. These shears usually consist of tiny angular pieces of quartzite (up to 4mm in diameter) surrounded by fine white crushed quartzite powder. Occasional small en-echelon faults filled with this powdery white gouge are found. A more even hangingwall (often with impressions of pebbles from the reef) further indicates that this weakening has occurred, as a strong contact would produce a much more hackly surface. This weakened contact would result in less

penetration of the production blast into the hangingwall, resulting in less fracturing. As a consequence of the reduced number of these fractures, the hangingwall quality is better in preconditioned areas.

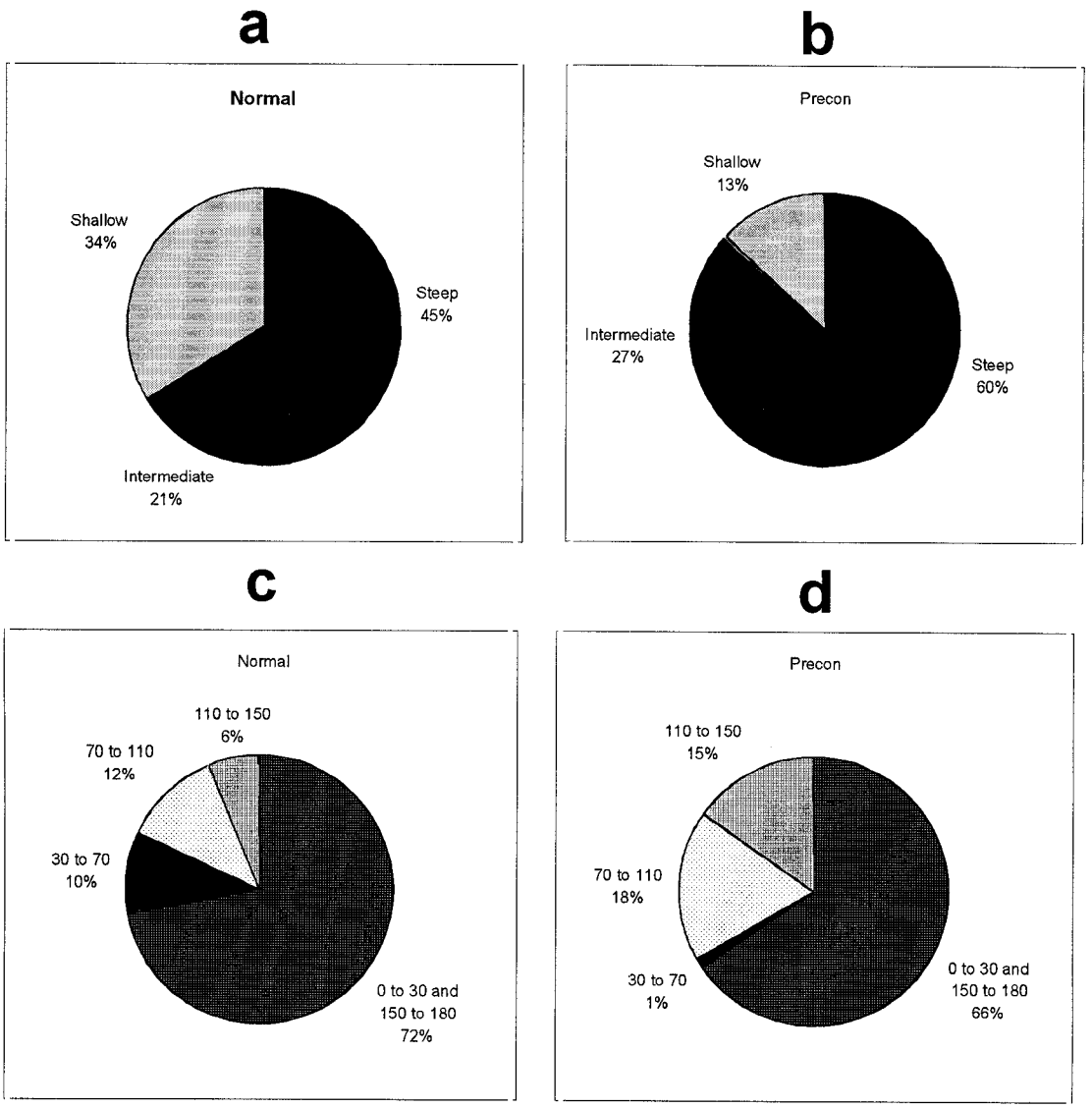

Figure 4.10: Pie charts of orientations of fractures prior to and after preconditioning. Note shallow dipping fractures have a dip of 0° to 30°, intermediately dipping fractures have a dip of between 30° and 60° and steep fractures a dip of 60° to 90°.
a) dip orientation prior to preconditioning
b) dip orientation after preconditioning
c) strike orientation (in degrees) prior to preconditioning
d) strike orientation (in degrees)after preconditioning.

There has been a significant increase in the frequency of occurrence of Group II fractures. In certain cases, the fractures have changed character from only joints (in unpreconditioned areas) to gouge filled faults and joints. It is suggested that preconditioning does not cause new fractures to develop in this orientation, but rather extends pre-existing fractures (Figure 4.11). This is because the preconditioning blast, which is detonated in a 3m face-perpendicular hole, occurs within the zone of the face parallel fracturing. Evidence from the edge of the panel next to the lag shows that the zone of face parallel fracturing extends to depths of approximately 3m ahead of the face. In any given slice (such as the stope itself) through the rock mass more fractures would be intersected, giving the impression of increased fracturing. This apparent increase in face parallel fractures has led to an improved face advance, with production holes again causing any fractures to be extended further. Thus

the exposed preconditioned face is highly fractured when compared to unpreconditioned ones. It is also much easier to bar down.

Table 4.IV: Summary of the characteristics of the various fracture groups.

Group	I	II	III	IV	V
Dip vector plunge (normal)	4.1°	84.8°	75.4°	41.4°	-59.6°
Dip vector plunge (precon)	7.9°	85.4°	77.5°	47.2°	-48.3°
Strike vector azimuth (normal)	9.9°	1.7°	99.1°	14.6°	17.6°
Strike vector azimuth (precon)	27.3°	177.6°	85.9°	175.5°	163.7°
Percentage (normal)	26	38	21	7	5
Percentage (precon)	15	47	24	11	5
Spherical Variance (normal)	0.7689	0.5503	0.2404	0.4848	0.2420
Spherical variance (precon)	0.1237	0.5641	0.1623	0.2787	0.0442

The Group II fractures connect up with the more shallowly dipping Group IV fractures. This is more common in preconditioned areas than unpreconditioned areas. It appears that preconditioning extends the pre-existing fractures and in this case causes them to join. Preconditioning appears to affect fractures by extending them or by causing movement on them.

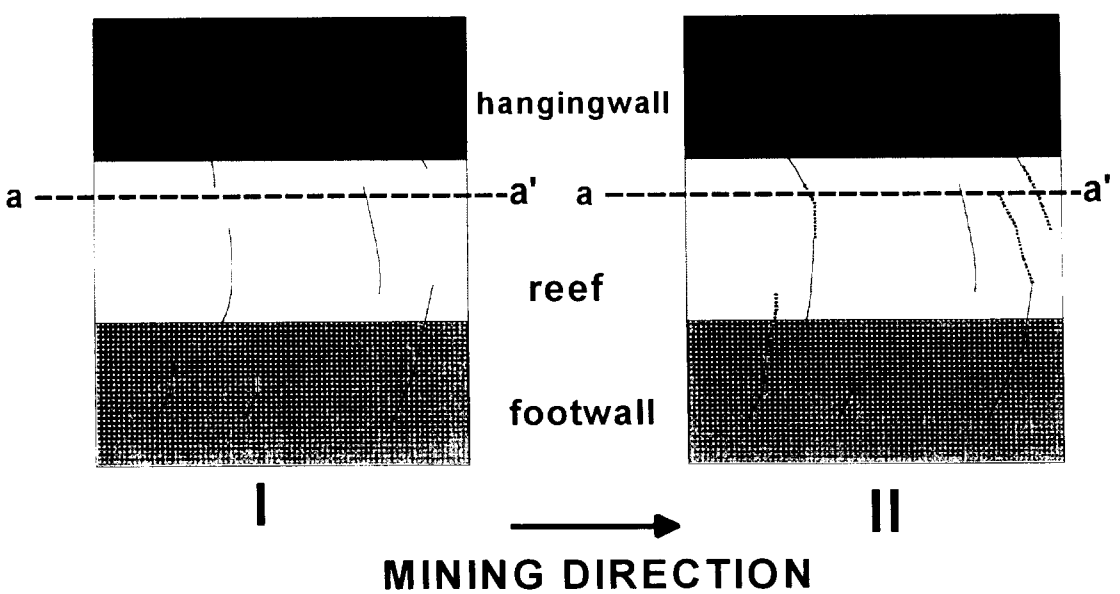

Figure 4.11: Sketch diagrams to show reason for apparent increase in abundance of Group II fractures. I) An idealised section through rockmass ahead of stope-face. Note that line a-a' only intersects one fracture II) The same area ahead of the face, but after a preconditioning blast has caused extension of pre-existing fractures. Now line a-a' intersects four fractures. Note the change in dip of fractures as they pass through the reef horizon. Certain fractures interconnect to form a continuous surface.

The Group III fractures show almost no variation in abundance between preconditioned and normal areas. This is probably because they formed much earlier than the other fractures in the stope. The stresses that caused the fracturing in this orientation were thus probably no longer dominant, which would prevent the preconditioning blast from causing further fracture growth. As the majority of the fractures in this group (apart from those developed in the 3m wide zone parallel to the lag) already show intense shearing, most likely due to seismic events in the stope, it is difficult to determine if preconditioning has caused any further

shearing. However this seems unlikely as fractures do not show any major variations in appearance in preconditioned and unpreconditioned areas.

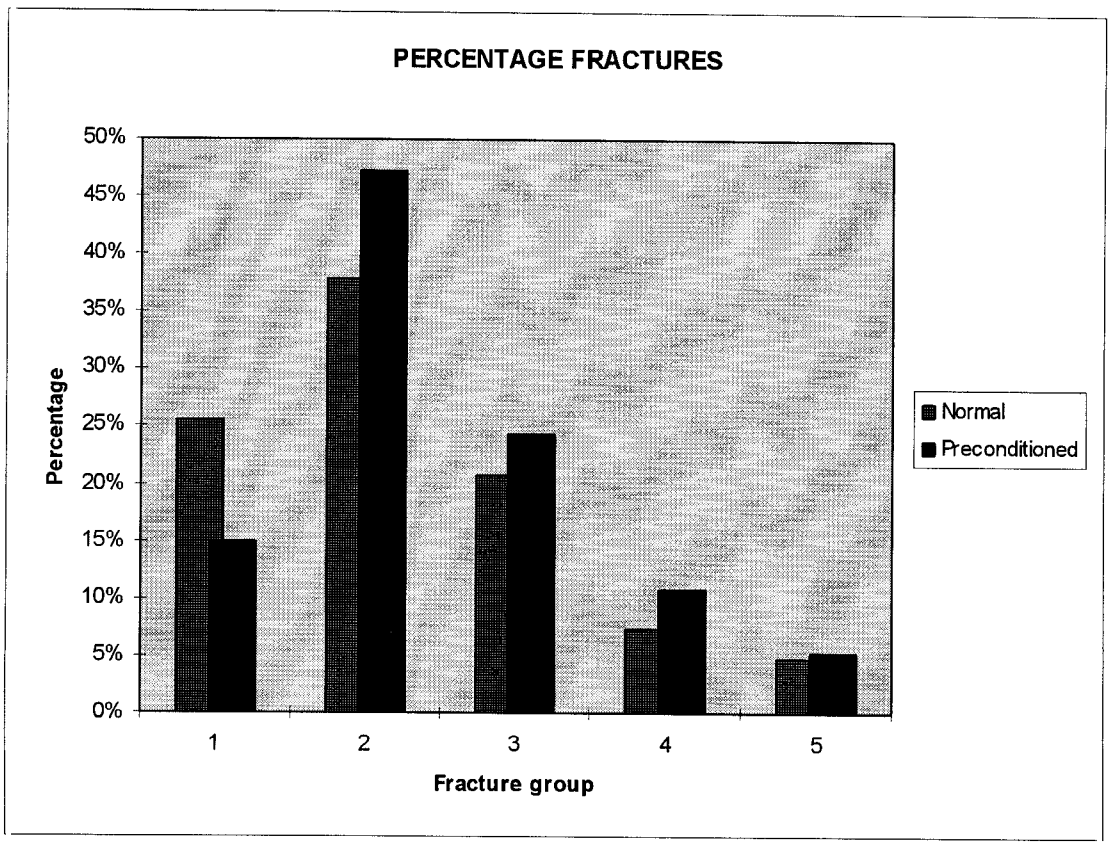

Figure 4.12: Graph showing relative abundance of the various fracture groups in normal and preconditioned areas. Note the increase in Group II fractures and decrease in Group I fractures

Preconditioning does not cause the development of new fracture sets. Rather, the relative abundance of pre-existing fracture sets is modified (Figure 4.12). In preconditioned areas, there is better clustering of the fractures into groups. This suggests that preconditioning actually reduces the randomness of fracturing by enhancing the fractures in certain specific orientations.

Group I fractures show a decrease in occurrence in the preconditioned area, most likely due to separation on the reef-hangingwall contact induced by the preconditioning blast. In contrast to this there is a definite increase in abundance of Group II fractures. This increased abundance is not due to the development of new fractures, but rather the extension of small pre-existing fractures by the preconditioning and later the production blast. Group IV and V fractures are thought to be formed when blocks created by Group I and II fractures lock against one another and the compressive forces cause further fracturing. However in preconditioned areas it is thought that this occurs further ahead of the face.

It could be argued that preconditioning initiates fracturing that merely lies parallel to pre-existing fractures. King and Sammis (1992) show that brittle deformation exploits either pre-existing or deformation induced points of weakness. They term these "starter defects". The stressed zone of intense face parallel fracturing due to the creation of a void by mining is riddled with such deformation induced defects (as well as pre-existing fractures). A preconditioning blast detonates within this zone. It therefore reasonable to assume that the blast would exploit these points of weakness when causing further fracturing. Indeed, there is evidence (such as shearing of pre-existing joints) that pre-existing planes of weakness are indeed re-activated.

In conclusion it appears that the mechanism of stress redistribution by preconditioning is through the enhancement and remobilization of pre-existing fractures and not via the development of unique sets of faults, joints or fissures.

4.2.5 Worker Perceptions

The benefit of preconditioning is the reduced risk of face bursting following the implementation of preconditioning This also has the added benefit that the attitude of the people in the stope improves resulting in a more efficient workforce. In one stope, the preconditioning technique has been referred to as "the jumpers that stop the bumps" and in another, production personnel said they would never go back working as before preconditioning was introduced. (This further illustrates the importance of having a subjective evaluation process or people's attitudes and how they change as preconditioning is introduced.)

4.3 COST ANALYSIS

The success of the implementation of preconditioning on a large scale in South African gold mines is dependent upon the economic viability of the technique. Even if a rockburst control technique can be proven to drastically reduce the risk of face bursting, its implementation will only be limited to very high grade areas if the costs cannot be kept to a minimum. The cost analysis presented here compares the actual cost of materials as supplied to Western Deep Levels South Mine for preconditioning with the actual 1995 escalated stoping costs as supplied in early November 1995.

This analysis contains several assumptions which are considered entirely realistic and based on information and studies carried out by the mine's industrial engineering personnel. The main assumptions include the following:

- stoping costs are based on information from stores requisitions
- no additional material waste due to the additional work of preconditioning
- preconditioning holes are considered safety holes and no additional money (in the form of bonuses) will be paid for drilling them
- no additional labour is provided to drill the holes
- preconditioning is currently taking place in a pack supported stope; costs will reflect the difference between this and backfilled stopes
- there is no variation in the 1995 escalated and 1996 base labour costs

The average stores costs can be divided into the following general categories and quoted in terms of Rands per centare mined (Table 4.V). Certain costs cannot be separated from stoping and development operations and they are therefore not considered in any part of this analysis. These include mainly pumping, compressed air and transportation costs.

Table 4.V: Average cost for timber supported stopes (stores and labour).

R 18.96 /ca	Explosives
R 5.20 /ca	Drilling - steels only
R 123.85 /ca	Support - timber and other
R 38.90 /ca	Other - incl. trackless equipment, services, scraping, etc.
R 186.91 /ca	Stoping stores costs (subtotal)
R 195.72 /ca	Labour costs - stoping
R 382.63 /ca	Total stoping costs

A detailed labour cost break-down was not provided for 1995 but a planned average stoping cost for 1996 (included labour) was obtained from Industrial Engineering personnel. From the average stoping costs for timber and backfill supported stopes and assuming that backfill accounts for only 10% of stope support, the average labour cost can be estimated (assuming

escalated 1995 and planned 1996 costs are equivalent). The break down of costs is summarised in Table 4.V.

The stope in which preconditioning is being carried out is being blasted with fuse and igniter cord, although there is work towards changing to an electronic system with millisecond delays. Cost calculations are based on the fuse initiation system. The implementation of preconditioning with such an initiation system has resulted in the entire panel changing to longer fuses to prevent confusion during charging operations. The assumptions regarding the implementation of preconditioning are listed below:

- the entire panel uses 2.1m long fuses (1.2m originally)
- the same explosive is used in the preconditioning holes as production holes (Powergel 816)
- every preconditioning hole is tamped
- preconditioning holes are drilled to 3.0m
- 38mm knock-off bits can drill 60m before being replaced
- each drill stem lasts for 210m
- the rock drill is the new Seco Nova 70 that is expected to replace the existing 815 model. This is depreciated over 5 years.
- production holes are 1.15m long, with 30 holes/shift for 20 shifts/month

The cost to drill one preconditioning hole based on the assumptions above are given in Table 4.VI

Table 4.VI: Normalised cost to drill and blast one 3.0m preconditioning hole

Explosives:	Powergel 816 -15 cartridges 25mm x 200mm	R 6.00
	Fuse 2.1m long	R 1.47
	Tamping - 8 clay cartridges	R 1.16
	subtotal - explosives	R 8.63
Drilling:	38mm bit	R 2.02
	3.0m drill stem	R 2.05
	Rock drill	R 0.62
	subtotal - drilling	R 4.69
	Total cost of one preconditioning hole	R 13.32

To extend these costs into one full production blasted shift, it is assumed that the face length is 15m requiring, five preconditioning holes and 60 production holes (Table 4.VII). The production blast results in a 1.0m average face advance (as is currently being achieved with preconditioning). The cost per blasted shift is shown in Table. The cost per centare of preconditioning is only R 5.88. Table 4.VIII compares this to the cost of stoping in terms of stores costs only and total cost including labour. Since it is assumed that there is no additional labour involved with preconditioning, the additional cost to the normal stoping operation is only 1.5%.

Table 4.VII: Total cost of preconditioning for one production blast

Five preconditioning holes	R 66.60
Additional cost of longer production fuses	R 21.60
Total preconditioning cost per blast	R 88.20
Preconditioning cost per centare	R 5.88

Table 4.VIII: Comparison of the cost of preconditioning to normal stoping costs

	Stoping cost (R/m²)	Cost increase with preconditioning
Preconditioning cost	5.88	
Stoping stores cost	186.91	3.1 %
Total stoping cost	382.63	1.5 %

It has been observed that the average face advance per blast prior to preconditioning of a panel was 0.7m. This has now increased to 1.0m face advance. This increased face advance will result in a considerable improvement in the productivity and thus a reduction in production cost. A 43% improvement in face advance does not however relate to an equivalent reduction in stoping costs as some items are not affected by production rate, such as support and cleaning costs. The costing areas noted in Table 4.V that are affected by the increased productivity include drilling, blasting and labour. Table 4.IX compares the total cost of the implementation of preconditioning including the cost benefit obtained by the increased face advance. A final stoping cost reduction of R 60/m² or 15.7% is being achieved in the preconditioning panels at the mine.

Table 4.IX: Comparison of total costs per centare with and without preconditioning

	Stoping cost without preconditioning	Stoping cost due to improved productivity with preconditioning	Cost of preconditioning	Total stoping costs with implementation of preconditioning
Drilling	R 5.20	R 3.64	R 1.56	R 5.20
Blasting	R 18.96	R 13.27	R 4.32	R 17.59
Other stores	R 162.75	R 162.75	-	R 162.75
Labour	R 195.72	R 137.00	-	R 137.00
Total	R 382.63	R 316.66	R 5.88	R 322.54

5. PRECONDITIONING TO TRIGGER LARGE SEISMIC EVENTS

The potential for triggering large seismic events as a result of preconditioning has, to date, only been studied at the Blyvooruitzicht Gold Mine 24-17W experimental preconditioning site (see Section 3). Since the change to breast mining at this site in September 1992, 48 large ($M \geq 1.0$) seismic events have been recorded from the 17-24W preconditioning site. Of these, 45 were located less than 50 metres ahead of the stope face (the other three events were located within the core of the pillar, between 50 and 100 metres ahead of the faces). More than half (24) of these 45 events occurred during blasting time and the majority of the remainder occurred within a few hours thereafter. In fact, some 40 of the 45 events were associated with a clearly recognisable trigger mechanism, in the form of preconditioning or production activity. The remainder resulted from the accumulation of stress via time-dependent effects at work in the rock mass ahead of the advancing faces. Only four larger events took place during the day shift, when workers were present in the stope, and none of these resulted in injury to any of the workers. Table *5.I* summarises the various triggering conditions associated with the large events.

Table *5.I*. Occurrence of large ($M \geq 1.0$) seismic events at 17-24W preconditioning site.

	Number of events	Percentage of total
Recorded preconditioning blasts	7	15.6
Triggered (precon only)	5	11.1
Triggered (precon & production)	2	4.4
Triggered (production after precon) [1]	5	11.1
Not directly triggered (after precon) [1]	1	2.2
Subtotal: Related to preconditioning	**20**	**44.4**
Triggered (production only)	21	46.7
Not triggered	4	8.9
Total within 50 m of stope face [2]	**45**	**100.0**

[1] within 2 days of preconditioning blast
[2] excludes 3 events in core of pillar

From Table *5.I*, it can be seen that 44.4 per cent of the 45 larger seismic events were associated with preconditioning activity in some way. This included the blasts themselves being recorded as large events as well as the direct or indirect triggering of separate large events by preconditioning. On the other hand, 46.7 per cent of the larger events were triggered by production blasting. Given that there have been 51 preconditioning blasts set off at the site in the time period under consideration, compared with six times that number (317) of full-face production blasts, the preconditioning has clearly been more efficient in terms of the triggering of larger seismic events, and thereby the controlled release of stored strain energy from the rock mass, than has normal production activity. Table *5.II* compares the preconditioning and production triggering rates in more detail.

Table *5.II*. Occurrence of larger ($M \geq 1.0$) seismic events in association with preconditioning and production activity.

		Triggering blasts	Total blasts	Triggering percentage
Preconditioning	Panel 1	[1] 2	19	10.5
	Panel 2	[1] 6	22	27.3
	Stub	[1] 2	10	20.0
	Total	**10**	**51**	**19.6**
Production	Panel 1	1	[2] 104	1.0
	Panel 2	13	[2] 108	12.0
	Stub	8	[2] 105	7.6
	Total	**21**	**317**	**6.6**

[1] includes $M \geq 1.0$ blast events
[2] full-face blasts only

While the numbers in Table *5.I* are given in terms of the total number of large events, those in Table *5.II* are given in terms of the total number of preconditioning and production blasts associated with those large events. On several occasions, single preconditioning or production blasts have triggered multiple large events. From Table *5.II*, it is clear that preconditioning blasting is more efficient than production blasting in terms of the triggering of large seismic events. Also, for both preconditioning and production, blasts in panel 2 have the highest yield of large events, while those in panel 1 trigger large events very seldom. This result is clearly related to the fact that the rock mass ahead of panel 1 carries significantly less load than that ahead of panel 2, and that the regular preconditioning of panel 1 has resulted in the effective redistribution of stress from panel 1 into panel 2.

The stress transfer associated with a preconditioning blast can be readily deduced from a study of the spatial migration of microseismicity induced by the blast. The triggering of larger events by production blasting, on the other hand, seems to be a complicated function of the production history of the stope prior to the events. This triggering appears to depend on such factors as the production rate, the sequence of production from one panel to another, and the time-dependent effects which operate in the rock mass between production blasts.

Clearly, well controlled preconditioning blasts do act to redistribute stresses effectively and can also serve to control the timing of the release of stored strain energy from the rock mass. Poorly controlled preconditioning blasts, on the other hand, either do not redistribute stress effectively, or can act to induce unfavourable stress redistribution (i.e. moving the stress towards the face of the "preconditioned" area, rather than away from it). Actual preconditioning blasts which have been set off too far ahead of the face, in the region of highly confined rock, have not induced any observable stress changes in the rock mass. However, some larger seismic events which have located further ahead of the face than the usual position of a preconditioning hole have induced unfavourable stress redistribution by effectively "destressing" the source region and driving the stress back onto the closest panel face. While preconditioning clearly cannot control the larger-scale behaviour of the pillar (larger seismic events will continue to occur as the rock mass of the pillar responds to the stress changes induced by mining), preconditioning has been effective in the vicinity of the stope faces, both in terms of the relaxation of stress there and in terms of the creation of a "buffer" zone which serves to reduce the adverse effects of larger seismic events on the working areas.

6. SEISMIC TOMOGRAPHY

Tomography is a method in which data collected at the boundaries of a region are used to produce an image of some physical property within the region (Carneiro, 1995). Seismic tomographic imaging maps the spatial variation in some seismic property (typically, the P-wave velocity) of a rock mass. Velocity images can be used to infer variations in the state of stress throughout the rock mass, as velocity variations reflect differences in stress state: under high stress conditions, fractures are preferentially closed, which corresponds to an increase in seismic velocity (Maxwell and Young, 1995). According to Maxwell and Young, zones of concentrated seismic activity have been found to be associated with zones of anomalously high velocity, while low-velocity zones tend to be aseismic.

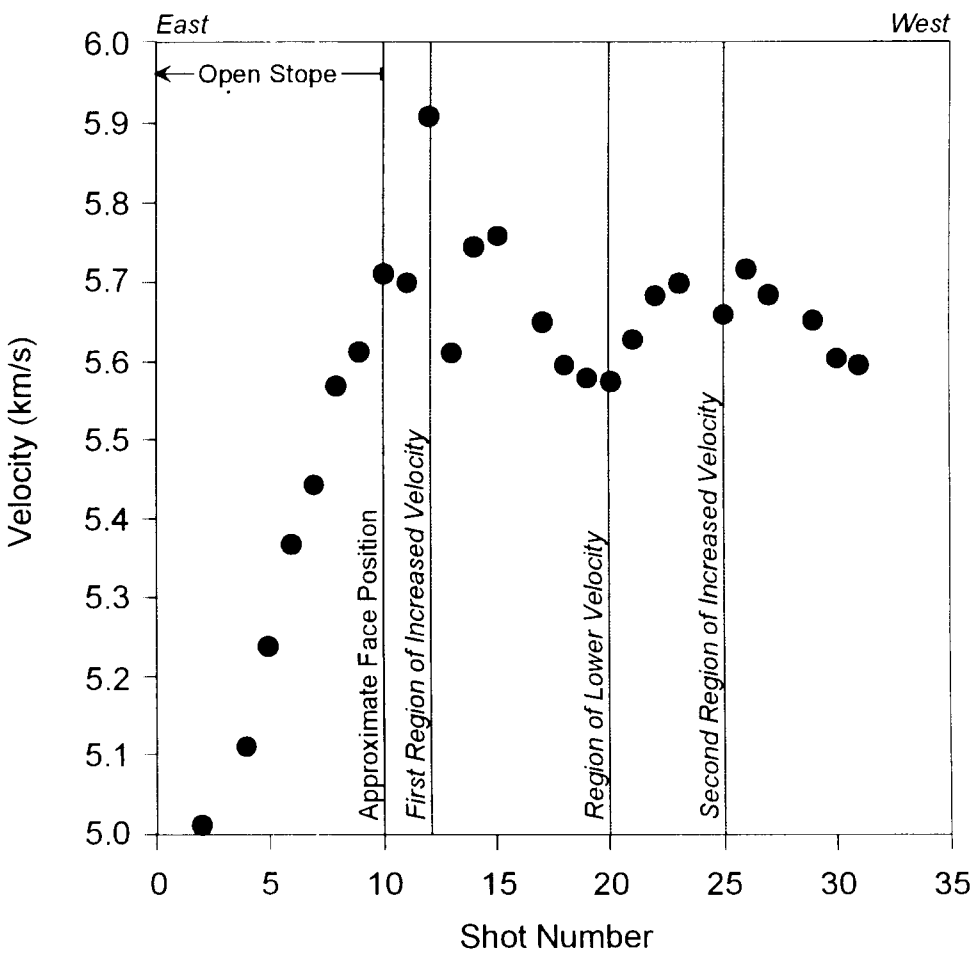

Figure 6.1: Plot of the straight ray apparent velocity measured between common shot and receiver hole numbers, showing the velocity variation from east to west (after Maxwell and Young, 1995).

A seismic tomography experiment was performed in March 1995 at Blyvooruitzicht Gold Mine to characterise the 17-24W stability pillar in terms of a controlled-source seismic velocity image. The velocity survey was repeated after the preconditioning blast in panel 1 on 6 March, 1995 in an attempt to assess the associated effects on the stress state of the pillar. The footwall and hangingwall drives to the north and south of the pillar were used for the survey. A series of 30 moderately downwards dipping three-metre long boreholes spaced at between two and three metres were drilled into the south sidewall of the footwall drive. Hydrophone sensors were placed in each of these water-filled holes. Similarly, a series of 35 upwards dipping boreholes were drilled into the north sidewall of the hangingwall drive. During the surveys, individual explosions (generated by single sticks of Tovex) were

detonated in each of these holes in turn. The blasts were recorded on a seismometer monitoring the hydrophone sensors and the exact detonation time for each blast was measured at the source. The acquisition geometry resulted in dense ray coverage of the survey area (Carneiro, 1995).

Some 1070 P-wave travel-times to each hydrophone were computed by visually picking the arrival-times (Maxwell and Young, 1995). Good signal-to-noise ratios and clear onsets were evident in the waveforms obtained from each sensor and the travel-times were accurately measured to within two samples on average (Maxwell and Young, 1995). Similar quality data were acquired from an accelerometer sensor mounted directly on the tunnel wall surface This showed that the fracturing around the tunnel extended beyond the ends of the hydrophone holes, so that similar signal attenuation was experienced at both sensor positions. This suggests that it could be feasible to use surface sensors in future surveys, which would speed up the data acquisition considerably.

Using the surveyed locations of the blast and sensor boreholes, the apparent velocities for the rock mass were computed on the assumption of straight ray paths between source and receiver through the pillar (Maxwell and Young, 1995). Significant velocity variations were detected in the pillar, with velocities of between 4.96 and 6.00 km/s being measured, the average value being 5.67 km/s (standard deviation 0.16 km/s). Figure 6.1 shows the variation in velocity from east to west, measured directly across the pillar between common source and receiver holes. A low-velocity zone in the east, corresponding to the open stope, is evident in the figure; ahead of the face (at approximately position #10 in the figure), there is a region of increased velocity, corresponding to the expected high-stress anomaly in the pillar. Beyond this (position #20), there is a region of lower velocity, followed by (position #25) a second region of moderately high velocity, which will be discussed later.

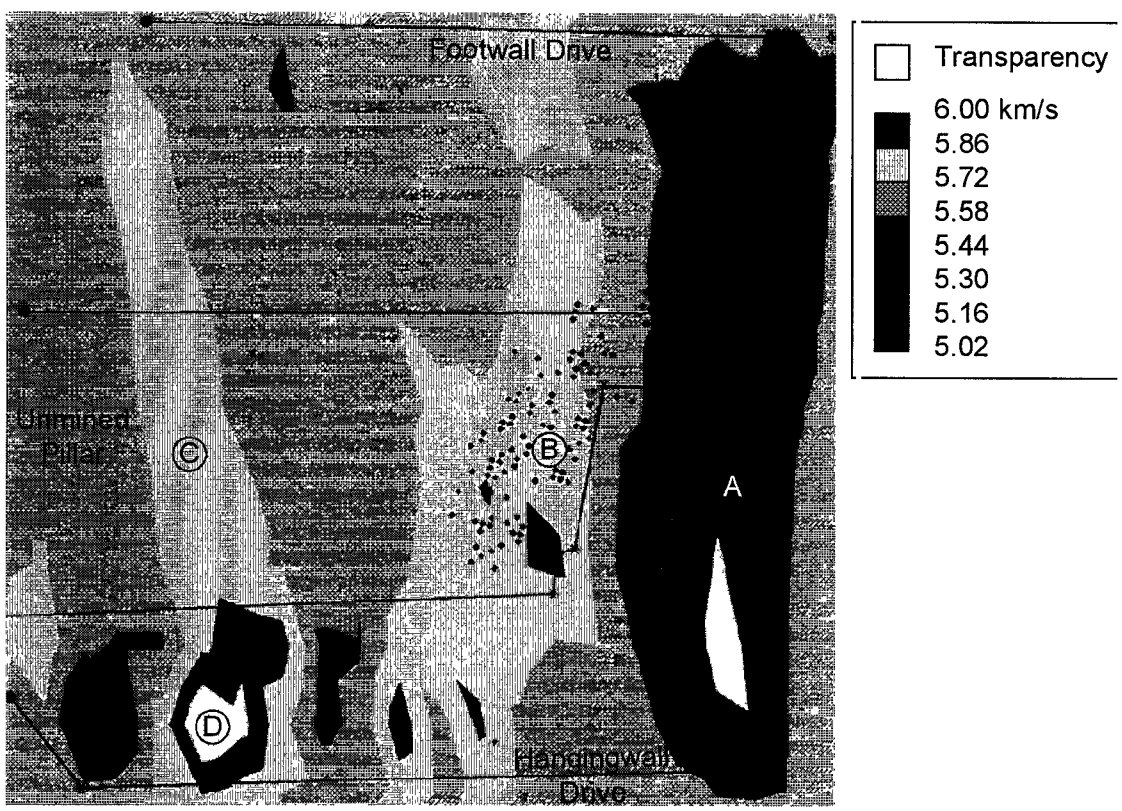

Figure 6.2: Straight ray velocity image produced from the seismic tomography survey. The tunnels used for acquisition are indicated, as is the outline of the unmined pillar. The locations of seismic events recorded during the period of the survey are shown by the small dots. The circled letters are at regions of interest discussed in the text. (After Maxwell and Young, 1995.)

A pervasive apparent-velocity anisotropy (i.e. the apparent velocity has different values in different directions through the rock mass) of some 7.5 per cent was found consistently throughout the data set (Maxwell and Young, 1995). The fast direction is parallel to strike, while the apparent velocity is slower in the dip direction. The anisotropy is most likely produced by the strongly developed alignment of fracturing which has been observed parallel to the top and bottom edges of the pillar. A correction was applied to the data to minimise the influence of the anisotropy on the inversion to the velocity image.

A velocity image with a 5-by-10 metre resolution (Figure 6.2) was produced by inverting the travel-times. The maximum estimated stochastic errors were 0.1 km/s and these were reduced to 0.06 km/s in the relatively well-resolved central portion of the image (Maxwell and Young, 1995). The image shows low velocities in and around the open stope (Feature 'A' in Figure 6.2), where the ray paths either propagated through the (closed) excavation or were diffracted around the stope face. According to Maxwell and Young (1995), the low-velocity anomaly is smeared to the footwall and hangingwall drives due to the limited ray path coverage in the corners of the image.

A high-velocity region extends from north to south across the pillar ahead of the stope face in the image (Feature 'B' in Figure 6.2). This increased velocity can be attributed to the expected stress increase ahead of the advancing face. The mining-induced seismicity recorded by the monitoring PSS during the period of the surveys tended to concentrate in this high-velocity region, as can be seen in Figure 6.2. The highest velocities were found in the southern portion of this region, ahead of the face between panel 2 and the advance heading (stub). This is an area of the pillar which is believed to be ineffectively preconditioned due to the geometries of the panel 2 and the stub preconditioning holes as well as the influence of the stemming at the collars of the holes. It was the site of a large (M=2.3) damaging seismic event in April 1994, after the stub was preconditioned out of sequence before the preconditioning of panel 2. This appeared to add to the stress concentrated in the area and trigger the failure of the instability.

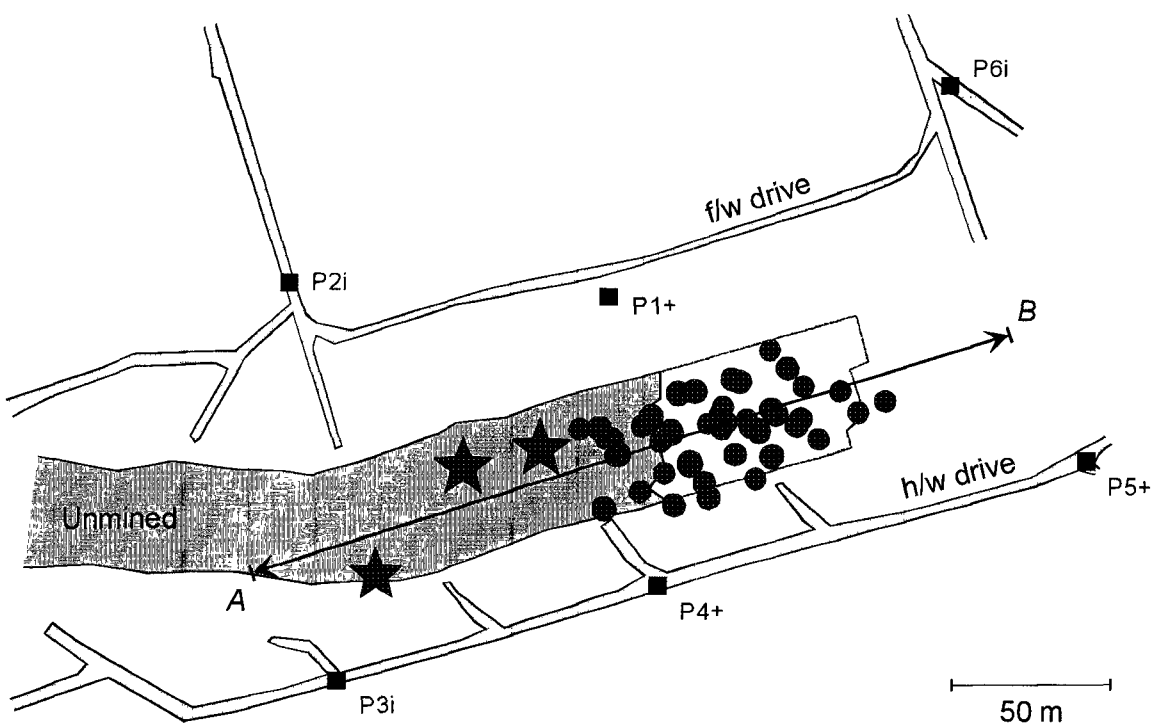

Figure 6.3. Plan of the locations of the larger seismic events (filled circles) recorded from the BGM 17-24W preconditioning site during breast mining. The three events discussed in the text are shown as filled stars. The line *A–B* is the section line used for Figure 6.4. The position of the stope faces at the start of the time period is shown by the dashed line.

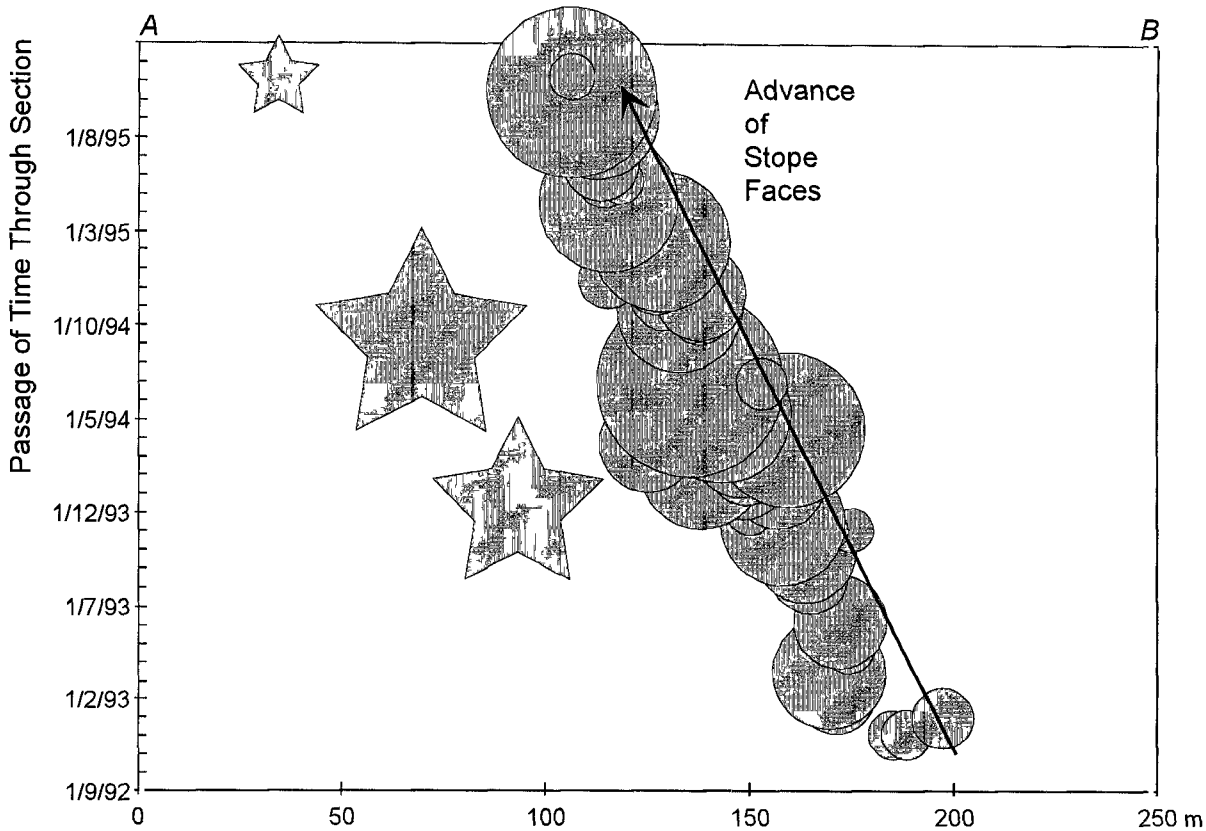

Figure 6.4: Time-section along line *A–B* of Figure 6.3. The larger seismic events associated with the advancing stope faces are shown as filled circles, while the three events discussed in the text are shown as filled stars.

Within the pillar, the image shows a second moderately high velocity anomaly, roughly 50 metres ahead of the stope face (Feature 'C' in Figure 6.2), which appears to correspond to a secondary stress anomaly. Both of the high-velocity regions extend from the footwall drive to the hangingwall drive in the image: according to Maxwell and Young (1995), ray path smearing was to be expected in the north-south direction from the acquisition geometry. A secondary cluster of seismic activity has been observed within the core of the pillar. Figure 6.3 shows the locations of the larger (M>1.0) seismic events which have been recorded by the PSS since the change to a breast-mining geometry at the site. Figure 6.3 shows the locations in plan, while Figure 6.4 shows a time-section in which the locations of the events through time are projected onto the line *A–B* (Figure 6.3). As can be seen in Figure 6.3, most of the events located in the pillar ahead of and relatively close to the advancing stope faces, while the three events highlighted in the figure located between 50 and 100 metres ahead of the faces. This observation tends to confirm the presence of the secondary high-velocity anomaly in the image (Figure 6.2), and suggests that this secondary region of stress concentration has been advancing with the stope faces through time, possibly indicating a degree of progressive failure of the core of the pillar.

The series of alternating high- and low-velocity regions along the southern boundary of the image (Feature 'D' in Figure 6.2) appear to be localised, near-shot velocity variations; the average velocities show a similar, consistent trend over a number of shot holes (Maxwell and Young, 1995). The velocity anomalies are thought to coincide with regions of relatively more and less fractured rock between the hangingwall drive and the pillar.

Carneiro (1995) reprocessed the travel-time data, using a curved ray tracing algorithm (which caters for the effects of refraction of the seismic waves as they pass through the rock mass

between source and receiver). The 5-by-10 metre pixels used by Maxwell and Young (1995) were thought to introduce interpolation-related numerical artifacts into the resulting image. The resolution of the image was improved by subdividing the surveyed area into 1-by-1 metre pixels, ensuring that almost every pixel was crossed by at least one ray path. The resultant image (Figure 6.5) is similar to that produced by Maxwell and Young, but without the interpolation artifacts and with a clearer definition of the high-velocity regions.

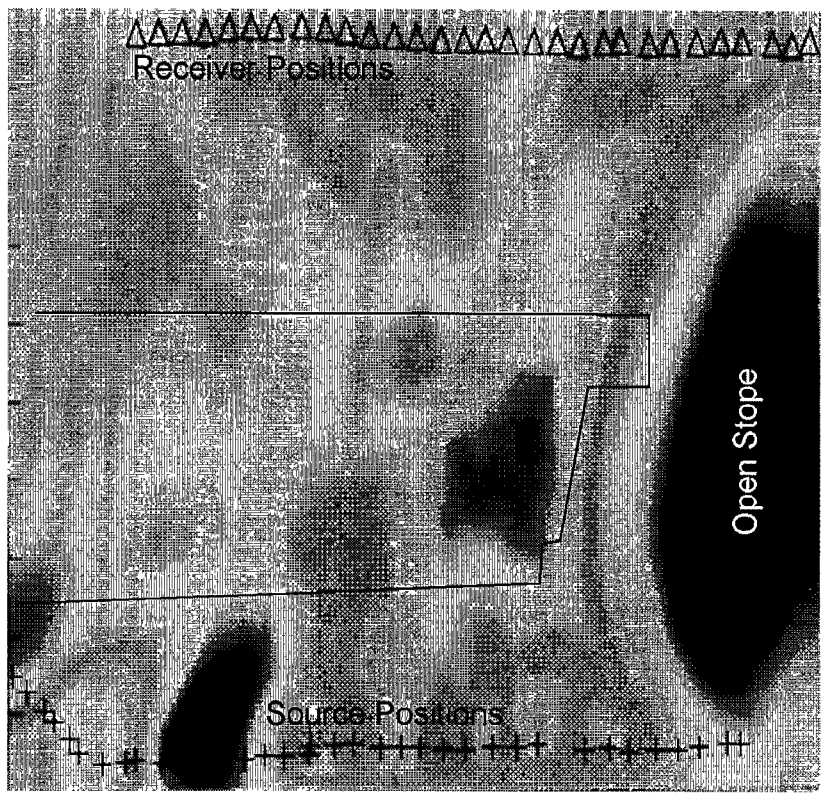

Figure 6.5: Velocity image of Figure 6.2 reconstructed using curved ray tracing. Higher velocities are represented by shades of red, lower velocities, by shades of blue. (After Carneiro, 1995.)

The velocity survey was repeated after the preconditioning blast of 6 March in panel 1. According to Maxwell and Young (1995), the preferred method for computing velocity changes between consecutive surveys is to invert the travel-time changes measured by cross-correlating common ray paths (i.e. comparing the waveforms on a mathematical basis). This is thought to be more accurate and precise than simply subtracting the two velocity images, each of which has its own relatively high errors.

Unfortunately, the source explosions for the tomography did not generate signals with the desired degree of repeatability (the local fracturing produced in the boreholes by the repeated blasts resulted in variations in the energy transfer from the explosive to the rock). The estimated data uncertainty was thus of the same order as the observed variability in the measurements, so that there was considerable uncertainty as to whether any significant velocity changes would be detectable with such imprecise measurements (Maxwell and Young, 1995).

The imaged velocity changes (Figure 6.6) shows velocity variations from -0.22 km/s to +0.20 km/s (measured with respect to a datum of 5.65 km/s), with an estimated maximum error of 0.16 km/s (0.08 km/s in the centre of the image). The alternating high- and low-velocity regions at the northern boundary of the image (Feature 'A' in Figure 6.6) are thought to be

noise-related, as the anomalies are smaller than the error in this portion of the image and are thus not significant. However, the velocity increase of 0.12 km/s near the top of the pillar (Feature 'B' in Figure 6.6) is probably significant (being larger than the error in that portion of the image), and indicates an increase in stress ahead of panel 1 and into panel 2 as a result of the transfer of stress away from the vicinity of the preconditioning blast. The seismicity recorded by the PSS after the preconditioning blast migrated away from the blast location in panel 1, as shown in Figure 6.7, confirming the interpretation of stress transfer by preconditioning.

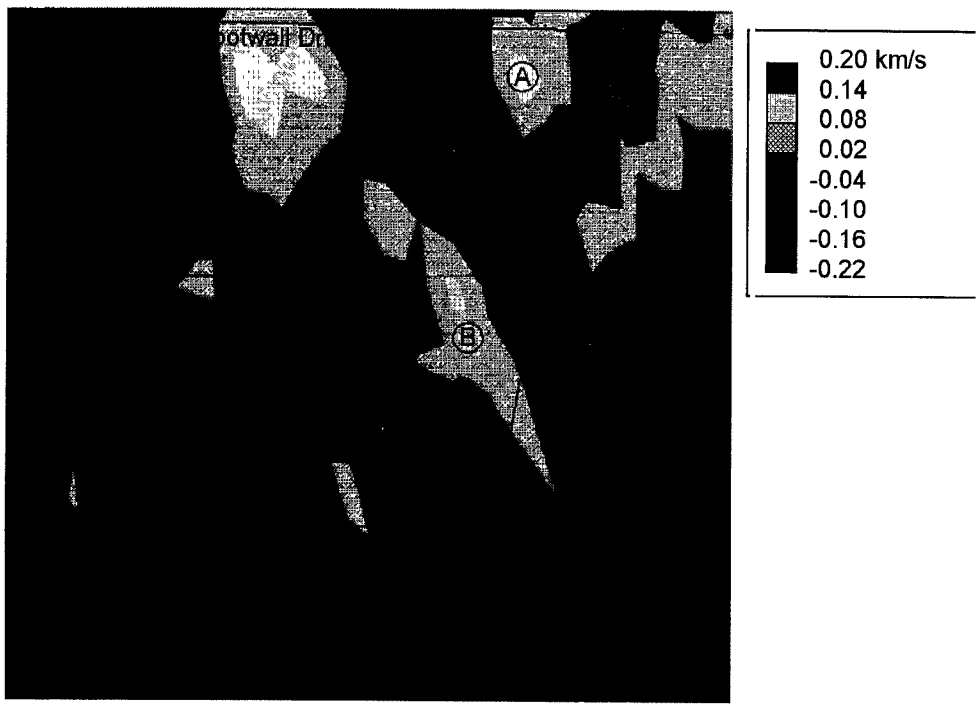

Figure 6.6: Straight ray tomographic image of the velocity change following the preconditioning blast. The circled letters are at regions of interest discussed in the text. (After Maxwell and Young, 1995.)

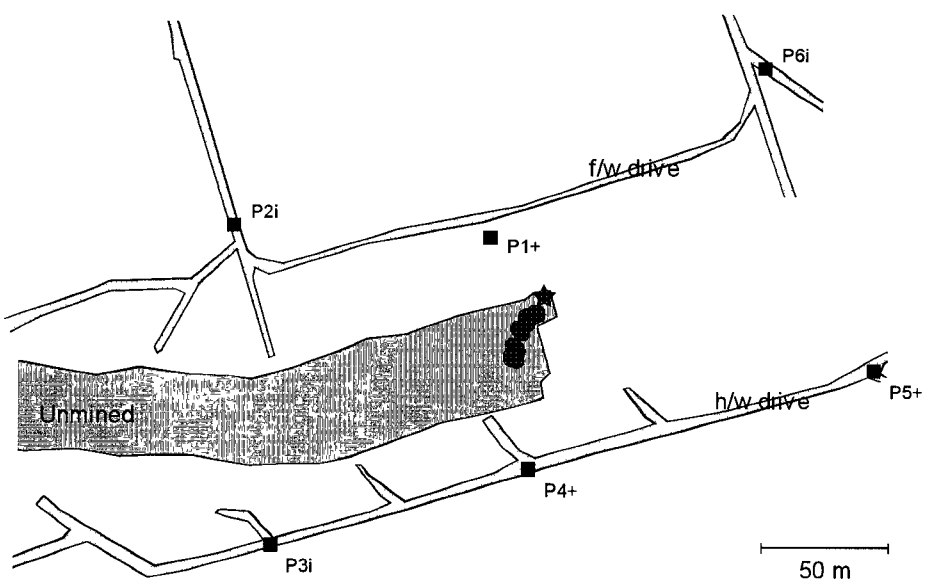

Figure 6.7: Plan of the seismicity (filled circles) recorded after the preconditioning blast (filled star) discussed in the text.

7. NUMERICAL MODELLING

The main thrust of the numerical modelling in this project area has been intended to address three separate but related issues concerning preconditioning. These are:-

- the effect of a single preconditioning blast in a bedded but intact highly confined rock mass
- the mechanism by which a preconditioning blast affects the rock mass ahead of a mining face
- the influence of geological joints and the fractured rock mass around a stope face has on the tendency for face bursts to occur

The first issue involved the use of three separate computer programs in pursuit of the necessary answers. As will be discussed below the approach was not able to solve the problem that was posed. In fact no computer program or combination of currently available programs could be acquired to fully address the problem at hand.

In the case of the second aspect, the work has concentrated on modelling the effect of a gas blast in a stressed rock mass ahead of a stope face. Two factors of interest were investigated: the mechanism of preconditioning, and the effect of the position of a face parallel preconditioning blast on the efficiency of the preconditioning process.

In the third category of research discontinuum modelling has been used to investigate the mechanics of mining in a fractured rock mass and how face bursts develop in this environment.

7.1 PRECONDITIONING IN CONFINED ROCK

The computer program DIGS (Discontinuity Interaction Growth Simulation) (Napier, 1991, Napier and Hildyard, 1992 and Napier and Pierce, 1995) was used to simulate the propagation of multiple fractures from a blasthole due to the gas pressure generated by the explosive charge. In order to do that a two dimensional displacement discontinuity method was used to model a plane perpendicular to the borehole axis, in which vertical fractures may propagate.

A series of DIGS models were formulated to determine which physical parameters significantly affected the growth of the fractures and the change in field stresses in the vicinity of the blasthole. In all these models the tensile growth criterion was used. Another objective of this study was to simulate the underground experiment at West Driefontein Gold Mine undertaken in 1993, and re-evaluate the results obtained from this study and to gain an understanding of the blasting mechanism as well as the factors involved in the process.

According to the numerical procedure for modelling the fracture growth process, each fracture is modelled as a series of displacement discontinuity boundary elements that are joined end to end to form the fracture path in an incremental growth sequence. Each crack tip is advanced incrementally in a direction that maximises the specified growth criterion and fracturing is assumed to continue from an existing crack tip if a specified failure criterion is met at a designated point ahead of a crack tip.

The blast is simulated by applying a gas pressure on each of the faces of a fan of cracks emanating from a point. To avoid the complexity in description of pressure- time history for blast loading, it was assumed that all the points on the blasthole walls in contact with the entire length of charge will be loaded with the same pressure at any instant in time. Multiple fractures are checked sequentially for crack growth, and segments are added until the rupture criteria is no longer exceeded. Following the growth of fractures from the extremities of the pressurised cracks, the blast pressure is removed from the fan and is replaced by a residual opening dilation on each crack.

Various models were designed by changing the inclination of bedding planes (0, 30, 60, 90 degrees) and blast pressure (500 or 1000 MPa) (Appendix D Figures 1 to 30). The friction angle and the cohesion for the bedding planes were assumed as 30 degrees and zero respectively. All other relevant parameters were assumed according to the field data (Table 7.I).

Table 7.I. Parameters used for DIGS Models

Field Stresses	σv= 100 MPa, σh= 50 MPa
Rock Properties	E= 71.9 GPa, ν= 0.23
Growth Elements	Non-mobilised, C=50 MPa, ϕ= 37° Mobilised, C= 0 MPa, ϕ= 37°
Bedding Planes	C= 0 MPa, ϕ= 30°, Spacing = 30cm (No, 0°, 30°, 60°, 90°)
Blast hole	Fan shaped 12 growth elements (Each 10cm long)
Blast Pressure	500 or 1000 MPa

The numerical modelling (DIGS) results (Given in Appendix G) show some degree of similarity with the field observations. Longer blast induced fractures were observed in the direction of maximum principal stress and the stress field around the blast hole was changed both in magnitude and direction.

Figure 1 of Appendix G shows the stress field around a blast hole for the model with no bedding plane and it is clear that the change in the orientation of the principal stresses is controlled by the stress field (i.e. the longer blast induced fractures in the direction of major principal stress). However ,in the other models, it seems that re-orientation of the principal stresses is mainly controlled by the orientation of bedding planes (Appendix G: Figures 6, 11, 21 and 26). The contour plots of principal stresses of each model have shown in Appendix G: Figures 3, 4, 8, 9, 13, 14, 18, 19, 23, 24, 28 and 29. The very high stress concentrations are observed in immediate vicinity around the blast hole in the models with 500 MPa blast pressure regardless of the bedding plane orientation, but it is transferred further away in the model with double blast pressure (Appendix G: Figure 16).

The blast induced fractures are generally captured between nearest bedding planes. In other words the blast damage to the surrounding rock was limited in the same stratum where the blast took place. Since this is not the case in the model with double blast pressure, it is clear that 500 MPa blast pressure was not sufficient to grow fractures further after they intersect the bedding plane. As it was expected, the blast induced fractures are extended by doubling the blast pressure (Appendix D: Figure 16). The 0 and 90 degrees models showed relatively longer blast induced fractures parallel to the bedding planes.

The displacement vector plots of each model are presented in Appendix D: Figures 5, 10, 15, 20, 25 and 30. The maximum displacement calculated for 500 MPa models is 2mm and for 1000 MPa model is 5mm.

7.2 THE MECHANICS OF PRECONDITIONING

Rorke and Brummer (1988) proposed two possible mechanisms to explain the process of preconditioning. These mechanisms are:-

1. The explosive energy generates fractures in the intact rock immediately ahead of the fracture zone which alter the rock's properties and lower its load carrying ability. As the stope faces approach this blast-fractured rock, it will yield under the increased load and thus encourage shear movement between blocks of rock in the hangingwall and footwall and result in further propagation of mining-induced fractures.

2. The explosive energy breaks asperities and locking mechanisms in the fractured rock thus encouraging shear movement and the growth of the fracture zone under mining-induced stresses.

They went on to suggest that each mechanism would be favoured by a different drilling position. It was proposed that a blast placed ahead of the mining induced fracture zone would favour the first mechanism and a blast detonated within the zone of fracture ahead of the stope face would result in the second mechanism.

Practical considerations concerning the field experiments with preconditioning at the Blyvooruitzicht Gold Mine (described in a previous chapter of this report) dictated that research should concentrate on one or other of these methods. The question was: which was the most likely mechanism to provide the more efficient preconditioning. This posed an ideal challenge for a modelling exercise.

Both mechanisms have many things in common but of greatest significance to solving the particular problem posed was the fact that both involve the interaction of a fractured or fracturing rock mass with an explosive detonation. Hence, the numerical analysis had to be able to incorporate a reasonable representation of fractured rock and a detonation. At the time four main numerical modelling packages were available for use in the analysis. These were:-

- Minap : a two dimensional static, linear, elastic boundary element code that allows for the representation of a limited number of explicit, non-intersecting rock fractures or stopes using displacement discontinuity elements.

- Minsim-D : a three dimensional version of Minap.

- FLAC : a two dimensional continuum finite difference code developed for the analysis of non-linear behaviour in granular materials such as soils. Full dynamic analysis is possible (Itasca, 1992).

- UDEC : a two dimensional distinct element / finite difference code developed for the analysis of non-linear behaviour in jointed rock masses. Full dynamic analysis is possible (Itasca, 1993).

FLAC was ruled out as a potential candidate for the analysis as it is essentially a continuum code and could not represent the fractured rock mass in a manner necessary to address the problem. The geometry initially described by Rorke and Brummer (1988) was a two dimensional slice through a stope face. Inspection of the situation at the Blyvooruitzicht Gold Mine field site confirmed that it could be represented as a two dimensional plane strain problem at least to a first order of approximation. For this reason the use of Minsim-D was ruled out in favour of the potential use of Minap. The effect of detonating an explosive charge in a fractured rock mass could be simulated in Minap by applying normal tractions to the displacement discontinuity element to represent an internal gas pressure produced by the explosive. However, Minap cannot easily handle multiple intersecting fractures. The UDEC program was designed to simulate the behaviour of jointed or fractured rock. In addition to this, pore pressures can be applied directly in the domains that represent the fractures. For these reasons UDEC was chosen as the tool for this analysis.

The rock mass ahead of a stope face was modelled as an assemblage of more than 5 000 small triangular blocks(Figure 7.1) that were internally elastic (Kullmann, et al, 1995). The blocks themselves were closely packed and able to slip on joints governed by a cohesionless Mohr-Coulomb law (a friction angle of 30°). Alternatively the blocks are able to separate as the joints have no tensile strength. The reasoning behind using a block assembly that has no cohesive or tensile strength is that it was intended to represent the fracture zone ahead of a deep-level mining stope where the rock has already failed.

The blast was modelled as a pore pressure applied within the joint domains as a step function. In order to compare the effects of preconditioning at different positions ahead of the stope face the pore pressure was applied to different regions of the block assembly representing the reef horizon for a number of different simulations.

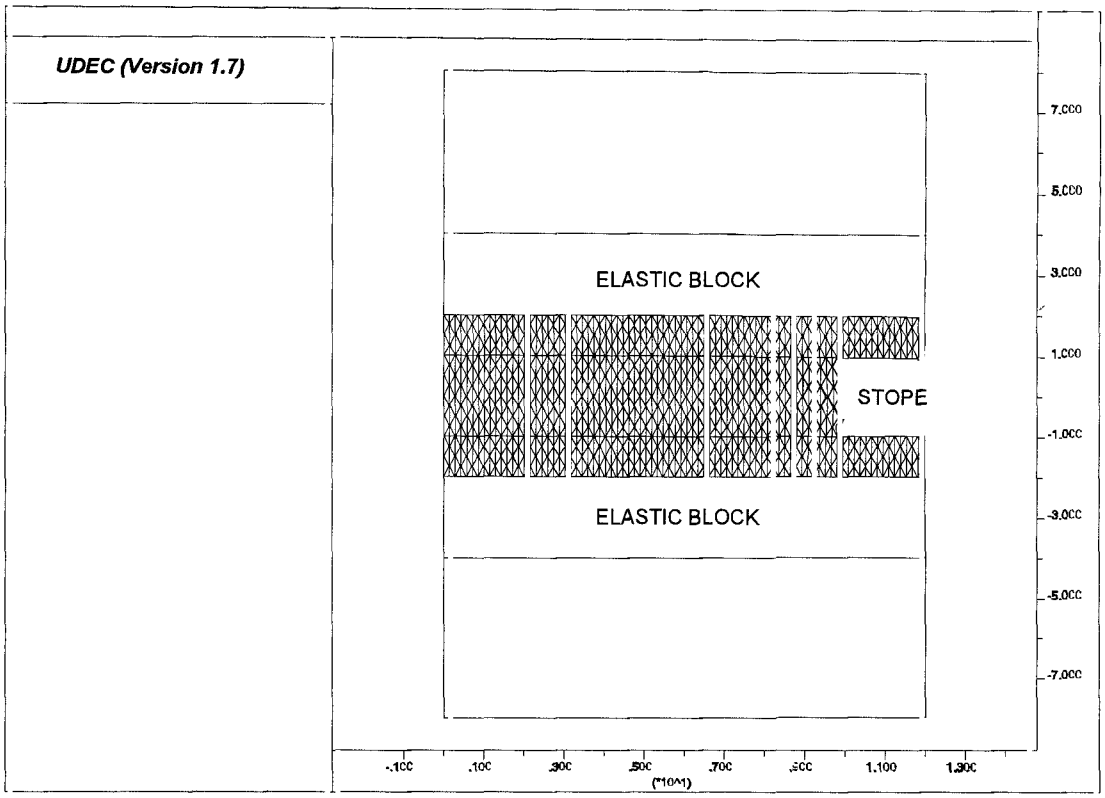

Figure 7.1: The mesh used for the "preconditioning" analyses. Only the rock mass in the immediate vicinity of the reef horizon is modelled as a blocky assemblage. The rock mass above and below this zone is represented by elastically deformable plattens.

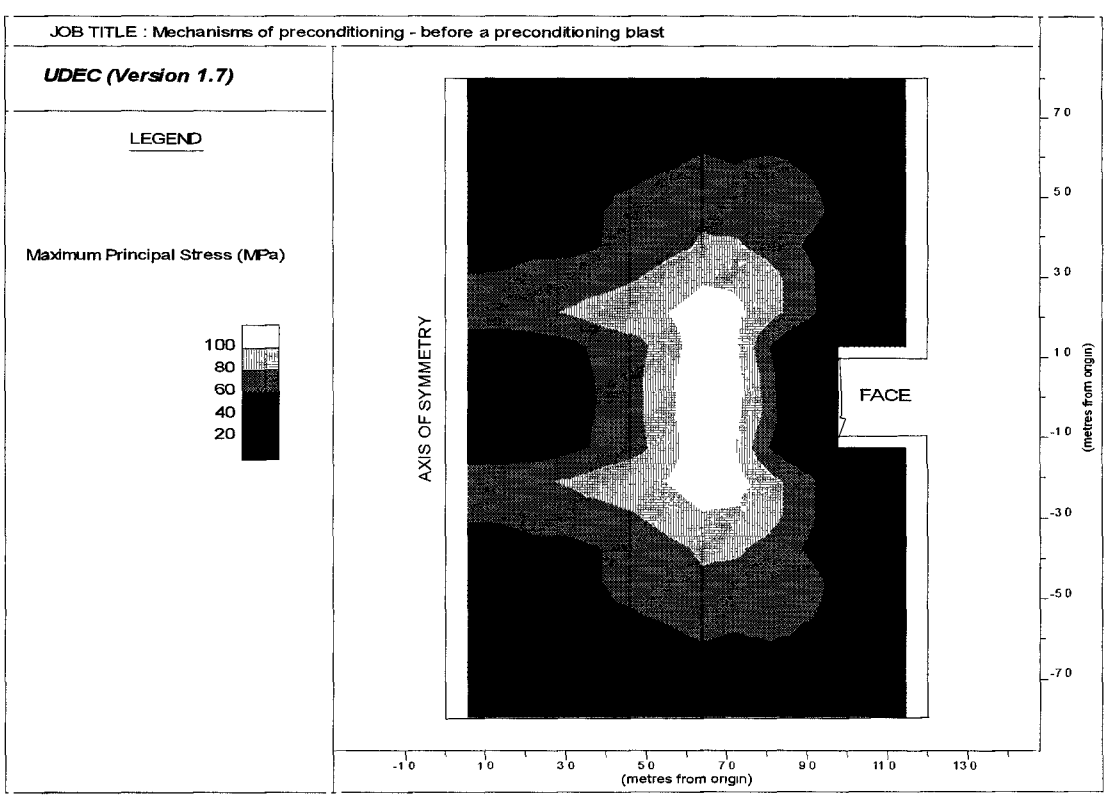

Figure 7.2: Maximum principal stress contours in an unaltered discontinuum model. The stress peak occurs roughly 5m behind the face. The lobes trailing off to the left are artifacts of the mesh but are acceptable within the constraints of the analysis.

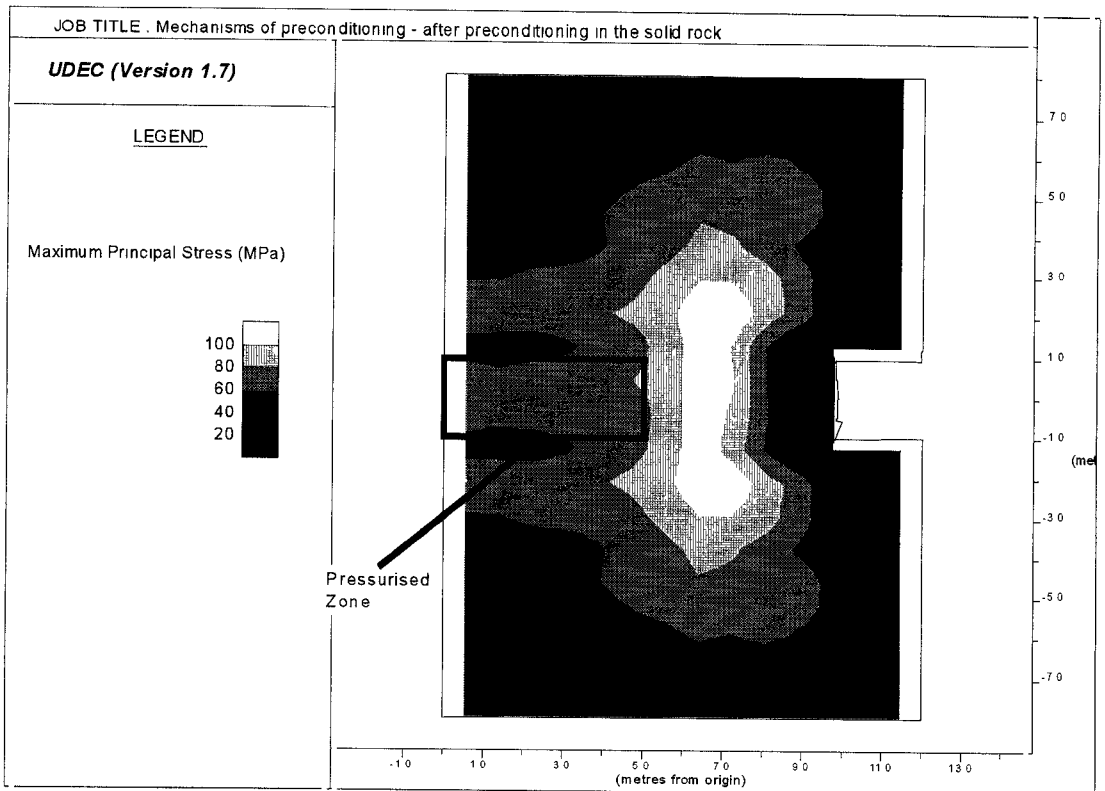

Figure 7.3: Contours of maximum principal stress after applying a pore pressure to the confined rock well ahead of the stope face. There is little difference between this situation and that prior to "preconditioning" (Figure 7.2).

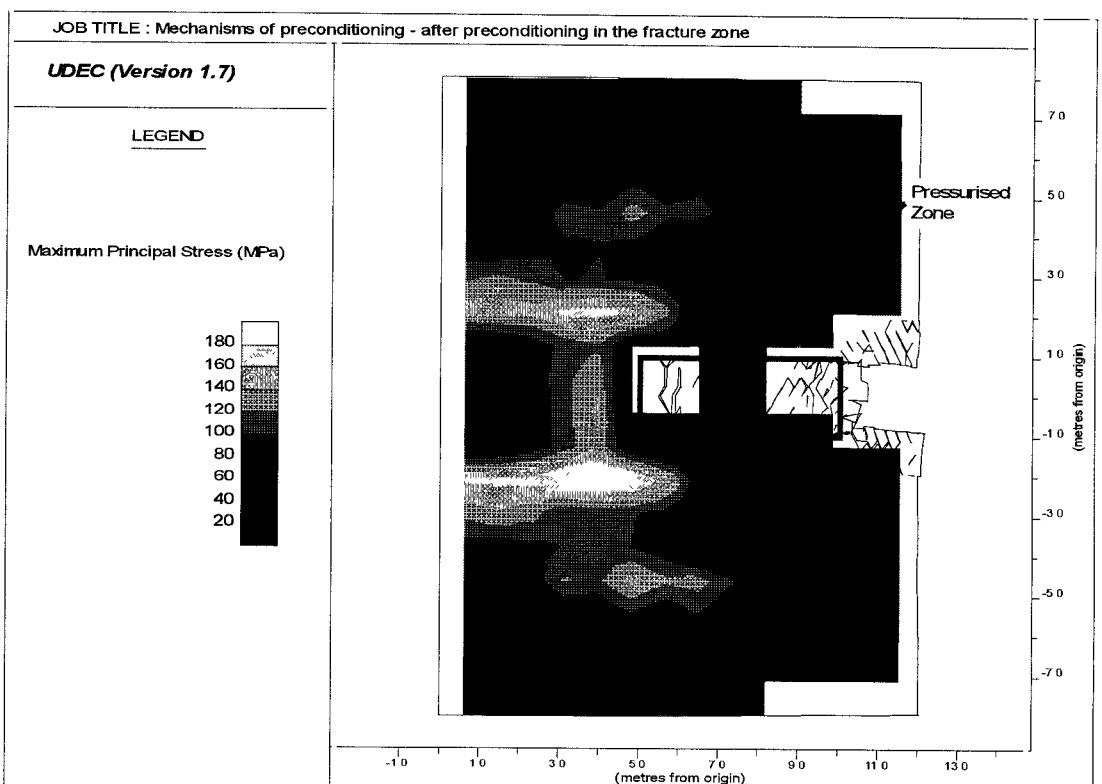

Figure 7.4: Contours of maximum principal stress after applying a pore pressure in the fracture zone immediately ahead of the face. The stress peak has been transferred further ahead of the face than without the "preconditioning" (compare to Figure 7.2).

Initially, the intact block assembly was brought to equilibrium under an applied vertical load of 50MPa and a horizontal confining load of 25MPa. A small region of the reef horizon blocks were then removed to simulate a mining face. The assembly was again cycled to equilibrium and the stress state ahead of the face was determined at this point (Figure 7.2). A pore pressure was then applied to a region between 5 and 10 metres ahead of the face to simulate a preconditioning blast in the solid relatively far ahead of the face. Again the model was brought to equilibrium and the new stress state was determined (Figure 7.3). A second blast simulation was performed in which the pore pressure was applied to the between 0 and 5 metres ahead of the face to simulate the preconditioning in the fracture zone immediately head of the face. Again the system was brought to equilibrium (Figure 7.4).

The difference between the results in figures 7.3 and 7.4 results from the preconditioning blast being located in the fracture zone immediately ahead of the stope face and interacting directly with the high stress peak found in the discontinuous rock mass ahead of the face. In addition the blocks effected by the applied pore pressure have a free face providing a void into which large scale dilation can occur.

Subsequent to the simulated preconditioning blast close to the stope face it is clear that the over-burden load being carried by the blocks representing the reef horizon is the same before and after the blast. What has happened is that load has been shifted from the preconditioned rock mass to the blocky system further ahead of the face. This work is reported in more detail in Kullmann, et al, 1995.

7.3 FACE BURSTING IN A JOINTED ROCK MASS

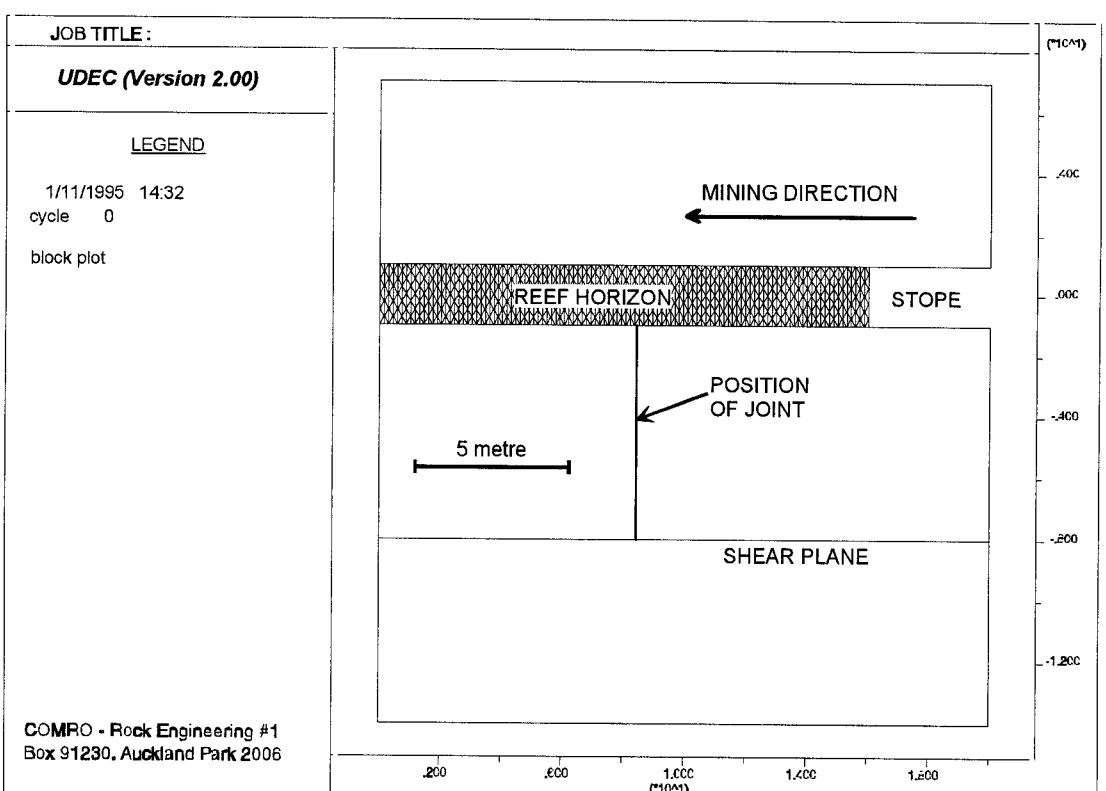

Figure 7.5: The block assembly used in the joint stope interaction analyses. The Footwall joint did not exist in the first phase but was present in the second phase of the simulations.

Field evidence from the Western Deep Levels South Mine suggested that the frequency and magnitude of face bursts that had occurred previously at the site might be associated with geological jointing (Lightfoot, et al, 1994). It was postulated that geological joint sets oriented parallel to the overall longwall face orientation might be a contributing factor in the occurrence of face bursts. The situation is essentially plane strain and discontinuous and lends itself well to an analysis using UDEC.

Only the reef horizon itself was modelled as a blocky rock mass assemblage in order to reduce the time required for computational analysis. A 20 metre stope span was simulated that was mined progressively from right to left (Figure 7.5). The reef was mined in a series of 2 metre steps. In the first simulation both the hangingwall and the footwall were modelled as continuous elastic blocks. In the second phase of the analysis a joint was introduced in the footwall (Figure 7.5).

In the simulation without footwall or hangingwall joints the mining proceeded in a fairly stable manner. At the point at which the intact block assembly reached equilibrium (convergence stopped) a small amount of loose blocks were still being ejected from the face at relatively low velocities (Figure 7.6).

The simulation incorporating a footwall joint resulted in a very different picture. As the influence of the fractured face took effect on the footwall joint it began to slip causing compression on the broken rock mass in the face area. This resulted in a large disturbance at the face with a large amount of material being mobilised (Figure 7.7).

Geological joints are a potential source of amplification of face instabilities and should be considered as an integral aspect of mine design. In the second phase of the analysis described here the joints are implicitly oriented parallel to the "mining induced" fracture orientation: which is a worst case scenario. However, the plane strain analysis without jointing could be assimilated to a three dimensional analysis where the mining induced fractures are perpendicular to the geological joint sets: this is a best case scenario. In practice it would seem that the angle of incidence between geological joints and mining induced fractures may well be a contributing factor towards the incidence and severity of face bursts experienced on deep-level mines. This could have significant implications for mine design.

8. SEISMIC RISK ASSESSMENT

A seismic risk assessment method has been developed under the auspices of the preconditioning project. The aim of the risk assessment is to be able to quantify the level of risk of occurrence of damaging seismicity on a daily basis, so that workers can be withheld from the working areas during periods of increased risk. During such periods, steps could also be taken to address the problem by such means as preconditioning the stope face. There has been no attempt to develop a risk assessment based on a fundamental understanding of the mechanics of rockburst formation, as it is thought that the processes at work within a rock mass are too complex for such an approach to be viable. The approach that has been taken is to define the historical behaviour of the seismicity associated with damaging events and use those patterns as indicators of the probable evolution of large seismic events in the future.

Multiple, quasi-independent seismic parameters were included during the development of the method in order that various aspects of the rock mass behaviour associated with the formation of damaging seismic events might be incorporated into the risk assessment. Single parameters monitored in isolation have proved to be unsatisfactory indicators of risk, as they do not consistently display precursory behaviour prior to the occurrence of large seismic events.

The risk assessment method has been developed from the large database of seismicity established at the Blyvooruitzicht Gold Mine 17-24W preconditioning site. For the method to be applied to other mining sites, it would be necessary for those sites to have a long enough seismic record to enable the risk assessment parameters to be defined with adequate statistical confidence.

The development of the risk assessment method has passed through three phases. The first phase took place during the up-dip mining at the preconditioning site; the results from that analysis were described by Stewart and Spottiswoode (1993). After the change to breast mining, the method was applied to the database of seismicity recorded from the altered mining geometry; the results from that analysis were described by Stewart (1995). The method was then refined and further developed during the most recent phase.

One of the primary goals in the development of the method was to be able to minimise any loss of production necessitated by the identification of periods of increased risk. A 'gain' factor Γ was defined as

$$\Gamma = \frac{\varepsilon_R}{\varepsilon_T} \Big/ \frac{\tau_R}{\tau_T} \qquad (1)$$

where ε_R is the number of 'potentially-damaging' events that took place during a period of increased seismic risk,
ε_T is the total number of 'potentially-damaging' events in the data set,
τ_R is the number of days for which the seismic risk was determined to have increased, and
τ_T is the total number of days in the data set.

For example, if 40 per cent of the recorded 'potentially-damaging' events took place during some 20 per cent of the total time for which the seismic risk was determined to have increased (and which would, in practice, represent lost production time), the gain would be $\Gamma = 2$. Obviously, in the ideal case, a considerably greater proportion of damaging events would take place during periods of high apparent seismic risk than outside such periods. The lost production time need not necessarily reduce overall productivity, as the workers could still be productive away from the stope faces (for example, in ensuring the integrity of the excavation and of the support system). 'Potentially-damaging' events are defined as those within the area of interest which have a magnitude greater than some critical magnitude M_C often associated with damage to the working areas.

Stable fracture growth in front of an advancing stope face should result in regular extension of the fracture zone ahead of the face, dilation of the face towards the back area and a broad, low stress peak in front of the face. In contrast, instability in the development of fracturing in front of the advancing face could manifest itself through retardation of the extension of the fracture zone ahead of the face and/or reduction in the amount of dilation of the face (as existing fractures lock up against one another). Indications of the development of unstable stope fracturing would thus include changes in stope convergence-ride measurements, reduction in face dilation (possibly measured via sophisticated techniques such as digital photogrammetry), and various seismic measurements (b-values, spatial clustering of seismicity, S-to-P moment and energy ratios, stress drops, seismic attenuation, etc.).

Thus far, the parameters which have been included in the seismic risk assessment method are all derived from seismic measurements. It is intended to incorporate non-seismic parameters (such as convergence-ride measurements) in the future. The ten parameters which are currently in use are largely independent and reflect different aspects of the rock mass behaviour associated with large seismic events. All of the parameters were formulated so that their values would be expected to increase during periods of increased seismic risk.

Parameter *P1* is derived from Gutenberg-Richter frequency-magnitude statistics, which are described by the relation

$$\log N = a - bM \qquad (2)$$

where N is the number of seismic events of magnitude greater than or equal to M, recorded from a given area during a given time period, and
a and b are constants for that area and time period.

Parameter *P1* is proportional to the value of N determined at the critical magnitude M_C. Calculated from 30 events.

Parameter *P2* is derived from the fractal dimension of spatial clustering of seismicity, which has been found to decrease prior to large seismic events.

Parameter *P3* is derived from scaled peak particle velocities, is proportional to the extent of critically stressed ground.

Parameter *P4* monitors changes in stress drop of the recorded seismicity.

Parameter *P5* is derived from the intensity of spatial clustering of the seismicity, which has been found to increase prior to large events.

Parameter *P6* *is* derived from the S-to-P wave moment ratios.

Parameter *P7* is derived from the S-to-P wave energy ratios.

Parameter *P8* monitors variations in the degree of seismic attenuation by the rock mass.

Parameter *P9* is derived from the P-wave seismic viscosity (a measure which incorporates both seismic energy and seismic moment).

Parameter *P10* is derived from the S-wave seismic viscosity.

While parameters such as *P2* and *P5*, *P3* and *P4*, and *P9* and *P10* appear to be closely related to each other, their variations are, in fact, not well-correlated (i.e. the behaviour of one does not mirror that of another). This suggests that all ten parameters do behave independently, to a degree. Each parameter is thus useful as an indicator of a different aspect of the response of the rock mass to impending large seismic events.

The risk assessment method was developed by analysing the behaviour of the parameters on a daily basis, over the entire database of seismicity recorded during breast mining at the BGM 17-24W preconditioning site. The parameter values were determined from a certain number of events recorded from a specific area around the preconditioning site before 22:00 on each day. This was to simulate a routine implementation which would involve an assessment of the risk just prior to the night shift on any given day. The parameter values were determined from the ratio of the value calculated from 30 events and the value calculated from 200 events, in order to smooth the short-term fluctuations over a longer period of time.

The parameter values were then compared with the occurrences of potentially-damaging events recorded between 22:00 and 13:00 on the following day. This was so as to simulate the outcome of a risk assessment performed at 22:00 in terms of the seismic activity during the following working (night and day) shifts. Recorded preconditioning blasts were excluded from this analysis, as they typically generate seismic events with magnitudes greater than the critical magnitude, M_C = 0.0. The analysis was also split into two categories, according to whether or not a production blast had been taken in the stope on the day of the analysis, as such blasts have a significant effect on the recorded seismicity, which must be taken into account.

Each parameter was examined individually in this way, with 'critical levels' being assigned to each parameter in such a way as to maximise the gain, Γ, for that parameter. A 'critical level' is that value of a parameter above which the risk of damaging seismicity is judged to be significant. In the simulation of a routine risk assessment, the parameters were then combined in a single risk indicator, according to whether the values of a given number of parameters had all risen above their individual critical levels simultaneously. The use of multiple parameters in the risk assessment leads to an enhanced statistical confidence in the results of the analysis.

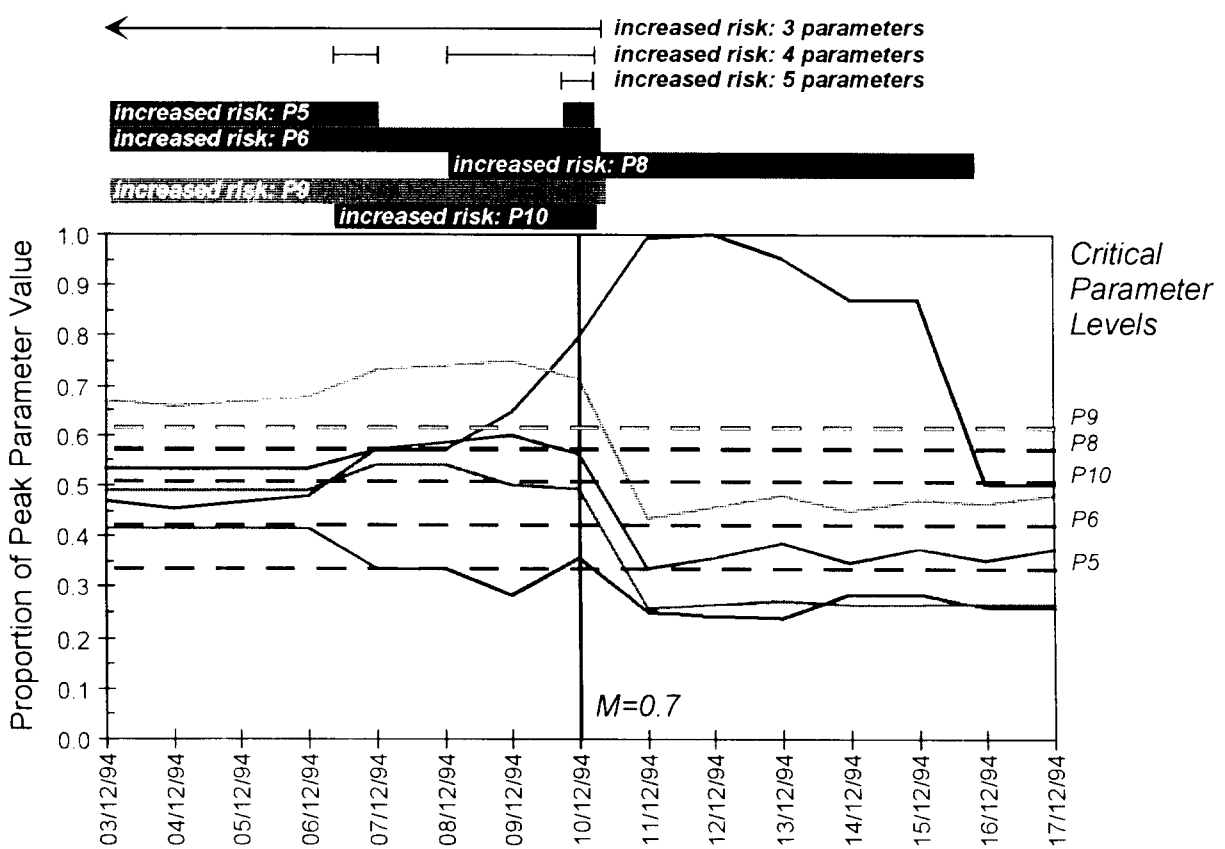

Figure 8.1 Variations in some parameter values during a two-week period. The time of occurrence of a larger seismic event recorded from the BGM 17-24W site is indicated, as are

periods of apparent increased risk for the parameters considered individually and in combination.

Figure *8.1* shows an example of actual parameter variations during a two-week period in December 1994. The maximum value of each parameter for the entire analysis period was scaled to unity. The critical level for each parameter is indicated in the figure, as is the time of occurrence of a recorded magnitude $M = 0.7$ seismic event. Clearly, the various parameters do exhibit different responses, indicating that each is responding differently to changing conditions in the rock mass ahead of the stope face.

At the start of the time period shown in Figure *8.1*, three parameters (*P5*, *P6* and *P9*) were all above their critical levels. This means that, if the risk assessment had been based on any three (or fewer) parameters being above their individual critical levels, the 'high-risk' period would have extended from before the start of this period up until shortly after the larger event. Between 6 and 7 December, *P10* rose above its critical level. If the assessment had been based on any four parameters, the 'high-risk' period would have started three days before the event (although *P5* dipped below its critical level between 8 and 9 December, *P8* rose to take its place at the same time). All five parameters were above their individual critical levels simultaneously only after 9 December (when *P5* rose back above its critical level). If the assessment had been based on any five parameters, the 'high-risk' period would have lasted just for the day of the event (between 10 and 11 December, four of the five parameters, all except *P8*, fell below their critical levels, signalling the end of any 'high-risk' period based on more than one parameter).

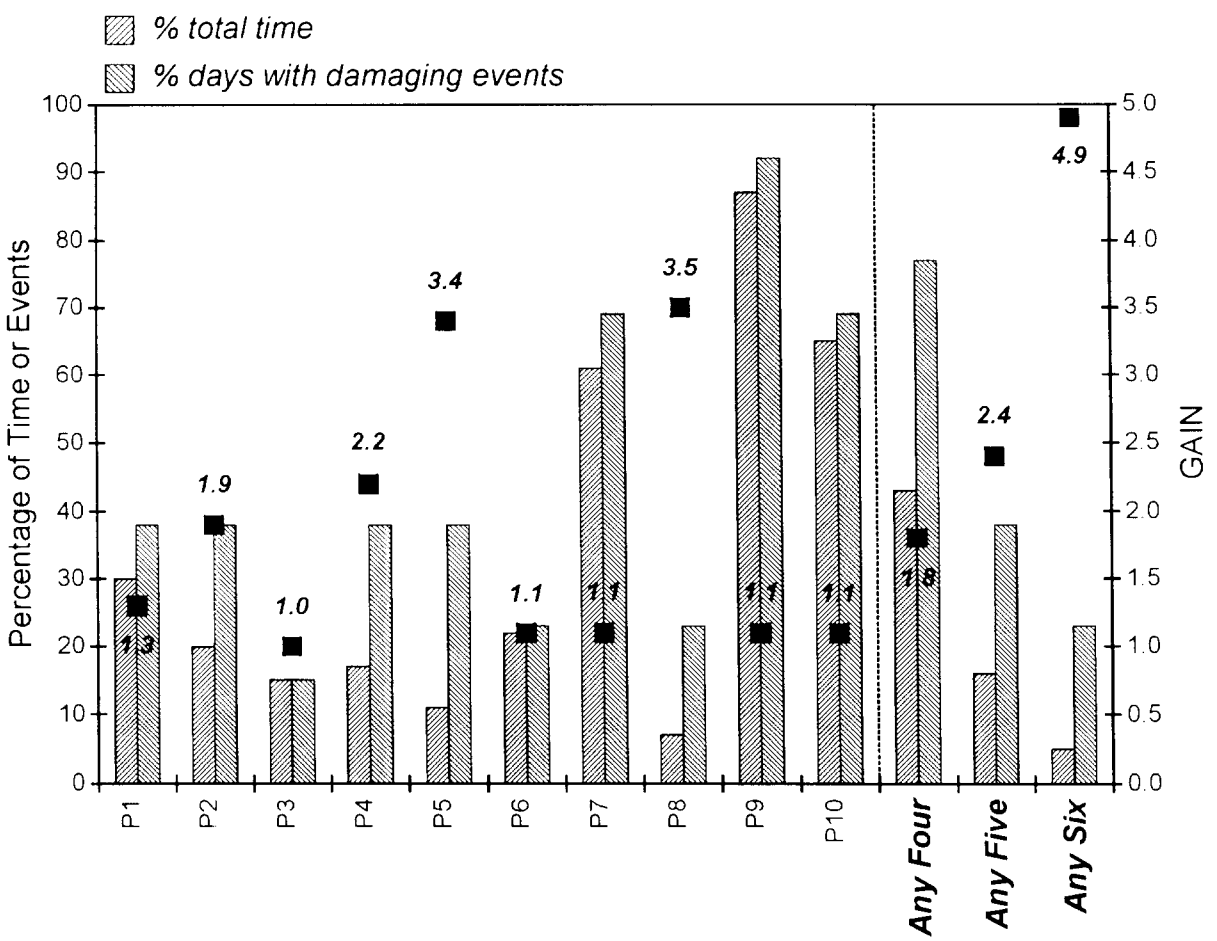

Figure 8.2: Results from the application of the risk assessment method to the entire seismic database recorded from the BGM 17-24W site, for the case of "blast yesterday".

Admittedly, this example was chosen for its efficacy, but it serves to illustrate the general principle. The loss of production time can be minimised by making the requirements for the 'high-risk' definition more stringent and thereby invoking the power of multi-parameter risk assessment. Unfortunately, as will be seen, the stricter the 'high-risk' definition, the fewer the events that are "captured" during the high-risk periods (i.e. the greater the chance of having a damaging event while workers are still in the working areas).

Figures *8.2* and *8.3* summarise the results from the analysis of the entire database, for the two categories of a production blast on the day before the day of the assessment (Figure *8.2*) and no blast on the day before (Figure *8.3*). The vertical bars for each parameter show the percentage of time for which each was above its critical level, and the percentage of the total number of potentially-damaging events which occurred during that time. The labelled points are the gain values (Γ, in equation 1). Clearly, some parameters (e.g. *P10*) captured a large proportion of events, but at a low gain (i.e. necessitating a substantial loss of production time), while other parameters (e.g. *P8*) achieved a high gain (i.e. operated very efficiently, with relatively small loss of production), but captured a smaller proportion of events. On the other hand, some parameters (e.g. *P3*) captured few events at a low gain, which would have rendered them useless, if not for their usefulness in combination with other parameters.

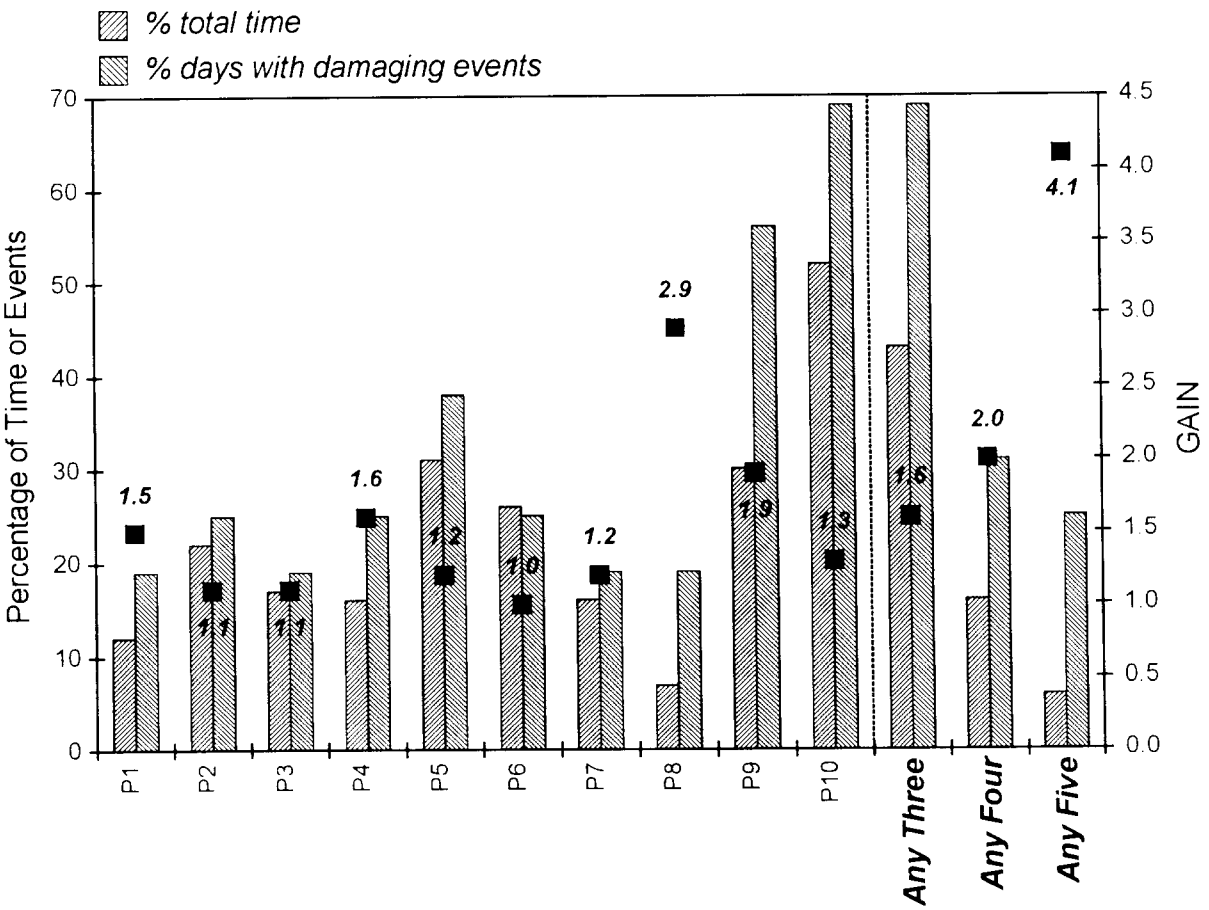

Figure 8.3: Results from the application of the risk assessment method to the entire seismic database recorded from the BGM 17-24W site, for the case of "no blast yesterday".

When the assessment was performed on the basis of multiple parameters being simultaneously above their individual critical levels, the trend is clear from Figures *8.2* and *8.3*: the more stringent the requirements (i.e. the more parameters that are required to be above their critical levels), the greater the gain (i.e. the smaller the loss of production), but the fewer the events that occurred during periods of 'high risk'. For a given proportion of lost time, the use of multiple parameters achieved better gains than those from any single

parameter acting in isolation. Prior to implementation of this seismic risk assessment method at any site with sufficient seismic coverage, a full analysis would have to be performed on the recorded database of seismicity from that site. A decision could then be made as to whether the gains would be good enough to justify the loss of a certain proportion of potential production time during periods of 'high risk' that should contain a significantly greater proportion of the total number of potentially-damaging events.

9. DISCUSSION

Although the fracture mapping and subsequent analysis of the Blyvooruitzicht Gold Mine (BGM) site has been extremely valuable the really exciting results are from the Western Deep Levels South Mine (WDLS). This is because it was possible to determine the nature of the rock fracturing in the region before preconditioning began and then repeat the process after it had been underway for some time. Five fracture groups were identified in the initial analysis prior to preconditioning and all five fracture groups were identified in the post-preconditioning panels. No new fracture groups were found to occur in the preconditioned panel. If the mechanism of preconditioning was primarily one of new fracture generation one would have expected to have found new fracture groups peculiar to the preconditioning panels. As this is not the case then it may be concluded that the most likely mechanism to describe the effect of the preconditioning blast on the rock mass is that of causing slip on pre-existing fractures. This concurs with the modelling work undertaken during the course of this project which predicted that slip on already existing fractures in the fracture zone ahead of the stope face would have the most significant preconditioning effect.

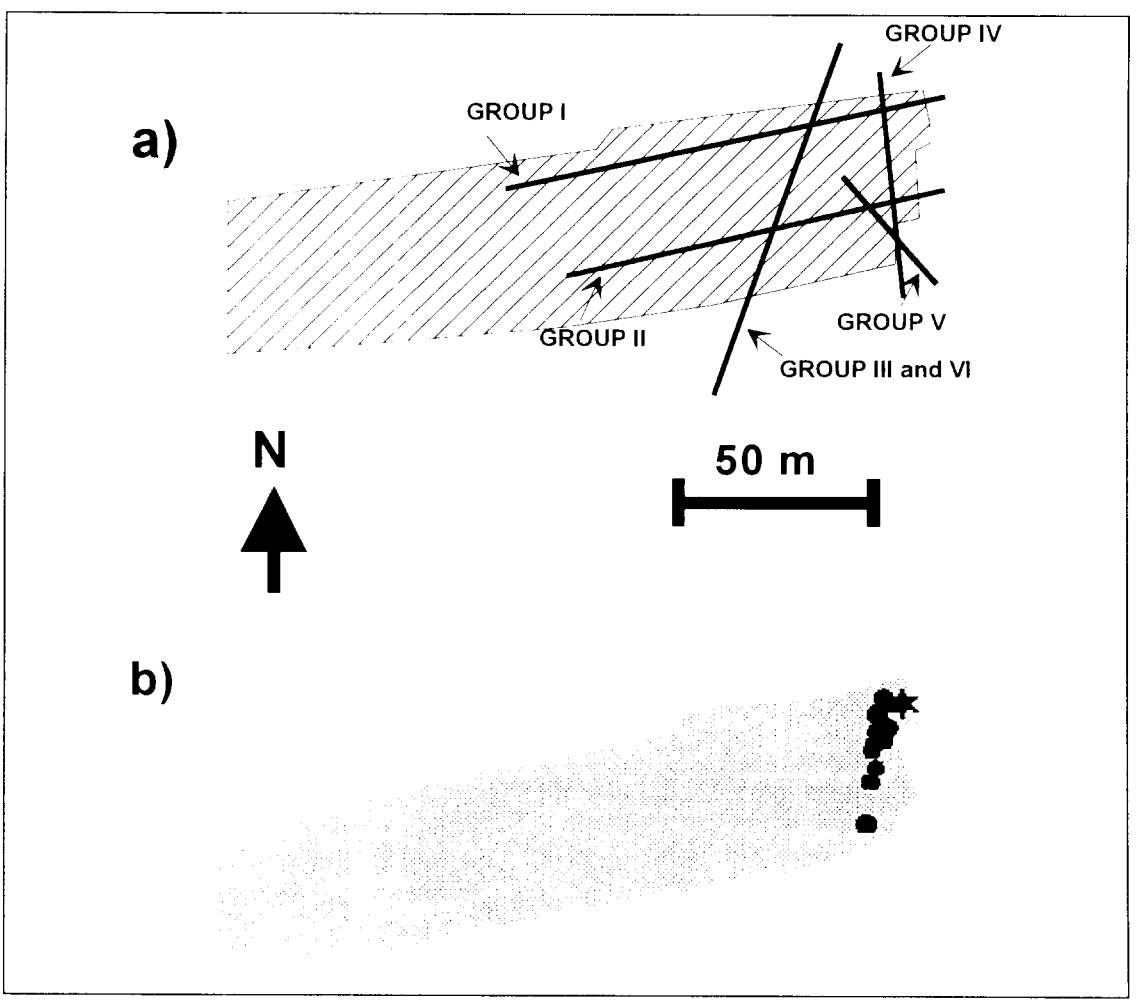

Figure 9.1a : Sketch plan showing the orientation of the various fracture groups in relation to the 17-24W pillar. Note the orientations of Group III and VI fractures
Figure 9.1b : Plot of seismic events (blue circles) recorded after a preconditioning blast (red star) showing the events propagating in the same direction as the Group III fractures

Although the evidence from the BGM site is less direct there are strong however an indication of re-activation of pre-existing fracture surfaces in the preconditioned area. This is most noticeable in the Group III fractures, with evidence of both horizontal and lateral movement at a later stage. Certain Group IV and VI fractures within the shear zones of

Group III change character from fine joints into millimetre thick bands of crushed quartzite gouge, indicating further movement has occurred along the fracture plane. There is strong evidence to suggest that the direction of propagation of seismic events directly after the preconditioning blasts are in the same orientation as that of the Group III fractures (Figures 9.1a and 9.1b). This further indicates that the mechanism of stress redistribution is by re-activation of existing fractures.

The way in which the preconditioning blast actually causes slip on the fracture surfaces is not absolutely certain. It would appear that there are two possible mechanisms. The first would involve the gas produced by the blast penetrating through the fractures at high pressure, reducing the effective stress acting across the fractures and, possibly, even propping them open. This could allow shear across previously jammed asperities enabling slip on larger areas of the fracture surface. The second mechanism involves the shake-up of the rock mass as a result of the blast. This could allow previously jammed asperities or lock-up points in the jointed rock mass to slip allowing for further slip across the whole fracture. The preconditioning could provide one or both of these mechanisms. Indeed, it appears that both mechanisms would operate but which is more dominant (if there is a dominance of one over the other) is unclear. Understanding the actual method on this scale is important to the optimal design of the preconditioning blast itself. If gas is the dominant mechanism then, clearly, a high gas generating explosive, or even a propellant, would provide for the most effective preconditioning of the rock mass. However, if shake-up is more important then an explosive producing a high degree of ground vibration is desirable.

The mechanics of preconditioning involves 'destressing' of the immediate rock mass as a result of local stress transferral. Local readjustments in the state of stress in the zone of fractured rock mass ahead of the face that is subjected to the preconditioning process results in the over-burden load it was carrying prior to the blast being shifted to adjacent areas of the rock mass outside the direct influence of the preconditioning blast. The benefit to the mining personnel is that a low stressed 'cushion' of rock is produced in the immediate stope face. High stress in the immediate face that results in face bursts in non-preconditioned stopes is no longer present and hence the incidence of face bursting is drastically reduced.

The effect of preconditioning is very localised. In order to avoid a face burst on a specific face the face itself must be preconditioned. This was well illustrated at the WDLS preconditioning site on the 87/49 Longwall west when a large magnitude seismic event (M=2.0) which was located very close to the preconditioning panel (West 4) occurred on 25 July 1995. Although significant damage was observed in the both the adjacent West 5 and West 3 panels there was no damage to the preconditioning panel.

Although the most controllable effects of preconditioning are local it has been seen to have a more wide spread effect on occasion when large events occur subsequent to a preconditioning blast (Section 5). The most likely cause of these large events either immediately after a preconditioning blast or some time later (sometimes hours) is related to the stress transferral occurring in the rock mass. The preconditioning blast initiates the immediate transferral of load from the preconditioned rock onto the adjacent rock mass. However, if this adjacent rock mass was already highly stressed and in a condition of unstable equilibrium then it will also undergo a phase of readjustment. This readjustment results in a further stress transferral onto other adjacent rock. This process can propagate through the rock mass in a form of 'chain-reaction' as local zones of rock readjust and re-equilibriate. Ultimately the system as a whole must once again reach a state of equilibrium but if in the course of this transition to a new equilibrium state a large local instability is encountered then a large seismic event can be initiated or 'triggered'.

There is clearly a physical mechanism that can be invoked to explain how preconditioning blasts sometimes trigger large seismic events. However, such a mechanism involves a highly complex, fractured and fracturing rock mass ahead of the stope face. Such complexity makes it hard to foresee a time when it will be possible to predict whether a given preconditioning blast will trigger an event or not. For this reason triggering should not be considered a goal of the preconditioning process but rather an added benefit should it occur.

The effect of preconditioning is localised both in space and time. As the mechanism of preconditioning is one of stress transferral resulting from induced deformations in the fracture zone ahead of the face rather than one of actually modifying the material properties of the rock the zone that is preconditioned is still capable of carrying high loads. After a face has been preconditioned it is possible that subsequent mining will result in the transfer of stress back onto the preconditioned rock mass if nothing is done to prevent it. An example of just such a situation occurred in August 1995 on the WDLS 87/49W longwall.

Preconditioning of the original longwall panel (Panel 'E') began on 23rd May 1995 and continued for approximately 10 weeks. The accelerated advance rate on this panel resulting from preconditioning caused it to advance more rapidly than was planned. As a result of this the panel was stopped on the 14th August 1995 to allow the re-establishment of the correct face sequence. Mining continued on the adjacent panel (Panel 'F') and the closely neighbouring panel (Panel 'C'). Preconditioning of Panel 'C' began on 28th August. On the 31st August, some two weeks after the stoppage of Panel 'E' a magnitude M=1.1 event occurred in the region. This appears to have triggered a face burst on Panel 'E' which totally destroyed an adjacent pack. There was no damage to Panel 'C'. It is likely that while Panel 'E' was standing and mining continued on nearby panels that load built up in the fracture zone ahead of Panel 'E': stress had been transferred back onto the rock that had previously been 'destressed' by preconditioning.

Of practical significance here is that the process of stress transfer is a dynamic, ongoing process. The stress shifts around in the rock mass in response to the mining and the preconditioning. The preconditioning process must be integrated into the production cycle in a controlled sequential manner. This sequence must be engineered to ensure that the most favourable stress distribution for maximum face stability is maintained at all times. In the case of the Blyvooruitzicht pillar preconditioning this means that the order of preconditioning must be sequential through the panels (i.e. panel 1, then panel 2, then the stub and back to panel 1). In the case of the WDLS longwall preconditioning must be maintained as an integral part of the production blast cycle: every production blast must be accompanied by an effective preconditioning blast.

Two different methods of preconditioning have been developed, these are face perpendicular preconditioning and face parallel preconditioning. Currently, face perpendicular preconditioning is being used to precondition the faces of a deep level longwall on Western Deep Levels South Mine and face parallel preconditioning is being used to precondition a stability pillar on Blyvooruitzicht Gold Mine. In the present circumstances each method is well suited to the environment in which it is being used. However, it may be that one or other of the methods is more efficient at causing stress transferral in which case it should be recognised as the method of choice. Currently there seems to be no fundamental rock mechanics reason reason why either method should be eliminated from any given mining environment. However face parallel preconditioning does impose certain constraints on the mining cycle and problems have been encountered with stemming of holes for this method. However, if the current model of the mechanics of preconditioning is correct it is likely that face parallel preconditioning is likely to prove the most efficient of the methods from a rock mechanics point of view if these problems could be eliminated.

The rock mass surrounding the portion of a face parallel preconditioning hole that is not charged but contains the stemming is not effectively preconditioned. It appears that the preconditioning blast can actually result in stress being transferred onto this portion of the rock mass as a consequence of the preconditioning blast. This is highly undesirable as this region will always be close to a free face and consequently adjacent to areas where people have access. It is important to rectify this situation. Currently, numerical simulations are being carried out of the behaviour of stemming materials in an attempt to optimise the design of the stemming in order to reduce the length of hole that must be stemmed. However, the ultimate solution may lie in a type of charge that requires no stemming. Such a solution is still to be investigated.

The ultimate goal of the preconditioning project is an implementable tool to reduce the hazard of face bursting associated with highly stressed mining faces. Successful

implementation will rely on two additional but inter-related aspects that have not yet been addressed in the research programme to date. The first of these is the development of a preconditioning team that can "champion" preconditioning to the mining industry. The second is worker acceptance of preconditioning.

The structure of the implementation team is not entirely clear but it should consist of members that can relate at all levels of the mining infrastructure, from management to the face worker. The team should be able to work for some period at a mine or site to help in the practical knowledge transfer of the preconditioning technique to ensure successful implementation.

The initial phase of addressing the question of worker attitude towards preconditioning involves ascertaining the current perception that workers operating in preconditioning stopes have towards the method. In addition to this, the perceptions of their fellow workers who work in stopes that are not preconditioned should be ascertained. Knowledge of current worker perceptions should be used to both gauge the success of the preconditioning system and to help develop practical ways of ensuring its acceptance with the labour force on relevant mines.

10. CONCLUSIONS

At this stage of the preconditioning programme a number of conclusions have been derived based on the current status of knowledge.

- Preconditioning reduces the incidence of face bursts.
- The mechanism of preconditioning is one of stress transferal and the process is
    - local and
    - temporary
- The mechanism of preconditioning does not involve the prolific generation of new fractures but, rather, involves slip on existing fractures.
- Whether the cause of this slip is a change in the local effective stress as a result of the injection of gases into the fracture or the dynamic shake up of the local rock mass as a whole is not clear at this stage.
- Two methods of preconditioning have been demonstrated for different mining environments
- Current methods of tamping the preconditioning holes are not ideal.
- Results from seismic tomography support those from normal seismic analysis
- A stochastic risk assessment technique has been developed but requires proving.
- Preconditioning can trigger larger seismic events, however, this should not be the sole purpose of a preconditioning programme but rather an additional benefit.
- Preconditioning is a potentially implementable tool that has achieved enthusiastic and widespread acceptance of the work force on at least one mine.
- Face perpendicular preconditioning is cost effective, indeed it may increase profitability under favourable circumstances.

11. RECOMMENDATIONS

In order to assure the successful implementation of preconditioning in the mining industry as a whole the following issues must still be addressed:-

- Quantify the effects of preconditioning. This important for the future ability to assess the success of preconditioning in any given circumstance, i.e. has it made the situation better or worse?

- Ascertain the actual mechanism of preconditioning. This is an important aspect for explosive design, both the chemical content and the emplacement.

- Improve the tamping system. The current tamping system may result in detrimental loading of the rock mass adjacent to the stemmed portions of the preconditioning hole. This situation must be rectified.

- Expand to other mines and mining situations. The current experiments have concentrated on two specific situations. It is important to identify any problems that may exist in transferring the technology to the numerous other mining environments that exist in the industry.

- Develop an implementation programme. Build a specialist Miningtek preconditioning team that can transfer preconditioning technology to the mining industry as a whole. This team should include members representing all levels of the mining system from top management to workers on the face.

- Optimise integration into the mining strategy. Perhaps new mining systems based on the use of preconditioning must be designed?

REFERENCES

Adams. G.R. and Jager A.J. 1980. Petroscopic observations of rock fracturing ahead of stope faces in deep level gold mines. J.S.A. Inst. of Mining & Met 80:204-209

Adams, G.R., Jager, A.J. and Roering, C. 1981. Investigations of rock fracture around deep level gold mine stopes. Proc. 22nd U.S. Symposium on Rock Mechanics, MIT.

Adams, D.J., Gay, N.C. and Cross, M.C. 1993. Preconditioning - A technique for controlling rockbursts., pg 29-33 in Rockbursts and Seismicity in Mines, R.P. Young (ed.) Balkema. Rotterdam.

Brummer, R.K. 1987. Fracturing and deformation at the edges of tabular gold mining excavations and the development of a numerical model describing such phenomena. Unpublished Ph.D. thesis -Rand Afrikaans University, Johannesburg, South Africa, 204 pp

Carneiro, D. 1995. Blyvooruitzicht Seismic Imaging Experiment: Alternative Images Produced by MES Software. Internal Report.

Giltner, S.G. 1992. Proposed method preconditioning stope faces with small diameter blastholes. Comro internal note No. 06/92

Hill, FG and Plewman, RP. 1957. Destressing: a means of ameliorating rockburst conditions. Part 2: implementing de-stressing with a discussion of the results so far obtained. J. S. Afr. Inst. Min. Met., October 1957

Itasca, 1992. FLAC Fast Lagrangian Analysis of Continua. Version 3.2 User's Manual.

Itasca, 1993. UDEC Universal Distinct Element Code. Version 2.0 User's Manual.

King, G.C.P. and Sammis, C.G. 1992. The mechanisms of finite brittle strain. Pageoph. 138(4):611-640

Kullmann, DH, Stewart, R.D. and Lightfoot, N. 1994. Verification of a discontinuum model used to investigate rock mass behaviour around a deep-level stope. The Application of Numerical Modelling in Geotechnical Engineering, SANGORM, Pretoria

Kullmann, D, Stewart, R.D., Lightfoot, N and Longmore, P. 1995. Interim report on the progress towards the implementation of preconditioning as a technique for controlling face bursting on deep-level mines, Mining Technology Division of CSIR, SIMRAC Interim Project Report

Lightfoot, N. 1993. The use of numerical modelling in rockburst control. Proceedings of the 3rd International Symposium on Rockbursts and Seismicity in Mines, Balkema, Rotterdam

Lightfoot, N., Kullmann, D.H. and Leach, A.R. 1994. A conceptual model of a hardrock, deep level, tabular ore body that incorporates the potential for face bursting as a natural product of mining. Proceedings of the 1st North American Rock Mechanics Symposium. In) Nelson, P.P. and Laubach, S.E. (eds) Rock Mechanics Models and Measurements Challenges From Industry. Balkemea, Rotterdam.

Lightfoot, N., Kullmann, D.H., Stewart, R.D. and Toper, A.Z. 1995. Guidelines for preferable layouts for preconditioning with appropriate explosive and stemming: Revision 1. CSIR: Mining Technology, SIMRAC Interim Project Report, November 1995.

Maxwell, S. C. and Young, R. P. 1995. Blyvooruitzicht Seismic Imaging Experiment: Report on Imaging Results and Interpretation to CSIR Mining Technology. Internal Report.

Moody, J.D. and Hill, M.J. 1956. Wrench-fault tectonics. Bull. Geol. Soc. Am 67:1207-1246

Napier, J.A.L. 1991. Energy changes in a rock mass containing multiple discontinuities. J.S. Afr. Inst. Min. Metall., 91, 145-157.

Napier, J.A.L. and Hildyard, M.W. 1992. Simulation of fracture growth around openings in highly stressed brittle rock. J.S. Afr. Inst. Min. Metall., 92, 159-168.

Napier, J.A.L. and Pierce, A.P. 1995. Simulation of extensive fracture formation and interaction in brittle materials. In H.P. Rossmanith (ed), Mechanics of jointed and faulted rock: 709-715. Balkema, Rotterdam.

Pattrick, K. W., Kelly, A. M. and Spottiswoode, S. M. 1990. A Portable Seismic System for Rockburst Applications. International Deep Mining Conference: Technical Challenges in Deep Level Mining. Johannesburg, SAIMM.

Piper, P and Gürtunca, RG. 1987. Measuring Convergence and Ride. SANGORM News, Feb. 1987

Ramsey, J.G. 1980. Shear zone geometry: a review. J. Struc. Geol **2**:83-99

Roering, C. 1979. Confidential Report to Chamber of Mines Organisation

Rorke, AJ, Brenchley, PR and Janse van Rensburg, AL. 1988. Preliminary preconditioning results obtained at West Driefontein, 32/12 stope and proposed future work at this site. Chamber of Mines Research Organisation (COMRO), Unpublished Internal Note

Rorke, AJ, Cross, M, Van Antwerpen, HEF, and Noble, K. 1990. The mining of a small up-dip remnant with the aid of preconditioning blasts, International Deep Mining Conference: Technical Challenges in Deep Level Mining. Johannesburg, SAIMM

Rorke, A.J. and Brummer, R.K. 1990b. The use of explosives in rockburst control techniques. Proceedings of the 3rd International Symposium on Rockbursts and Seismicity in Mines, Balkema, Rotterdam

Roux, A.J.A., Leeman, E.R. and Denkhaus, H.G. 1957. De-stressing: a means of ameliorating rockburst conditions. Part I - The concept of de-stressing and the results obtained from it's application. J. S.Afr. Inst. of Mining and Met , October 101-119

Smit, J.L. and Rüther, H. 1995. The 3D mapping of a textured surface using digital photogrammetric techniques. Department of Surveying and Geodetic Engineering, UCT, Research Report, November 1995.

Stewart, R. D. 1995. Development of seismic risk assessment method for application to rockburst-prone sites in deep-level South African gold mines. Transactions of the Institution of Mining and Metallurgy, 104, A87-A95.

Stewart, R. D., and Spottiswoode, S. M. 1993. A technique for determining the seismic risk in deep-level mining. Rockbursts and Seismicity in Mines, Young (ed.). Balkema, Rotterdam. 123-128.

Toper, A.Z., Janse van Rensburg, A. and Lightfoot, N. 1995. Guidelines for layouts for face perpendicular preconditioning with appropriate explosive and stemming. CSIR: Mining Technology, SIMRAC Interim Project Report, November 1995.

Wilcox, R.E., Harding, T.P. and Seely, R. 1973. Basic wrench tectonics. AAPG Bull 57(1):74-96

APPENDIX A

Criteria by which preconditioning blasts at Blyvooruitzicht Gold Mine 17-24W pillar preconditioning site are judged

These criteria are the result of an attempt to minimise subjectivity in the assessment of the effectiveness of individual preconditioning blasts.

The criteria

1. The seismic magnitude of the recorded blast event: the size of the seismic event recorded by the monitoring PSS network at the time of the blast, related to the amount of explosive used for the blast.
2. The number of seismic events recorded from the site in the 24 hours following the blast: adjusted according to whether or not there was a production blast in another panel on the same day.
3. The largest magnitude of the subsequent seismicity: seismic events of $M \geq 0.0$ indicate additional release of stored strain energy over and above that released by the blast itself.
4. The evidence of spatial migration of the subsequent seismicity: migration of subsequent seismicity away from the site of the blast indicates the effective redistribution of stress in the rockmass by the blast.
5. The convergence recorded on the following day: adjusted according to whether or not the measurement was made in the panel of the blast or in another panel, and whether or not there was a production blast in another panel on the same day.

The critical values and rating system

The rating system described below is ordered with the values for a "typical" preconditioning blast given first, followed by those for an underachieving blast and then those for an exceptional blast.

0. Start with **0** points.
1. Blast magnitude (M_{Blast}):
    - If M_{Blast} lies in the range *(kg explosive/100)*$\pm$*0.5*, add **1**
    - If M_{Blast} is *below* this range, add **0**
    - If M_{Blast} is *above* this range, add **2**
2. Number of subsequent events:
    - If there was no production blast
        * If there are *between 10 and 19 events*, add **1**
        * If there are *fewer than 10 events*, add **0**
        * If there are *20 or more* events, add **2**
    - If there was a production blast
        * If there are *between 20 and 39 events*, add **1**
        * If there are *fewer than 20 events*, add **0**
        * If there are *40 or more events*, add **2**
3. Largest subsequent event magnitude:
    - If the largest event magnitude is in the range $0.0 \leq M < 1.0$, add **1**
    - If the largest event magnitude is $M < 0.0$, add **0**
    - If the largest event magnitude is $M \geq 1.0$, add **2**
4. Spatial migration:
    - If there is *some* evidence of migration, add **1**
    - If there is *no* evidence of migration, add **0**
    - If there is *convincing* evidence of migration, add **2**

5. Convergence:
    - If the convergence was measured in the panel of the preconditioning blast
        * If the convergence is *15 mm or more but less than 30 mm*, add **1**
        * If the convergence is *less than 15 mm*, add **0**
        * If the convergence is *30 mm or more*, add **2**
    - If the convergence was measured in another panel and there was no production blast
        * If the convergence is *10 mm or more but less than 20 mm*, add **1**
        * If the convergence is *less than 10 mm*, add **0**
        * If the convergence is *20 mm or more*, add **2**
    - If the convergence was measured in another panel and there was a production blast
        * If the convergence is *20 mm or more but less than 40 mm*, add **1**
        * If the convergence is *less than 20 mm*, add **0**
        * If the convergence is *40 mm or more*, add **2**
6. Rate the preconditioning blast out of a possible total of **10** points.

APPENDIX B

Tables giving summary information for each preconditioning blast at Blyvooruitzicht Gold Mine 17-24W preconditioning site since the change to breast mining in September 1992.

Preconditioning in 1992.

Date of Blast	Panel Number	Mass of Explosive (kg)	Explosive Type	Length of Hole (m)	Length of Stemming (m)	Seismic Magnitude of Blast	Number of Events Following (24 h)	Largest Magnitude of These	Evidence of Spatial Migration?	Convergence in Panel of Blast (mm)	Distance to Face (m)	Blast Rating (%)
09/09/92	2	150	anfo	17.0	5.0	[1]?	5	-1.1	?	?	?	—
08/10/92	2	125	emulsion	17.0	5.0	0.8	35	-0.7	yes	?	?	63
05/11/92	2	150	anfo	[11]22.0	7.0	[1,2]0.8	5	-0.7	?	11	7.1	00
26/11/92	1	75	anfo	14.0	5.0	0.7	19	-0.3	yes	35	1.8	60
03/12/92	2	150	anfo	[11]22.0	5.0	1.2	8	1.2	some	18	3.8	50

NOTES:

[1] seismic data acquisition problems experienced
[2] event magnitude obtained from BGM mine-wide seismic system
[3] production blast in panel 1 on same day
[4] production blast in panel 2 on same day
[5] production blast in stub on same day
[6] includes effects of production blast on following day
[7] measured in panel 1
[8] measured in panel 2
[9] blasted same hole again
[10] hole drilled too far ahead of face
[11] drilling difficulties experienced: blockages in hole, etc.
[12] two holes drilled, one charged
[13] hole diameter 76 mm
[14] first attempt misfired

Preconditioning in 1993.

Date of Blast	Panel Number	Mass of Explosive (kg)	Explosive Type	Length of Hole (m)	Length of Stemming (m)	Seismic Magnitude of Blast	Number of Events Following (24 h)	Largest Magnitude of These	Evidence of Spatial Migration?	Convergence in Panel of Blast (mm)	Distance to Face (m)	Blast Rating (%)
02/01/93	1	75	anfo	[10]15.0	5.0	0.2	5	-0.8	yes	7	7.0	20
18/01/93	2	118	anfo	[11]18.0	6.0	0.8	[3]9	*0.4*	some	12	[7]4.8	30
22/01/93	stub	50	anfo	[12 13]10.0	5.0	-0.1	[3]10	-1.0	no	19	[7]6.4	00
19/02/93	1	75	anfo	15.0	5.0	0.8	[4]43	*0.4*	yes	?	?	*75*
02/03/93	2	95	anfo	15.0	5.0	0.8	[3]20	*0.1*	no	16	5.8	40
15/03/93	stub	75	anfo	10.0	5.0	[2]2.0	8	-1.3	some	41	[8]5.8	*50*
31/03/93	1	81	emulsion	[13]17.0	5.0	0.8	12	*0.4*	yes	3	[8]2.9	*50*
16/04/93	2	81	anfo	[12]15.0	5.0	0.8	8	-1.0	some	14	2.9	20
14/05/93	1	93	emulsion	14.0	5.0	0.8	5	-0.8	some	30	3.2	40
07/06/93	2	100	anfo	16.0	5.0	0.6	22	[2]*1.8*	some	64	4.7	*80*
29/06/93	1	100	anfo	14.5	5.0	0.5	2	-1.6	no	4	5.0	10
12/07/93	stub	43	anfo	10.0	5.0	0.2	[3]12	-0.1	no	11	[7]2.4	10
19/08/93	1	100	anfo	13.5	5.0	0.8	15	-0.8	yes	9	4.2	40
30/09/93	2	125	anfo	18.0	6.5	[1,2]1.9	?	?	?	20	2.9	*75*
04/11/93	1	100	emulsion	13.5	5.0	1.0	[4,5]57	*0.3*	some	16	2.3	*60*
22/12/93	2	100	anfo	16.5	5.0	1.0	18	-0.9	yes	13	2.3	40

Preconditioning in 1994.

Date of Blast	Panel Number	Mass of Explosive (kg)	Explosive Type	Length of Hole (m)	Length of Stemming (m)	Seismic Magnitude of Blast	Number of Events Following (24 h)	Largest Magnitude of These	Evidence of Spatial Migration?	Convergence in Panel of Blast (mm)	Distance to Face (m)	Blast Rating (%)
10/01/94	stub	69	anfo	10.5	5.5	-0.0	9	-0.6	yes	4	[8]4.9	20
17/01/94	1	88	anfo	13.0	5.0	0.9	[5]29	*0.5*	some	12	2.2	40
10/02/94	2	100	anfo	[10]18.0	6.5	-1.1	8	-1.1	no	2	6.4	00
28/02/94	[9]2	100	anfo	16.5	5.0	1.3	14	-0.3	some	39	3.1	*50*
17/03/94	1	62	anfo	12.0	5.0	0.6	12	-0.6	yes	11	4.8	40
11/04/94	stub	50	anfo	10.0	5.0	0.4	[4]39	*0.0*	no	26	[8]4.0	40
15/04/94	2	130	emulsion	20.0	5.0	1.4	11	[2]*2.3*	some	47	4.3	*70*
18/05/94	1	75	emulsion	13.0	5.0	0.8	7	-1.5	some	4	4.3	20
24/06/94	2	138	anfo	20.0	5.0	1.0	14	-0.2	yes	21	2.7	*50*
20/09/94	1	80	emulsion	15.0	5.0	0.8	13	-0.9	yes	13	1.9	40
26/09/94	2	85	anfo	[12]21.0	5.0	0.8	5	-1.2	some	3	2.3	20
29/09/94	stub	40	anfo	9.0	5.0	-0.2	[3]17	*0.2*	no	2	4.7	10
28/10/94	1	75	emulsion	13.0	5.0	0.9	[5]18	[2]*2.1*	yes	26	5.6	*60*
06/12/94	2	100	anfo	17.5	5.0	0.8	11	*0.3*	some	15	4.0	*50*
15/12/94	stub	75	anfo	[11]11.0	6.5	0.3	21	*1.5*	yes	19	5.2	*80*

APPENDIX C

Comparison of the recorded precondition blast event magnitudes with the amount of explosives used for each blast.

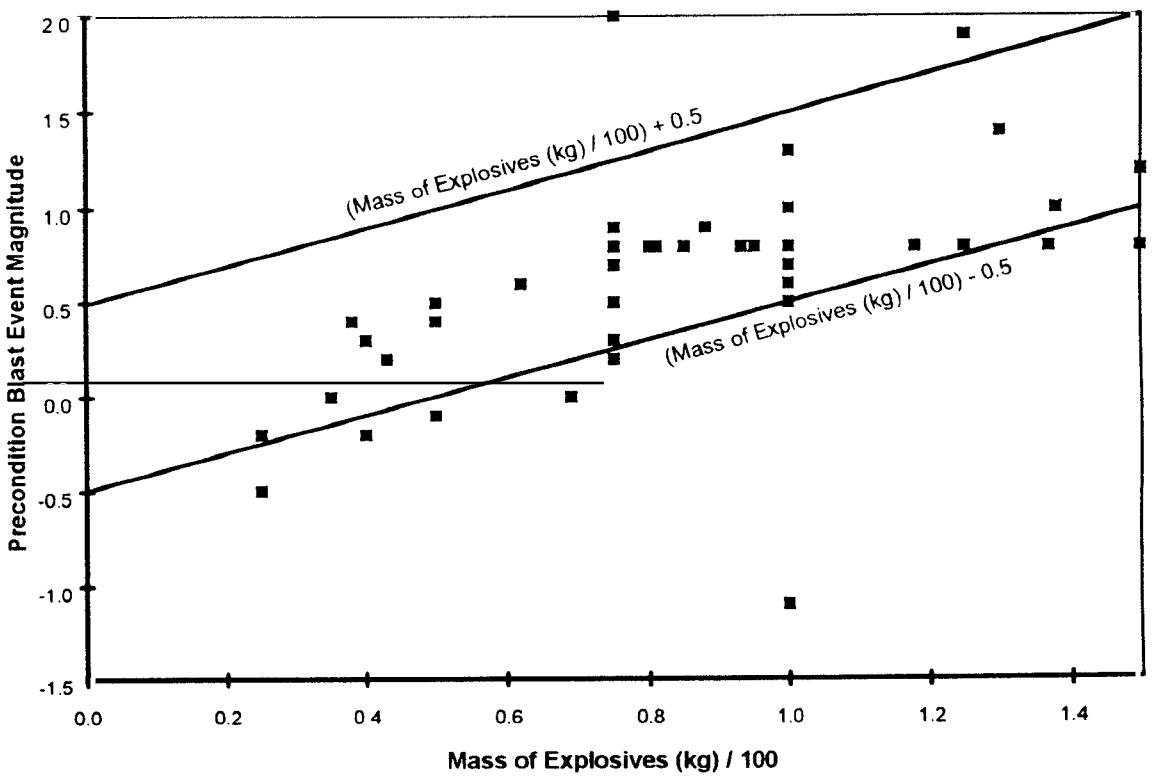

Summary information for each preconditioning blast since the commencement of breast mining at the Blyvooruitzicht Gold Mine 17-24W preconditioning site.

Preconditioning in 1995.

Date of Blast	Panel Number	Mass of Explosive (kg)	Explosive Type	Length of Hole (m)	Length of Stemming (m)	Seismic Magnitude of Blast	Number of Events Following (24 h)	Largest Magnitude of These	Evidence of Spatial Migration?	Convergence in Panel of Blast (mm)	Distance to Face (m)	Blast Rating (%)
10/01/95	1	75	emulsion	13.5	5.0	0.8	19	-0.6	yes	7	2.5	40
03/02/95	2	100	anfo	20.0	5.0	0.7	26	-0.6	yes	16	4.3	*60*
06/03/95	1	75	emulsion	12.0	5.0	0.7	9	-0.7	yes	10	6.9	30
29/03/95	2	75	anfo	[11,12]12.0	2.0	0.3	17	-0.1	some	6	[7]4.3	30
05/04/95	stub	25	anfo	[11,13]3.0	1.0	-0.2	10	-1.0	yes	3	[7]4.3	40
19/05/95	1	40	emulsion	[11]9.0	4.5	0.3	[4]59	-0.6	some	6	4.2	40
01/06/95	2	75	anfo	[11,13]20.0	5.0	0.5	[3]14	*0.2*	some	7	[7]6.1	30
06/06/95	stub	35	emulsion	[11,13]6.0	2.0	0.0	[3]23	-0.6	no	9	[7]8.6	20
01/08/95	1	50	anfo	9.0	5.0	0.4	[5]23	-0.5	some	5	2.4	30
09/08/95	2	137	anfo	20.0	5.0	0.8	[3]50	-0.6	yes	34	3.4	*60*
18/08/95	stub	25	anfo	4.5	2.0	-0.5	[3]25	-0.3	no	7	[8]1.5	10
[14]23/09/95	1	38	emulsion	10.0	5.0	0.4	3	-0.9	no	14	2.6	10
04/10/95	2	100	emulsion	[11,12,13]20.0	6.5	1.0	[3]10	-0.5	no	21	5.2	20
16/11/95	1	50	emulsion	8.0	3.0	0.5	7	*0.8*	yes	19	2.1	*50*
05/12/95	2	100	emulsion	[11]12.0	5.0	0.8	[6]17	*0.1*	some	11	4.6	30

APPENDIX D

Average daily convergences measured in each panel for various blast types and positions.

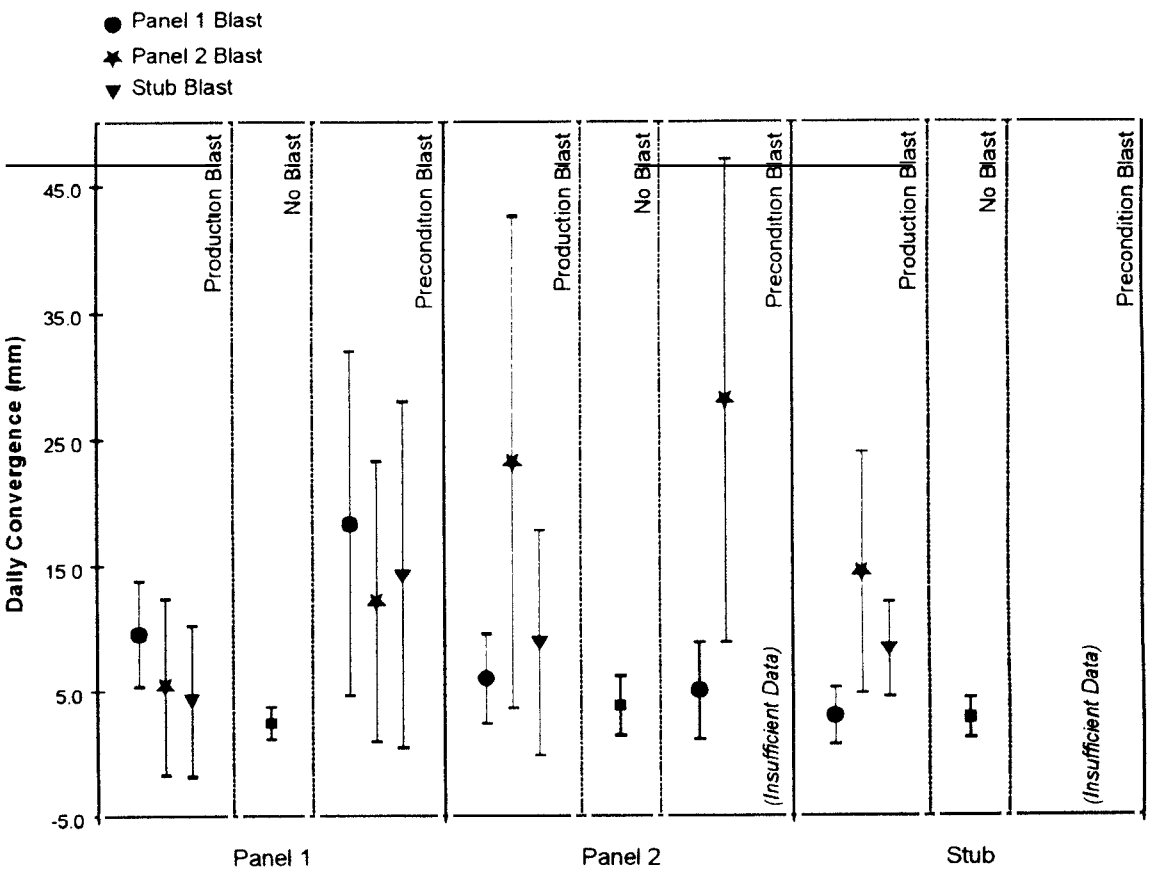

APPENDIX E

Comparison of the b-values determined from the seismic data recorded from panel 'E' before and after the commencement of preconditioning in that panel.

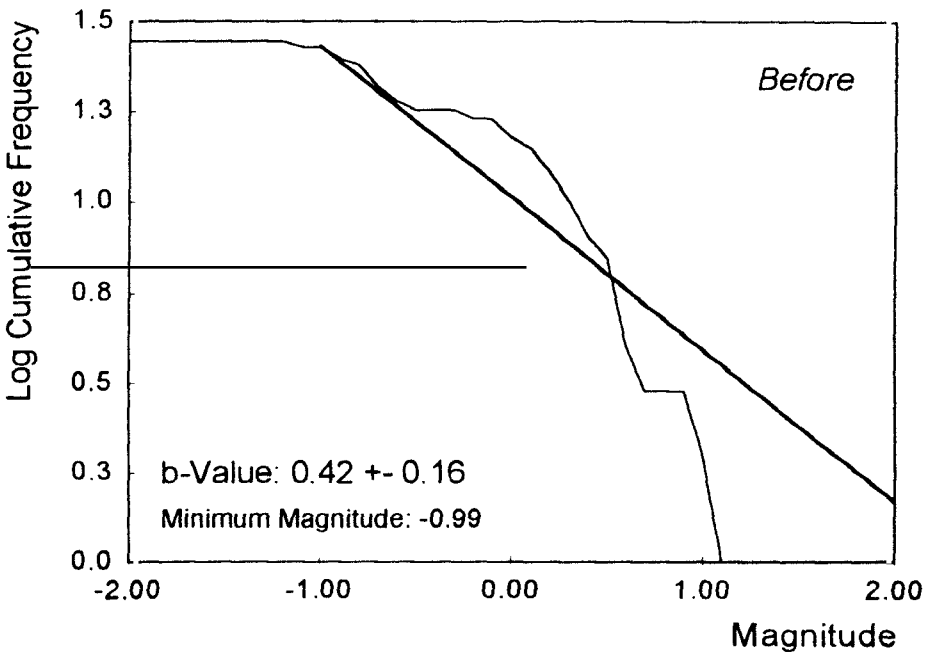

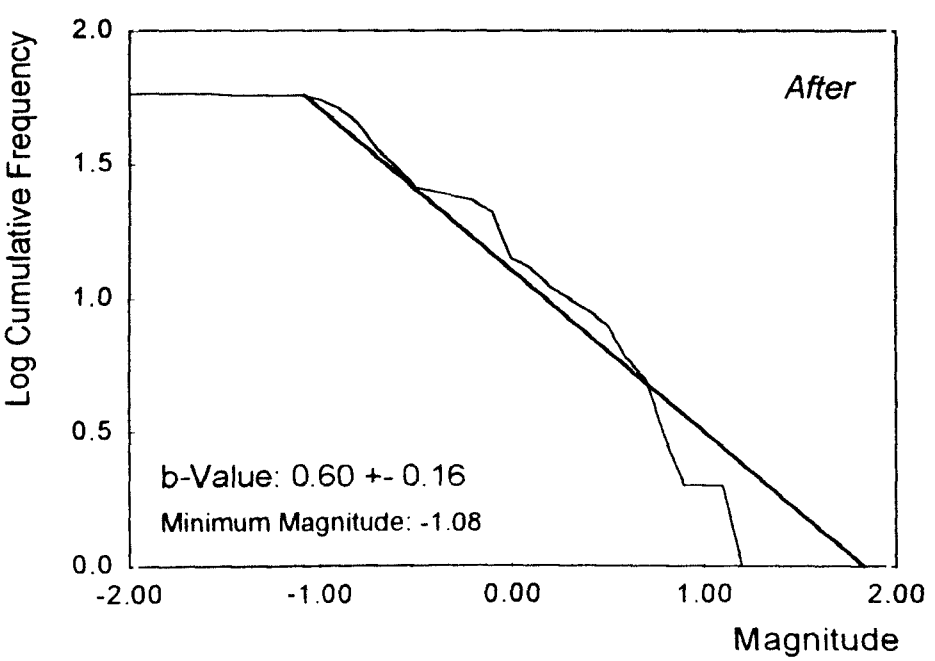

APPENDIX F

Graphs of convergence ride data from Western Deep Levels South Mine 84-49W *longwall preconditioning site discussed in* Section 4.2.2.

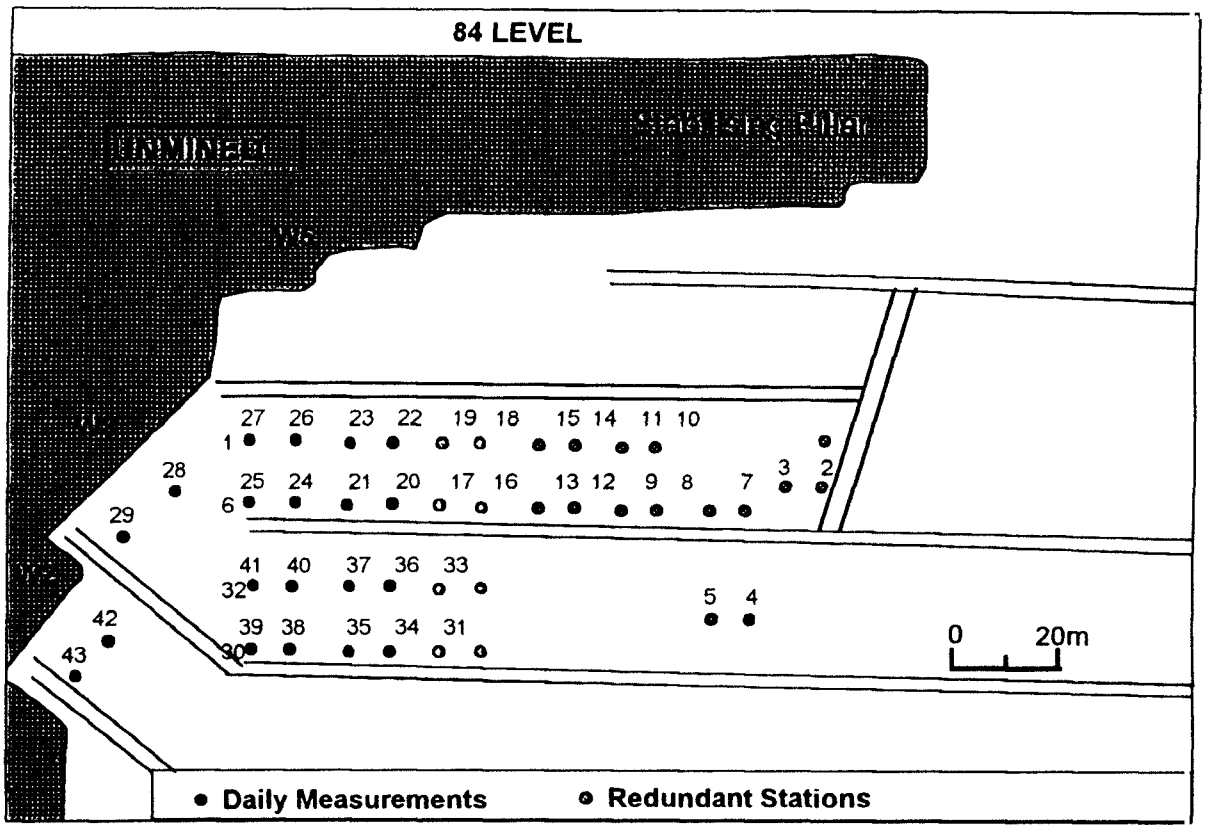

Figure 4.5. Positions of Convergence-Ride Measurement Stations. The relationship between the station numbers in this plan and the actual station numbers used in the following graphs is given in the table below.

NUMBER (FIG.4.5)	STATION NAME	NUMBER (FIG.4.5)	STATION NAME
1	4WE02A	23	4WW01E
2	4WE01A	24	4WE00F
3	4WW01A	25	4WW00F
4	3WE01A	26	4WE01F
5	3WW01A	27	4WW01F
6	4WE00A	28	3WE00J
7	4WW00A	29	3WW00J
8	4WE00B	30	3WE00D
9	4WW00B	31	3WW00D
10	4WE02B	32	3WE01D
11	4WW02B	33	3WW01D
12	4WE00C	34	3WE00E
13	4WW00C	35	3WW00E
14	4WE02C	36	3WE01E
15	4WW02C	37	3WW01E
16	4WE00D	38	3WE00F
17	4WW00D	39	3WW00F
18	4WE01D	40	3WE01F
19	4WW01D	41	3WW01F
20	4WE00E	42	2WE00K
21	4WW00E	43	2WW00K
22	4WE01E		

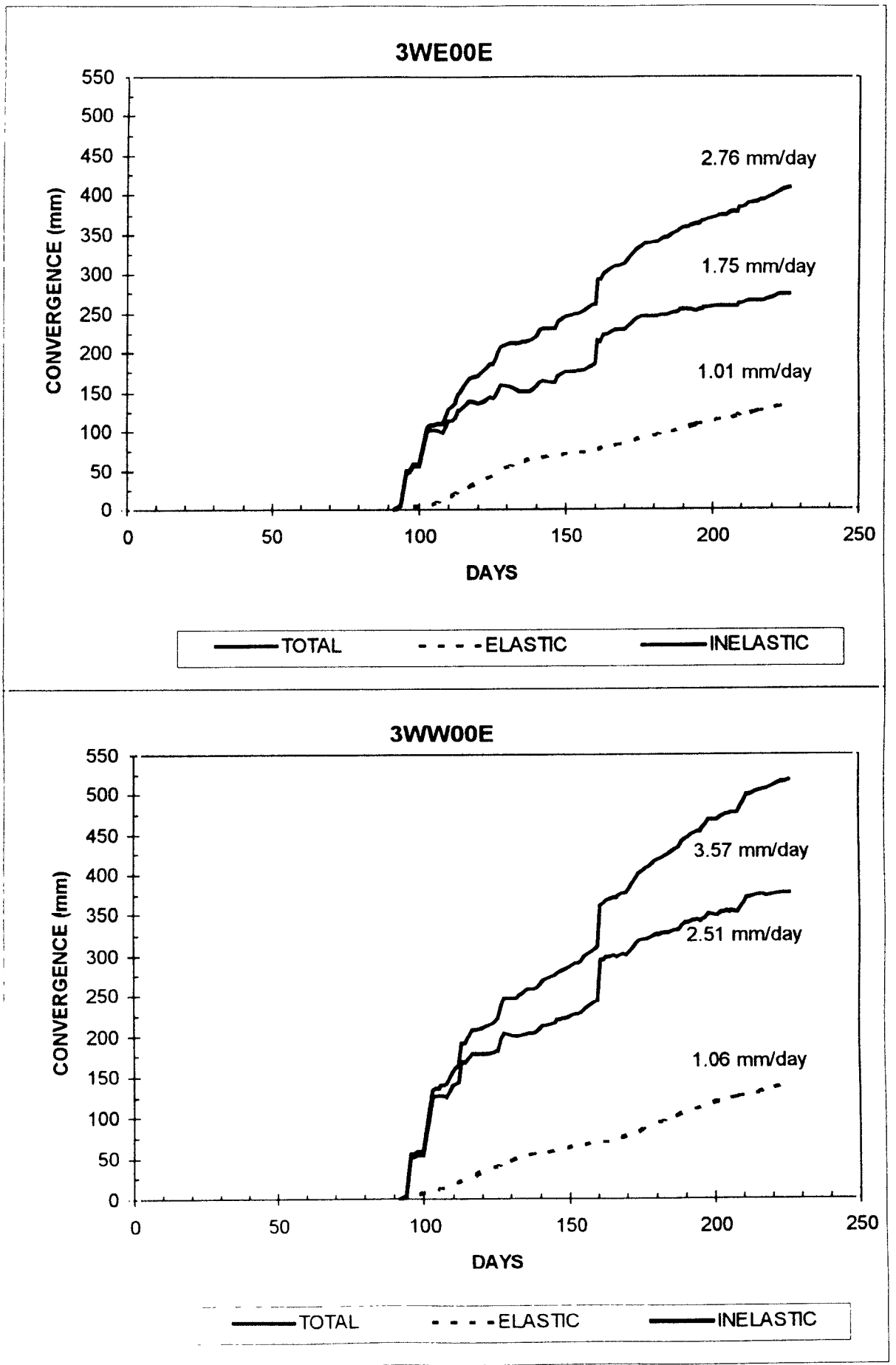

Figure 1. Convergence - Ride Measurements (Stations 3WE00E & 3WW00E)

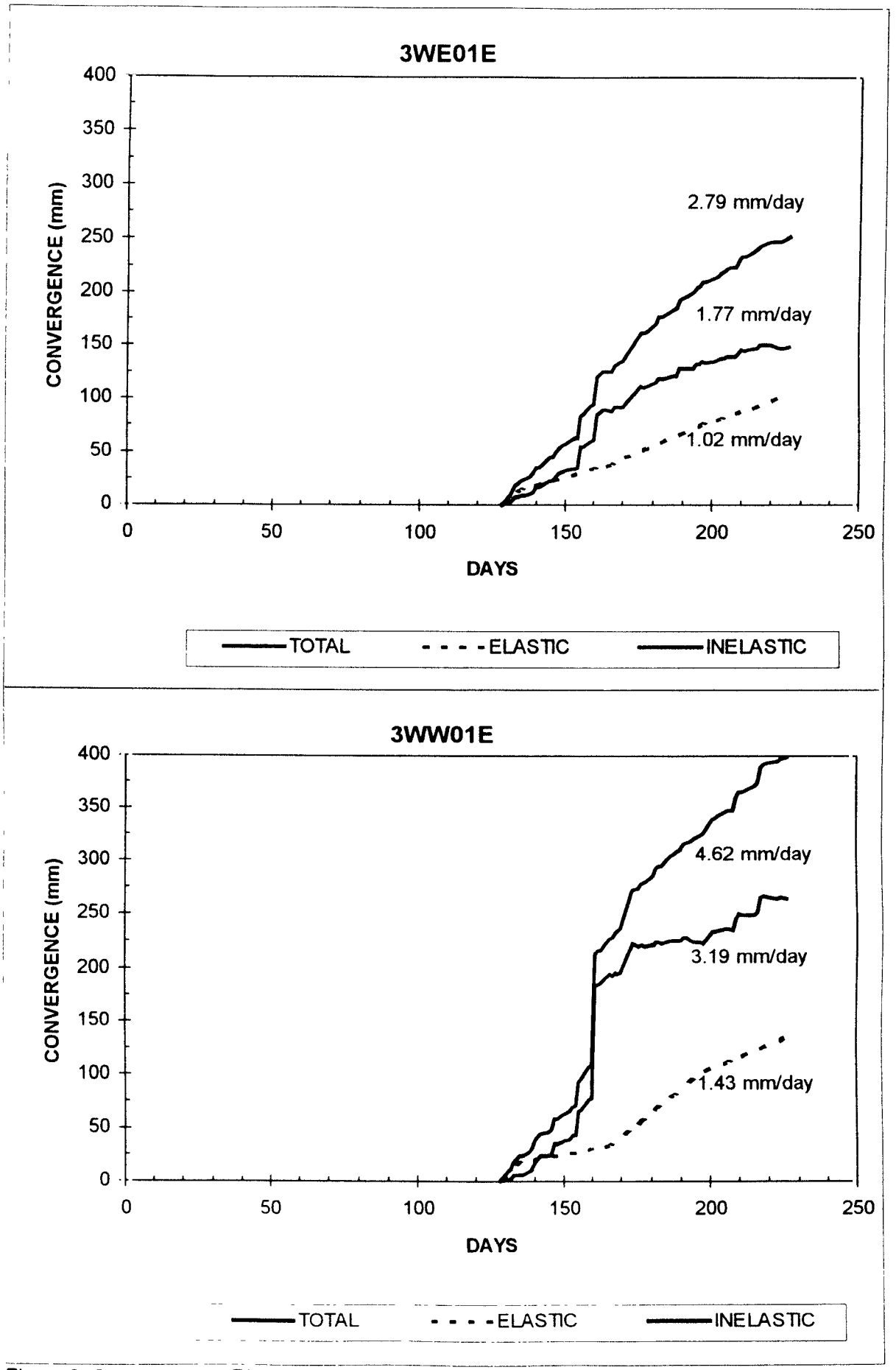

Figure 2. Convergence - Ride Measurements (Stations 3WE01E & 3WW01E)

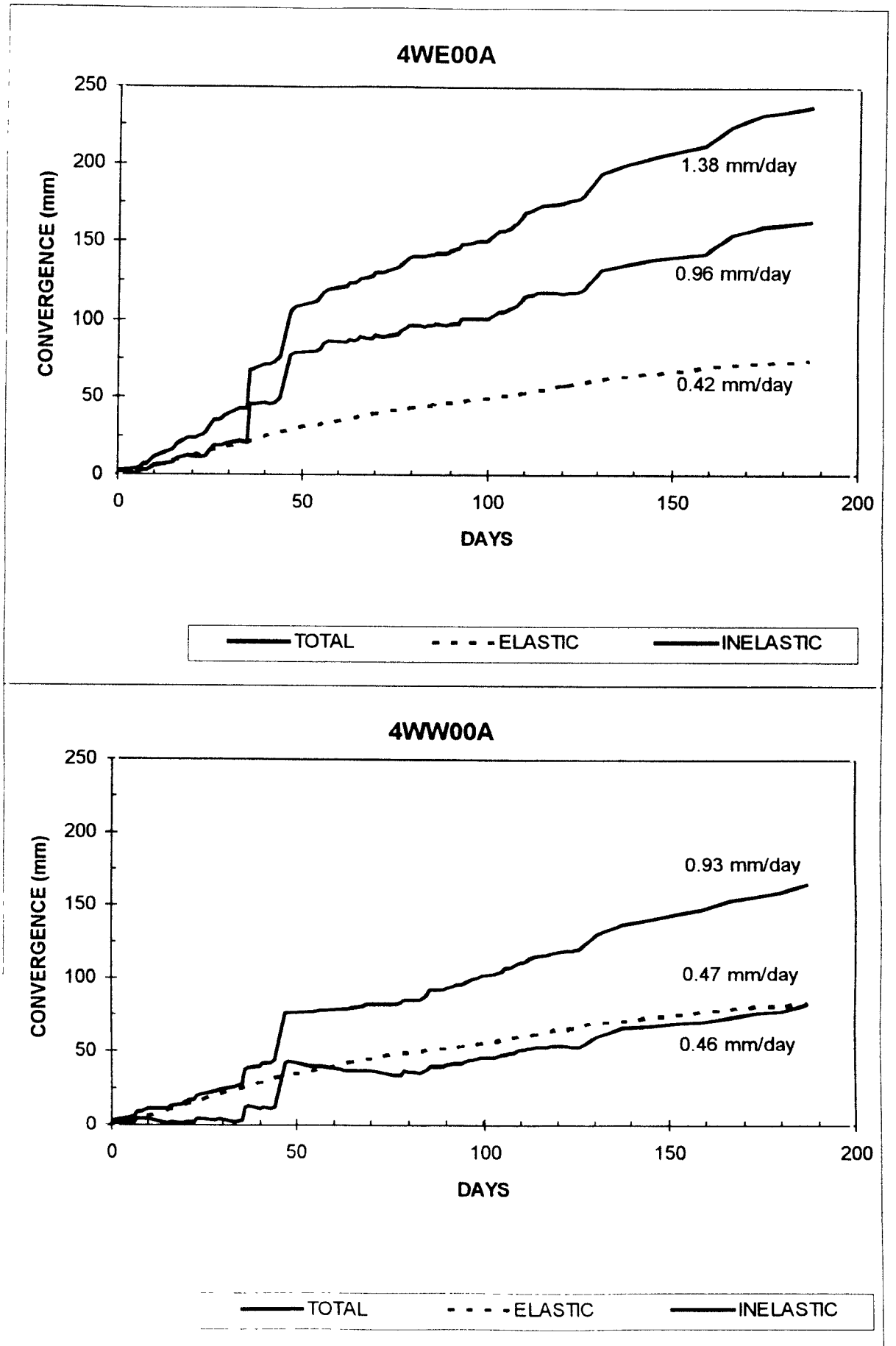

Figure 3. Convergence - Ride Measurements (Stations 4WE00A & 4WW00A)

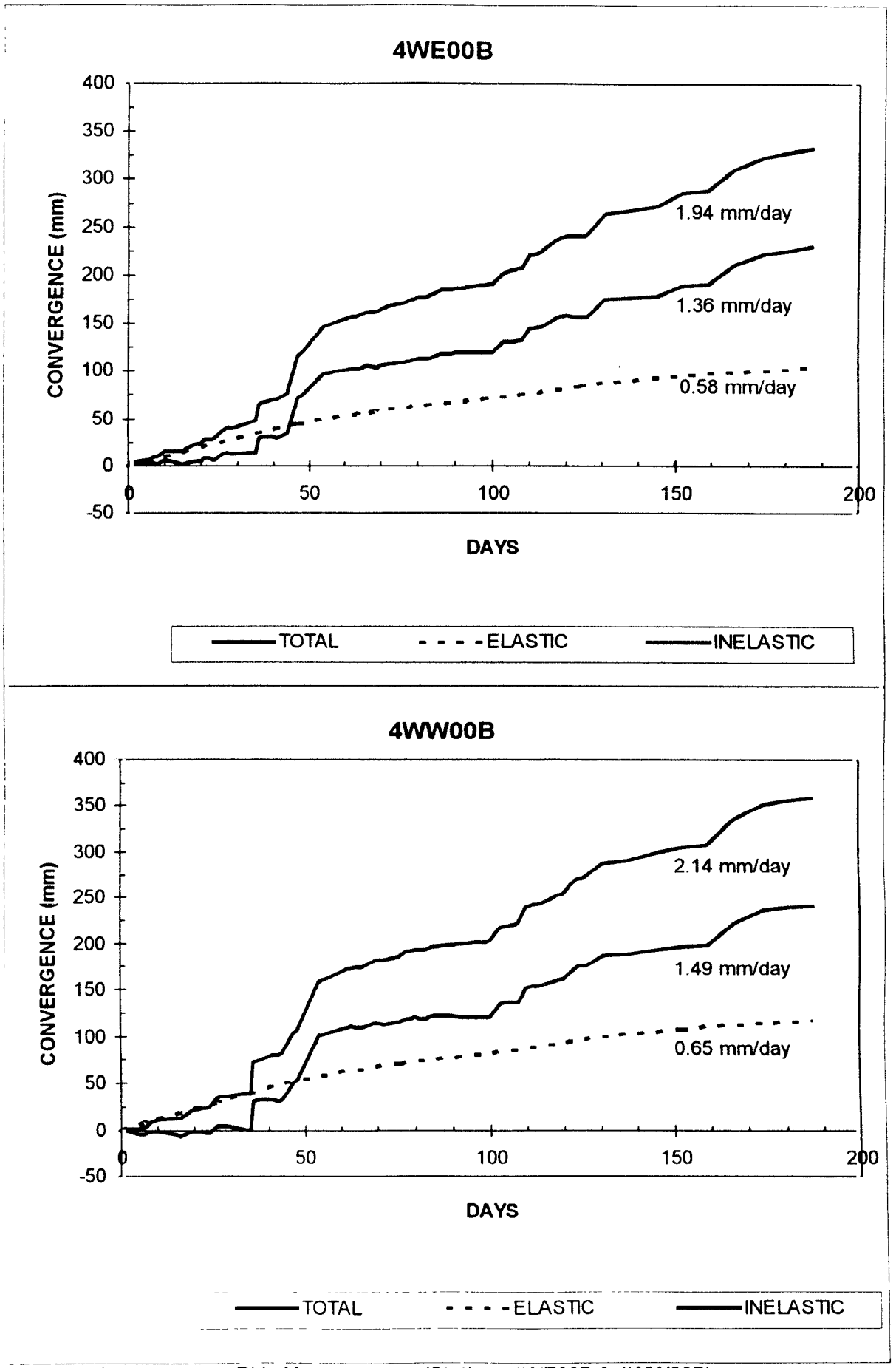

Figure 4. Convergence - Ride Measurements (Stations 4WE00B & 4WW00B)

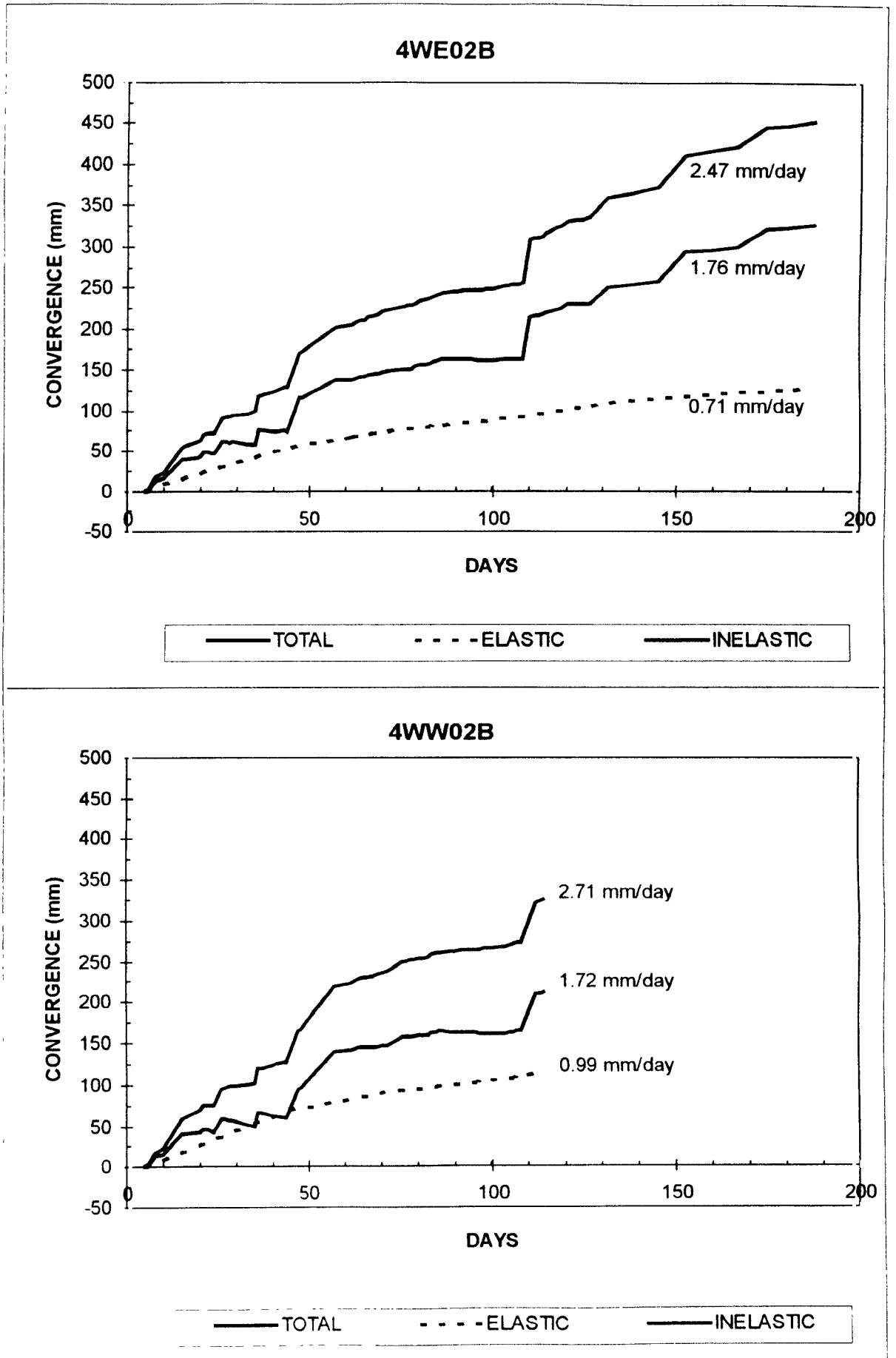

Figure 5. Convergence - Ride Measurements (Stations 4WE02B & 4WW02B)

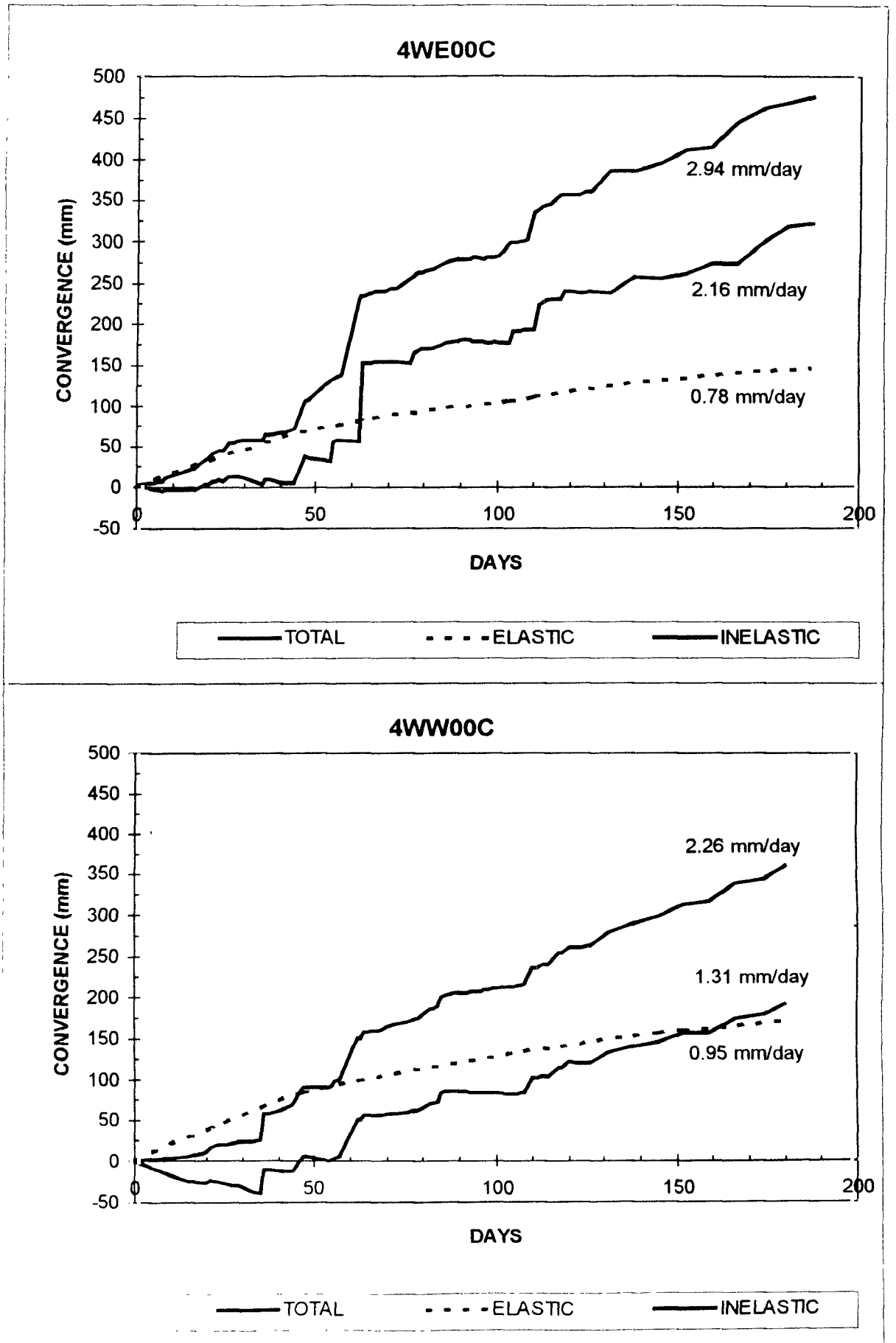

Figure 6. Convergence - Ride Measurements (Stations 4WE00C & 4WW00C)

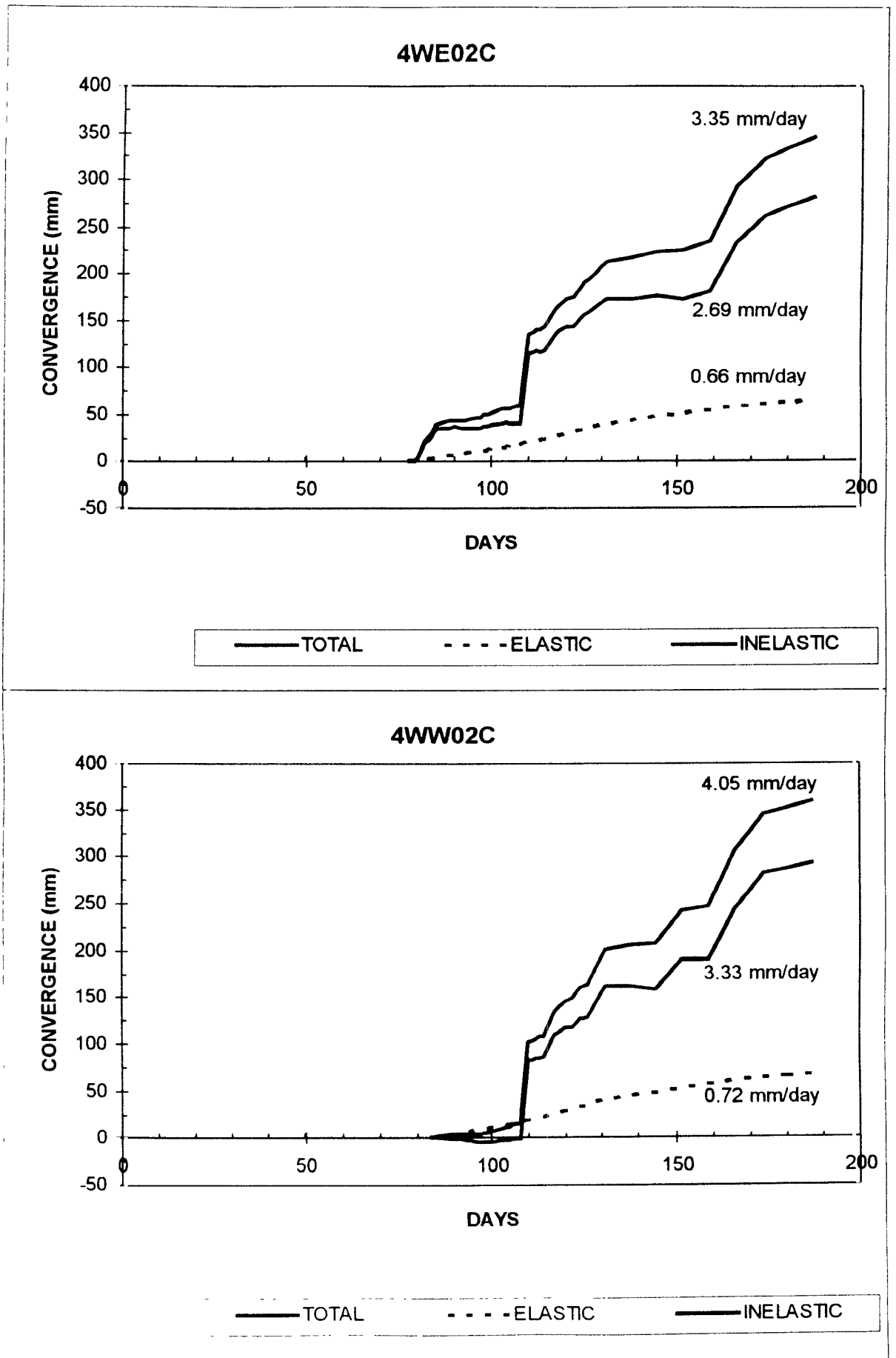

Figure 7. Convergence - Ride Measurements (Stations 4WE02C & 4WW02C)

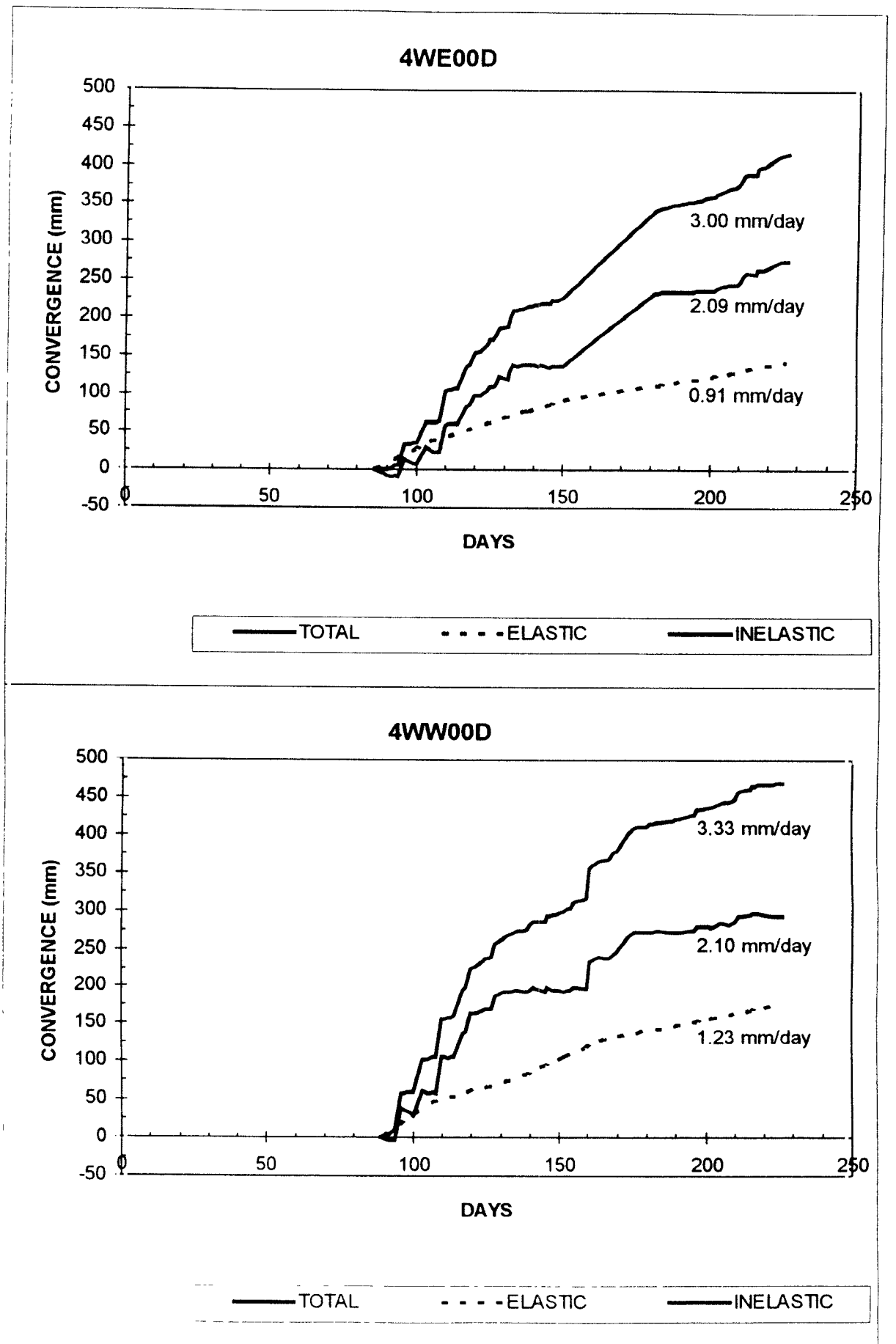

Figure 8. Convergence - Ride Measurements (Stations 4WE00D & 4WW00D)

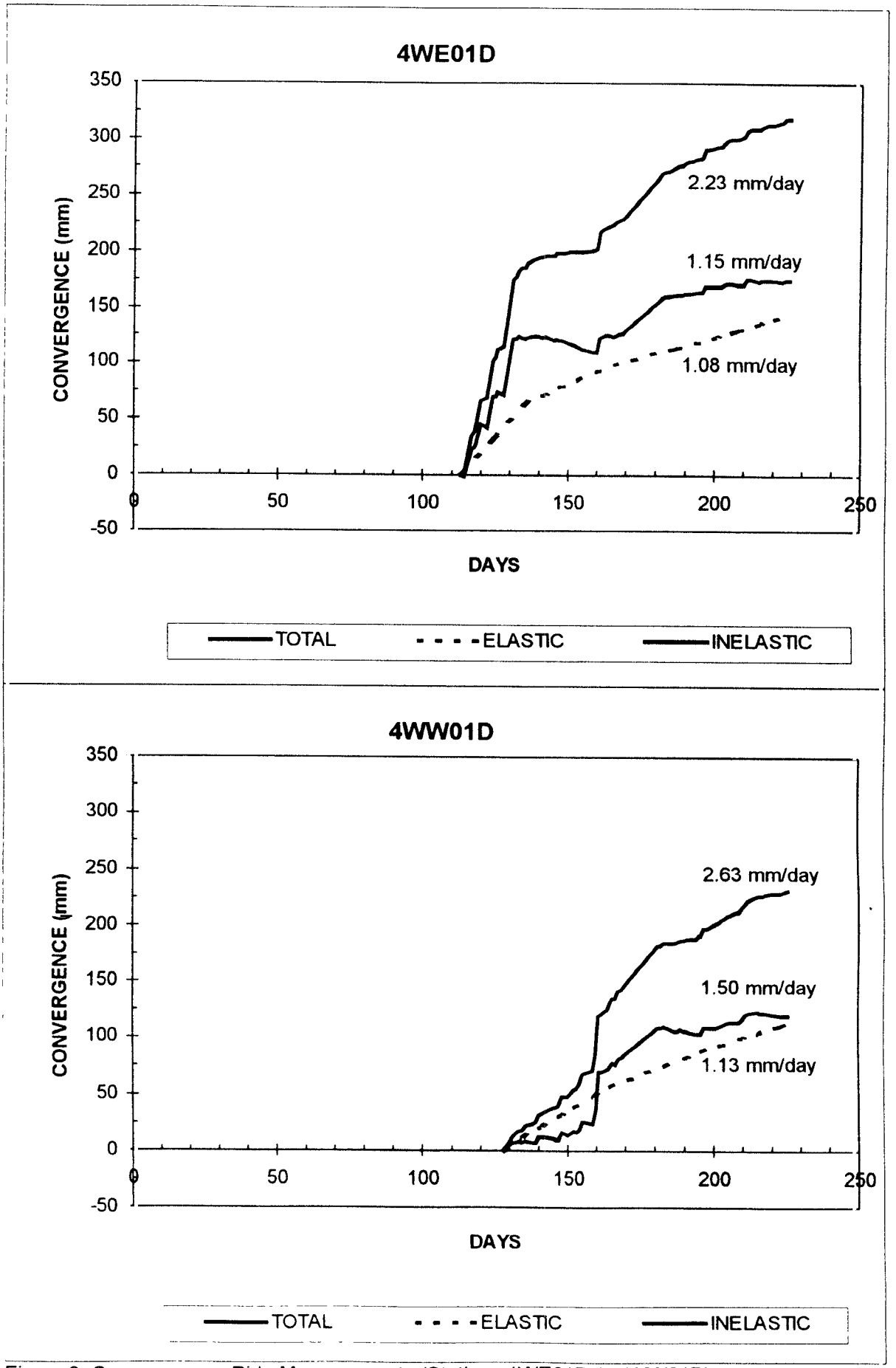

Figure 9. Convergence - Ride Measurements (Stations 4WE01D & 4WW01D)

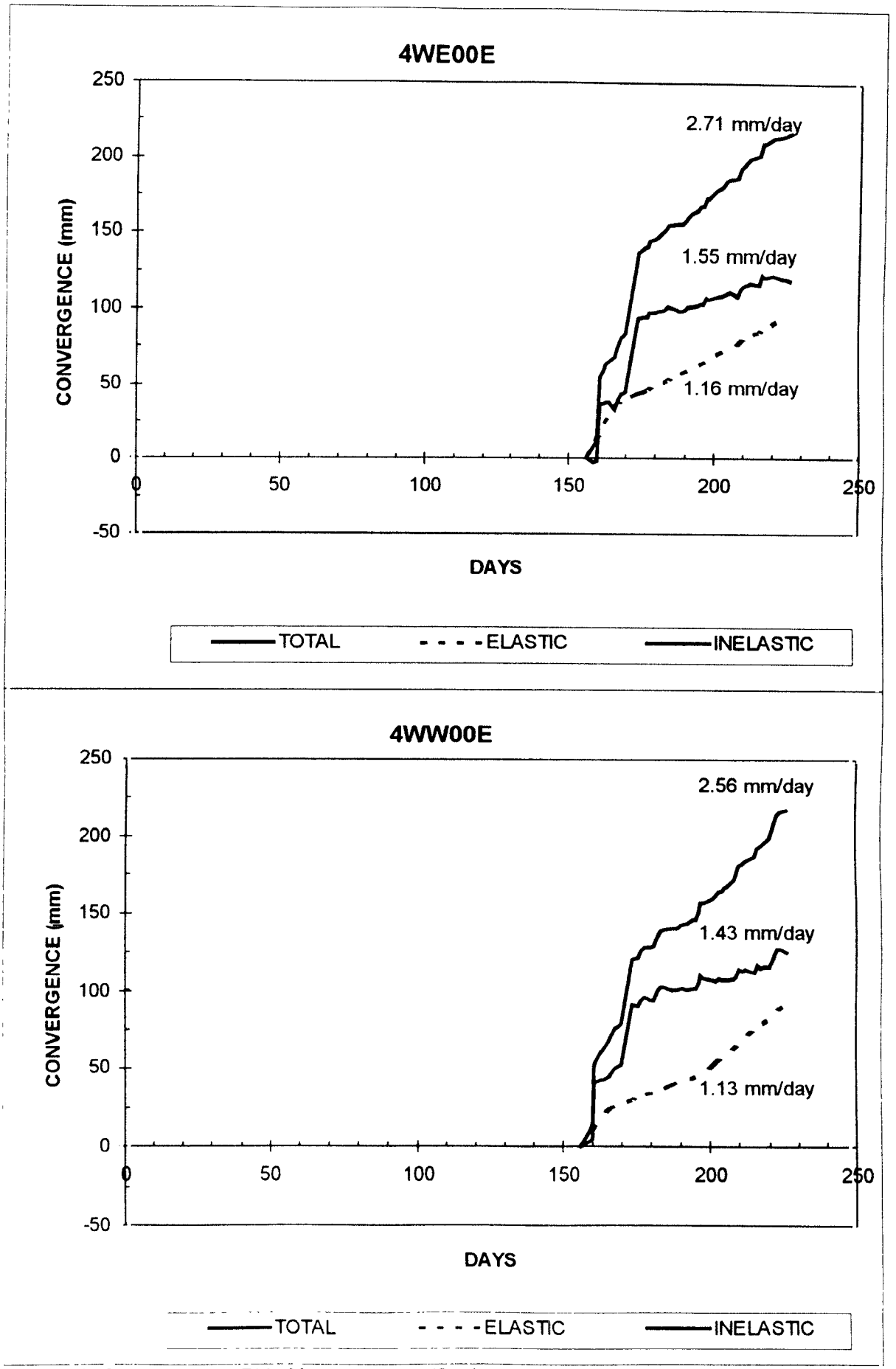

Figure 10. Convergence - Ride Measurements (Stations 4WE00E & 4WW00E)

APPENDIX G

Output from the computer program DIGS used to analyse the effects of detonating a large amount of explosives in a confined rock mass: discussed in Section 7.1.

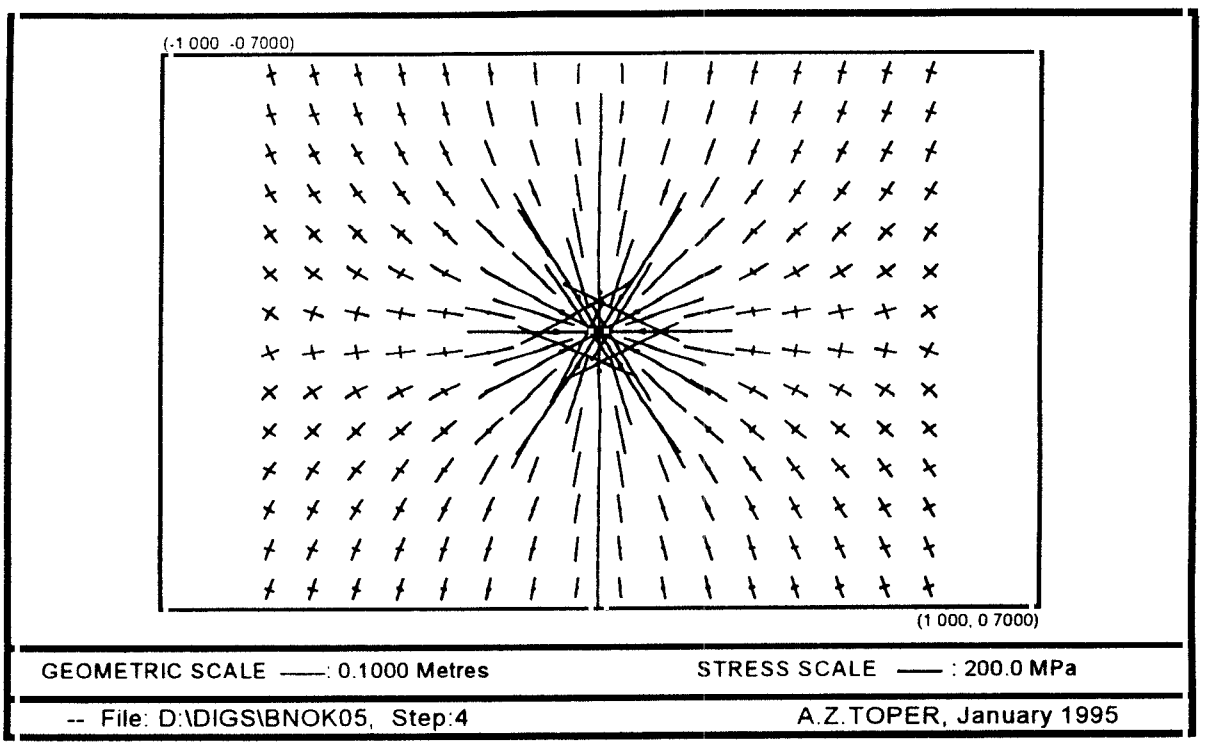

Figure1. Stress Vectors (No bedding plane, Blast Pressure = 500 MPa).

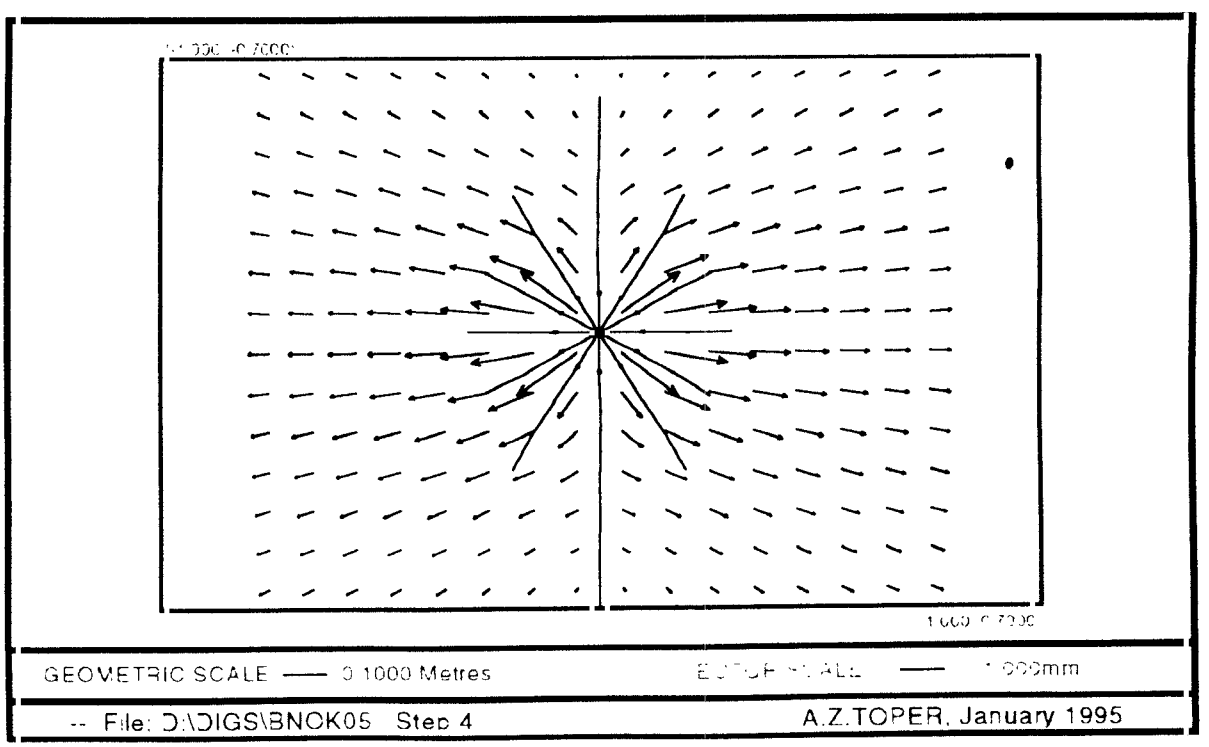

Figure 2. Displacement Vectors (No bedding plane, Blast Pressure = 500 MPa).

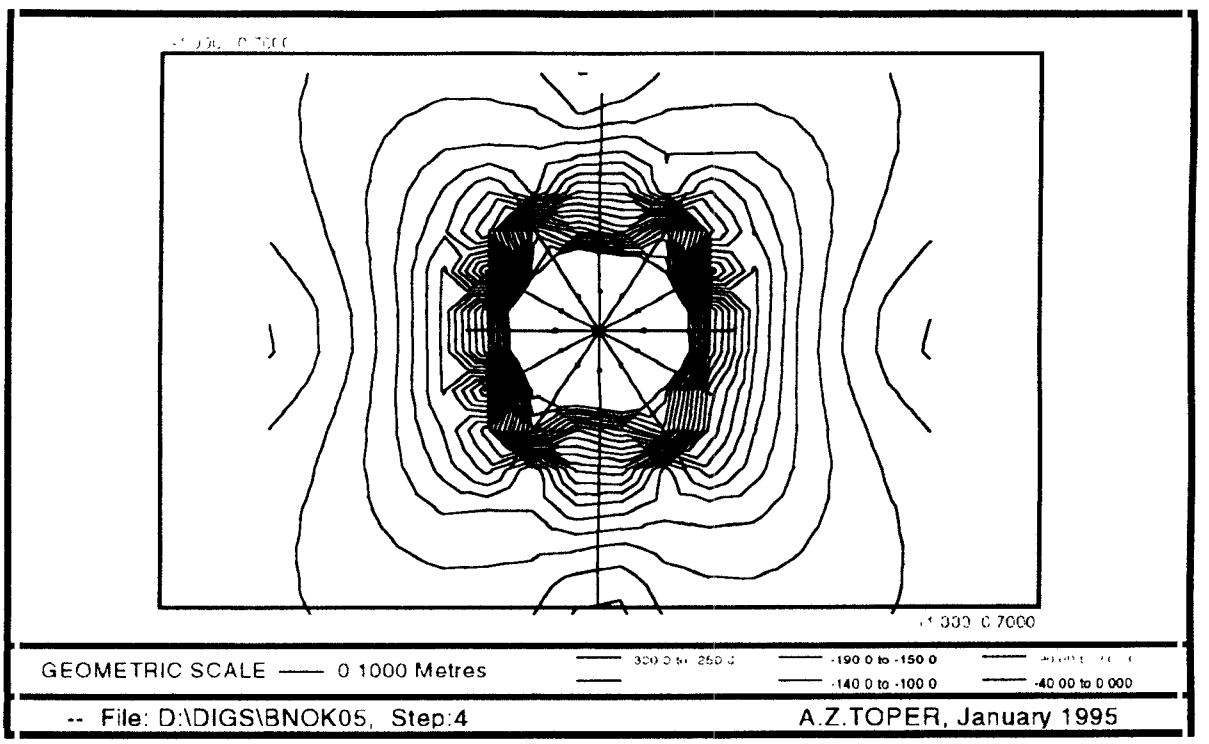

Figure 3. Major Principal Stress Contours (No bedding plane, Blast Pressure = 500 MPa).

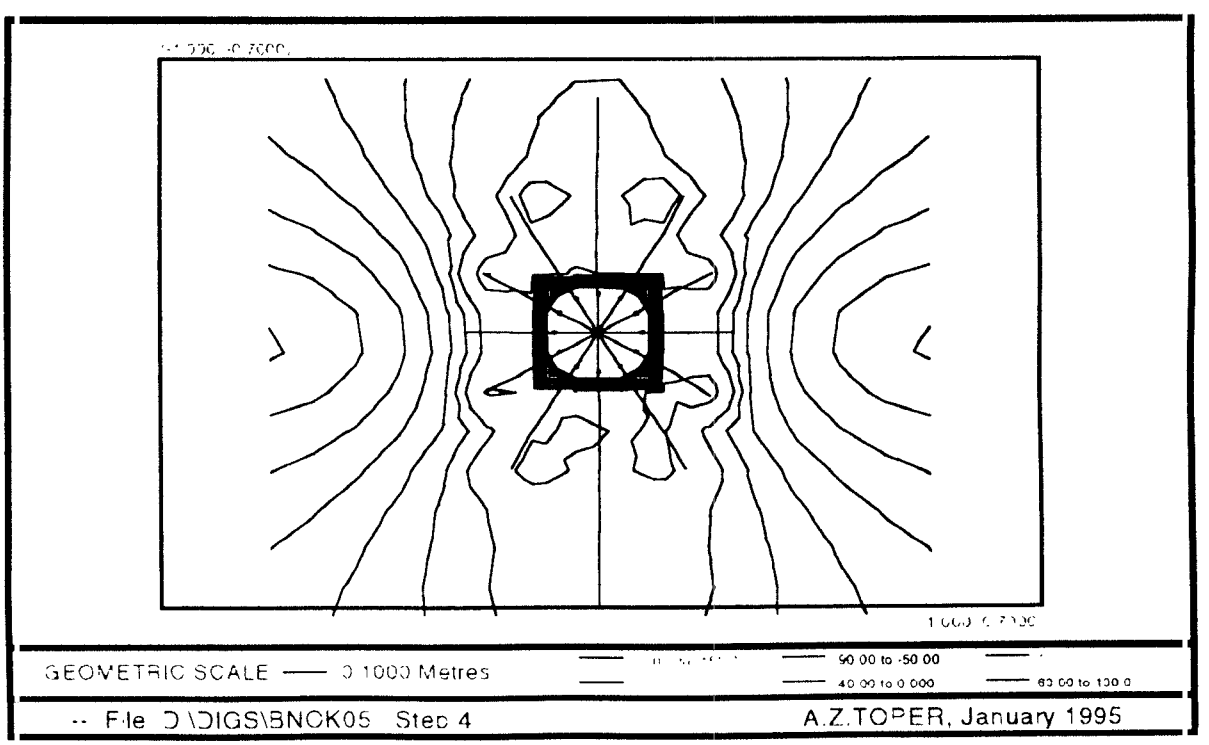

Figure 4. Minor Principal Stress Contours (No bedding plane, Blast Pressure = 500 MPa).

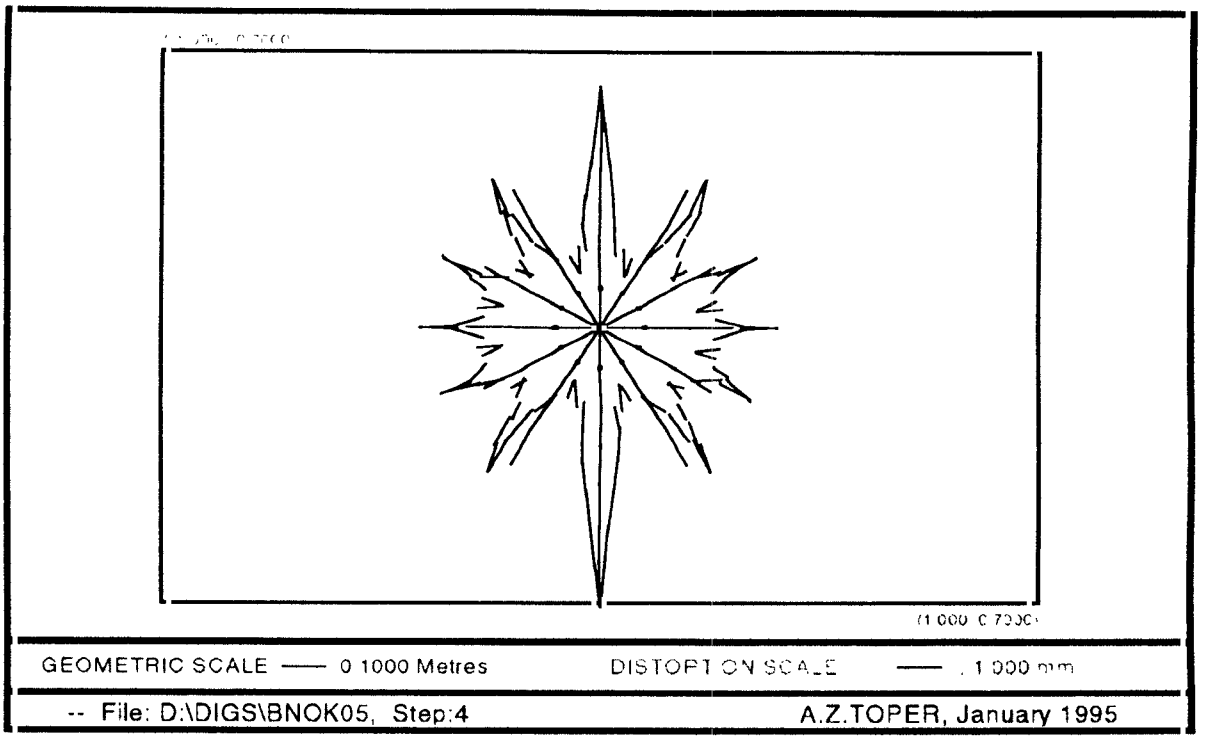

Figure 5. Distorted Geometry (No bedding plane, Blast Pressure = 500 MPa).

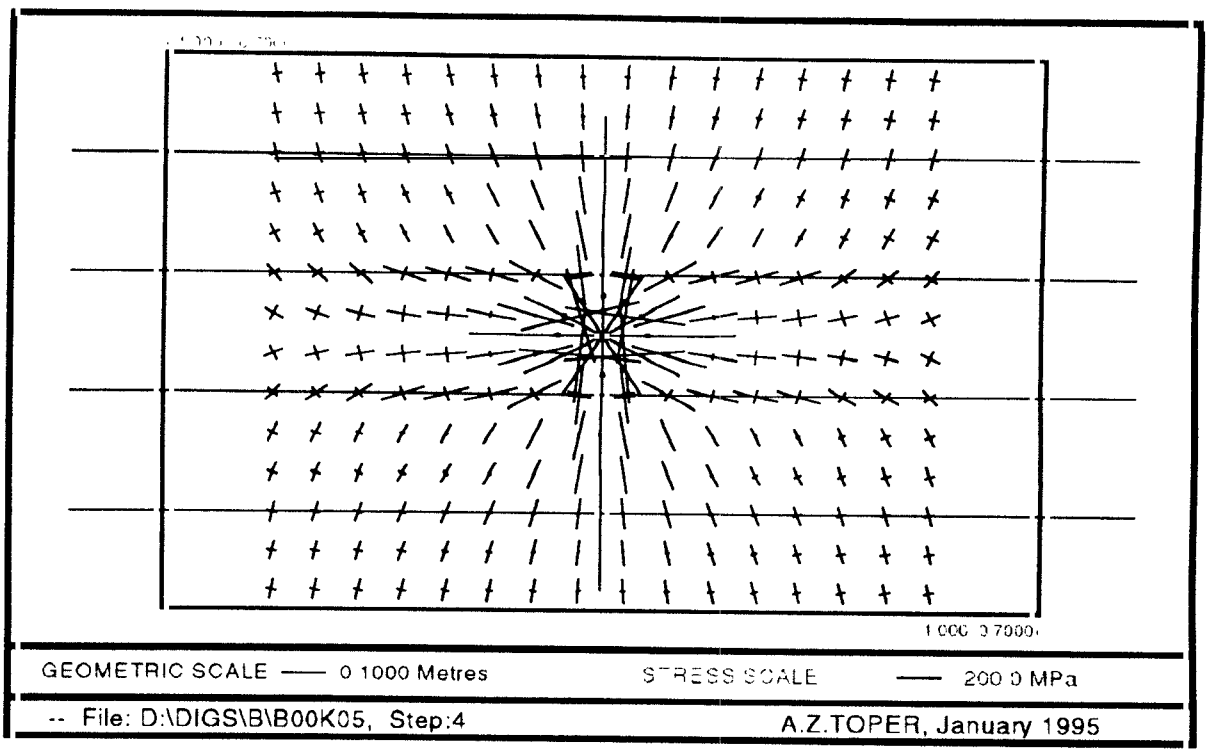

Figure 6. Stress Vectors (Bedding plane : 0°, Blast Pressure = 500 MPa).

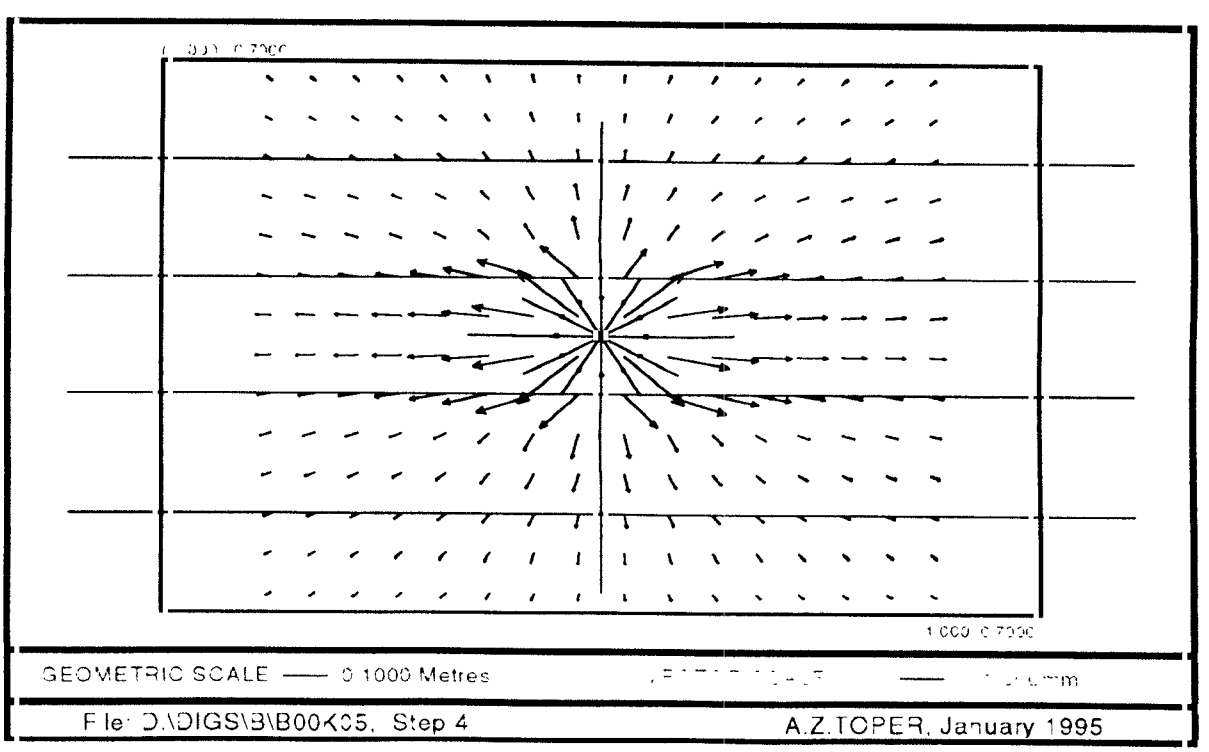

Figure 7. Displacement Vectors (Bedding plane : 0°, Blast Pressure = 500 MPa).

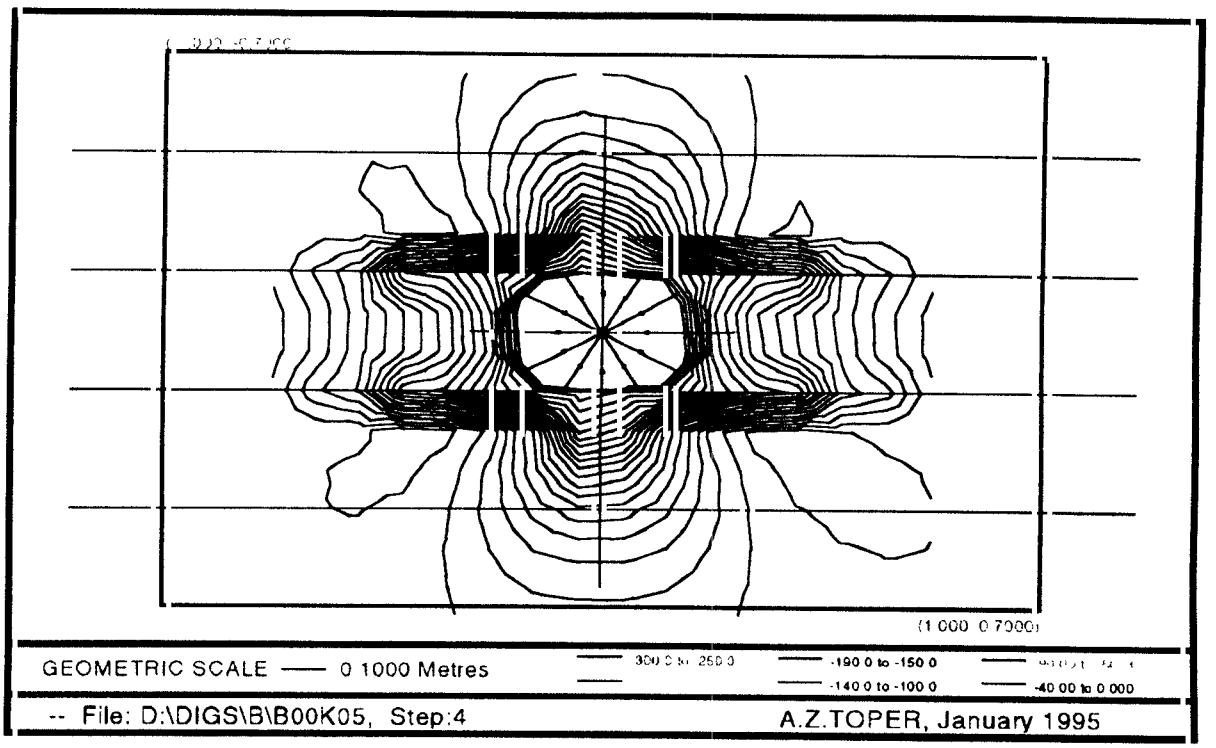

Figure 8. Major Principal Stress Contours (Bedding plane : 0°, Blast Pressure = 500 MPa).

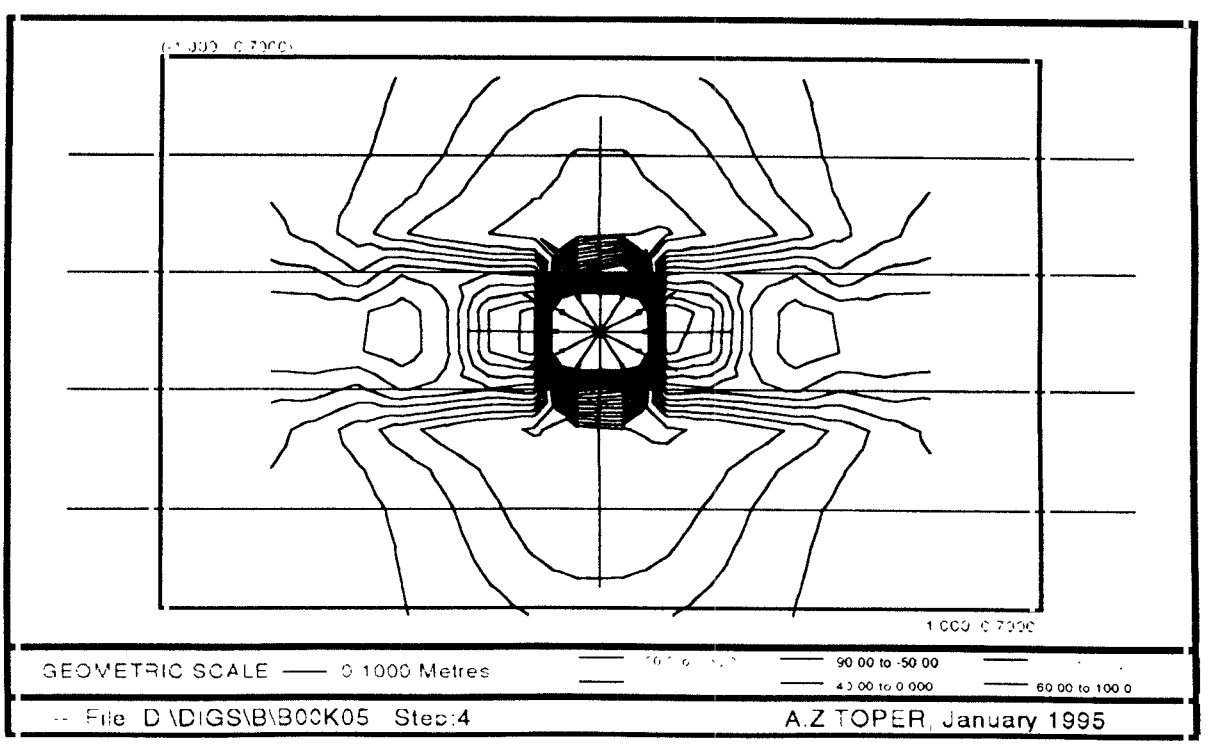

Figure 9. Minor Principal Stress Contours (Bedding plane : 0°, Blast Pressure = 500 MPa).

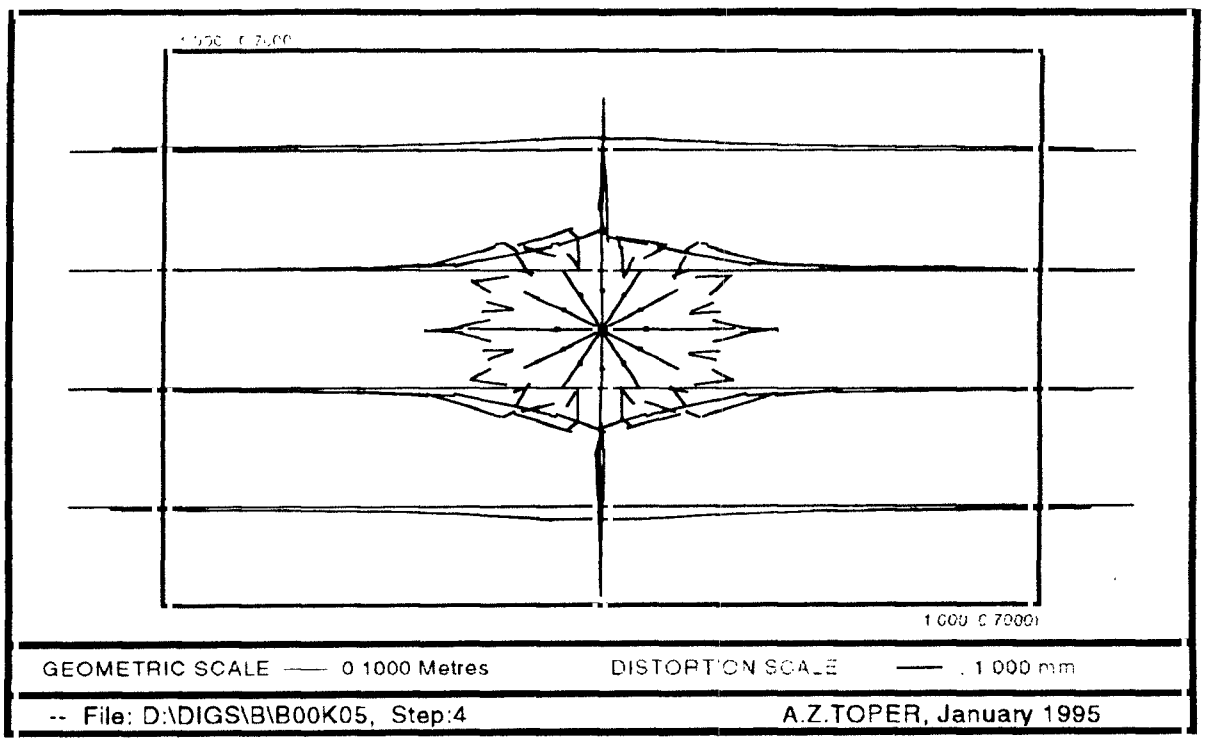

Figure 10. Distorted Geometry (Bedding plane : 0°, Blast Pressure = 500 MPa).

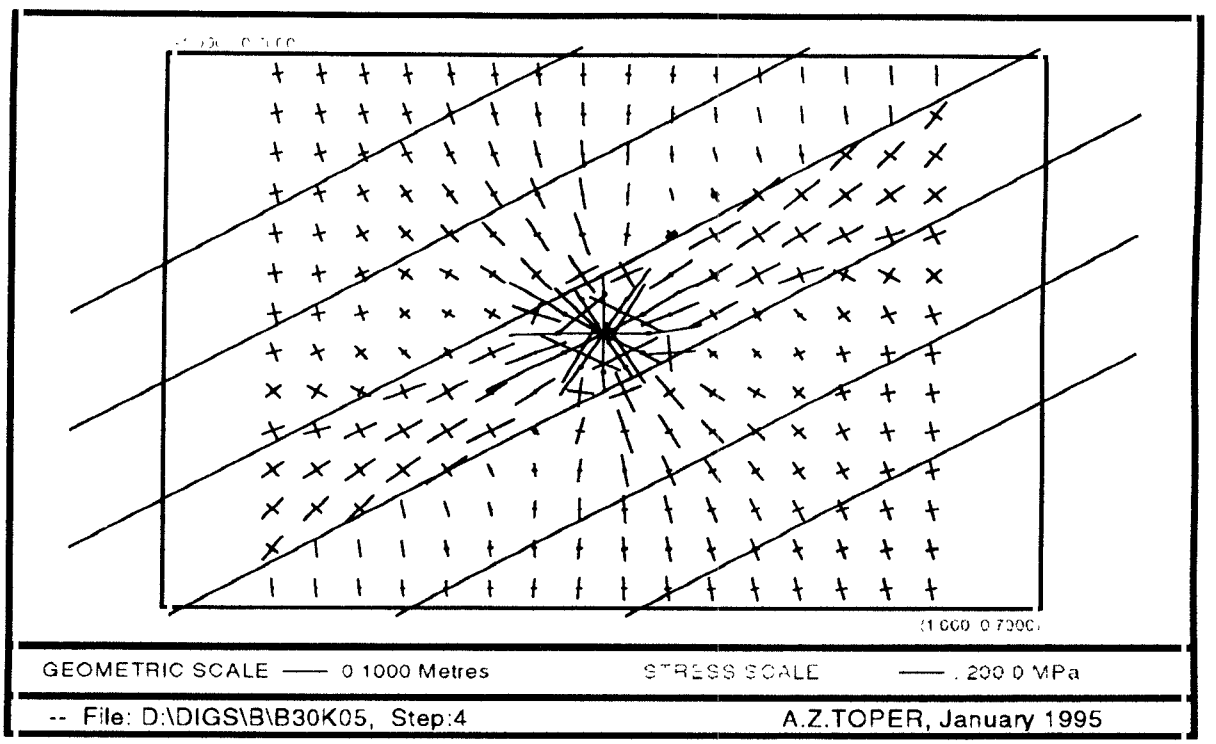

Figure 11. Stress Vectors (Bedding plane : 30°, Blast Pressure = 500 MPa).

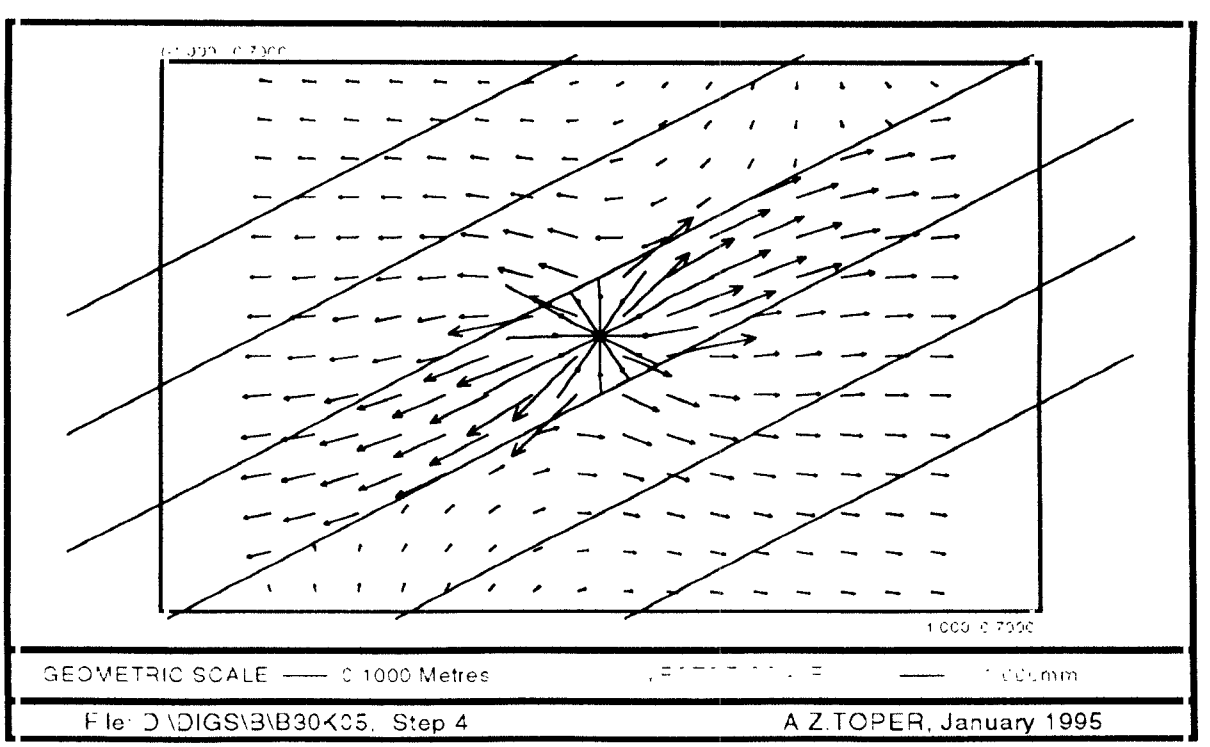

Figure 12. Displacement Vectors (Bedding plane : 30°, Blast Pressure = 500 MPa).

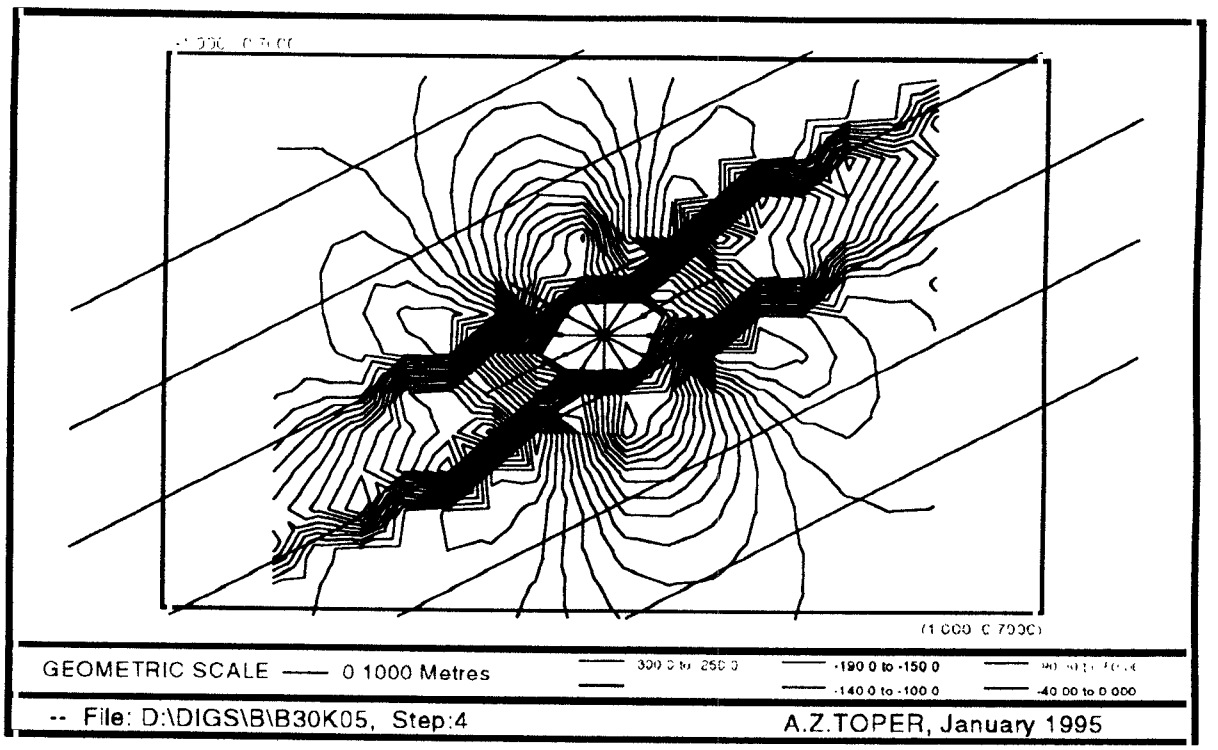

Figure 13. Major Principal Stress Contours (Bedding plane : 30°, Blast Pressure = 500 MPa).

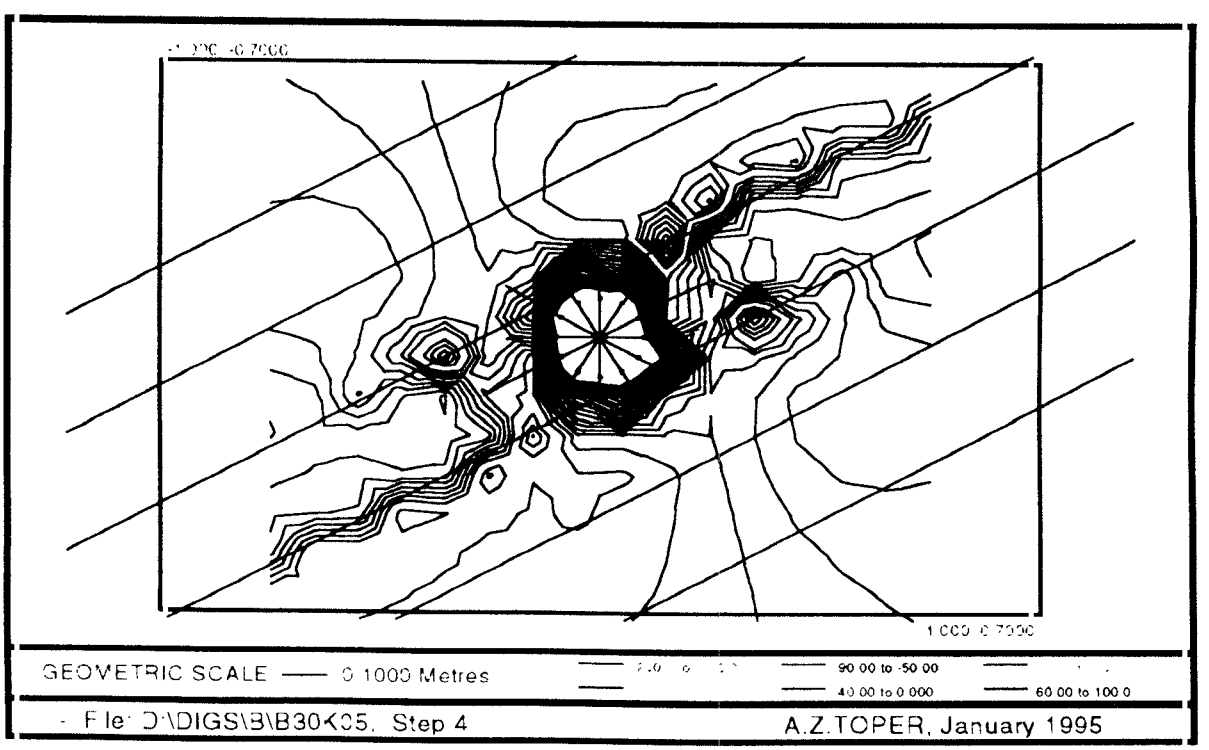

Figure 14. Minor Principal Stress Contours (Bedding plane : 30°, Blast Pressure = 500 MPa).

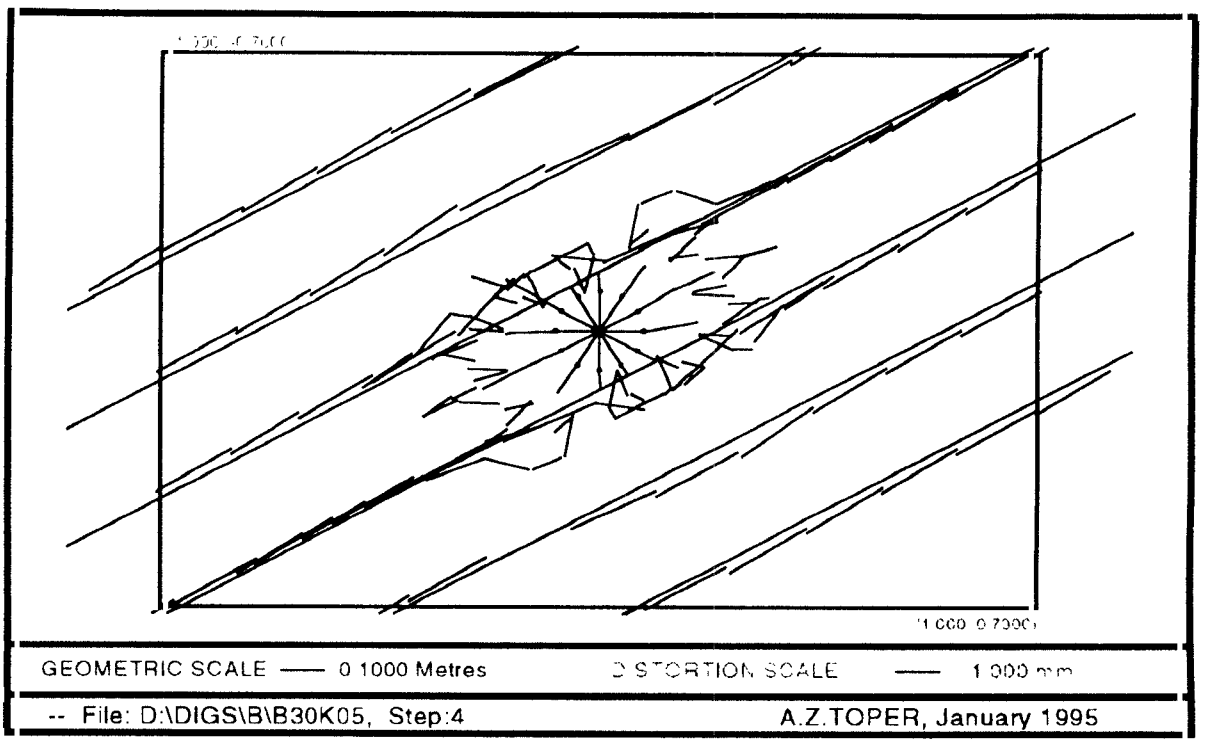

Figure 15. Distorted Geometry (Bedding plane : 30°, Blast Pressure = 500 MPa).

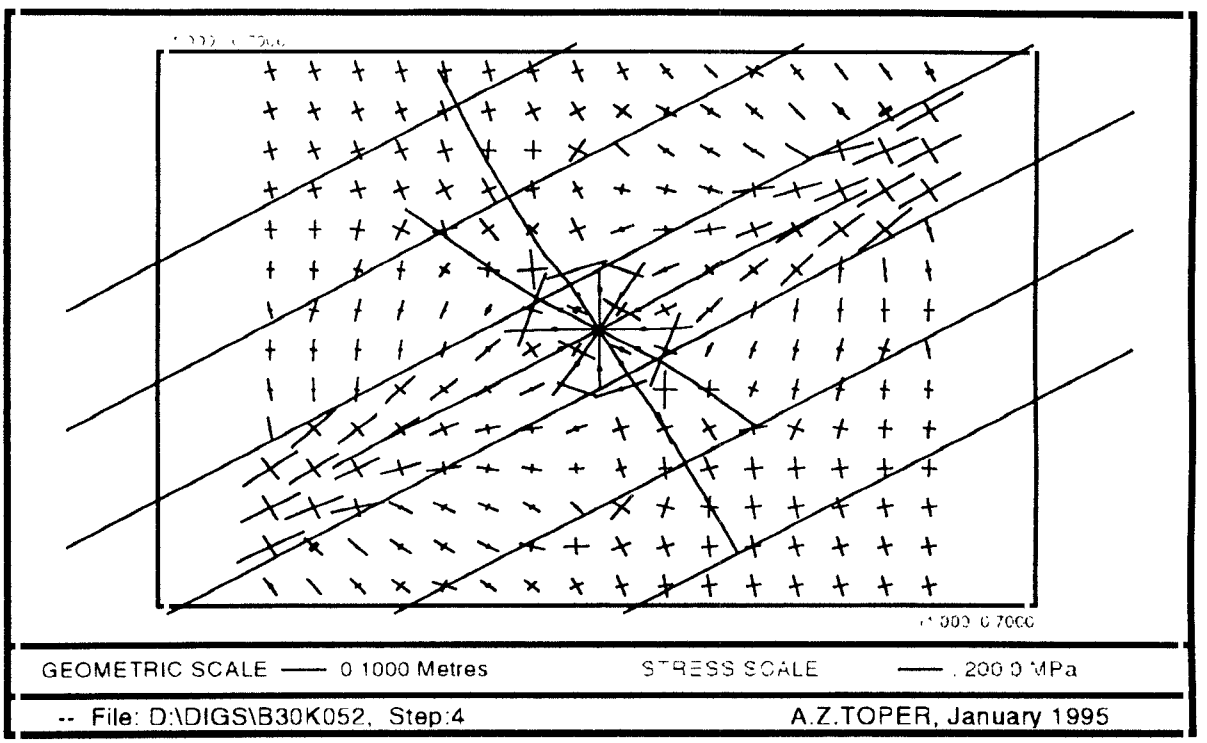

Figure 16. Stress Vectors (Bedding plane : 30°, Blast Pressure = 1000 MPa).

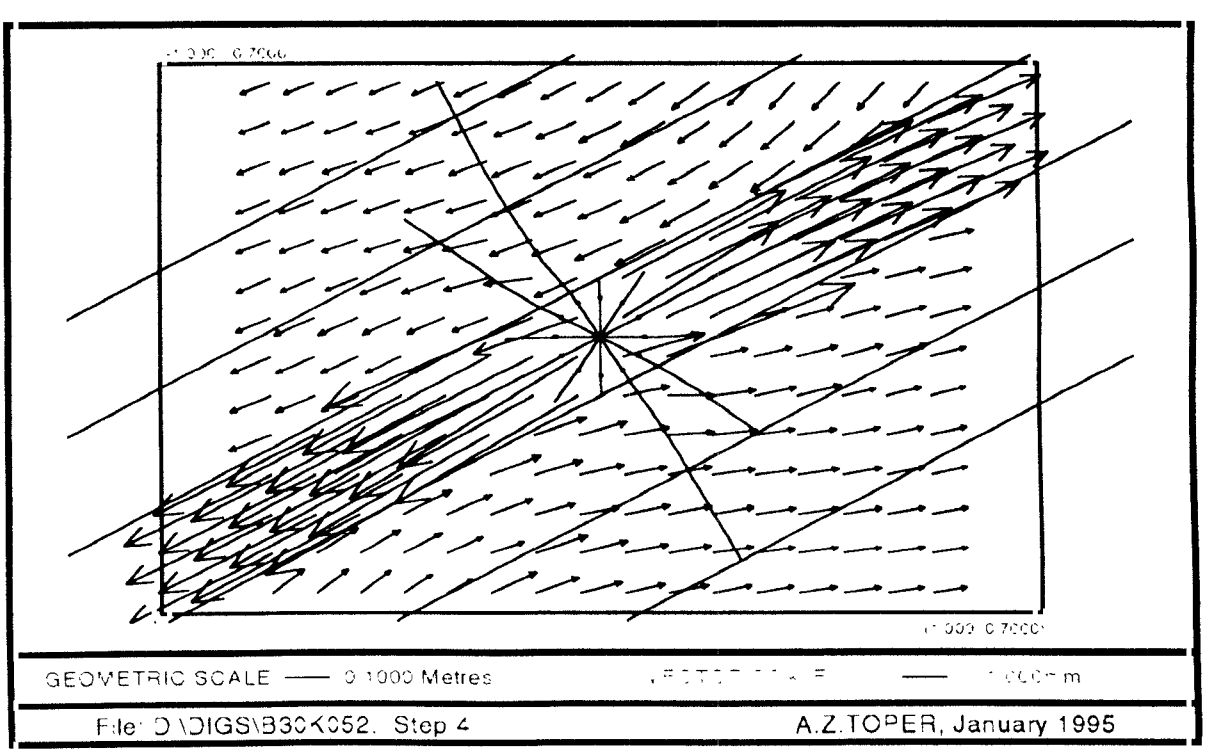

Figure 17. Displacement Vectors (Bedding plane : 30°, Blast Pressure = 1000 MPa).

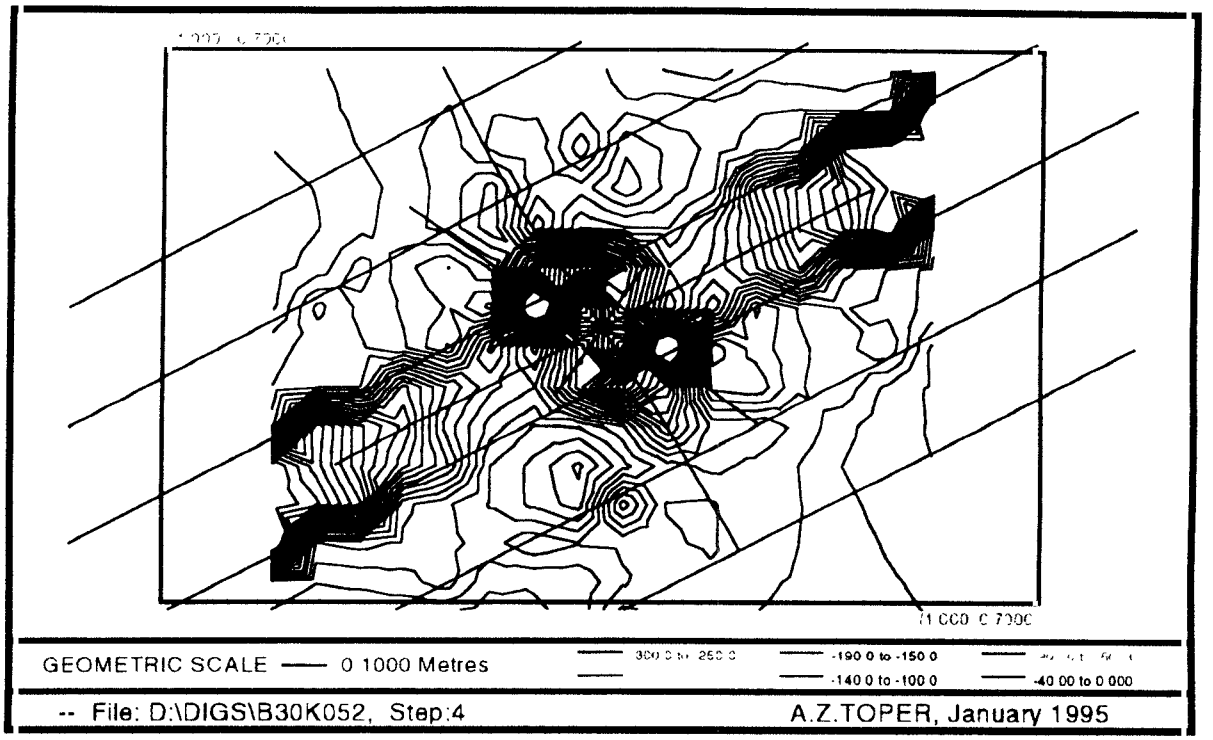

Figure 18. Major Principal Stress Contours (Bedding plane : 30°, Blast Pressure = 1000 MPa).

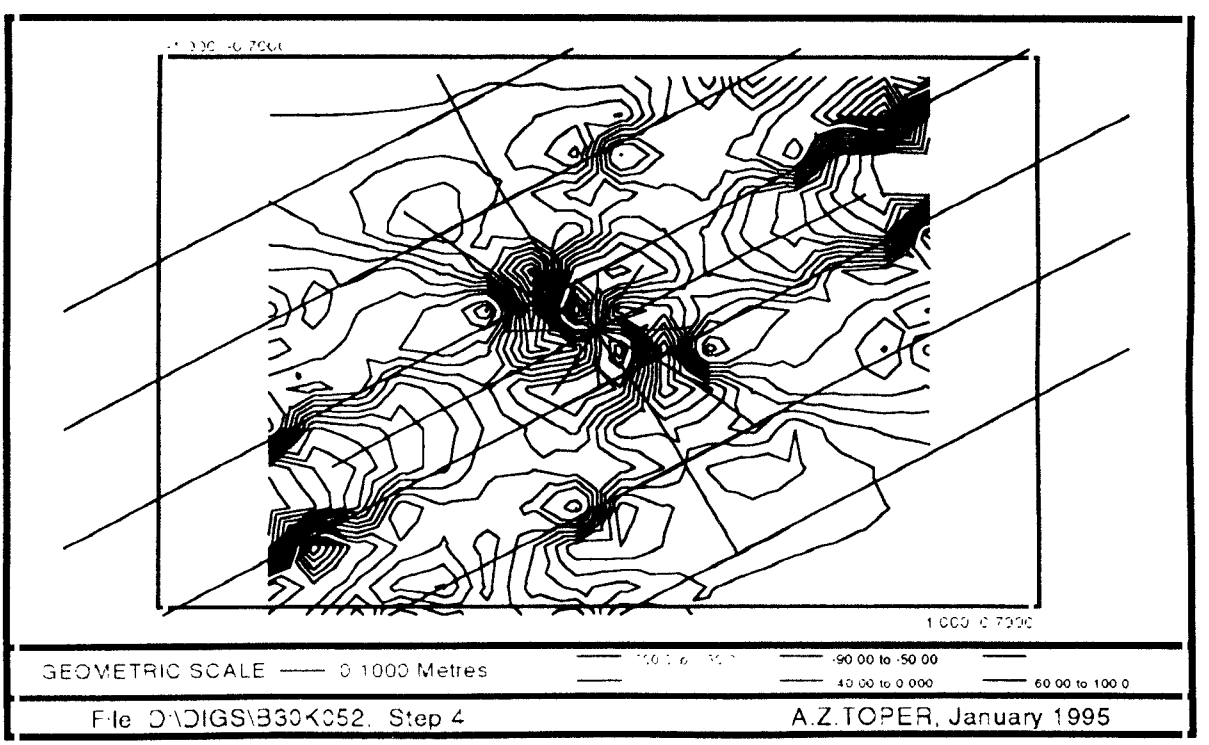

Figure 19. Minor Principal Stress Contours (Bedding plane : 30°, Blast Pressure = 1000 MPa).

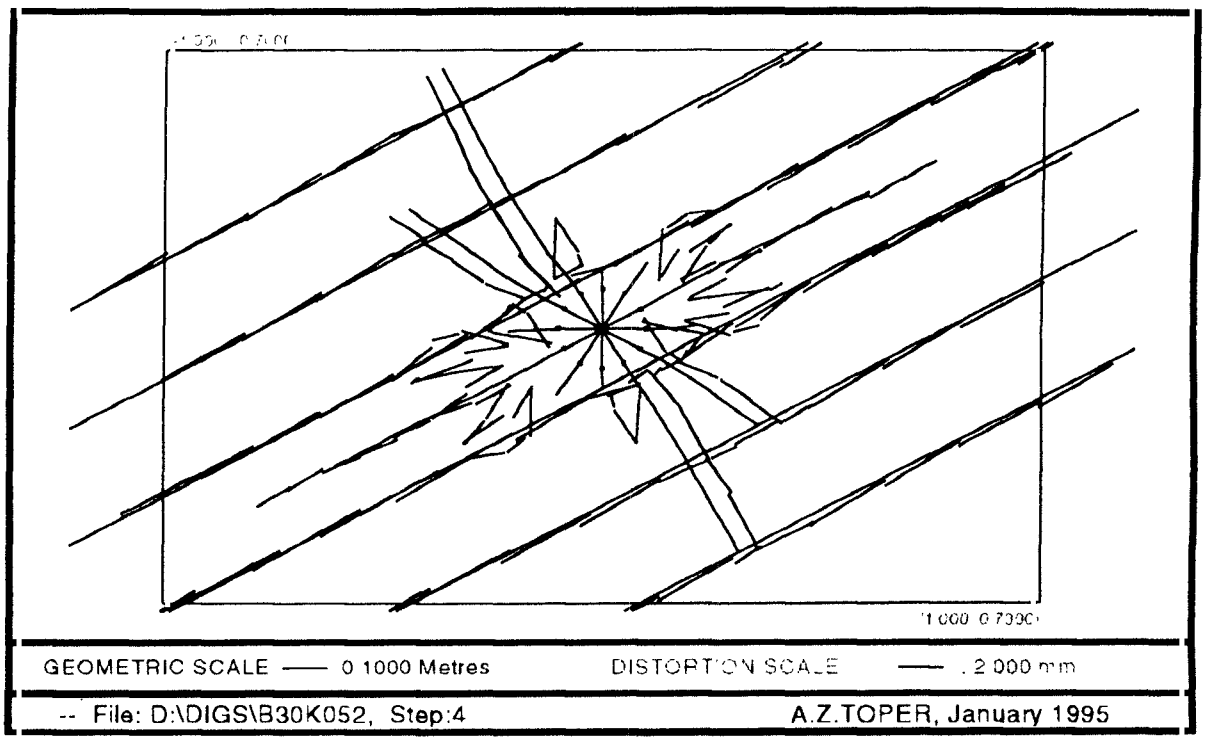

Figure 20. Distorted Geometry (Bedding plane : 30°, Blast Pressure = 1000 MPa).

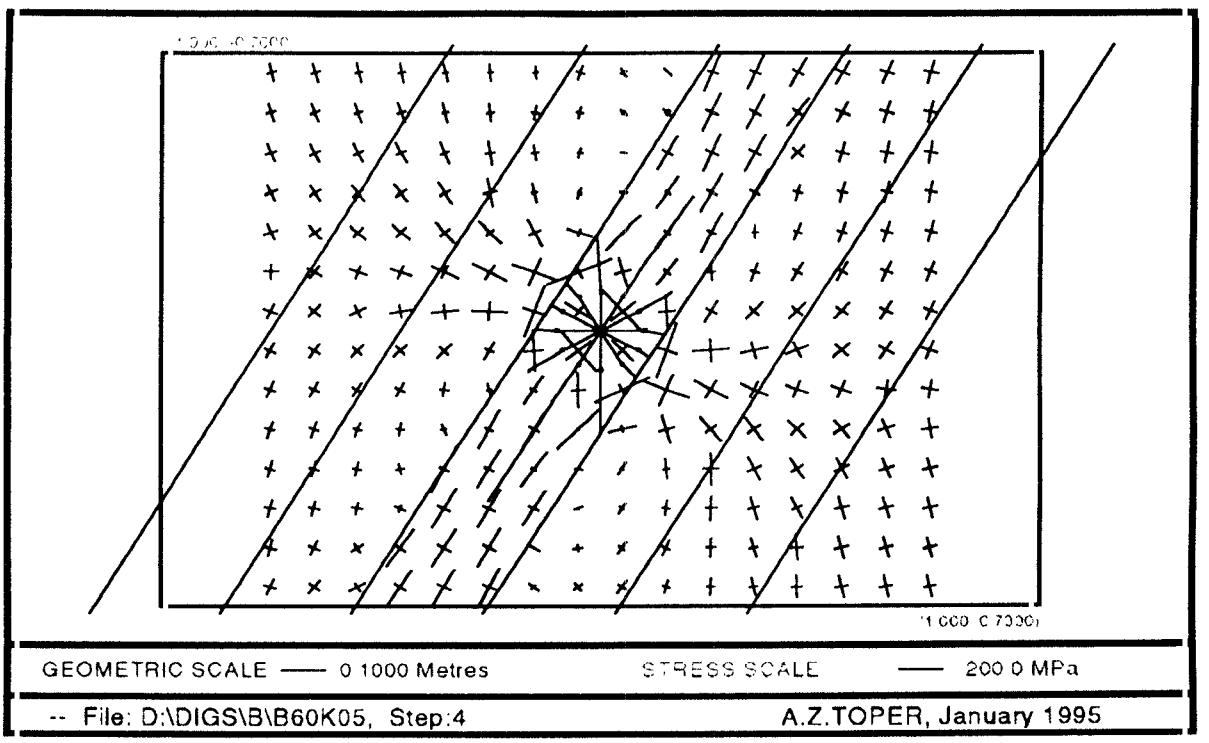

Figure 21. Stress Vectors (Bedding plane : 60°, Blast Pressure = 500 MPa).

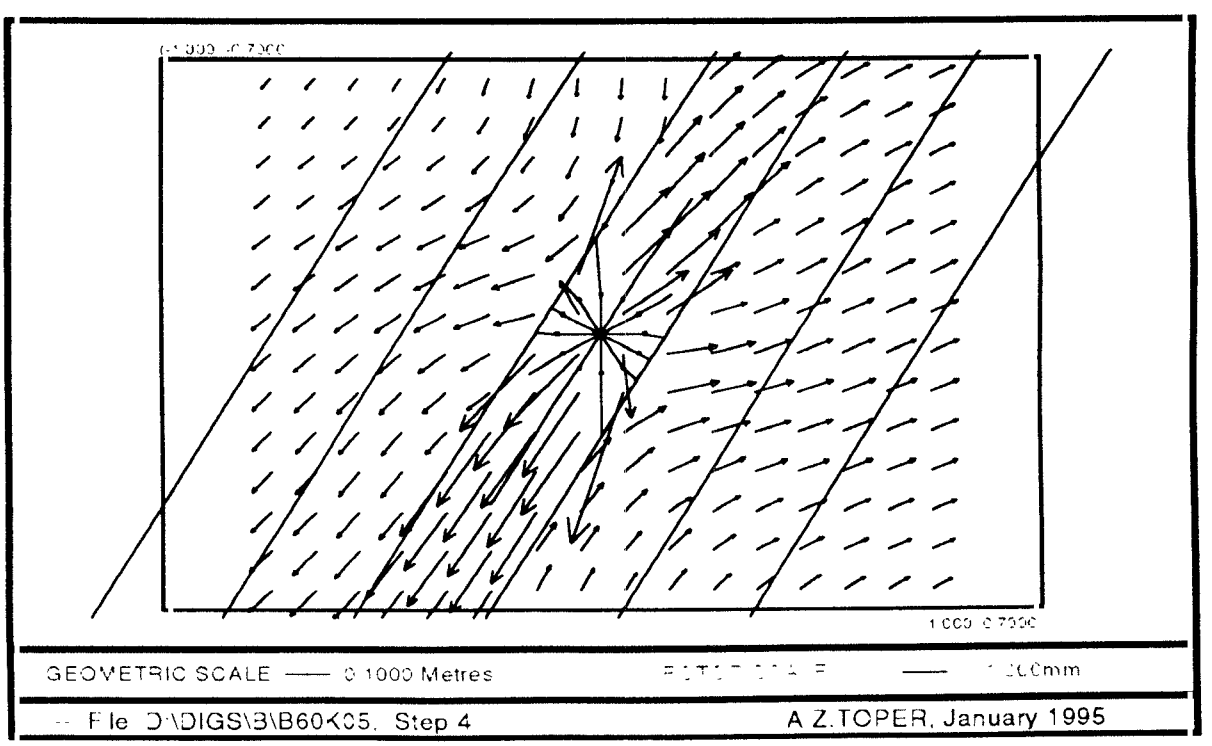

Figure 22. Displacement Vectors (Bedding plane : 60°, Blast Pressure = 500 MPa).

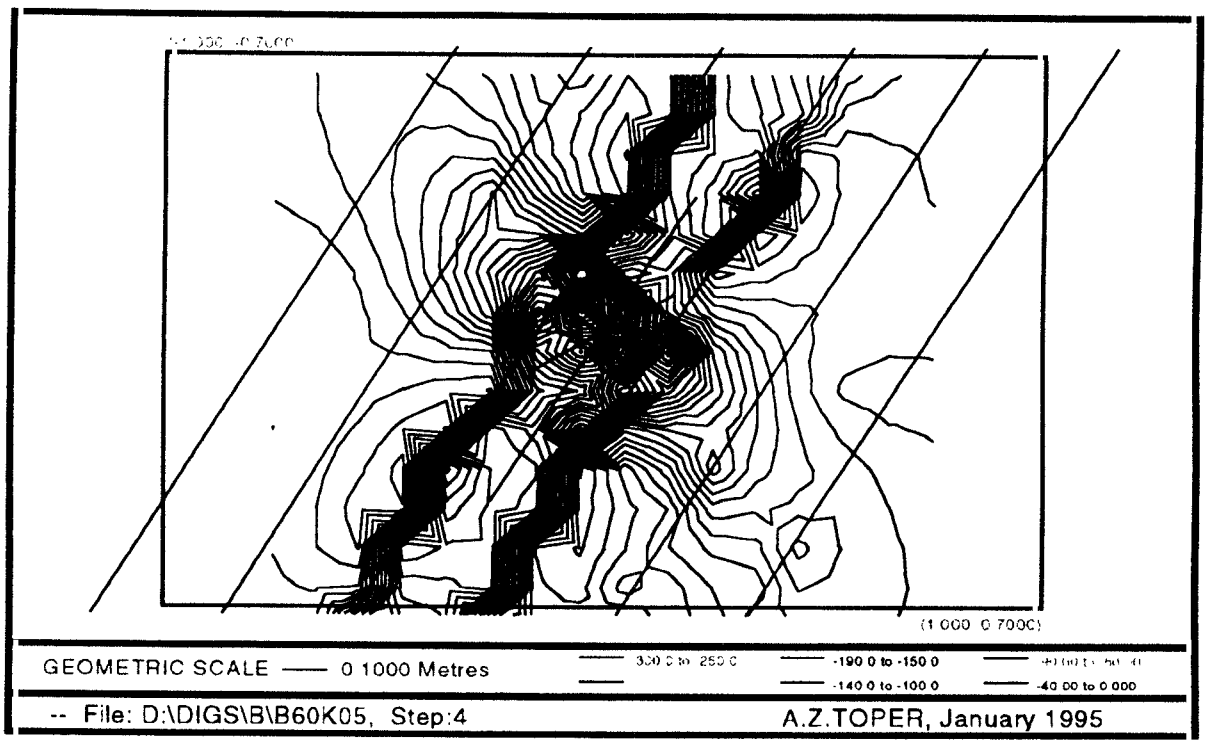

Figure 23. Major Principal Stress Contours (Bedding plane : 60°, Blast Pressure = 500 MPa).

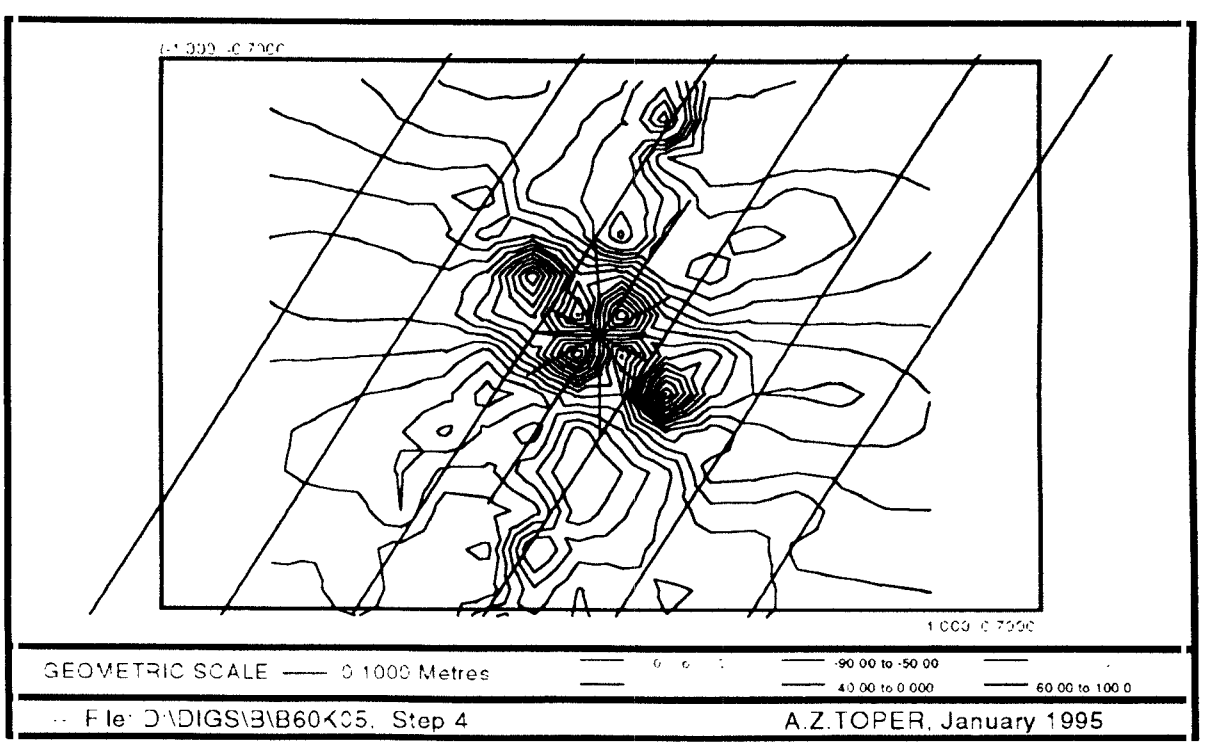

Figure 24. Minor Principal Stress Contours (Bedding plane : 60°, Blast Pressure = 500 MPa).

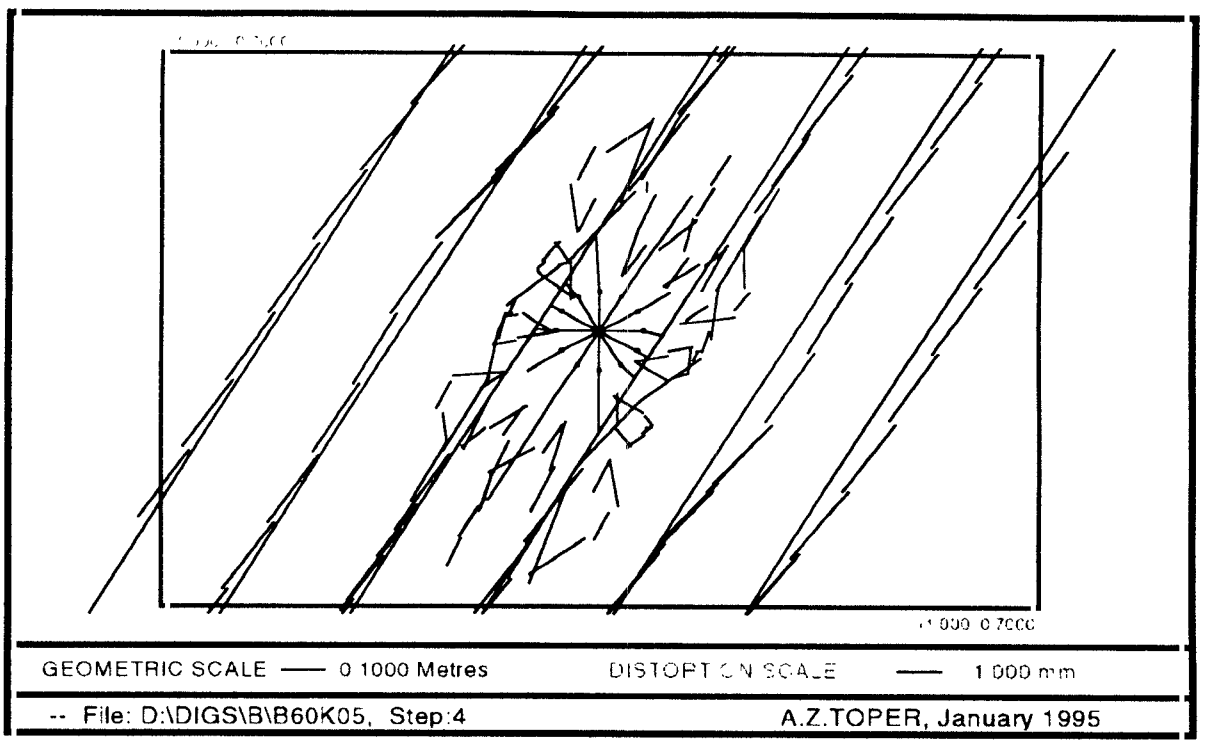

Figure 25. Distorted Geometry (Bedding plane : 60°, Blast Pressure = 500 MPa).

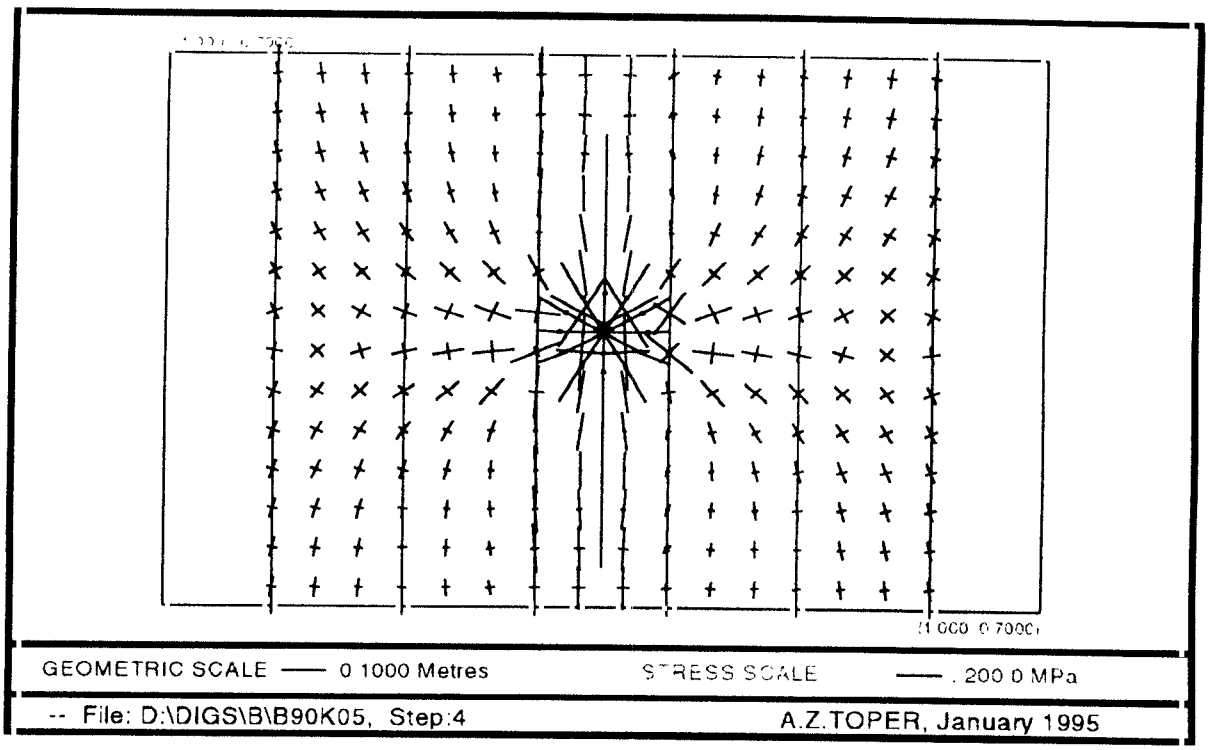

Figure 26. Stress Vectors (Bedding plane : 90°, Blast Pressure = 500 MPa).

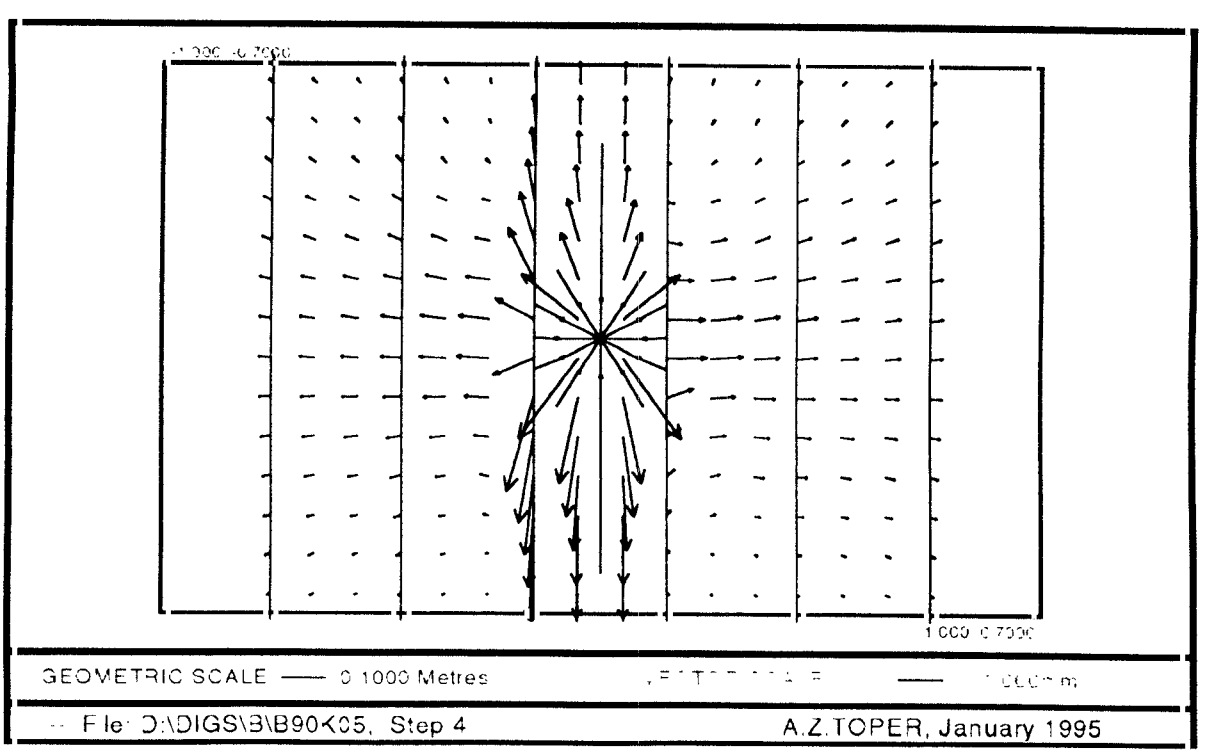

Figure 27. Displacement Vectors (Bedding plane : 90°, Blast Pressure = 500 MPa).

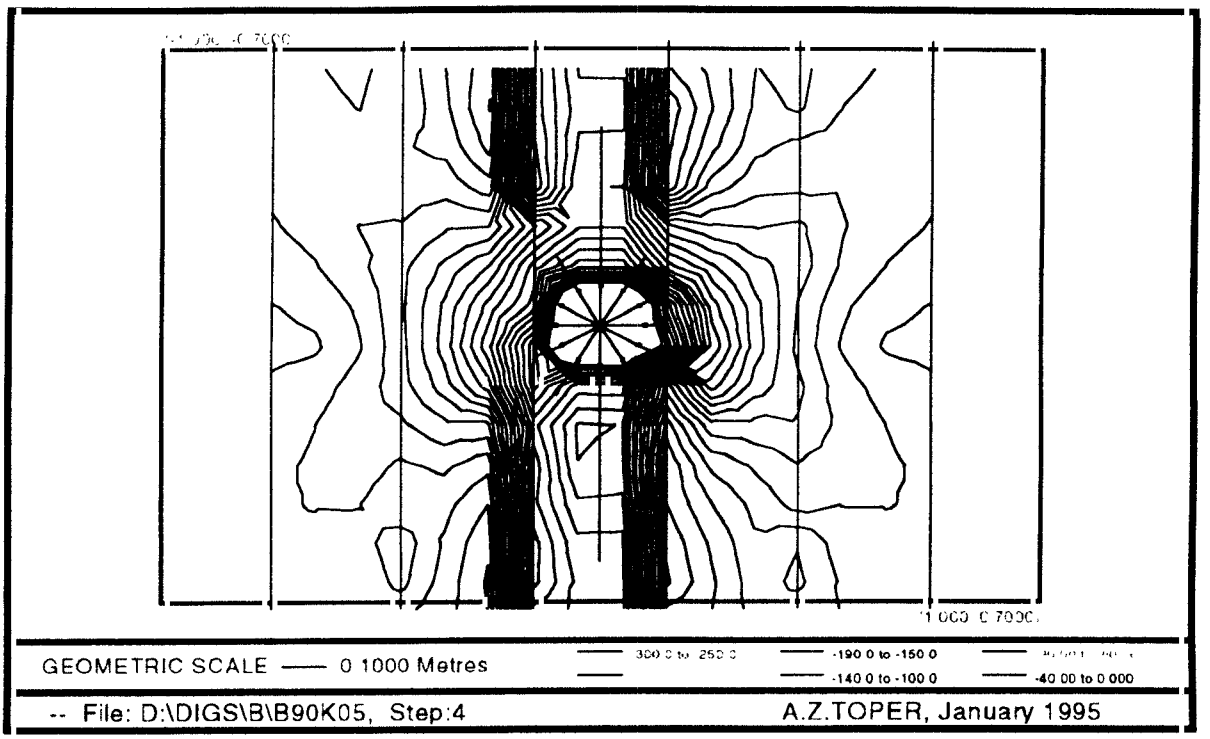

Figure 28. Major Principal Stress Contours (Bedding plane : 90°, Blast Pressure = 500 MPa).

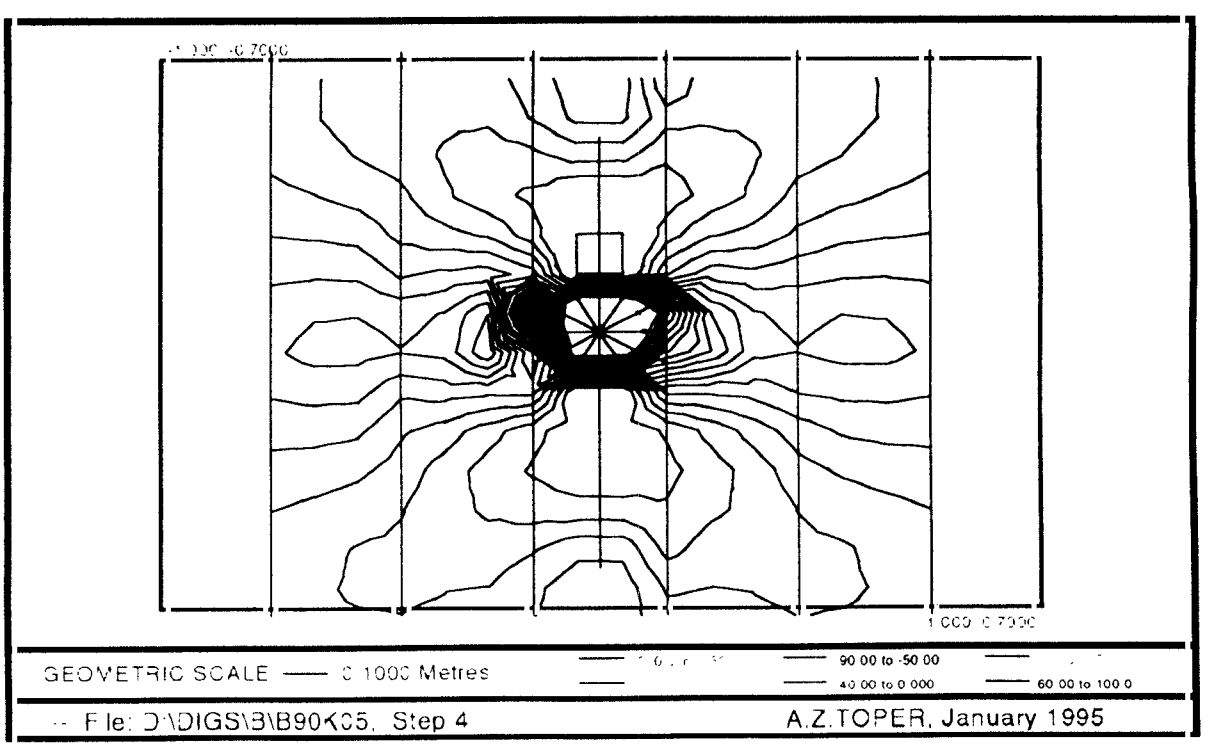

Figure 29. Minor Principal Stress Contours (Bedding plane : 90°, Blast Pressure = 500 MPa).

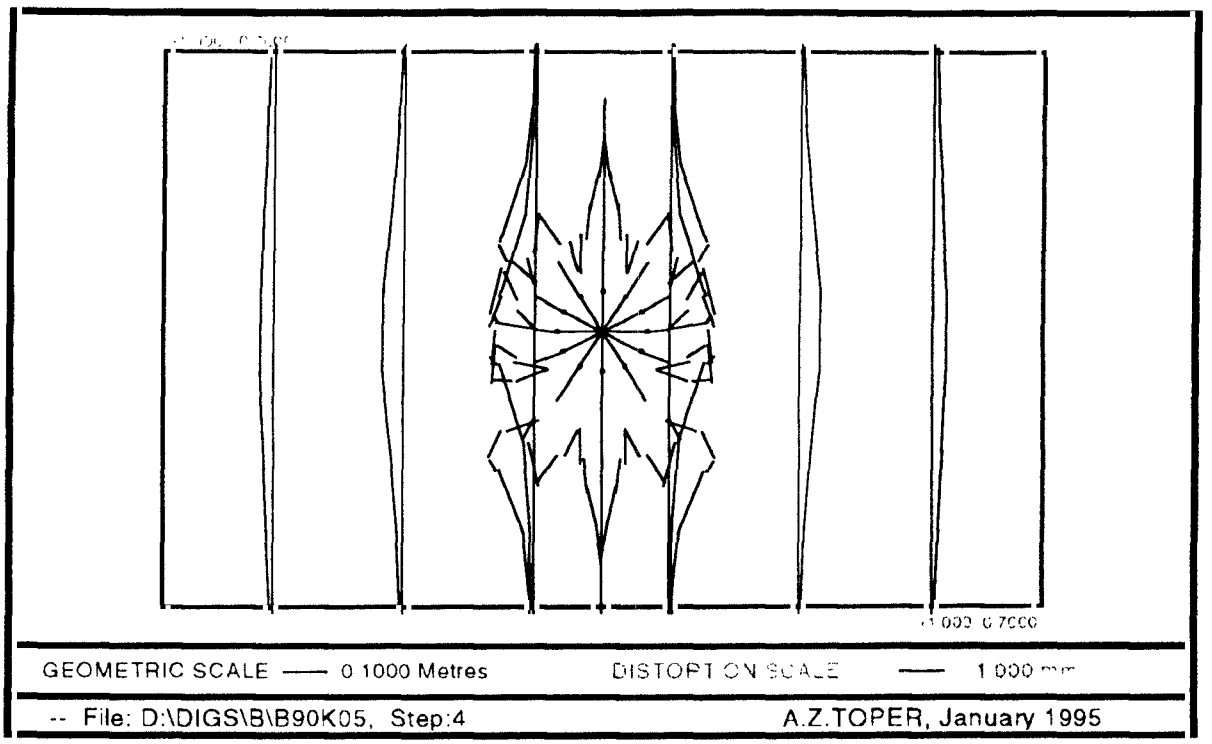

Figure 30. Distorted Geometry (Bedding plane : 90°, Blast Pressure = 500 MPa).